



**TECHNISCHE
UNIVERSITÄT
WIEN**

**VIENNA
UNIVERSITY OF
TECHNOLOGY**

Institute for Building Construction and Technology

Center of Mechanics and Structural Dynamics

E206/3

DISSERTATION

DYNAMIC BEHAVIOR OF BELL TOWER LIKE STRUCTURES IN EARTHQUAKE ENVIRONMENT

Supervisors

Ao.Univ.Prof. Dipl.-Ing. Dr.techn. Rudolf Heuer

Prof. Dr.tech. Ali Kaveh

Ph.D. Candidate

M.Sc. S. Mehdi Yousefi

E0427672 (086610)

Vienna/Austria

January 2008

Preface

This dissertation is the result of my daily work for the last three years at the Institute of Mechanics and Structural Dynamics at the Technical University of Vienna.

First and foremost, I would like to deeply thank my main supervisor, Prof. Rudolf Heuer, for his invaluable guidance and unfailing enthusiasm throughout my entire study at the Technical University of Vienna. Beyond gaining academic knowledge, I am also indebted to him for all he taught me in life.

I am very grateful to Prof. Ali Kaveh, my second supervisor who followed the progress of my work at some distance. His hints and remarks have been more important than can be acknowledged in a single paragraph.

I benefited from the helpful knowledge and hospitality of Prof. Franz Ziegler and other institute members, my sincerest thanks to you all.

I would also like to offer my special thanks to Frau Dr. Theresia Laubichler for financial and institutional support.

My thanks are further due to my father and mother for their love and support.

Finally, I am grateful to my wife for her support and her patience over the last few years.

Abstract

In this thesis, the dynamic behavior of Bell-Tower (BT) like structures excited by various internal and external actions are investigated. A BT structure is considered as a linear elastic continuous cantilever beam (tower) together with a nonlinear single pendulum (bell). The formulation of the equation of motion is presented based on direct equilibrium position, as well as Lagrange equations, which is applicable to systems in both linear and nonlinear conditions. Parametric studies of the BT are performed for free and force vibrations and dynamic actions by bell swinging and earthquake forces. For this purpose, first the BT is introduced in discretized form with geometrically nonlinear behaviour corresponding to a simple pendulum combined with a linear Single-Degree-of-Freedom (SDOF) system (tower). Suitable analytical method is then performed and comparison is made between the responses obtained from the analytical method and a numerical approach by means of computer simulations.

In the next stage, the BT is studied as a hybrid system. In this case, the rigid pendulum is supported at the top of the linear elastic tower. The corresponding equations of motion are derived, considering nonlinear oscillation behavior of the pendulum and discretizing the continuous tower as a linear Multi-Degree-of-Freedom (MDOF) system. Special emphasize is placed on the nonlinear interaction between the dynamically excited tower and the movement of the bell that mechanically behaves like a rigid pendulum. This particular study gives a completely new insight into the complex dynamic behaviour of the BT structure. Comparison is also made between the characteristics in coupled and uncoupled systems.

Dynamic actions caused by ringing the bell are typical characteristic aspects in BTs. Thus the effect of the bell ringing on the tower is followed. Both the tower and bell system are studied under the effect of forced bell vibrations. In addition, particular study is performed for the nonlinear pendulum with special focus on subharmonics and superharmonics resonate frequencies. Vibrating forces are applied as an external moment, and nonstationary conditions in nonlinear pendulum is discussed.

Over the recent decades new vibration control methods are introduced using pendulum dynamic absorbers, which are extensively employed to reduce the tower's vibration level. A Pendulum Tuned Mass Damper (PTMD) is a device consisting of a suspended mass, and a damper that is attached to the tower in order to reduce the dynamic response of the structure. The primary eigenfrequency of the damper is tuned to a particular structural frequency so that when the system is excited, the damper will resonate out of phase with the tower motion and mitigates vibration. Energy is dissipated by the damping and inertia force acting on the structure. An introductory example of PTMD design and a description of the implementation of PTMDs in building structures like chimneys and BTs are presented. Time history and frequency domain responses for a continuous system connected to optimally PTMD and subjected to harmonic and random support excitations in linear and nonlinear conditions are studied. An assessment is made for the optimal placement of PTMD in the tower. Response against earthquake force with respect to seismic design criteria and record of real strong ground motion of Bam (Iran, 2003) is also estimated.

Dynamic analysis of the BT by means of the substructure method is introduced. The vibrations induced by the bell (pendulum) movements are treated as externally applied excitations and pendulum oscillatory movement is formulated to determine the time-variant forces applied to the tower. Subsequently, the responses of BT in quasi-static analysis are compared and the internal forces of the tower produced by dynamic excitations are evaluated by numerical nonlinear analysis.

Finally, the motion of the BT is controlled and modified by means of the action of control system. The bell works like an Active Pendulum Mass Damper (APMD) and dissipates energy by some external sources. Numerical nonlinear and time-step analyses are performed and the results are compared.

Kurzfassung

In der vorliegenden Arbeit wird das dynamische Verhalten von Glockenturm-ähnlichen (GT) Tragwerken, die durch verschiedene interne und externe Einwirkungen angeregt werden, untersucht. Die GT-Struktur wird als linear elastischer kontinuierlicher Kragträger mit einem nichtlinearen Einzelpendel (Glocke) modelliert. Die Formulierung der Bewegungsgleichungen, basierend auf der dynamischen Gleichgewichtsmethode, als auch die Lagrange'schen Gleichungen sind dabei für lineare und nichtlineare Bedingungen anwendbar. Es werden Parameterstudien der GT-Strukturen für freie und erzwungene Schwingungen durchgeführt und das dynamische Verhalten, verursacht durch Glocken schwingen und Erdbebenanregung, untersucht.

Zuerst wird die GT-Struktur in diskretisierter Form als ein geometrisch nichtlineares Phänomen, entsprechend einem einfachen Pendel kombiniert mit einem linearen Einmassenschwinger, vorgestellt. Eine passende analytische Methode wird beschrieben und die Ergebnisse mit jenen aus numerischen Simulationsrechnungen verglichen.

In der Folge wird der GT als hybrides System untersucht. In diesem Fall wird das starre Pendel an der Spitze des linear elastischen Turms gelagert. Die dazugehörigen Bewegungsgleichungen werden unter Berücksichtigung des nichtlinearen Schwingungsverhaltens des Pendels und des kontinuierlichen Turms, modelliert als diskretes lineares Mehrfreiheitsgrad-System, hergeleitet. Es wird besonders Wert auf die nichtlineare Interaktion zwischen dem dynamisch angeregten Turm und der Bewegung der Glocke, welche sich mechanisch wie ein starres Pendel verhält, gelegt. Die Studie gibt einen neuen Einblick in das komplexe dynamische Verhalten von GT-Strukturen. Es wird auch ein Vergleich des Schwingungsverhaltens von gekoppelten und entkoppelten Systemen angeführt.

Die dynamischen Reaktionen auf das Glockenläuten sind typische charakteristische Erscheinungen von den betrachteten Türmen. Das mechanische Verhalten von Turm und Glocke wird unter Berücksichtigung der erzwungenen

Glockenschwingung abgeschätzt. Unter der Wirkung eines externen Glocken-Antriebmomentes wird das nichtlineare Pendel in Bezug auf subharmonische und superharmonische Resonanzfrequenzen untersucht. Die nichtstationären Bedingungen des nichtlinearen Pendels werden diskutiert.

In den letzten Jahrzehnten wurde eine neue Methode der Schwingungsdämpfung entwickelt, die durch dynamische Pendelabsorber die Schwingungen von GT-Strukturen deutlich reduziert. Ein „Pendulum Tuned Mass Damper“ (PTMD) ist eine Einheit, bestehend aus einer pendelnd aufgehängten Masse und einem Dämpfer, der mit der Struktur verbunden ist um die Schwingungsantwort zu reduzieren. Die erste Eigenfrequenz des Dämpfers ist gezielt auf eine bestimmte Struktureigenfrequenz abgestimmt, so dass bei Anregung dieser Frequenz der Dämpfer durch ein phasenverschobenes Verhalten zur Turmbewegung die Schwingungen reduziert. Die Energie wird durch die Dämpfung und die Trägheitskraft, die auf die Struktur wirkt, dissipiert. Ein einführendes Beispiel eines PTMD und dessen Implementierung in Strukturen, wie Schornsteine oder Glockentürme, wird gezeigt. Zeitverläufe und Amplitudenfrequenzgänge werden für ein kontinuierliches System mit einem optimal abgestimmten PTMD, welches einer harmonischen oder stochastischen Fußpunkterregung ausgesetzt ist, unter linearen und nichtlinearen Bedingungen untersucht. Ebenso wird die optimale Position des Pendels diskutiert. Die Schwingungsantwort zufolge Erdbebenkräfte bezüglich seismischer Entwurfskriterien wird entsprechend der starken Bodenbewegung des Erdbebenereignisses in Bam (Iran, 2003) simuliert.

Ein Kapitel behandelt die dynamische Analyse von GT-Strukturen mittels Teilssystemtechnik. Die durch die Glocke induzierten Schwingungen werden als externe Anregung auf die Hauptkonstruktionen angesetzt um aus der Pendelbewegung die zeitvariablen Kräfte auf den Turm zu ermitteln. Diese werden mit den Kräften aus einer quasi-statischen Analyse verglichen, die dynamischen Schnittgrößen mittels numerischer nichtlinearer Analyse ermittelt.

Im letzten Abschnitt wird die Wirkungsweise von aktiv geregelten Pendeldämpfern in turmartige Baukonstruktionen analysiert.

TABLE OF CONTENTS

1	MECHANICAL MODEL OF A BELL-TOWER	1
1.1	Description of Bell-Tower like structures	1
1.2	Examples of existing pendulum tuned mass dampers	2
1.3	References	8
2	DYNAMIC ANALYSIS OF A TWO-DEGREE-OF-FREEDOM SYSTEM	9
2.1	Introduction	9
2.2	Equations of motion	9
2.3	Linear analysis	13
2.4	Numerical example for the linear system	15
2.5	Nonlinear vibrations of the simple pendulum	17
2.6	Equations of motion of the coupled nonlinear system	20
2.7	Numerical examples for the nonlinear system	21
2.7.1	Unit displacement base	23
2.7.2	Unit rotation Pendulum excitation	23
2.7.3	Unit acceleration base excitation	26
2.7.4	Harmonic base excitation	27
2.7.5	Stationary random base excitation	36
2.8	References	41
3	ANALYSIS OF THE HYBRID BELL-TOWER SYSTEM	43
3.1	Introduction	43
3.2	Generalized Multi-Degree-Of-Freedom (MDOF) system	43
3.2.1	Equilibration using energy principle	45
3.2.2	Equations of motion	46
3.3	Modal analysis of the BT	50
3.3.1	Eigenfrequencies and mode shapes	50
3.3.2	BT mode shapes and frequencies	53
3.3.3	Uncoupled equations of motion	56
3.4	Vibration analysis of the BT	56
3.5	Simulink controller of the BT	58
3.6	Numerical example for the BT	59
3.7	Analysis of the hybrid BT example	60
3.7.1	Unit acceleration base excitation	60
3.7.2	Harmonic support excitation	62
3.7.3	Stationary random base excitation	69
3.8	References	74
4	DYNAMIC BELL SWINGING ACTIONS IN THE BELL-TOWER	75
4.1	Introduction	75

4.2	Dynamic reactions by bell ringing	75
4.2.1	Secondary resonance of the pendulum	76
4.2.2	Forced introduced by bell ringing	78
4.3	Description of the BT	79
4.4	Analysis of the BT	80
4.4.1	Numerical modeling	81
4.5	Analysis of the BT example	83
4.5.1	Free oscillation	83
4.5.2	Harmonic external moment excitation	85
4.6	Nonstationary vibration in the BT	94
4.7	References	97
5	TOWER WITH PENDULUM TUNED MASS DAMPER SYSTEM	99
5.1	Introduction	99
5.2	An introductory sample of pendulum absorber	100
5.3	Generalized MDOF system with PTMD	101
5.4	The tower by nonlinear PTMD	109
5.4.1	Time-Harmonic excitation	110
5.4.2	Fundamental statistical parameters	114
5.4.3	Stationary random excitation	115
5.4.4	Bam strong ground motion	119
5.4.5	Earthquake excitation	121
5.4.6	Optimal location of PTMD	124
5.5	References	127
6	DYNAMIC ACTIONS OF PENDULUM AND FORCE CALCULATIONS	128
6.1	Introduction	128
6.2	Dynamic analysis via substructure method	128
6.3	Numerical example	131
6.4	Pendulum dynamic actions	135
6.5	Quasi-static analysis of the BT	139
6.6	BT forces induced by dynamic excitation	143
6.7	References	152
7	ACTIVE CONTROL IN THE BT	153
7.1	Introduction	153
7.2	Active Pendulum Tuned Mass Damper (APTMD)	153
7.3	BT with Active Pendulum Mass Damper (APMD)	154
7.4	The optimal state feedback control	156
7.5	Numerical analysis	158
7.6	References	162

8	CONCLUDING REMARKS	163
---	--------------------	-----

APPENDIXES		
A.	FUNDAMENTALS OF STRUCTURAL OSSILATIONS	166

A.1	Formulation of the equations of motion	166
A.1.1	Direct Equilibration Using d'Alembert's Principle	166
A.1.2	Principle of Virtual Displacements	167
A.1.3	Hamilton's Principle	168
A.1.4	Lagrange's equations of motion	169
A.2	Linear Single Degree of Freedom (SDOF) systems	171
A.2.1	Free Vibration	171
A.2.2	Forced vibration	173
A.3	Reference	175
B.	VIBRATION OF A SIMPLE PENDULUM	176

B.1	Nonlinear vibration of the simple pendulum	176
B.2	References	180
C.	NUMERICAL ANALYSIS OF NONLINEAR RESPONSE	181

C.1	Incremental formulation of nonlinear system	181
C.2	Step-by-Step integration	182
C.3	References	183
REFERENCES		184

1

MECHANICAL MODEL OF A BELL-TOWER

1.1 Description of Bell-Tower like structures

A Bell-Tower (BT) can be considered as a structure consisting of two substructures, namely the tower and the bell. Figure (1-1) shows a Bell-Tower system, where the bell ringing action is modeled as a simple pendulum.

The pendulum is suspended near the tower's upper part by a hinge bearing. The mechanical model of a tower is represented by a continuous structure and is idealized as a Multi-Degree-Of-Freedom (MDOF) system. Furthermore, the pendulum can be modeled as a tuned mass damper to improve the response of the entire structure under dynamic loads.

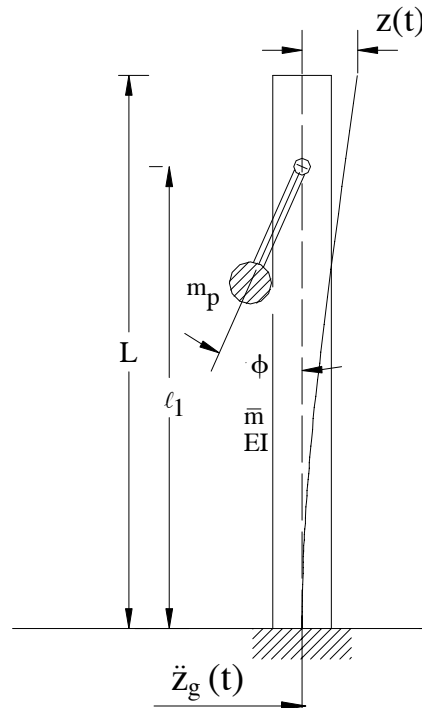


Figure 1-1 Mechanical model of a Bell-Tower (BT)

1.2 Examples of existing pendulum tuned mass dampers

Typical examples of pendulum-type dampers can be found in the Crystal-Tower located in Osaka of Japan, which is 157m high. A Pendulum Tuned Mass Damper (PTMD) was included to decrease the wind induced motion of the building by 50%. In this tower six, of the nine air cooling and heating ice thermal storage tanks are hanged from the top roof girders, which are used as a pendulum masses. Four tanks slide in the north-south direction, and the other two tanks slide in the east-west direction. Oil dampers connected to the pendulum are designed for dissipating the pendulum energy. A view of this building is illustrated in Figure (1-2).



Figure 1-2 Crystal Tower in Osaka of Japan

The skyscraper Taipei-101 in Taiwan is one the world tallest buildings with the height of 508m and 101 floors above ground, Figure (1-3). Since both earthquake and wind are important load cases in Taiwan, the designer of the building has taken extra precautions. A 660 ton PTMD is considered to reduce the oscillations of the main building and two further TMDs are especially designed for the pinnacle. The PTMD has a large spherical shape hanging as a simple pendulum, as shown in Figure (1-4), and it is visible to the public on the 88th and 89th stories, where a restaurant is situated in this part. When the building begins to sway either due to wind or an earthquake, the damper activates a restoring force. The Taipei-101 is built to withstand an earthquake of magnitude greater than 7 on the Richter scale.



Figure 1-3 Taipei-101 Tower



Figure 1-4 Taipei-101 Building PTMD

The AMP Sydney Tower, the tallest building in Australia, with 250m height and the base of the structure anchored to the roof of a 15-storey building. This tower stands 305m above the street level. The tower is one of the first buildings with the installation of a large-scale PTMD. The doughnut-shaped water tank near the top of the turret, which normally serves as the tower's water and fire protection supply, is incorporated into the design of the PTMD to reduce the wind-induced motions. The energy associated with relative movements between the tower and the water tank is dissipated by 8 shock-absorbers installed tangentially to the tank and anchored to the floor of the turret. A secondary PTMD of similar design was later installed on the intermediate anchorage ring to further increase the damping level, particularly in the second mode. A view of this tower is shown in Figure (1-5).

The Chifley Tower in Sydney of Australia represents one of the most advanced commercial office developments in this country with 209m height and 42 floors. The building is an all-steel structure including drywall core construction. A steel PTMD of 400 tons at the top of the tower is used to minimize the movement of the building, Figure (1-6).



Figure 1-5 AMP Tower in Sydney of Australia

Sydney has two towers with PTMD built into their structures; namely AMP Tower and Chifley Tower. Both are passive dampers. The damper in Chifley Tower is the largest damper of its type in the world.



Figure 1-6 Chifley Tower in Sydney of Australia

There are many Bell-Towers in Europe with different systems of bell ringing. The dynamic action caused by bell swinging is the characteristic aspect in Bell-Towers and the response of the building against wind and earthquake with respect to dynamic and seismic loading is a significant importance. In order to preserve the architectural heritage, the retrofit of this kind of structures is of vital importance. Figure (1-7) shows the view of a real Bell-Tower which is located at Schlossberg in Graz of Austria.



Figure 1-7 A Bell-Tower in Graz, Austria

In the present research, BT like structures are studied under dynamic loading, and in particular against earthquake excitation. Numerical studies for free and forced vibrations are performed by means of computer simulations. As a first step, the complete structure is modeled by a Two-Degree-Of-Freedom (2DOF) system “pendulum and sliding mass”, in order to give insight into its complex nonlinear dynamic behavior.

In the subsequent chapters both linear and nonlinear behavior of the system “Bell Structure and Pendulum” are studied. After applying appropriate analytical methods, parametric studies for forced and free vibration are performed by means of computer simulations. The nonlinear dynamic analysis of the forced vibrations are chosen in time domain by using numerical investigation, with emphasize on the

nonlinear interaction between the excited tower and movement of the bell, which mechanically behaves like a rigid pendulum. The dynamic actions caused by swinging of a bell, as the characteristic aspect in bell towers, are considered. Moreover the response of the building against earthquake is estimated with respect to seismic design criteria. This particular study gives an important insight into the complex dynamic behavior of the BT like structures. By interpreting pendulum as a passive absorber in the tower, it is intended to achieve a large decrease of damages in the main tower structures. Dynamic analysis by means of substructure method is introduced, and finally the active control in the BT is discussed.

1.3 References

1. Ziegler F., 'Mechanics of Solids and Fluids', Second edition, Technical University Vienna, Springer-Verlag, New York-Vienna, 1998.
2. Clough R.W., Penzien J., Department of Civil Engineering, University of California, 'Dynamic of Structures', McGraw-Hill, 1989.
3. Chopra A.K., University of California at Berkeley, 'Dynamics of Structures', second edition, Prentice Hall, 2001.
4. Haskett T., Breukelman B., Robinson J., Kottelenberg J., 'Tuned mass dampers under excessive structural excitation', Monitoring Inc, Guelph, Ontario, Canada.
5. EERC, structures with TMDs, <http://nisee.berkeley.edu/>.
6. Wikipedia, The Free Encyclopedia, <http://en.wikipedia.org>.
7. Civil Engineering Database, <http://pubs.asce.org>.

2

DYNAMIC ANALYSIS OF A TWO-DEGREE-OF-FREEDOM SYSTEM

2.1 Introduction

In this chapter, the mechanical model of a 2DOF system “pendulum and sliding mass” and the formulation of the corresponding equations of motion based on direct dynamic equilibrium equations, and the Lagrange equations are presented. The fundamentals for structural oscillations of a Single-Degree-Of-Freedom (SDOF) system are summarized in Appendix A.

The geometrically nonlinear phenomenon corresponding to a simple pendulum combined with a linear SDOF system is introduced. A suitable analytical method is described and comparison is made between the responses obtained from an analytical method and a numerical approach. Numerical analysis of nonlinear response is evaluated by means of computer simulations using the Matlab7 software. Furthermore, the response of the BT due to various load cases is found and a parameteric study is performed.

2.2 Equations of motion¹

The system of a rigid pendulum with mass m , radius of gyration i_s and a sliding mass m_1 , as it shown in Figure (2-1), has two degrees of freedom. According to the Lagrange formulation, described in Appendix A, the equations of motion are derived.

¹ Reference [1]

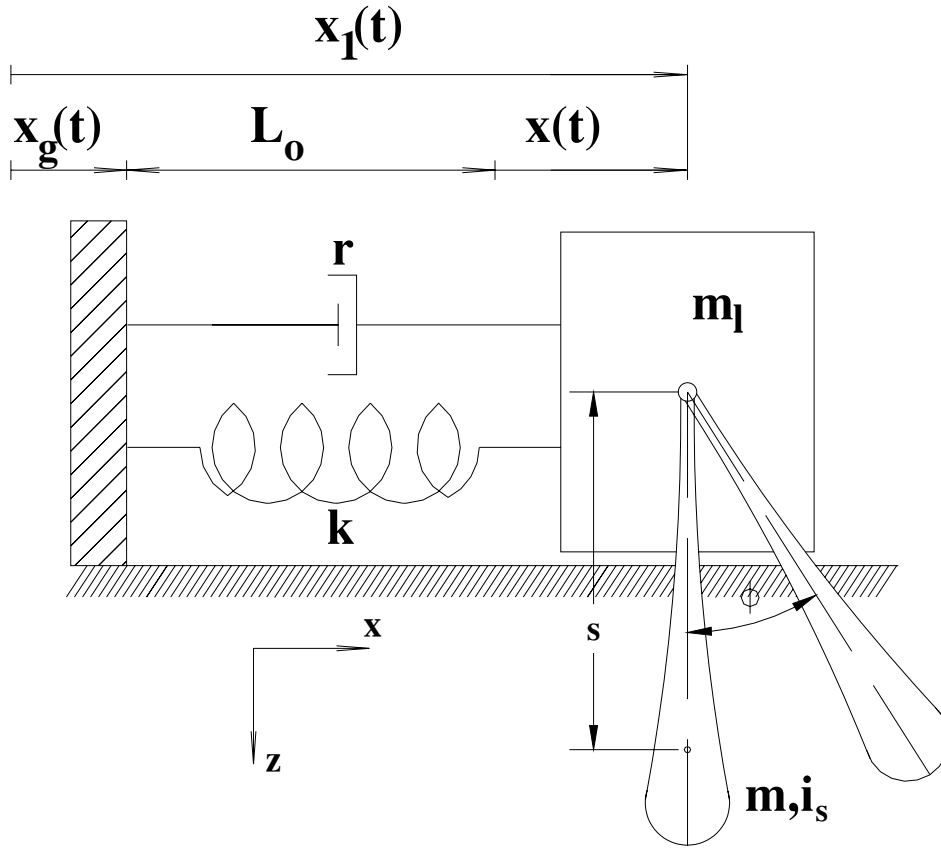


Figure 2-1 Pendulum with moving support

The generalized coordinates are selected as $q_1 = x$ and $q_2 = \phi$. The Cartesian coordinates of the centroid of the pendulum are geometrically related to the generalized coordinates by $x_s = x_1 + (s \sin \phi)$, $z_s = s \cos \phi$.

The square of the total velocity of the pendulum's centroid is

$$v_s^2 = \dot{x}_s^2 + \dot{z}_s^2 = \dot{x}_1^2 + (s\dot{\phi})^2 + 2s\dot{x}_1\dot{\phi}\cos\phi \quad (2-1)$$

$$x_1(t) = x(t) + L_0 + x_g(t) \Rightarrow \dot{x}_1 = \dot{x} + \dot{x}_g \quad (2-2)$$

where $x_g(t)$ represents a given support motion, and L_0 denotes the length of the unextended spring.

The total Kinetic energy is expressed as

$$\begin{aligned}
T &= \frac{1}{2} m_1 \dot{x}_1^2 + \frac{1}{2} m v_s^2 + \frac{1}{2} I_s \dot{\phi}^2 \\
&= \frac{1}{2} m_1 (\dot{x} + \dot{x}_g)^2 + \frac{1}{2} m v_s^2 + \frac{1}{2} I_s \dot{\phi}^2 \\
&= \frac{1}{2} m_1 (\dot{x}^2 + \dot{x}_g^2 + 2\dot{x}\dot{x}_g) + \frac{1}{2} m [(\dot{x} + \dot{x}_g)^2 + (s\dot{\phi})^2 + 2s(\dot{x} + \dot{x}_g)\dot{\phi}\cos\phi] + \frac{1}{2} I_s \dot{\phi}^2
\end{aligned} \tag{2-3}$$

where $I_s = m i_s^2$ stands for the moment of inertia of the rotating pendulum.

Differentiation of the kinetic energy leads to

$$\begin{aligned}
\frac{\partial T}{\partial \dot{x}} &= m_1 \dot{x} + m_1 \dot{x}_g + m \dot{x} + m \dot{x}_g + m s \dot{\phi} \cos \phi \\
&= (m_1 + m) \dot{x} + (m_1 + m) \dot{x}_g + s m \dot{\phi} \cos \phi
\end{aligned} \tag{2-4}$$

$$\frac{\partial T}{\partial \dot{\phi}} = m (s^2 + i_s^2) \dot{\phi} + m s (\dot{x} + \dot{x}_g) \cos \phi \tag{2-5}$$

$$\frac{\partial T}{\partial x} = 0 \tag{2-6}$$

$$\frac{\partial T}{\partial \phi} = -m s (\dot{x} + \dot{x}_g) \dot{\phi} \sin \phi \tag{2-7}$$

and further

$$\frac{d}{dt} \left(\frac{\partial T}{\partial \dot{x}} \right) = (m + m_1) \ddot{x} + (m + m_1) \ddot{x}_g + m (s \ddot{\phi} \cos \phi - s \dot{\phi}^2 \sin \phi) \tag{2-8}$$

$$\frac{d}{dt} \left(\frac{\partial T}{\partial \dot{\phi}} \right) = m (s^2 + i_s^2) \ddot{\phi} + m s (\ddot{x} \cos \phi - \dot{x} \dot{\phi} \sin \phi) + m s (\ddot{x}_g \cos \phi - \dot{x}_g \dot{\phi} \sin \phi) \tag{2-9}$$

The potential energy of the entire system is expressed as

$$V = -m g s \cos \phi + \frac{1}{2} k x^2 \tag{2-10}$$

and its derivatives become

$$\frac{\partial V}{\partial x} = kx \quad (2-11)$$

$$\frac{\partial V}{\partial \phi} = mgs \sin \phi \quad (2-12)$$

Substituting Equations (2-6), (2-7), (2-8), (2-9), (2-11) and (2-12) in Lagrange equations of motion (see Appendix A), one obtains

$$\frac{d}{dt} \left(\frac{\partial T}{\partial \dot{q}_i} \right) - \frac{\partial T}{\partial q_i} + \frac{\partial V}{\partial q_i} = Q_i \quad (2-13)$$

and two terms of generalized forces are

$$Q_1 = -r\dot{x} \quad (2-14)$$

$$Q_2 = 0 \quad (2-15)$$

leading to two coupled nonlinear equations

$$(m + m_1)\ddot{x} + r\dot{x} + kx + ms\ddot{\phi} \cos \phi - ms\dot{\phi}^2 \sin \phi = -(m + m_1)\ddot{x}_g \quad (2-16)$$

and

$$m(s^2 + i_s^2)\ddot{\phi} + ms \cos \phi \ddot{x} + mgs \sin \phi = -ms \cos \phi \ddot{x}_g \quad (2-17)$$

In the subsequent section linear and nonlinear behavior of this 2DOF system “Bell-Tower and pendulum” will be discussed

2.3 Linear analysis

By means of geometrical linearization about the equilibrium position²($\phi=0$), $\phi = \sin \phi$, $\cos \phi = 1$, and neglecting higher order terms of ϕ and its derivative, the dynamic equations of motion reduce to the linear system

$$(m_1 + m)\ddot{x} + r\dot{x} + kx + ms\ddot{\phi} = -(m_1 + m)\ddot{x}_g \quad (2-18)$$

$$(s^2 + i_s^2)\ddot{\phi} + gs\phi + s\ddot{x} = -s\ddot{x}_g \quad (2-19)$$

By replacing $\ell = \frac{s^2 + i_s^2}{s}$, Equation (2-19) can be expressed as

$$\ell\ddot{\phi} + g\phi + \ddot{x} = -\ddot{x}_g \quad (2-20)$$

In a matrix form, the complete set of relationship may be written as

$$\underset{\sim}{m}\ddot{\underset{\sim}{x}} + \underset{\sim}{r}\dot{\underset{\sim}{x}} + \underset{\sim}{k}\underset{\sim}{x} = -\underset{\sim}{m}\ddot{\underset{\sim}{x}}_g \quad (2-21)$$

where

$$\underset{\sim}{m} = \begin{bmatrix} m_1 + m & ms \\ 1 & \ell \end{bmatrix}, \underset{\sim}{r} = \begin{bmatrix} r & 0 \\ 0 & 0 \end{bmatrix}, \underset{\sim}{k} = \begin{bmatrix} k & 0 \\ 0 & g \end{bmatrix}$$

$$\underset{\sim}{x} = \begin{bmatrix} x \\ \phi \end{bmatrix}, \ddot{\underset{\sim}{x}}_g = \begin{bmatrix} \ddot{x}_g \\ 0 \end{bmatrix} \quad (2-23)$$

Considering a time-harmonic support excitation, $x_g = X_g e^{i\omega t}$, after decay of the transient effect, the steady-state response is of the following form

$$x = X e^{i\omega t}$$

$$\phi = \Phi e^{i\omega t} \quad (2-23)$$

where X and Φ stand for the unknown amplitude functions. Equation (2-21) is transferred to the frequency domain as

² Reference [1]

$$(-\nu^2 \tilde{m} + i \nu \tilde{r} + k) \begin{bmatrix} X \\ \Phi \end{bmatrix} = \nu^2 \tilde{m} \begin{bmatrix} X_g \\ 0 \end{bmatrix} \quad (2-24)$$

$$\begin{bmatrix} -\nu^2(m_1 + m) + i \nu r + k & -\nu^2 m s \\ -\nu^2 & g - \nu^2 \ell \end{bmatrix} \begin{bmatrix} X \\ \Phi \end{bmatrix} = \begin{bmatrix} \nu^2(m_1 + m) \\ \nu^2 \end{bmatrix} X_g \quad (2-25)$$

where the frequency response functions $X(\nu)$ and $\Phi(\nu)$ are the complex solutions of the linear system of equations (2-25). These are found in a closed form by using the software Matlab7

$$X = \frac{-X_g \nu^2 (m_1 g - \nu^2 m_1 \ell + m g - \nu^2 m \ell + \nu^2 m s)}{(\nu^2 m_1 g - \nu^4 m_1 \ell + \nu^2 m g - \nu^4 m \ell - i \nu r g + i \nu^3 r \ell - k g + k \ell \nu^2 + \nu^4 m s)} \quad (2-26)$$

$$\Phi = \frac{-\nu^2 X_g (i \nu r + k)}{(\nu^2 m_1 g - \nu^4 m_1 \ell + \nu^2 m g - \nu^4 m \ell - i \nu r g + i \nu^3 r \ell - k g + k \ell \nu^2 + \nu^4 m s)} \quad (2-27)$$

The two natural frequencies follow approximately from the homogeneous undamped system of equations

$$\begin{bmatrix} -\nu^2(m_1 + m) + k & -\nu^2 m s \\ -\nu^2 & g - \nu^2 \ell \end{bmatrix} \begin{bmatrix} X \\ \Phi \end{bmatrix} = \begin{bmatrix} 0 \\ 0 \end{bmatrix} \quad (2-28)$$

Setting the coefficient determinant to zero

$$(g - \nu^2 \ell)(-\nu^2 m_T + k) - \nu^4 m s = 0 \quad (2-29)$$

and using $m_T = m_1 + m$ leads to the frequency equation

$$(\ell m_T - m s) \nu^4 - (k \ell + m_T g) \nu^2 + k g = 0 \quad (2-30)$$

for the unknown eigenfrequencies ν_1, ν_2 .

2.4 Numerical example for the linear system

In order to discuss numerical results of the mechanical model, the magnitudes of the parameters of the system shown in Figure (2-1) are considered as follows

$$m_1 = 5 \text{ kg}, m = 1 \text{ kg}, r = 10 \frac{N \cdot s}{m}, k = 200 \frac{N}{m}, g = 9.81 \frac{m}{s^2}, s = 1 \text{ m}$$

$$i_s = \frac{1}{\sqrt{5}} \text{ m} \text{ and } \ell = 1.20 \text{ m} \quad (2-31)$$

Considering the numerical assumption of Equation (2-31) and substituting in Equation (2-30) follows that

$$6.20\nu^4 - 298.86\nu^2 + 1962.00 = 0 \quad (2-32)$$

Computing the two roots

$$\nu_1^2 = 7.84 \left(\frac{rad}{sec} \right)^2 \quad (2-33)$$

$$\nu_2^2 = 40.33 \left(\frac{rad}{sec} \right)^2 \quad (2-34)$$

leads to the circular eigenfrequencies of the linear 2DOF system as

$$\nu_1 = 2.80 \frac{rad}{sec} \quad (2-35)$$

$$\nu_2 = 6.35 \frac{rad}{sec} \quad (2-36)$$

The coupled system has two modes of oscillation. One may compare the above calculated frequency to the pendulum-like mode, $\omega_p = \left(\frac{g}{\ell} \right)^{1/2}$, and spring-like mode,

$\omega_r = \left(\frac{k}{m_1} \right)^{1/2}$, as the linear natural frequencies of the subsystems

$$\omega_p = \sqrt{\frac{9.81}{1.20}} = 2.8591 \frac{rad}{sec} \quad (2-37)$$

$$\omega_r = \sqrt{\frac{200}{5}} = 6.3245 \frac{rad}{sec} \quad (2-38)$$

In the next step, the unit amplitude of excitation is considered $X_g = "1"$ for the inhomogeneous coupled system. The system of equations (2-25) is of simplified form as

$$(-\nu^2(m_1 + m) + i \nu r + k)X - \nu^2 m s \Phi = \nu^2(m_1 + m) \quad (2-39)$$

$$-\nu^2 X + (g - \nu^2 \ell)\Phi = \nu^2 \quad (2-40)$$

rendering the amplitude functions Φ and X .

Figures (2-2) and (2-3) show the variation of X (mass displacement) and Φ (pendulum rotation angle), in frequency domain, respectively.

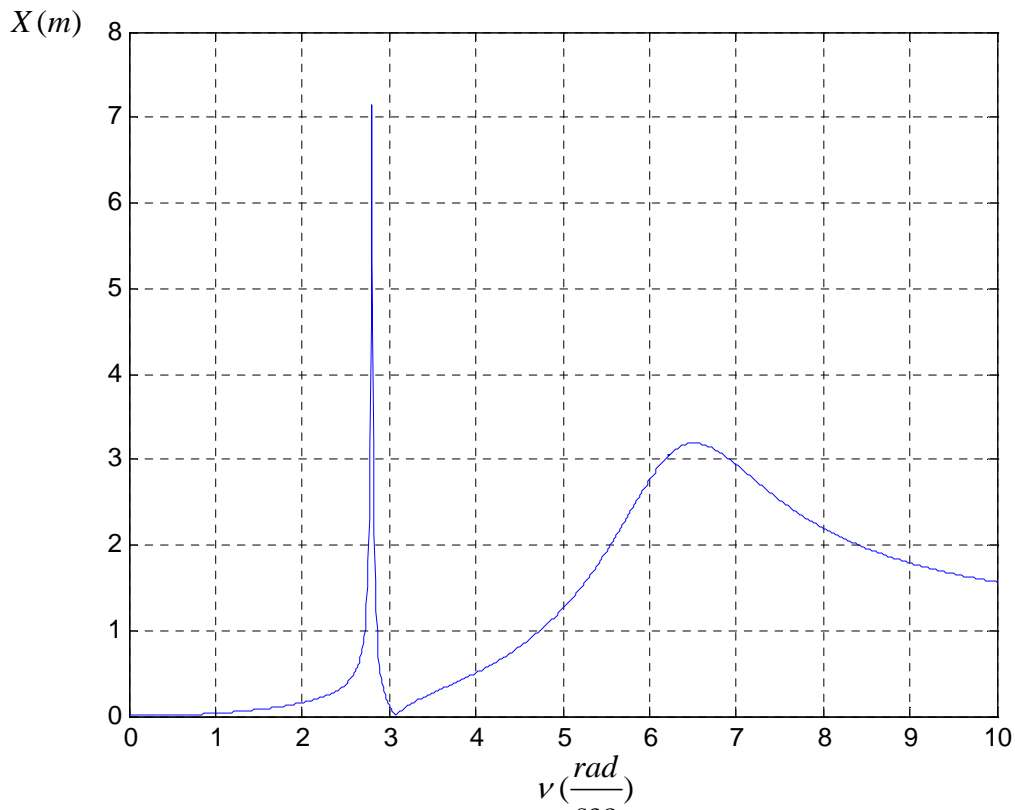


Figure 2-2 Mass displacement (X) versus frequency (ν)

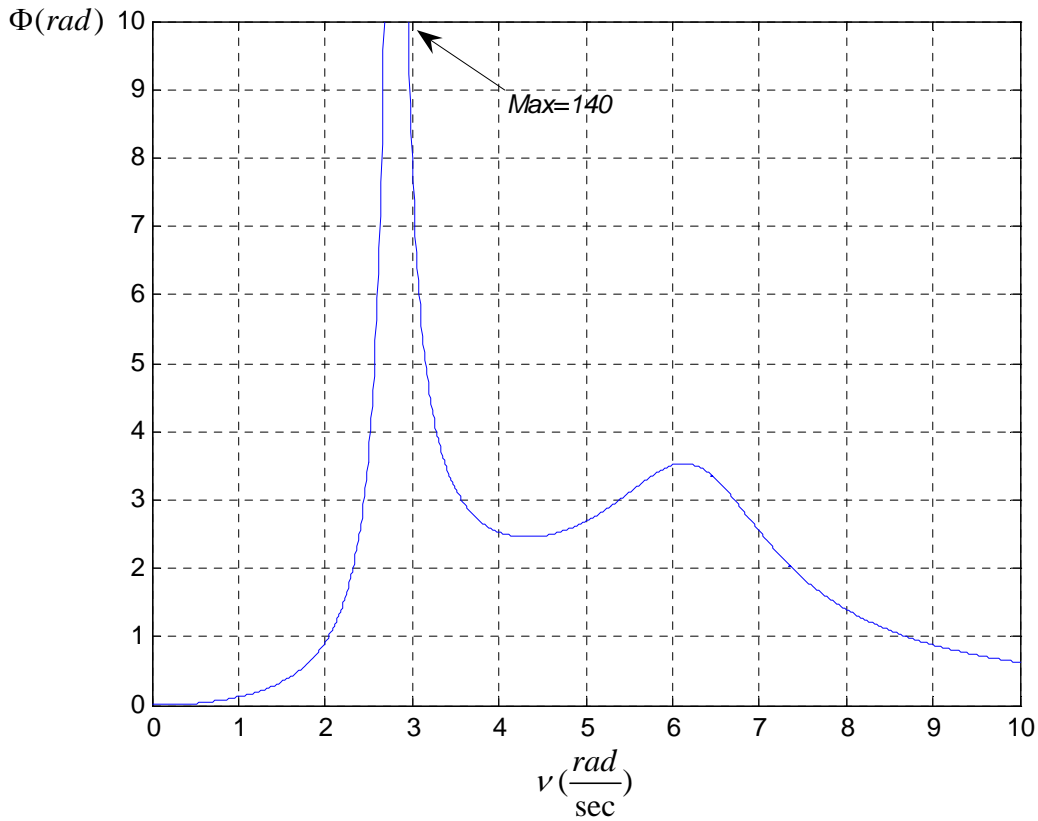


Figure 2-3 Pendulum deviation angle (Φ) versus frequency (ν)

2.5 Nonlinear vibrations of the simple pendulum

Considering a simple mathematical pendulum of a mass m attached to a hinged weightless rod of length ℓ , as shown in Figure (2-4), the corresponding equation of motion³ is obtained as

$$m \ell^2 \ddot{\phi} + m g \ell \sin \phi = 0$$

or

$$\ddot{\phi} + \omega^2 \sin \phi = 0 \quad (2-41)$$

where $\omega^2 = \frac{g}{\ell}$. The nonlinearity in this model is due to large rotation.

³ Reference [2]

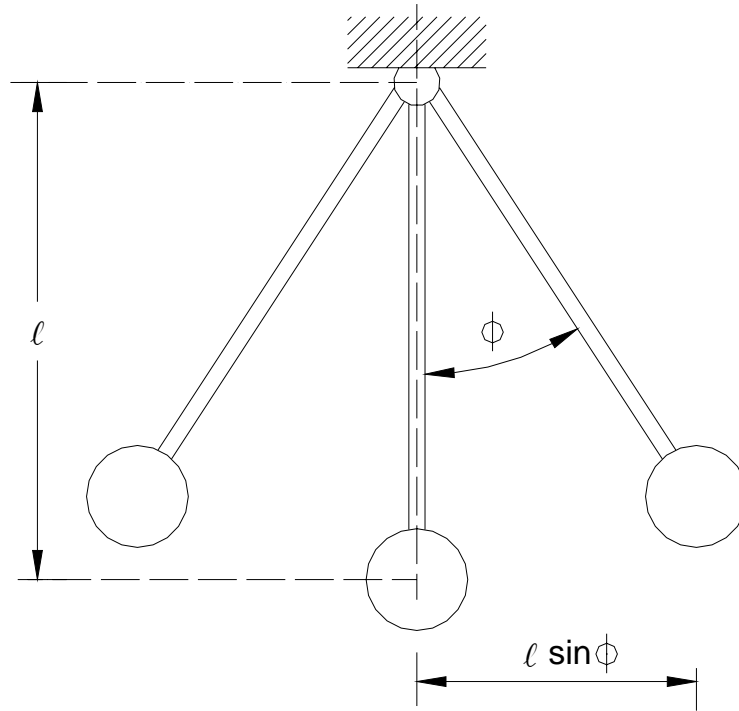


Figure 2-4 Simple pendulum

The analytical solution, renders the duration τ according to Equation (2-42), compare Appendix B. This is the standard form of the elliptic integral of the first kind and second order.

$$\tau = \frac{4}{\omega} \int_0^{\pi/2} \frac{d\theta}{\sqrt{1 - s^2 \sin^2 \theta}} = \frac{4}{\omega} F(s, \frac{\pi}{2}) \quad (2-42)$$

Numerical solution is obtained by using Simulink software, where a time step of 0.20 second is employed.

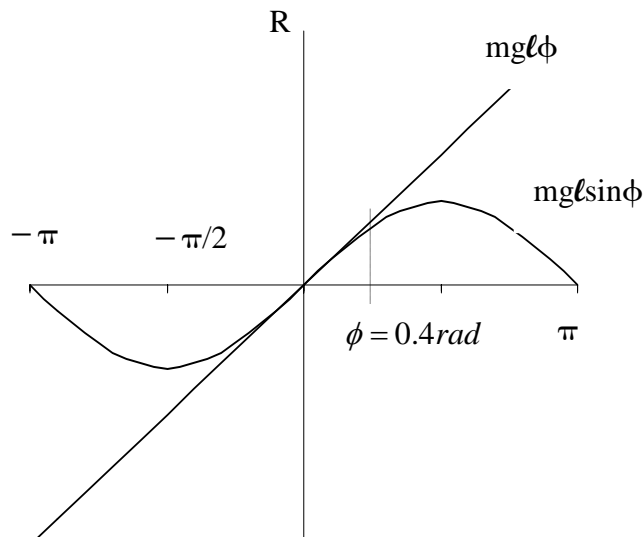
Table (2-1) shows that the ratio $\frac{T_N \text{ (Numerical)}}{T_A \text{ (Analytical)}}$ depends on ϕ (amplitude of rotation), and further discloses the accuracy limit of the numerical procedure.

Details of the analytical method for simple pendulum oscillation in linear and nonlinear conditions are provided in Appendix B.

$\phi[^\circ]$	0	10	20	30	40	50	60	70	80	90
$\frac{T_N}{T_A}$	1.000	1.000	0.9998	0.9995	0.9989	0.9960	0.9892	0.9820	0.9792	0.9650

Table (2-1) Comparison between the analytical and numerical solution

Within the range of $0 < \phi \leq 0.4 \text{ rad}$ it can be assumed that $\sin \phi \approx \phi$, thus a linearized analysis of natural frequency can be applied, see Figure (2-4a) for the restoring force.

**Figure 2-4a** Simple pendulum restoring force R in linear and nonlinear conditions

Computing the natural frequency $\omega = (\frac{g}{\ell})^{1/2}$ (in linear condition) and $\omega_N = \frac{2\pi}{T_N}$ (in nonlinear condition with $\phi = 0.4 \text{ rad}$) results in

$$\frac{|\omega_N^2 - \omega^2|}{\omega^2} \times 100 = 1.50\% \quad (2-43)$$

Figure (2-5) shows the variation of $\frac{\omega_N}{\omega}$ versus ϕ

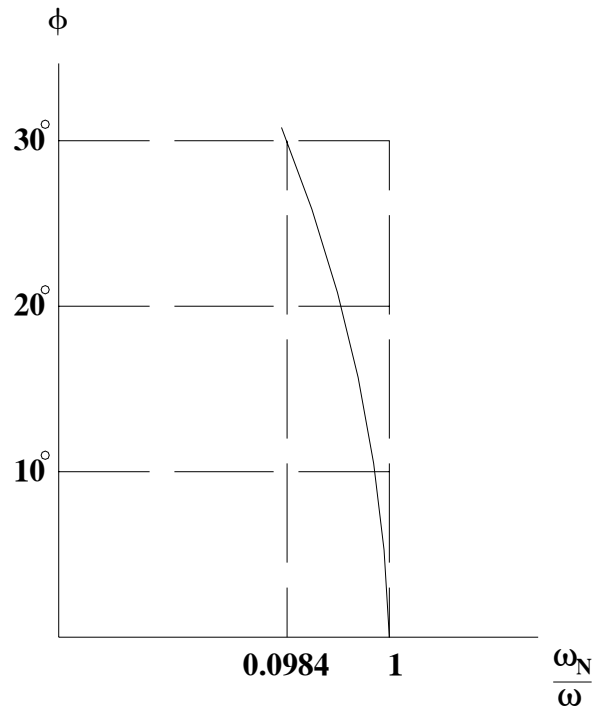


Figure 2-5 Variation of the ratio of nonlinear frequency versus linear frequency of a simple pendulum

2.6 Equations of motion of the coupled nonlinear system⁴

Considering the motion of a pendulum suspended of moving support as shown in Figure (2-1), the corresponding linear system exhibits two dominant modes of oscillation, namely a pendulum-like mode with the linear natural frequency

$\omega_p = (\frac{g}{\ell})^{1/2}$ and a spring-like (breathing) mode with the linear natural frequency

$$\omega_T = (\frac{k}{m_1})^{1/2}.$$

In the following, the nonlinear influence due to the motion of the pendulum is discussed. Combining the terms according to the Lagrange equations of motion and dividing through the coefficients of the highest order derivatives results in the nonlinear set of second-order differential equations, namely Equation (2-44) and Equation (2-45). For large motion of the pendulum one can not neglect the nonlinear terms.

⁴ Reference [4]

$$(m + m_1)\ddot{x} + r\dot{x} + kx + ms\ddot{\phi}\cos\phi - ms\dot{\phi}^2\sin\phi = -(m + m_1)\ddot{x}_g \quad (2-44)$$

$$\ell\ddot{\phi} + g\sin\phi + \cos\phi\ddot{x} = -\ddot{x}_g\cos\phi \quad (2-45)$$

$$\ell = s + \frac{i_s^2}{s} \quad (2-46)$$

2.7 Numerical examples for the nonlinear system

Numerical values for the two degrees of freedom system, shown in Figure (2-1), are assumed as follows

$$m_1 = 5 \text{ kg}, m = 1 \text{ kg}, r = 10 \frac{N s}{m}, k = 200 \frac{N}{m}, g = 9.81 \frac{m}{s^2}, s = 1 m$$

$$i_s = \frac{1}{\sqrt{5}} m \text{ and } \ell = 1.20 m \quad (2-47)$$

Thus Equation (2-44) and Equation (2-45) become

$$6\ddot{x} + 10\dot{x} + 200x + \ddot{\phi}\cos\phi - \dot{\phi}^2\sin\phi = -6\ddot{x}_g \quad (2-48)$$

$$1.20\ddot{\phi} + 9.81\sin\phi + \cos\phi\ddot{x} = -\ddot{x}_g\cos\phi \quad (2-49)$$

The equations of motion are solved in the time domain by Simulink and Matlab7 software computing $x, \phi, \dot{x}, \dot{\phi}$ at each time step Δt .

Procedure for the numerical nonlinear analysis, using a step-by-step method, can be found in Appendix C.

Here, the Simulink controller of the nonlinear system is discussed. Considering again Figure (2-1), the control parameters of this model are the displacement of moving support and the rotation angle of the pendulum.

Horizontal base acceleration applied to the mass of moving mass and pendulum, represents the input of this system. The pendulum is assumed to rotate without friction. Equations (2-48) and (2-49) represent motions of this system in each time step, where g is the acceleration due to gravity. Examining the equations of motion, one can notice that $\ddot{x}(t)$ and $\ddot{\phi}(t)$ appear in each equation. These can be interpreted as the output function of Simulink model with an algebraic loop.

The model consists of the input functions $x, \phi, \dot{x}, \dot{\phi}$. Figure (2-6) shows the Simulink model of the system.

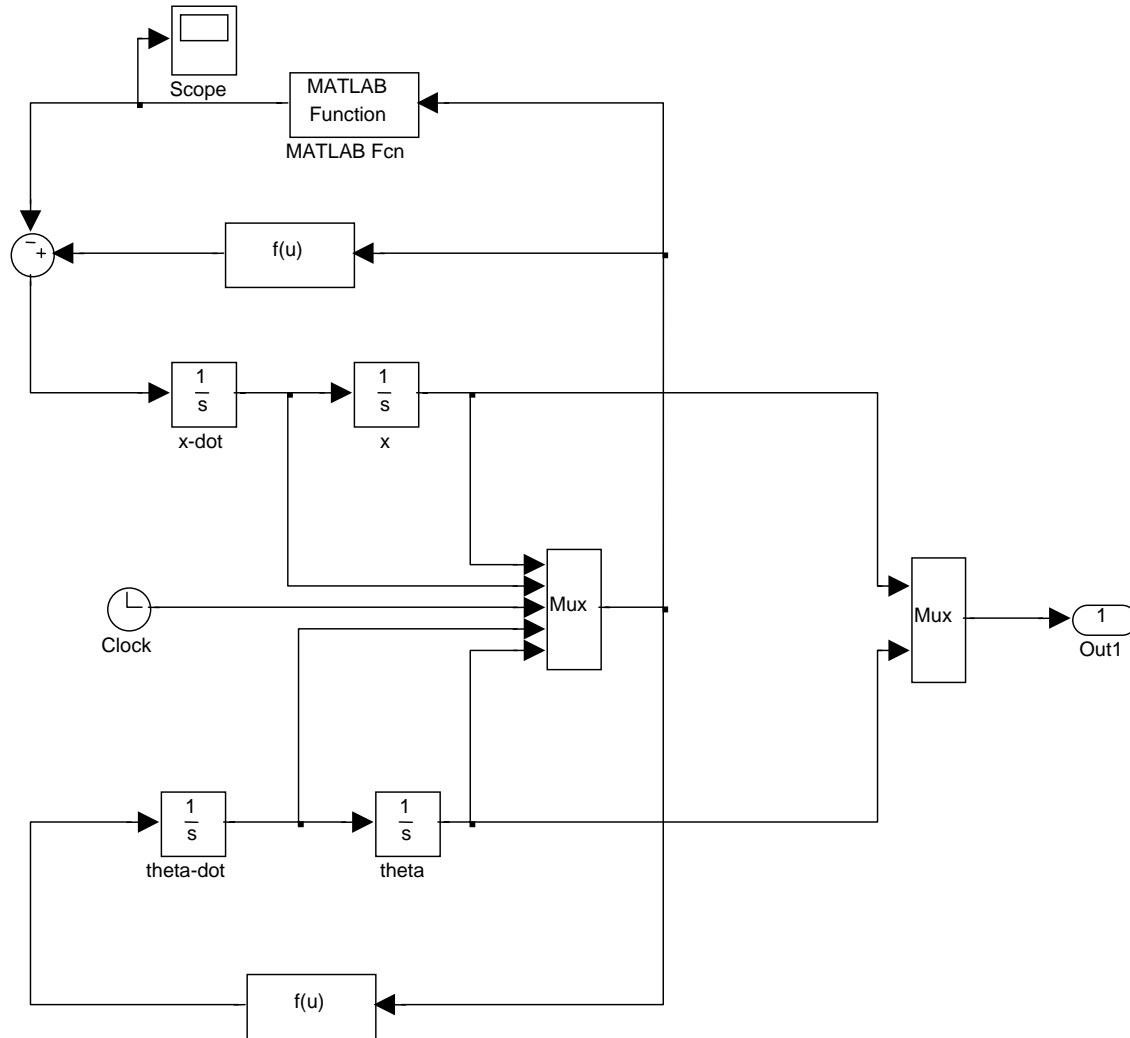


Figure 2-6 Simulink model of the nonlinear system

The equations of motion are computed using the above mentioned model. The system parameters are given in Equation (2-47) and excitation is introduced in the subsequent sections.

2.7.1 Unit displacement base

As shown in Figure (2-7), the undamped coupled system is excited by initial support excitation of Heaviside type⁵, $x_g(t) = x_0 H(t)$, $x_0 = 0.1 \text{ m}$, causing oscillation at both the pendulum and elastically supported mass around equilibrium position.

Figures (2-8a) and (2-8c) illustrate the displacement response of the moving mass and oscillation response of the pendulum. Figures (2-8b) and (2-8d) show the Fast Fourier transformation of both components of the system. Considering the time domain response of the 2DOF system, indicates that zero crossing for both displacements of the moving mass and oscillation of the pendulum occurs simultaneously. $\omega_1 = 2.78 \text{ rad/sec}$, $\omega_2 = 6.47 \text{ rad/sec}$ are resonance frequencies of the system which are very close to the values of the linear oscillation.

2.7.2 Unit rotation Pendulum excitation

As illustrated in Figure (2-9), the coupled system is excited by initial rotation of the pendulum, $t \geq 0$, $\phi(t) = \phi_0$, $\phi_0 = 10^\circ$.

Figures (2-10a) and (2-10c) indicate displacement of the moving mass and oscillation of the pendulum in the time domain. In Figures (2-10b) and (2-10d), the Fast Fourier transformations with regards to both the pendulum and the moving mass are illustrated.

Oscillations are in the neighborhood of $x_0 = 0$ and $\phi = 0$ position. Rotation angle of the pendulum and displacement of the moving mass decrease first slightly in time domain, and then bounded around equilibrium position where amplitude of oscillation tends to become zero by time decay. $\omega_1 = 2.78 \text{ rad/sec}$ (Resonance frequency of the system) shows a remarkable amplification in the response.

⁵ Reference [1]

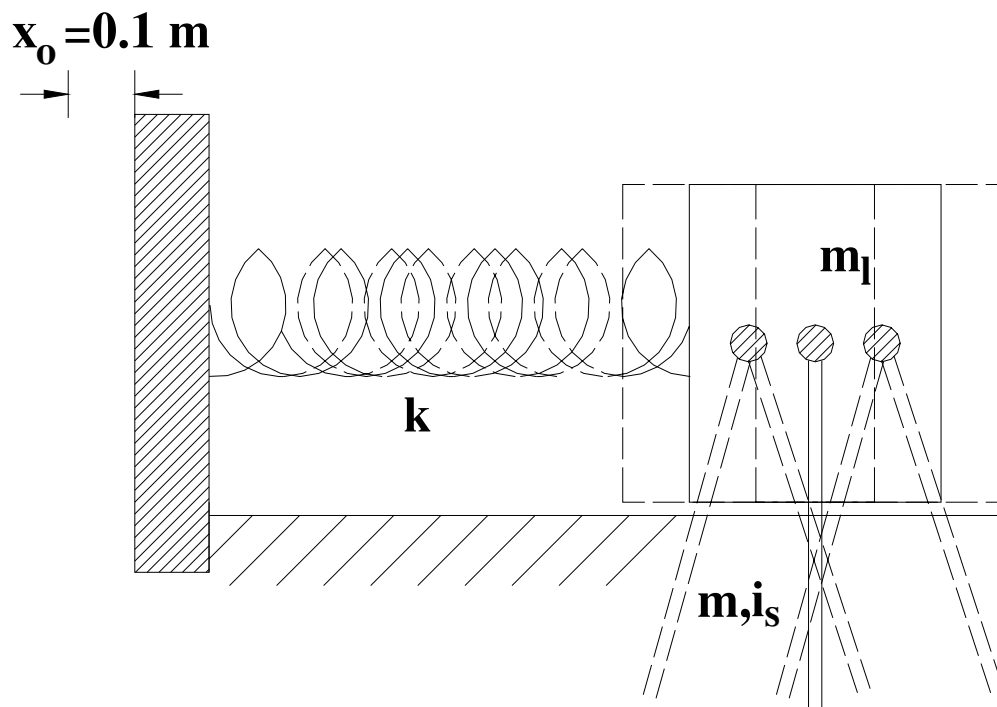


Figure 2-7 Base excitation

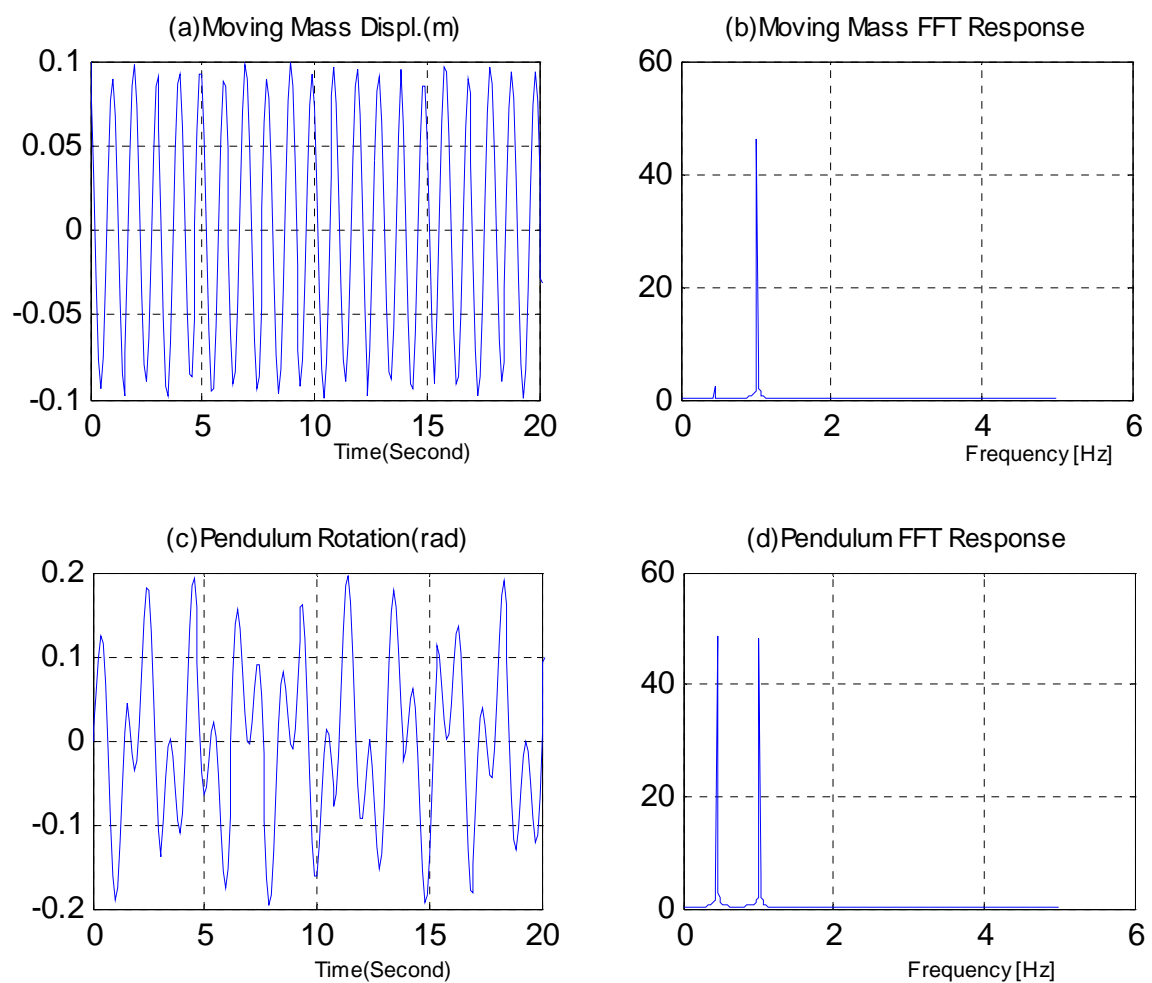
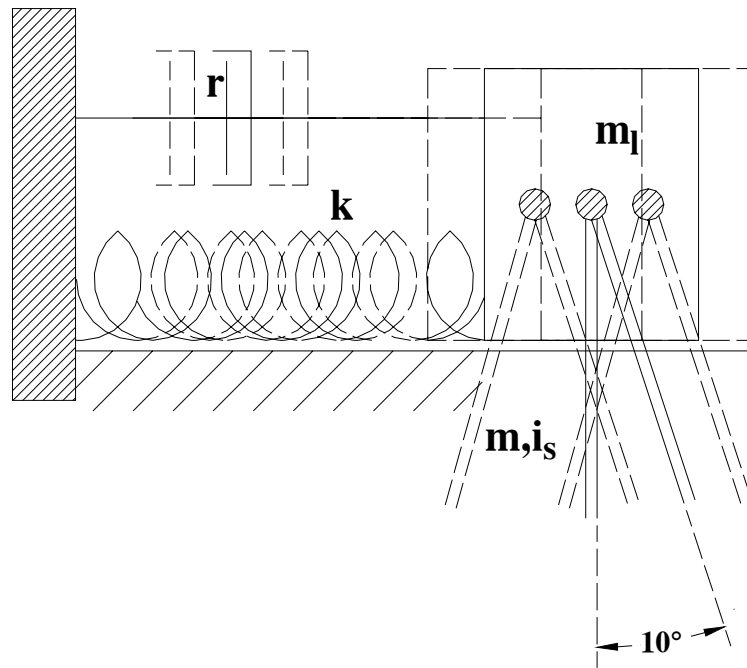
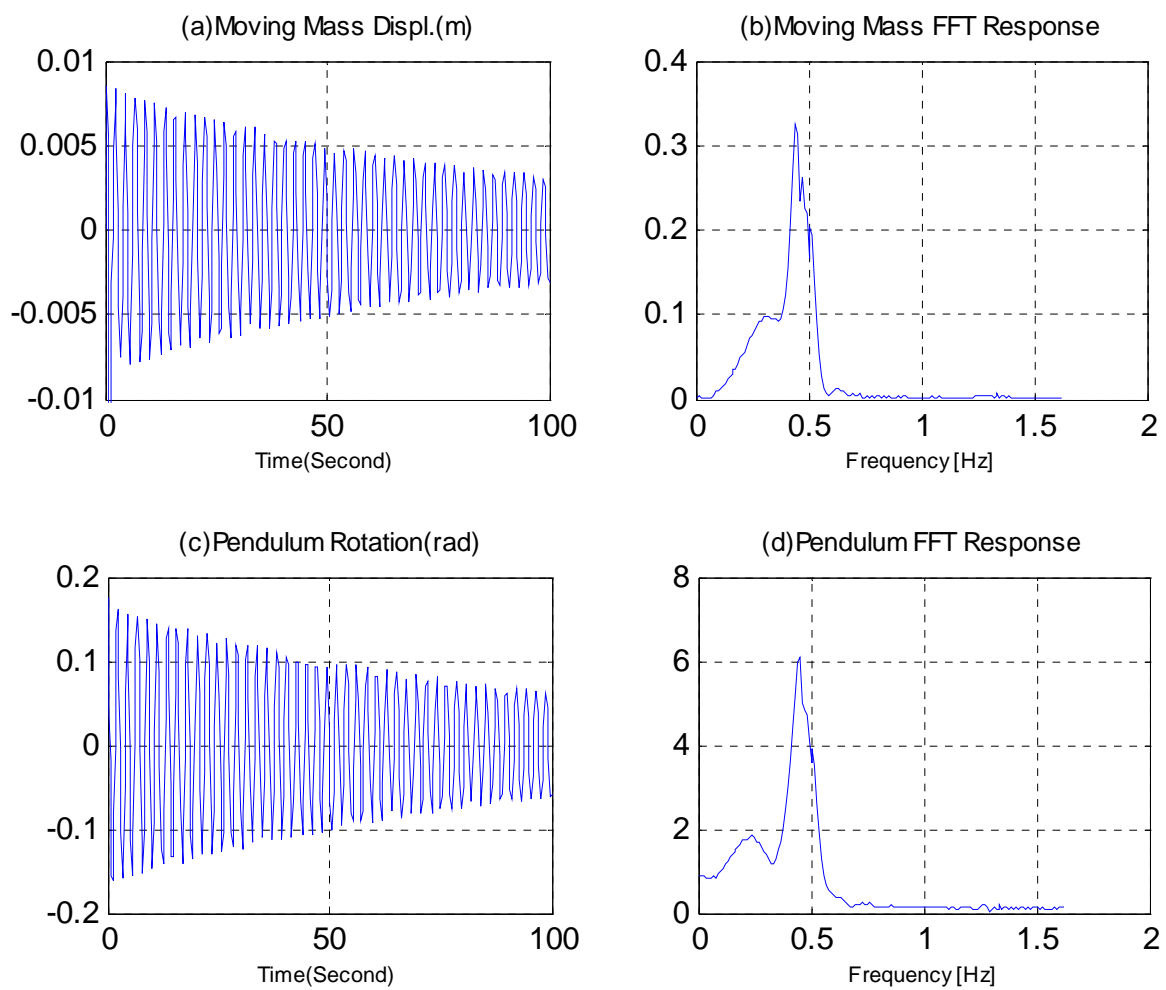


Figure 2-8 Time domain and FFT response

**Figure 2-9** Pendulum excitation**Figure 2-10** Time domain and FFT response

2.7.3 Unit acceleration base excitation

In this example, the coupled system is excited by a base excitation of the form $\ddot{x}_g(t) = 1.H(t)$, as it is shown in Figure (2-11).

Figures (2-12a) and (2-12c) illustrate the displacement of the moving mass and the rotation angle of the pendulum in time domain.

Likewise in Figures (2-12b) and (2-12d) Fast Fourier transformation in frequency domain with regards to both the pendulum and the moving mass are shown.

According to these figures, the rotation angle of the pendulum and displacement of the moving mass are decreased slightly and bounded in time domain. In contrast with models shown in Figures (2-7) and (2-8) Oscillations are not around equilibrium position and tend to become zero by time decay.

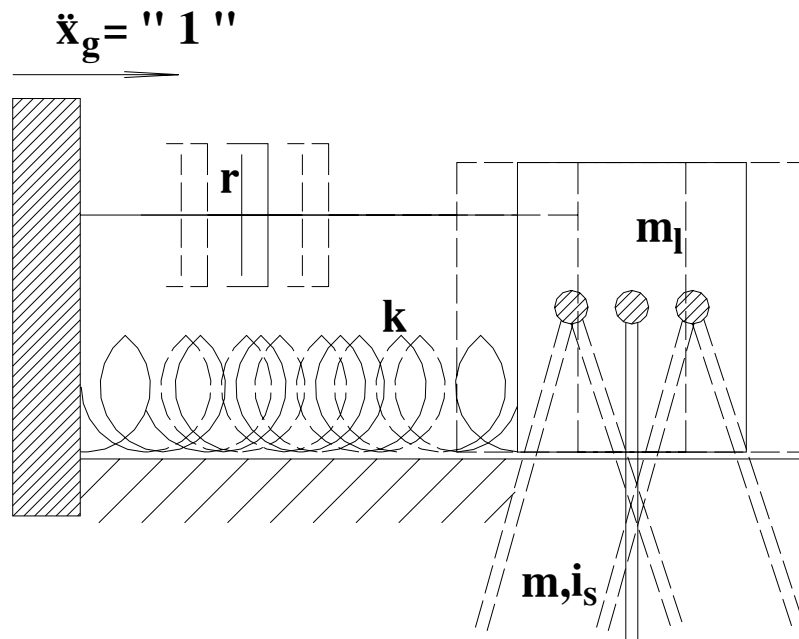


Figure 2-11 Base excitation by Heaviside step function

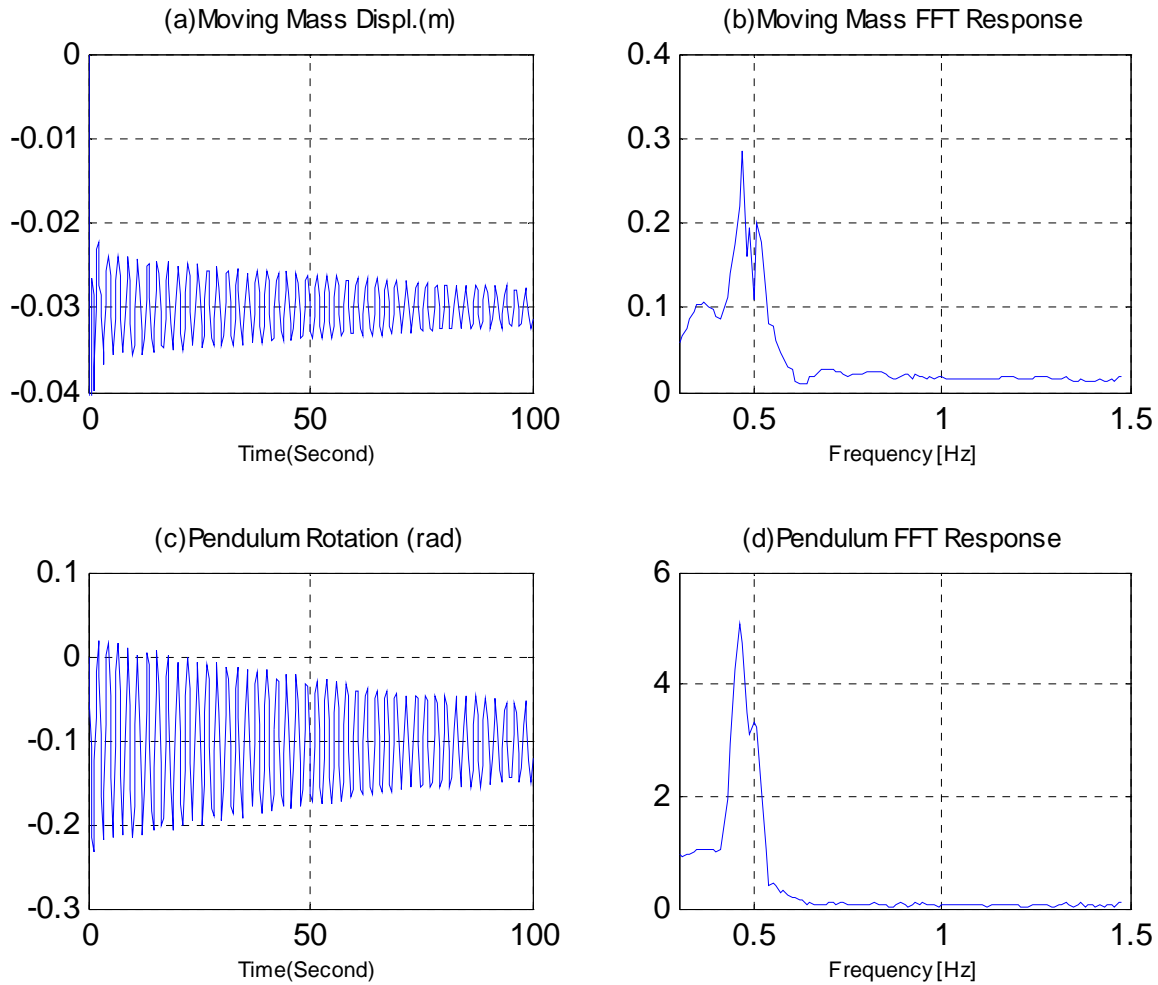
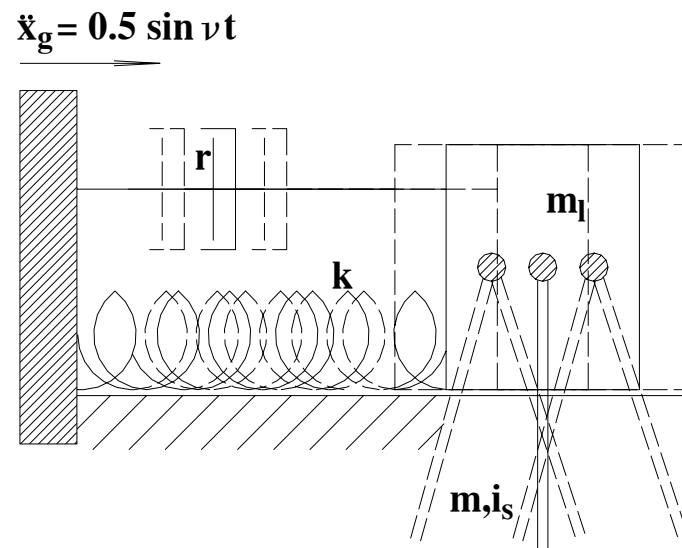
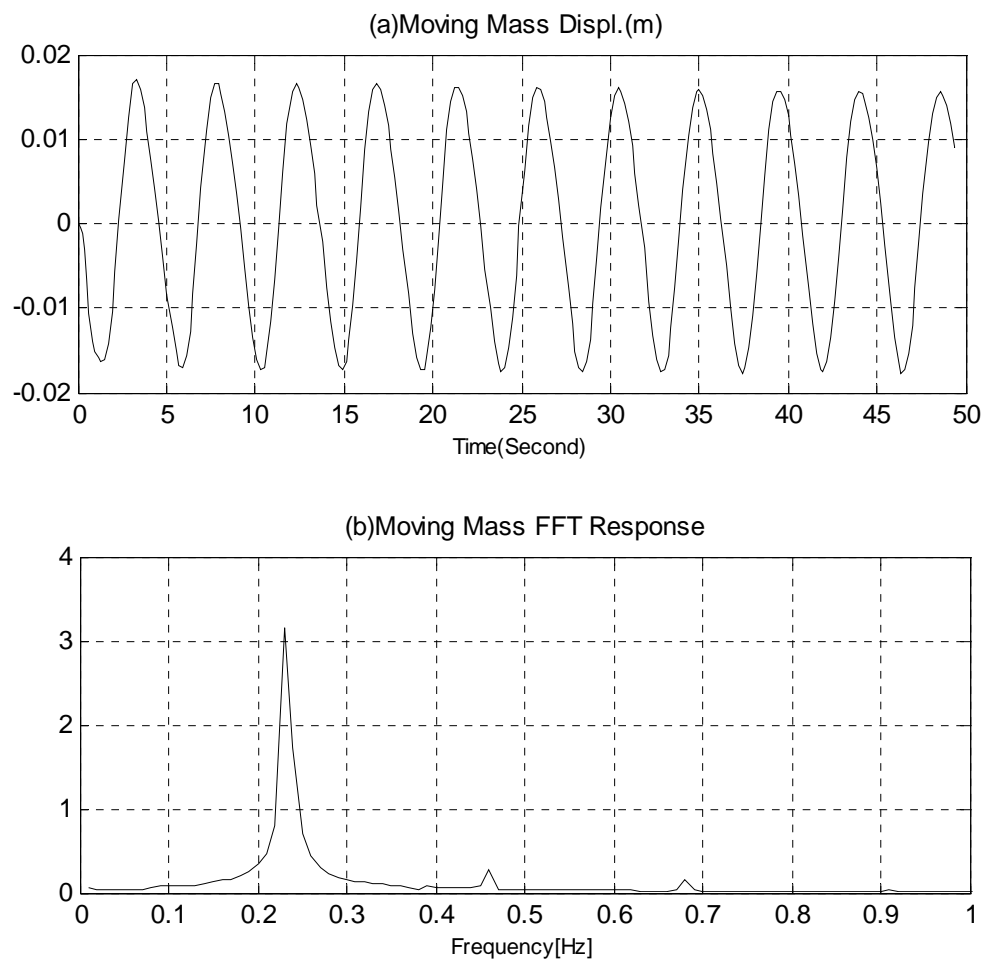


Figure 2-12 Time domain and FFT Response

2.7.4 Harmonic base excitation

The coupled system is excited by a harmonic support excitation $\ddot{x}_g = 0.5 \sin \nu t$ switched on at $t = 0$, as shown in Figure (2-13). The excitation frequency is chosen as $\nu = 1.39, 2.78, 5.56, 8.69 \text{ rad/sec}$. Figure (2-14) through Figure (2-21), indicate the response curve of displacement of the moving mass and rotation angle of the pendulum, as well as the Fast Fourier transformation response in frequency domain in the miscellaneous circumstances.

**Figure 2-13** Harmonic base excitation**Figure 2-14** Time domain and FFT response
 ν (frequency of excitation) = 1.39 rad/sec

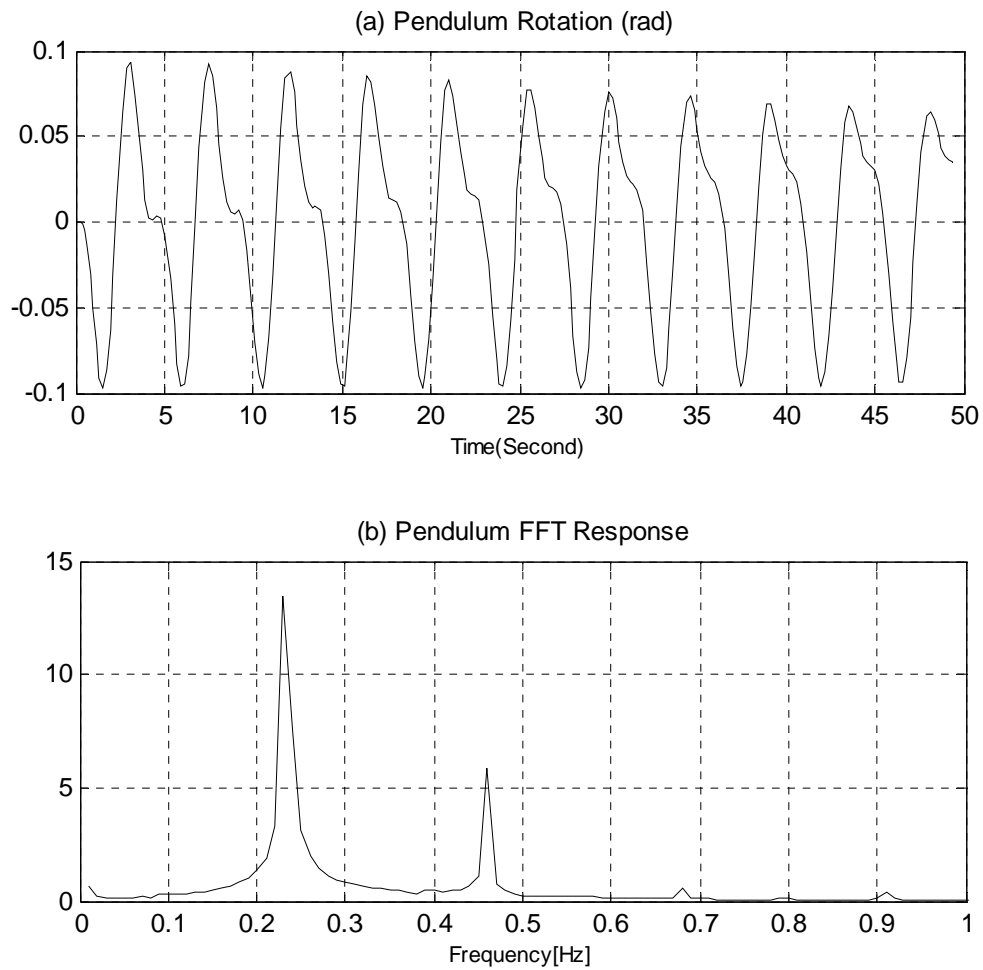


Figure 2-15 Time domain and FFT response
 ν (frequency of excitation) = 1.39 rad/sec

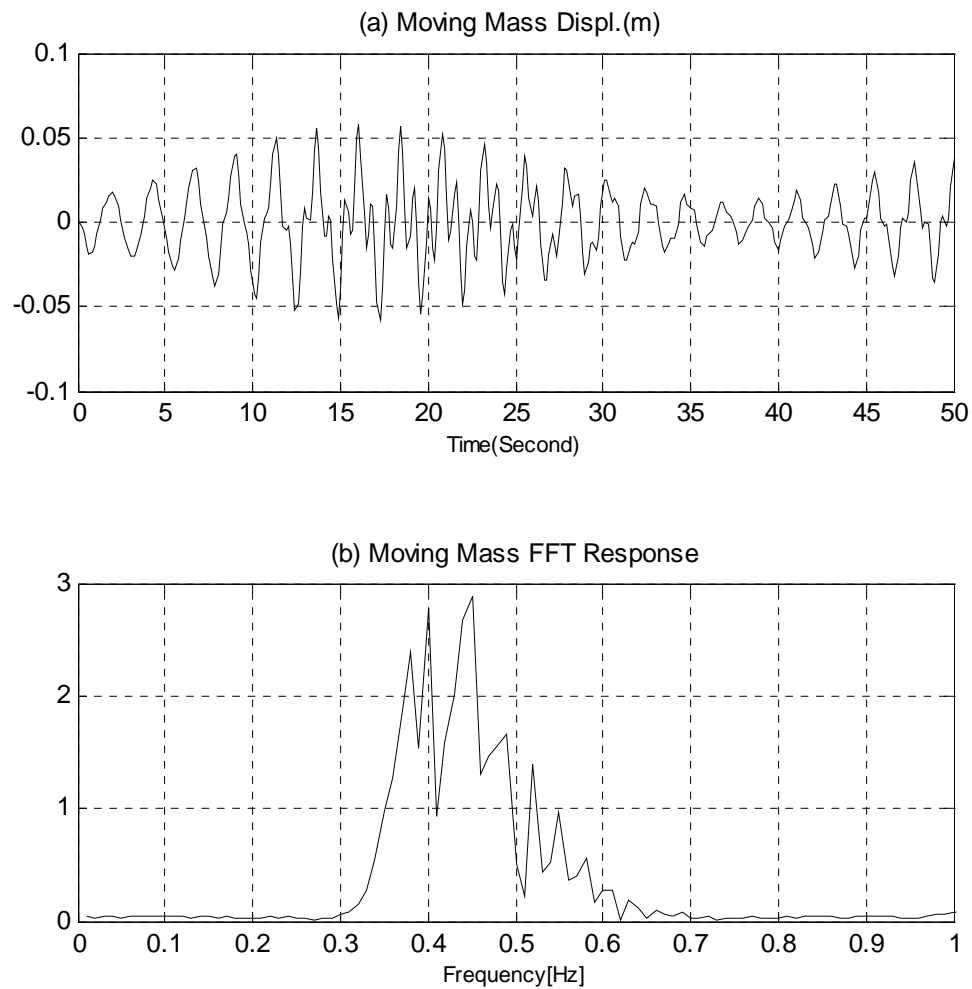


Figure 2-16 Time domain and FFT response
 ν (frequency of excitation) $= 2.78 \text{ rad/sec}$

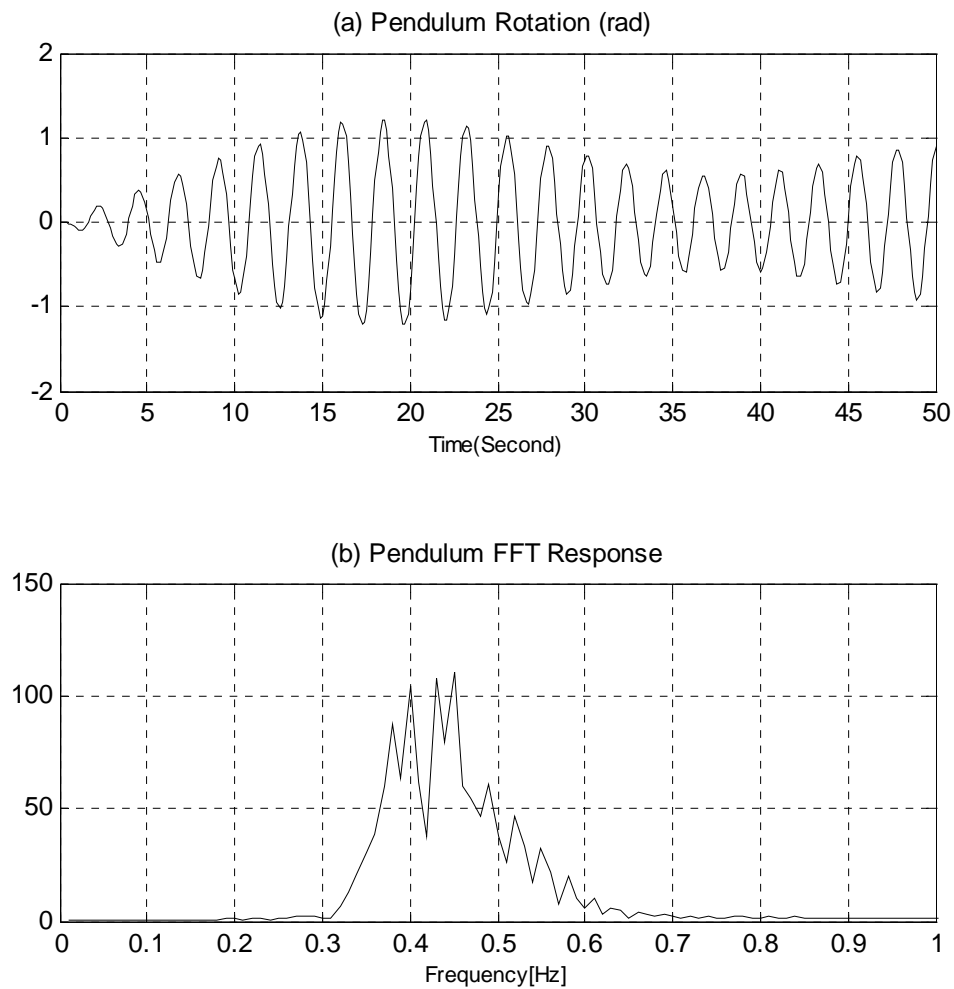


Figure 2-17 Time domain and FFT response
 ν (frequency of excitation) $\approx 2.78 \text{ rad/sec}$

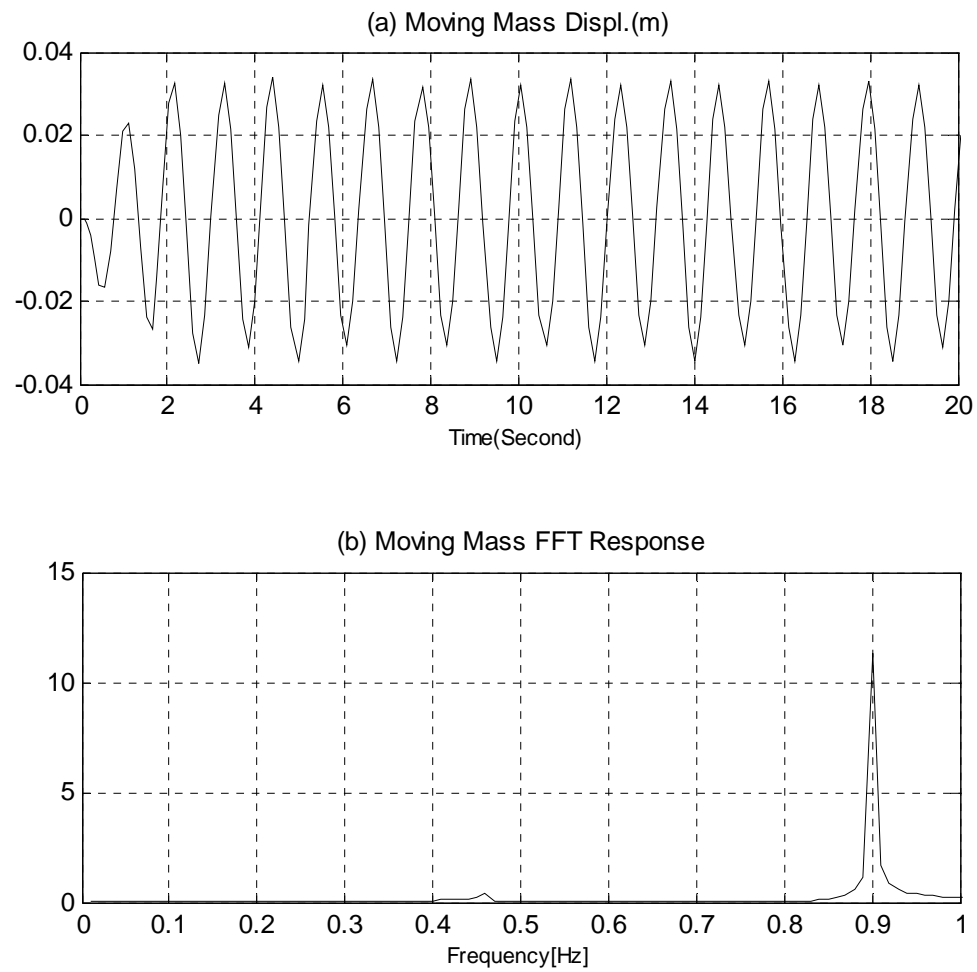


Figure 2-18 Time domain and FFT response
 ν (frequency of excitation) $\approx 5.56 \text{ rad/sec}$

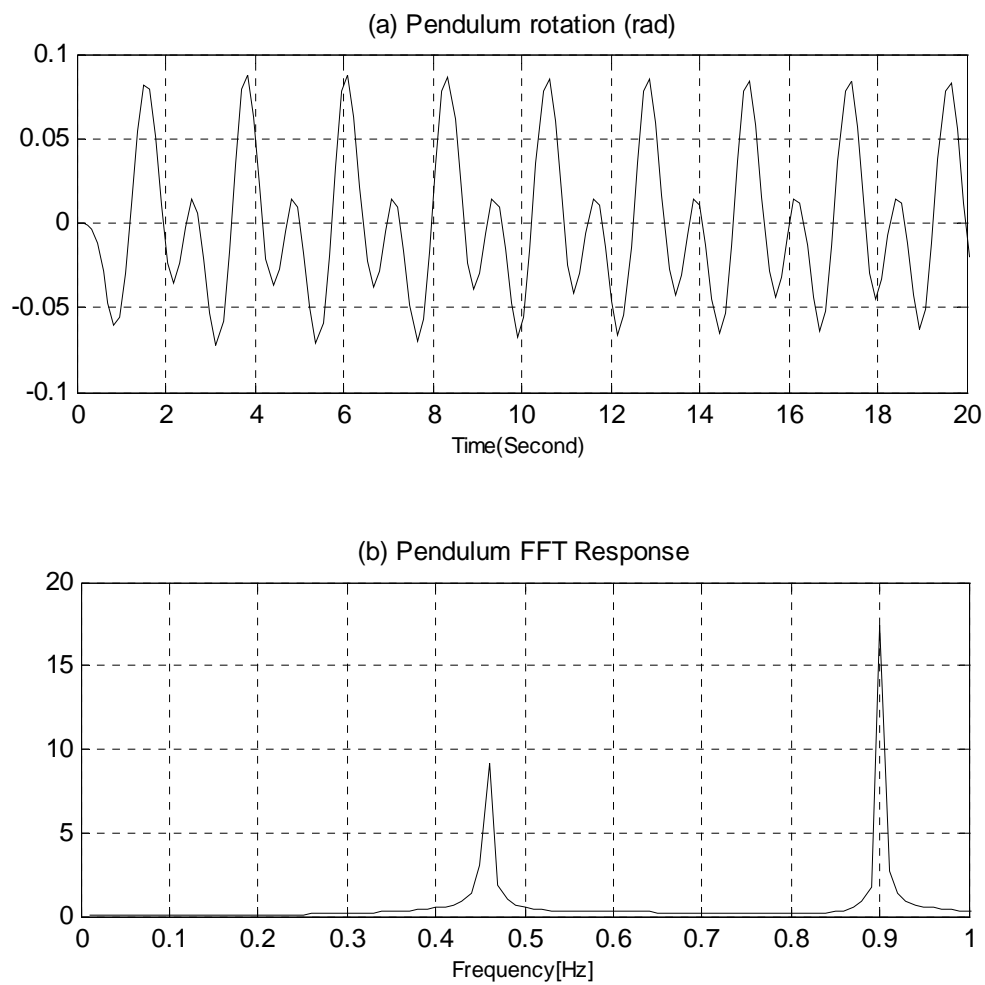


Figure 2-19 Time domain and FFT response
 ν (frequency of excitation) $\approx 5.56 \text{ rad/sec}$

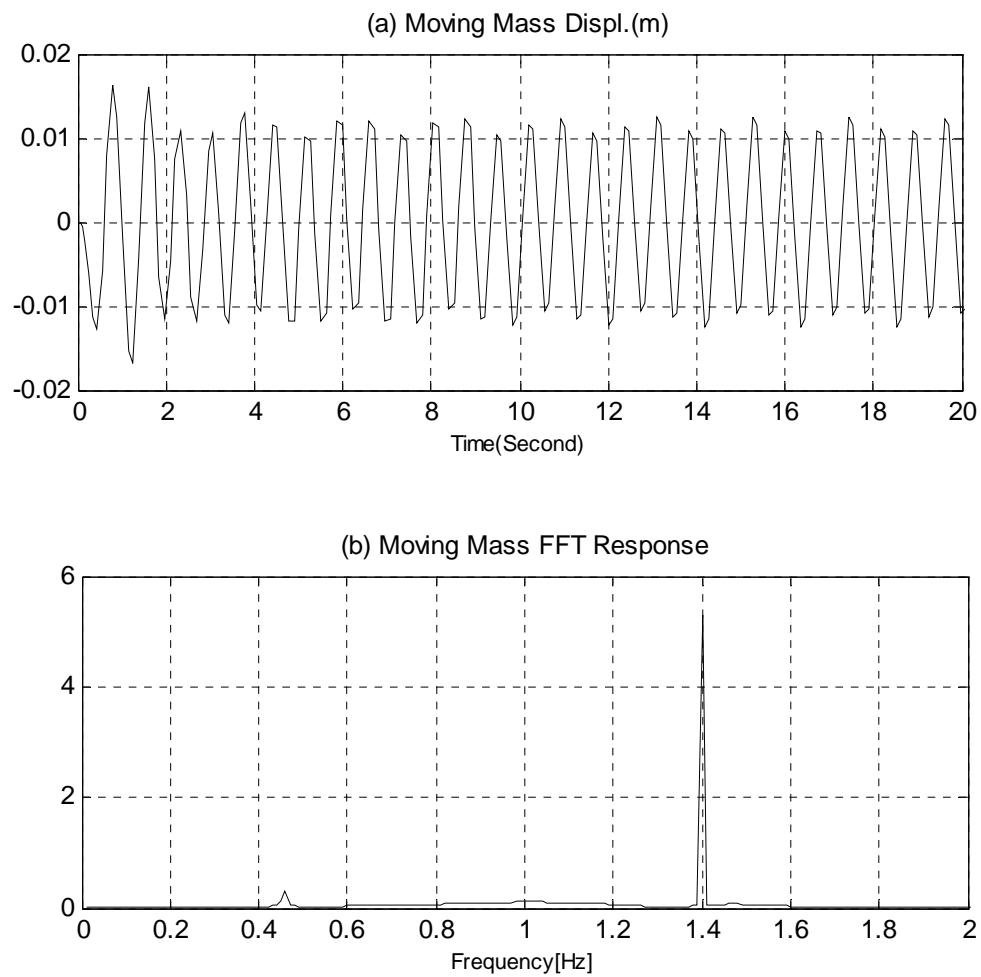


Figure 2-20 Time domain and FFT response
 ν (frequency of excitation) $\approx 8.69 \text{ rad/sec}$

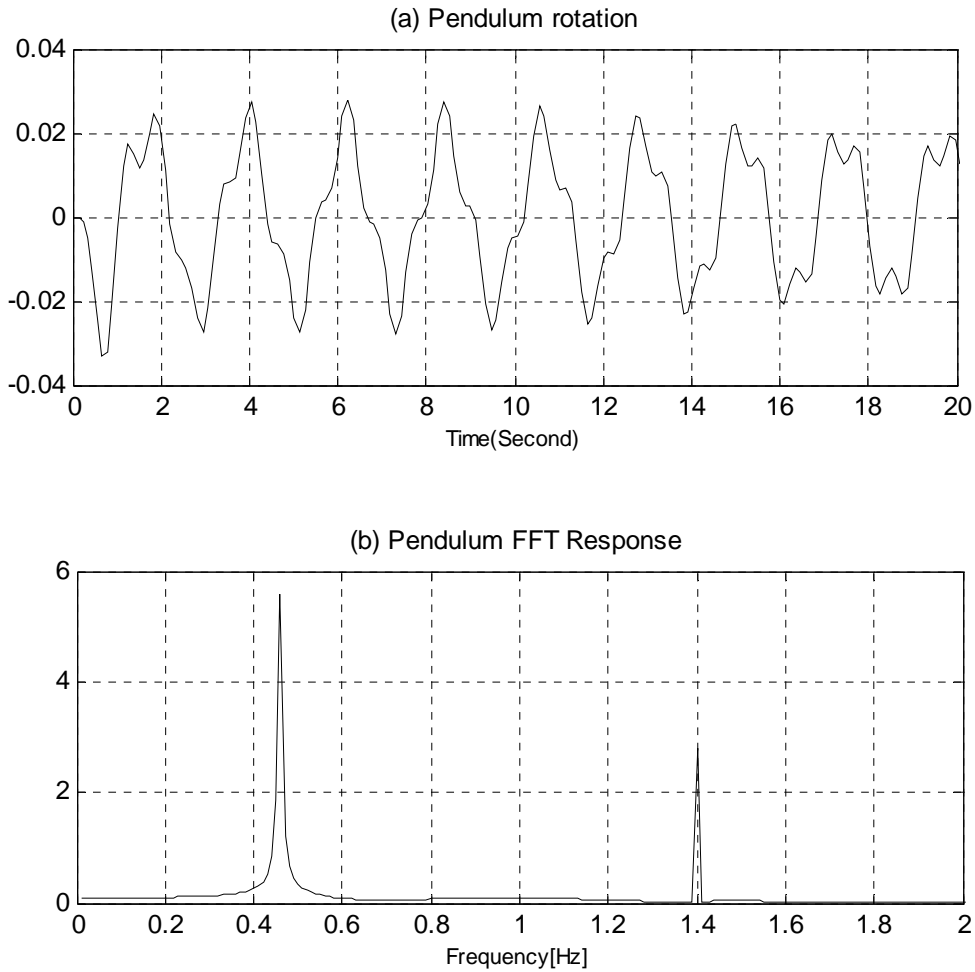


Figure 2-21 Time domain and FFT response
 ν (frequency of excitation) = 8.69 rad/sec

The response of the coupled nonlinear system is connected to the individual type of excitation. The first natural frequency of the system is shifted to $\omega_1 = 2.89 \text{ rad/sec}$ and the second natural frequency of the system has no influence on the response. This is due to the high damping ratio in the main mass, $\zeta = 35\%$. The influence of low frequency excitation and high frequency excitation are rendered in the described phenomenon. Response figures show that frequency of the response is a combination of two parts. The first part shows the oscillation at the forcing or exciting frequency which is called steady-state response and the second part shows the free vibrations of the system. By adjusting the excitation frequency around the natural frequencies of the system as it shown in Figures (2-16) and (2-17), the amplitude of the mass displacement and pendulum rotation grows enormously and decreases after time decay. An additional resonance of the

system also may be concluded whose frequency is due to nonlinearity to $\omega_p \approx \frac{1}{3}\nu$ (ν is frequency of the excitation) as the subharmonic resonance. Likewise an additional resonance of the system may be concluded whose frequency is changed by nonlinearity to $\omega_p \approx 3\nu$ (ν is frequency of the excitation) as the superharmonic resonance.

2.7.5 Stationary random base excitation

One can generate artificial sample function⁶ for excitation of the underlying random process $\ddot{x}_g(t)$ according to Equation (2-50), where $S(\nu)$ expresses an ensemble spectral density function as follows

$$\ddot{x}_g(t) = \sum_{n=1}^N \sqrt{4S(\nu)\Delta\nu} \cos(n\Delta\nu t - \varphi) \quad (2-50)$$

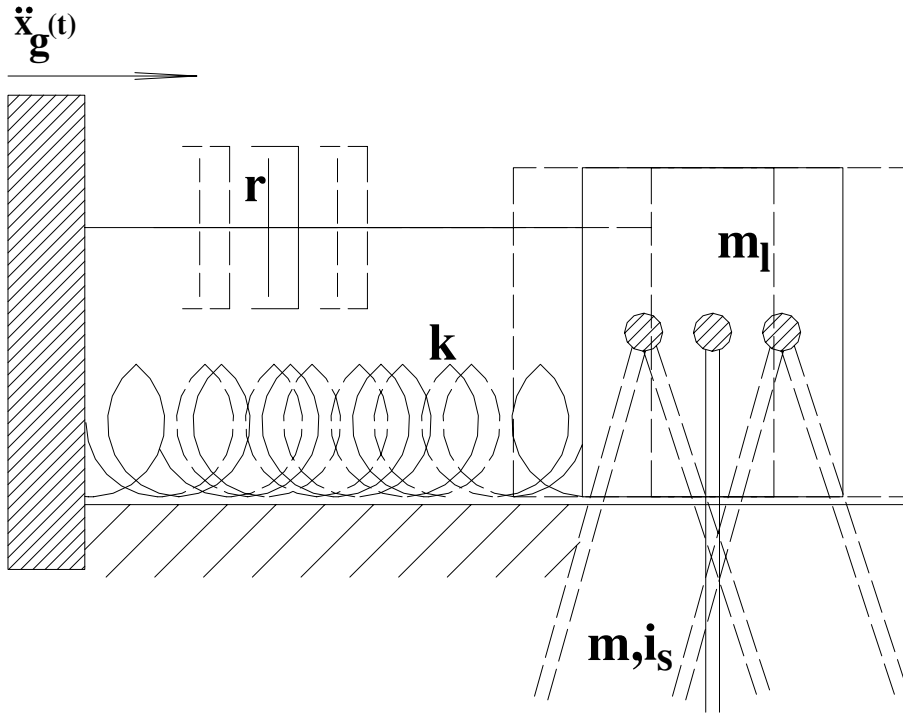


Figure 2-22 Random base excitation

⁶ Reference [6]

$\nu_i = i\Delta\nu$, $i = 1, 2, 3, \dots, 100$, $S(\nu)$ are determined in this example and $\Delta\nu$ is equal to ν_1 . Furthermore, a phase angle within the interval between $0 \leq \varphi \leq 2\pi$ is selected in the form of random number to advice a uniformly distributed random process. Numerical calculations lead to

$$S(\nu) = \{1\}, \{1.5\}, \{2\}$$

$$T = 100 \text{ sec}$$

$$\Delta\nu = \frac{2\pi}{T} = \frac{2\pi}{100} = 0.0628 \text{ rad/sec}$$

$$\nu_1 = \Delta\nu$$

$$S(\nu) = 1.5 \text{ m}^2/\text{sec}^3 \Rightarrow \ddot{x}_g(t) = \sum_{n=1}^{100} 0.6138 \times \cos(0.0628nt - \varphi) \text{ m/sec}^2 \quad (2-51)$$

$$\omega_{res} = 2.78 \text{ rad/sec}$$

$$\omega_p = \sqrt{\frac{g}{\ell}} = 2.86 \text{ rad/sec}$$

$$\omega_T = \sqrt{\frac{k}{m_1}} = 5.77 \text{ rad/sec}$$

$$\zeta = 15.81\%$$

The generated sample function $\ddot{x}_g(t)$ is illustrated in Figure (2-23a). Fast Fourier transformation analysis of a sample random vibration is obtained in Figure (2-23b) showing a constant energy level in time domain.

In Figure (2-24) through Figure (2-25), the response curves of the moving mass and the pendulum are illustrated, where $S(\nu)$ is selected as $\{1\}$, $\{1.5\}$ and $\{2\}$.

The response of the system depends on the type of excitation, natural frequency of the system, order of nonlinearity, and the type of damping mechanism.

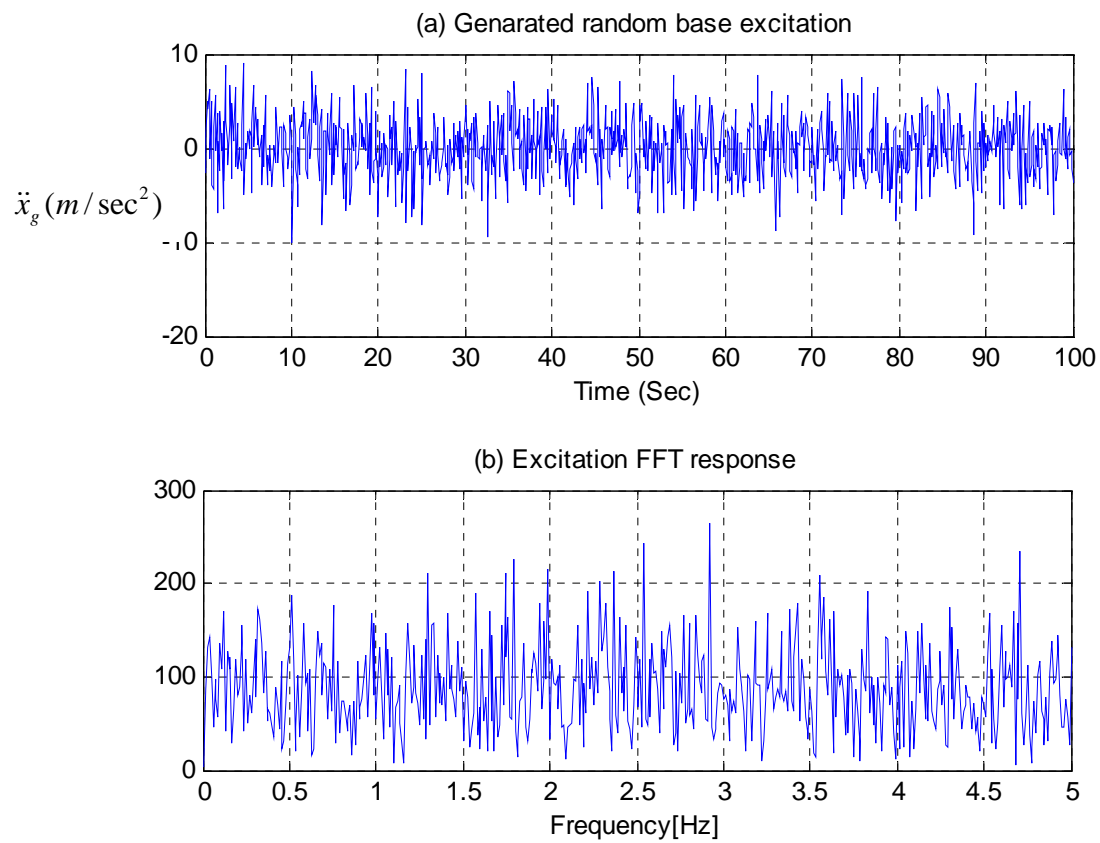


Figure 2-23 Time domain and frequency response-generated base acceleration

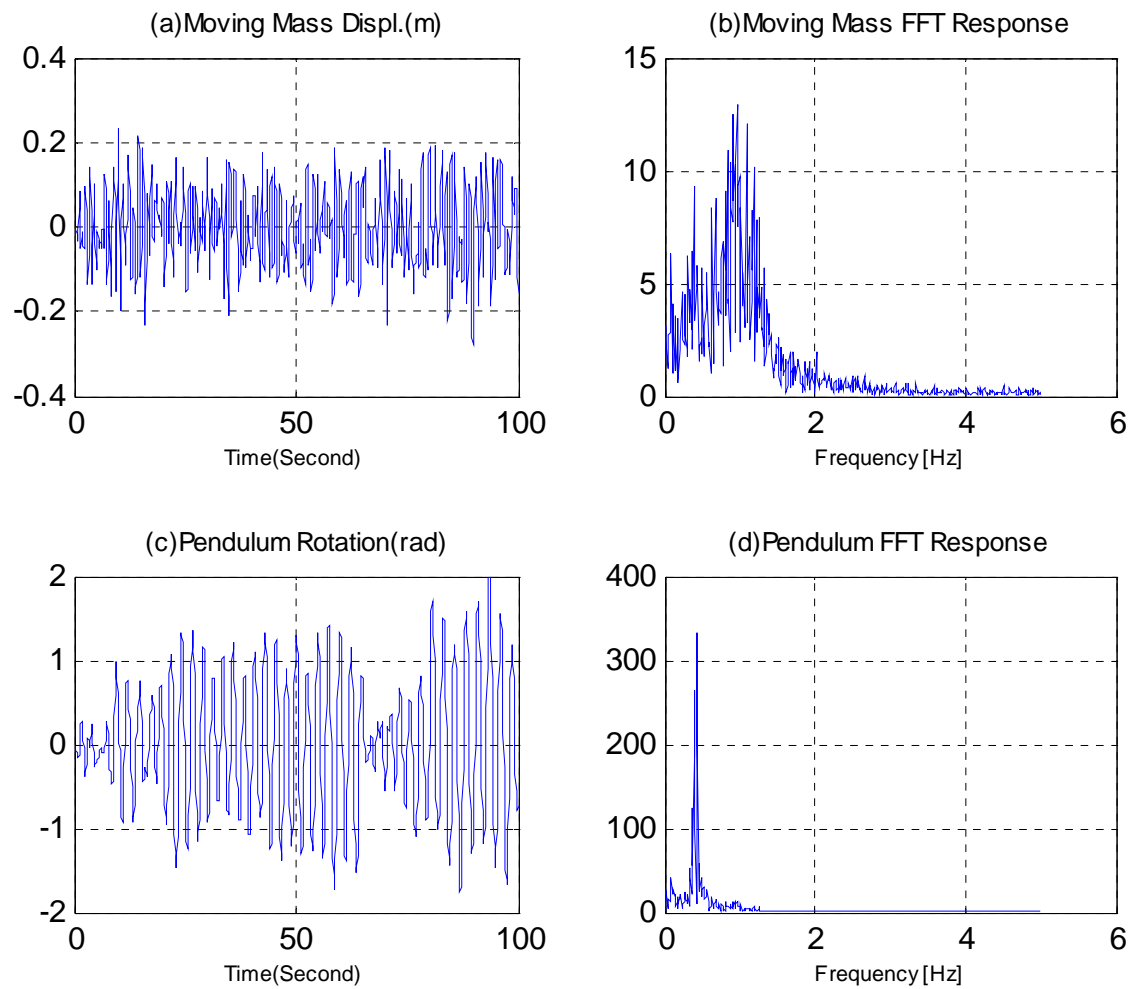


Figure 2-24 Time domain and frequency response
random excitation $S(\nu) = \{1\}$

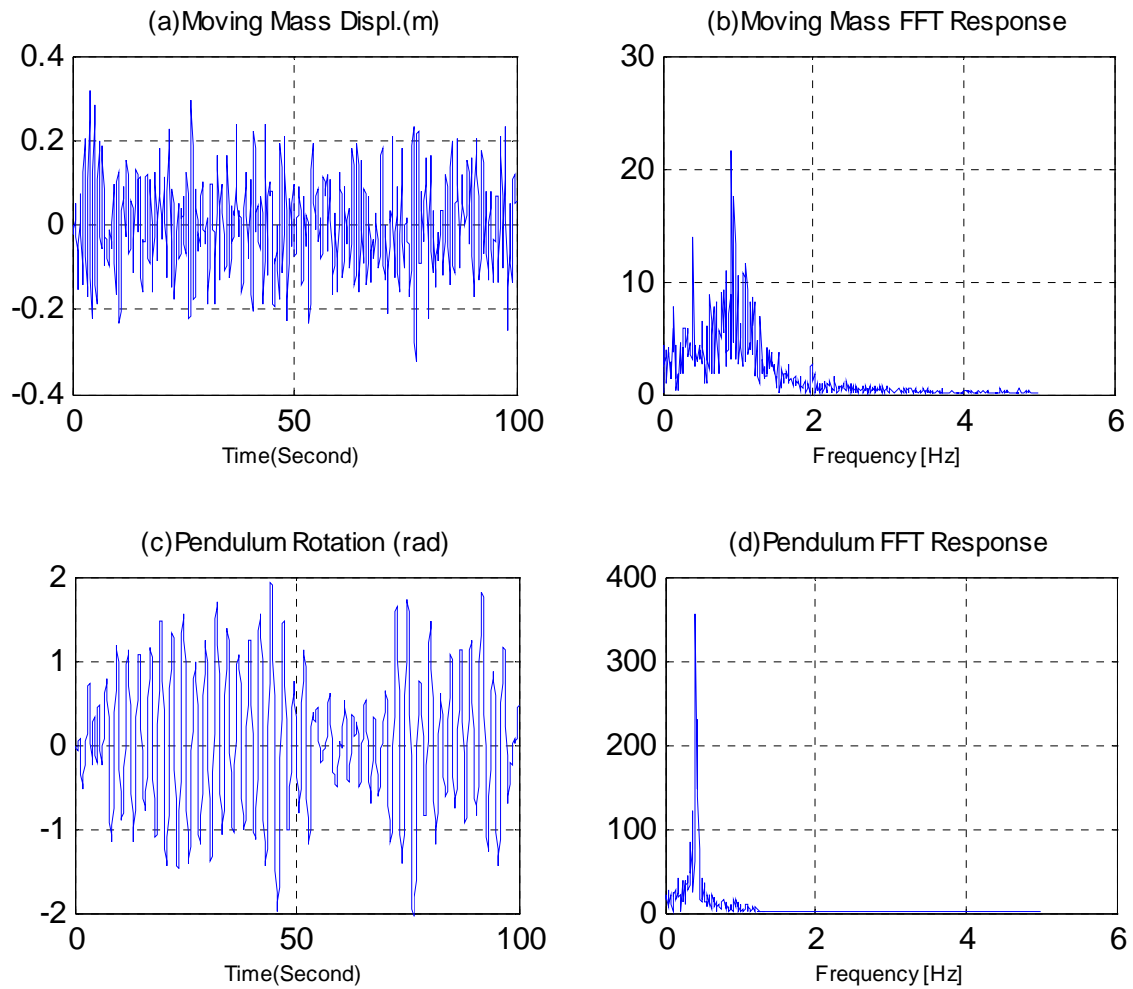


Figure 2-25 Time domain and frequency response
random excitation $S(\nu) = \{1.5\}$

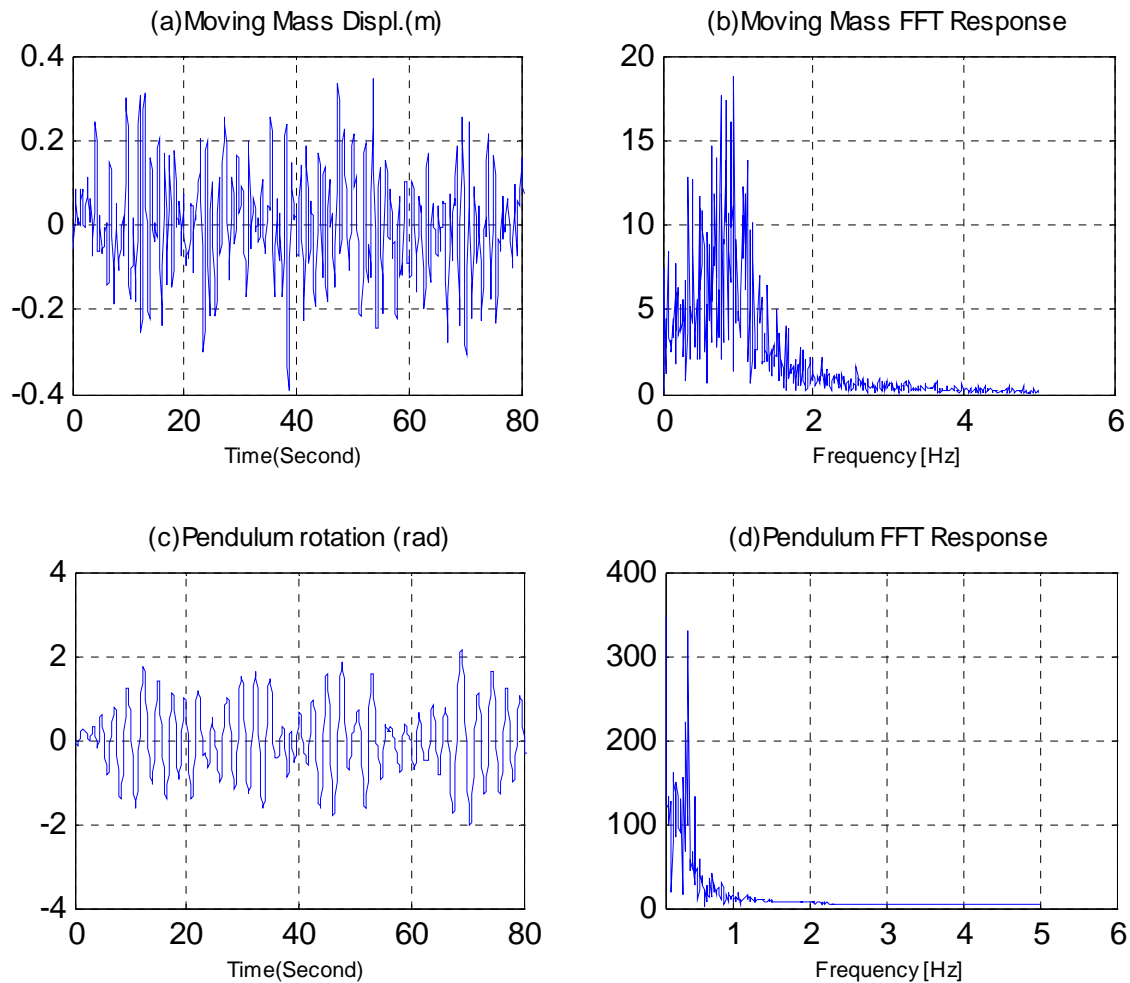


Figure 2-26 Time domain and frequency response
random excitation $S(\nu) = \{2\}$

When the amplitude of excitation is smaller than ω_p , a nonstationary state arises from the nonlinear response of the pendulum. Due to the nonstationarity, phase angle and amplitude of the response vary by time. In these cases, the frequency response curves may develop oscillations and deviate somewhat from the stationary case. This study will be discussed for the nonlinear pendulum in Chapter 4.

2.8 References

1. Ziegler F., 'Mechanics of Solids and Fluids', Second edition, Technical University Vienna, Springer-Verlag New York-Vienna, 1998.
2. Weaver Jr.W., Timoshenko S.P., Young D.H., Department of Civil Engineering, Stanford University, 'Vibration problems in engineering', Fifth edition, John Wiley & Sons, 1989.

3. Shabana A.A., Department of Mechanical Engineering, University of Illinois at Chicago, 'Theory of vibration', Springer-Verlag New York-Berlin Heidelberg, 1998.
4. Clough R.W., Penzien J., Department of Civil Engineering, University of California, 'Dynamic of Structures', McGraw-Hill, 1989.
5. Harris C.M., 'Shock and Vibration Handbook', Fourth edition, McGraw-Hill, 2003.
6. Yang C.Y., University of Delaware Newark, Delaware, 'Random vibration of structure', John Wiley & Sons, 1985.
7. Nayfeh A.H., Mook D.T., Department of Engineering Science and Mechanics Virginia, 'Nonlinear Oscillations', John Wiley & Sons, 1998.
8. Chopra A.K., University of California at Berkeley, 'Dynamics of Structures', second edition, Prentice Hall, 2001.

3

ANALYSIS OF THE HYBRID BELL-TOWER SYSTEM

3.1 *Introduction*

In this chapter the hybrid Bell-Tower (BT) system is studied. The structure is considered as a linear elastic continuous cantilever beam (Tower) together with a nonlinear single pendulum (Bell). The pendulum is supported at the top of the tower, and the corresponding equations of motion are derived. Oscillation of the pendulum is nonlinear and the tower has an infinitive number of degrees of freedom. Special emphasize is placed on the nonlinear interaction between the dynamically excited tower and the movement of the bell that mechanically behaves as a rigid pendulum. This particular study gives a completely new insight into the complex dynamic behavior of the BT structure. Responses of the BT for free and forced vibration are calculated by means of computer simulations. Comparison is made between the characteristics in coupled system and uncoupled system.

3.2 *Generalized Multi-Degree-Of-Freedom (MDOF) system*

The mechanical system consists of structural components having distributed mass and elasticity. Figure (3-1) shows a continuous BT system, where a pendulum is supported at the top of the tower. In spite of various possibilities for displacement of the tower, only one type of oscillation is possible in the pendulum. The tower is discretized as a linear system of a finite number of DOFs, and the pendulum is assumed to swing in nonlinear manner.

The essential properties of the tower consist of its flexural stiffness $EI(x)$ and its mass per unit length $\bar{m}(x)$, as well as the influence of damping denoted by $c(x)$.

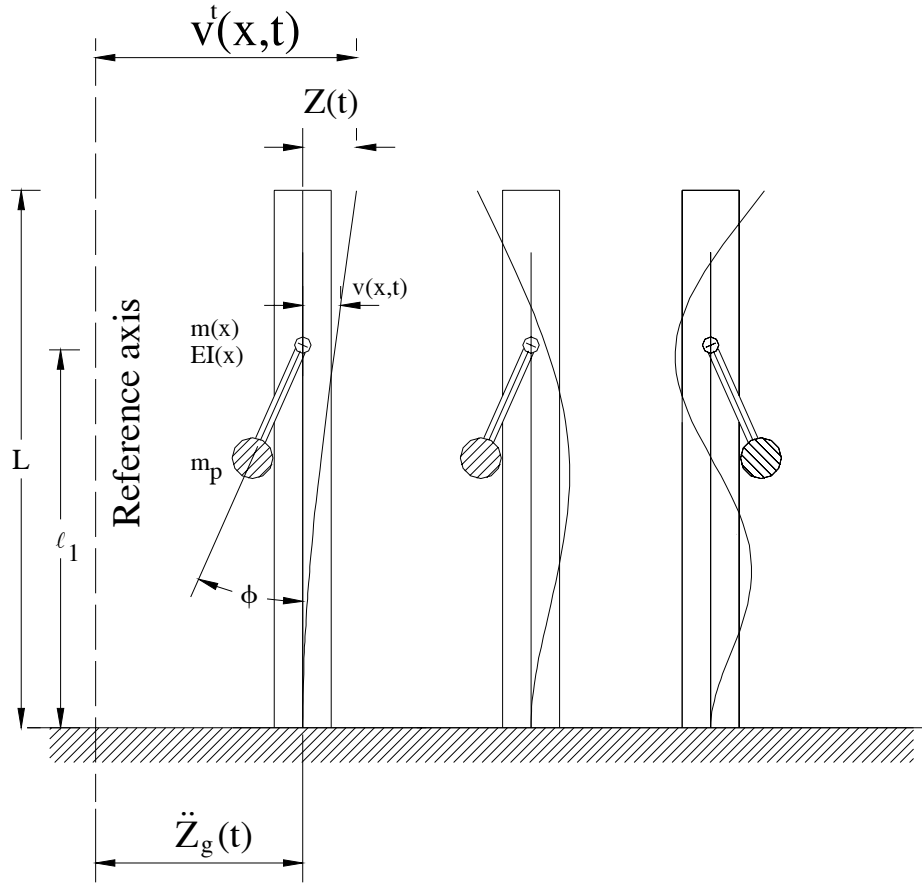


Figure 3-1 Generalized MDOF system

The BT is subjected to the ground motion excitation $\ddot{Z}_g(t)$. In order to approximate the motion of the tower, several mode shapes $\psi_i(x)$ are assumed for the deflection. The amplitudes of the motion are represented in the generalized coordinates $Z_i(t)$ ¹ thus

$$v(x,t) = \sum_{i=1}^n \psi_i(x) Z_i(t) \quad (3-1)$$

The generalized coordinates are selected as the model displacements of some convenient point of the tower such as its tip.

¹ Reference [4]

3.2.1 *Equilibration using energy principle²*

The kinetic energy of this system can be expressed as

$$T = \frac{1}{2} \int_0^L \bar{m} [\dot{v}'(x, t)]^2 dx + \frac{1}{2} m_p \dot{v}_p^2 \quad (3-2)$$

$$\dot{v}'(x, t) = \dot{Z}_g + \dot{v}(x, t)$$

where \bar{m} is the mass per unit length of the tower and m_p is the mass of the bell idealized as a “mathematical pendulum”.

Moreover, the pendulum velocity \dot{v}_p renders as

$$\dot{v}_p^2 = \left(\dot{v}(\ell_1, t) + \dot{Z}_g + s\dot{\phi} \cos \phi \right)^2 + \left(-s\dot{\phi} \sin \phi \right)^2 \quad (3-3)$$

and the potential energy for the system is given as

$$V = -m_p g s \cos \phi + \frac{1}{2} \int_0^L EI [v''(x, t)]^2 dx \quad (3-4)$$

in which EI is flexural stiffness of the tower and s is the length of the pendulum bar. By noting the following relationships, we have

$$\begin{aligned} v_i &= \psi_i(x) Z_i(t) \\ \dot{v}_i &= \psi_i(x) \dot{Z}_i(t) \\ \ddot{v}_i &= \psi_i(x) \ddot{Z}_i(t) \\ v'_i &= \psi'_i(x) Z_i(t) \\ v''_i &= \psi''_i(x) Z_i(t) \end{aligned} \quad (3-5)$$

² Reference [3]

Considering the special case with $\bar{m}(x) = \text{const.}$ and $EI(x) = \text{const.}$, the corresponding equations of kinetic and potential energy can be written as

$$\begin{aligned}
 T = & \frac{1}{2} \bar{m} \int_0^L \dot{Z}_g^2 + \frac{1}{2} \bar{m} \sum_{i=1}^n \sum_{j=1}^n \dot{Z}_i \dot{Z}_j \int_0^L \psi_i \psi_j dx + \bar{m} \dot{Z}_g \sum_{i=1}^n \dot{Z}_i \int_0^L \psi_i dx \\
 & + \frac{1}{2} m_p \sum_{i=1}^n \sum_{j=1}^n \dot{Z}_i \dot{Z}_j \psi_i(\ell_1) \psi_j(\ell_1) + \frac{1}{2} m_p \dot{Z}_g^2 + m_p \dot{Z}_g \sum_{i=1}^n \psi_i(\ell_1) \dot{Z}_i \\
 & + \frac{1}{2} m_p (s\dot{\phi})^2 + m_p s\dot{\phi} \cos \phi \sum_{i=1}^n \psi_i(\ell_1) \dot{Z}_i + m_p s \dot{Z}_g \dot{\phi} \cos \phi
 \end{aligned} \tag{3-6}$$

$$V = -m_p g s \cos \phi + \frac{1}{2} EI \sum_{i=1}^n \sum_{j=1}^n Z_i Z_j \int_0^L \psi_i'' \psi_j'' dx \tag{3-7}$$

3.2.2 Equations of motion

The generalized coordinates are selected $Z_i(t), \phi(t)$ and m_i, k_i, c_i are the modal mass, stiffness, and damping coefficients, respectively. By using the expressions for the kinetic and potential energies, and employing the following form of Lagrange equations of motion³, see Appendix A

$$\frac{d}{dt} \left(\frac{\partial T}{\partial \dot{q}_i} \right) - \frac{\partial T}{\partial q_i} + \frac{\partial V}{\partial q_i} = Q_i \tag{3-8}$$

two sets of equations of motion for the general coordinates Z_i and ϕ are in the form of

$$\frac{d}{dt} \left(\frac{\partial T}{\partial \dot{Z}_i} \right) - \frac{\partial T}{\partial Z_i} + \frac{\partial V}{\partial Z_i} = Q_i, \quad i = 1, 2, \dots, n \tag{3-9}$$

$$\frac{d}{dt} \left(\frac{\partial T}{\partial \dot{\phi}} \right) - \frac{\partial T}{\partial \phi} + \frac{\partial V}{\partial \phi} = 0 \tag{3-10}$$

³ Reference [6]

This procedure leads to the following partial differential expressions of kinetic and potential energy

$$\begin{aligned} \frac{\partial T}{\partial \dot{Z}_i} &= \sum_{j=1}^n \bar{m} \dot{Z}_j \int_0^L \psi_i \psi_j dx + \bar{m} \dot{Z}_g \int_0^L \psi_i dx \\ &\quad + \sum_{j=1}^n m_p \psi_i(\ell_1) \psi_j(\ell_1) \dot{Z}_j + m_p \dot{Z}_g \psi_i(\ell_1) \\ &\quad + m_p s \dot{\phi} \cos \phi \psi_i(\ell_1) \end{aligned} \quad (3-11)$$

$$\frac{\partial T}{\partial \dot{\phi}} = m_p s^2 \dot{\phi} + m_p s \cos \phi \sum_{i=1}^n \psi_i(\ell_1) \dot{Z}_i + m_p s \dot{Z}_g \cos \phi \quad (3-12)$$

$$\begin{aligned} \frac{d}{dt} \left(\frac{\partial T}{\partial \dot{Z}_i} \right) &= \sum_{j=1}^n \bar{m} \ddot{Z}_j \int_0^L \psi_i \psi_j dx + \bar{m} \ddot{Z}_g \int_0^L \psi_i dx \\ &\quad + \sum_{j=1}^n m_p \psi_i(\ell_1) \psi_j(\ell_1) \ddot{Z}_j \\ &\quad + m_p \ddot{Z}_g \psi_i(\ell_1) + m_p s \ddot{\phi} \cos \phi \psi_i(\ell_1) - m_p s \dot{\phi}^2 \sin \phi \psi_i(\ell_1) \end{aligned} \quad (3-13)$$

$$\begin{aligned} \frac{d}{dt} \left(\frac{\partial T}{\partial \dot{\phi}} \right) &= m_p s^2 \ddot{\phi} + m_p s \cos \phi \sum_{i=1}^n \psi_i(\ell_1) \ddot{Z}_i - m_p s \dot{\phi} \sin \phi \sum_{i=1}^n \psi_i(\ell_1) \dot{Z}_i \\ &\quad + m_p s \cos \phi \ddot{Z}_g - m_p s \dot{\phi} \sin \phi \dot{Z}_g \end{aligned} \quad (3-14)$$

$$\frac{\partial T}{\partial Z_i} = 0 \quad (3-15)$$

$$\frac{\partial T}{\partial \phi} = m_p s \dot{\phi} (-\sin \phi \sum_{i=1}^n \psi_i(\ell_1) \dot{Z}_i - \sin \phi \dot{Z}_g) \quad (3-16)$$

$$\frac{\partial V}{\partial Z_i} = EI \sum_{j=1}^n Z_j \int_0^L \psi_i'' \psi_j'' dx \quad (3-17)$$

$$\frac{\partial V}{\partial \phi} = m_p s g \sin \phi \quad (3-18)$$

Substituting Equations (3-13) through (3-18) in Lagrange equations of motion, Equations (3-9) and (3-10), and introducing modal damping terms results in

$$Q_i = -r_i \sum_{j=1}^n \dot{Z}_j \int_0^L \psi_i \psi_j dx \quad (3-19)$$

where r_i is the damping coefficient of the i -th mode.

The comprehensive equations for the hybrid system are expressed as

$$\begin{aligned} \sum_{j=1}^n \{ & \bar{m} \ddot{Z}_j \int_0^L \psi_i \psi_j dx + m_p \psi_i(\ell_1) \psi_j(\ell_1) \ddot{Z}_j \\ & + r_i \dot{Z}_j \int_0^L \psi_i \psi_j dx + EI Z_j \int_0^L \psi_i'' \psi_j'' dx \} \\ & + m_p s \psi_i(\ell_1) (\ddot{\phi} \cos \phi - \dot{\phi}^2 \sin \phi) = \\ & - \ddot{Z}_g \left(\bar{m} \int_0^L \psi_i dx + m_p \psi_i(\ell_1) \right) \end{aligned} \quad (3-20)$$

$$m_p s \cos \phi \sum_{i=1}^n \psi_i(\ell_1) \ddot{Z}_i + m_p s^2 \ddot{\phi} + m_p s g \sin \phi = -m_p s \cos \phi \ddot{Z}_g \quad (3-21)$$

The two mode shapes of the tower must satisfy orthogonality conditions⁴ as

$$\begin{aligned} \int_0^L \psi_i(x) \psi_j(x) \bar{m}(x) dx &= 0 & \omega_i &\neq \omega_j \\ \int_0^L \psi_i''(x) \psi_j''(x) EI(x) dx &= 0 & \omega_i &\neq \omega_j \end{aligned} \quad (3-22)$$

⁴ Reference [4]

Thus the corresponding equations reduce to

$$\begin{aligned} & \bar{m}\ddot{Z}_i \int_0^L \psi_i^2 dx + m_p \psi_i(\ell_1) \sum_{j=1}^n \psi_j(\ell_1) \ddot{Z}_j \\ & + r_i \dot{Z}_i \int_0^L \psi_i^2 dx + EI Z_i \int_0^L [\psi_i'']^2 dx + m_p s \psi_i(\ell_1) (\ddot{\phi} \cos \phi - \dot{\phi}^2 \sin \phi) = \\ & -\ddot{Z}_g \left(\bar{m} \int_0^L \psi_i dx + m_p \psi_i(\ell_1) \right) \end{aligned} \quad (3-23)$$

$$\cos \phi \sum_{j=1}^n \psi_j(\ell_1) \ddot{Z}_j + s \ddot{\phi} + g \sin \phi = -\cos \phi \ddot{Z}_g \quad (3-24)$$

The following relationships are introduced for further formulations

$$\begin{aligned} m_i &= \bar{m} \int_0^L \psi_i^2(x) dx \\ k_i &= EI \int_0^L [\psi_i''(x)]^2 dx \\ c_i &= r_i \int_0^L \psi_i^2(x) dx \\ m_{ip} &= m_p \psi_i^2(\ell_1) \\ m_i^* &= \bar{m} \int_0^L \psi_i(x) dx \\ m_{ip}^* &= m_p \psi_i(\ell_1) \end{aligned} \quad (3-25)$$

Considering Rayleigh Damping⁵ the modal damping coefficient c_i can be expressed as linear combination of the modal mass and stiffness coefficient m_i and k_i

$$c_i = a_0 m_i + a_1 k_i \quad (3-25a)$$

where the coefficient a_0 and a_1 have to be determined experimentally.

Substituting $k_i = m_i \omega_i^2$ yields

⁵ Reference [6]

$$c_i = m_i(a_0 + a_1\omega_i^2) \quad \text{and} \quad r_i = \bar{m}(a_0 + a_1\omega_i^2) \quad (3-25b)$$

Therefore two general sets of Lagrange equation are expressed as follows

$$\begin{aligned} m_i \ddot{Z}_i(t) + m_{ip}^* \sum_{j=1}^n \psi_j(\ell_1) \ddot{Z}_j(t) + c_i \dot{Z}_i(t) + k_i Z_i(t) \\ + m_{ip}^* s(\ddot{\phi} \cos \phi - \dot{\phi}^2 \sin \phi) = -(m_i^* + m_{ip}^*) \ddot{Z}_g(t) \end{aligned} \quad (3-26)$$

$$m_p s \cos \sum_{j=1}^n \psi_j(\ell_1) \ddot{Z}_j(t) + m_p s^2 \ddot{\phi} + m_p s g \sin \phi = -m_p s \cos \phi \ddot{Z}_g(t) \quad (3-27)$$

3.3 Modal analysis of the BT

In order to provide a representative solution of the BT, one should evaluate the mode shapes functions first. These functions are shown for the first three modes in Figure (3-1).

3.3.1 Eigenfrequencies and mode shapes⁶

Consider again the elementary case in which $EI(x)$ and $\bar{m}(x)$ have constants values EI and \bar{m} , respectively. The free vibration equation of motion for the undamped slender BT is expressed as

$$EI \frac{\partial^4 v(x,t)}{\partial x^4} + \bar{m} \frac{\partial^2 v(x,t)}{\partial t^2} = 0 \quad (3-28)$$

After dividing by EI and adopting the prime and dot notations to indicate partial derivatives with respect to x and t , respectively, this equation becomes

$$v^{iv}(x,t) + \frac{\bar{m}}{EI} \ddot{v}(x,t) = 0 \quad (3-29)$$

⁶ Reference [4]

Since $\frac{\bar{m}}{EI}$ is a constant, one form of solution of this equation can be obtained by separation of variables using

$$v(x,t) = \psi(x) Z(t) \quad (3-30)$$

which indicates that the free vibration motion is of a specific shape $\psi(x)$ having a time dependent amplitude $Z(t)$. Substituting this equation into Equation (3-29) results in

$$\psi^{iv}(x) Z(t) + \frac{\bar{m}}{EI} \psi(x) \ddot{Z}(t) = 0 \quad (3-31)$$

Dividing by $\psi(x) Z(t)$, the variables can be separated as follows

$$\frac{\psi^{iv}(x)}{\psi(x)} + \frac{\bar{m}}{EI} \frac{\ddot{Z}(t)}{Z(t)} = 0 \quad (3-32)$$

Since the first term in this equation is a function of x only, and the second term is a function of t only, the entire equation can be satisfied for arbitrary values of x and t only if each term is a constant in accordance with

$$\frac{\psi^{iv}(x)}{\psi(x)} = -\frac{\bar{m}}{EI} \frac{\ddot{Z}(t)}{Z(t)} = a^4 \quad (3-33)$$

where the single constant involved is designated in the form a^4 for subsequent mathematical convenience. This equation yields two ordinary differential equations

$$\ddot{Z}(t) + \omega^2 Z(t) = 0 \quad (3-34)$$

$$\psi^{iv}(x) - a^4 \psi(x) = 0 \quad (3-35)$$

in which

$$\omega^2 = \frac{a^4 EI}{\bar{m}} \quad \text{or} \quad a^4 = \frac{\omega^2 \bar{m}}{EI} \quad (3-36)$$

Equation (3-34) is the familiar expression for the free vibration of an undamped SDOF system having the solution as

$$Z(t) = A \cos \omega t + B \sin \omega t \quad (3-37)$$

The equation (3-35) can be solved in the usual way by introducing a solution of the form

$$\psi(x) = C e^{sx} \quad (3-38)$$

leading to

$$(s^4 - a^4) C e^{sx} = 0 \quad (3-39)$$

from which

$$s = \pm a, \pm ia \quad (3-40)$$

Incorporating each of these roots into Equation (3-38) separately and adding the resulting four terms, one obtains the complete solution as

$$\psi(x) = C_1 e^{iax} + C_2 e^{-iax} + C_3 e^{ax} + C_4 e^{-ax} \quad (3-41)$$

in which C_1, C_2, C_3 and C_4 must be treated as complex constants. Expressing the exponential functions in terms of their trigonometric and hyperbolic equivalents and setting the entire imaginary part of the right hand side of this equation to zero leads to

$$\psi(x) = A_1(x) \cos ax + A_2 \sin ax + A_3 \cosh ax + A_4 \sinh ax \quad (3-42)$$

These real constants must be evaluated so as to satisfy the known boundary conditions (displacement, slope, moment, or shear)

3.3.2 BT mode shapes and frequencies

The free vibration of the BT analysis requires all four terms in Equation (3-42). Consider the Bell-Tower shown in Figure (3-1) with four boundary conditions as

$$\psi(0) = 0 \quad \psi'(0) = 0 \quad (3-43)$$

$$M(L) = EI\psi''(L) = 0 \quad V(L) = EI\psi'''(L) = 0 \quad (3-44)$$

Substituting Equation (3-42) and its derivative expressions into these equations leads to

$$\begin{aligned} \psi(0) &= (A_1 \cos 0 + A_2 \sin 0 + A_3 \cosh 0 + A_4 \sinh 0) = 0 \\ \psi''(0) &= a(-A_1 \sin 0 + A_2 \cos 0 + A_3 \sinh 0 + A_4 \cosh 0) = 0 \\ \psi''(L) &= a^2(-A_1 \cos aL - A_2 \sin aL + A_3 \cosh aL + A_4 \sinh aL) = 0 \\ \psi'''(L) &= a^3(A_1 \sin aL - A_2 \cos aL + A_3 \sinh aL + A_4 \cosh aL) = 0 \end{aligned} \quad (3-45)$$

Making use of $\cos 0 = \cosh 0 = 1$ and $\sin 0 = \sinh 0 = 0$, the first two of these equations yield $A_3 = -A_1$ and $A_4 = -A_2$. Substituting these equalities into the latter two equations, changing all signs, and placing the resulting expressions in a matrix form one obtains

$$\begin{bmatrix} (\cos aL + \cosh aL) & (\sin aL + \sinh aL) \\ (\sinh aL - \sin aL) & (\cos aL + \cosh aL) \end{bmatrix} \begin{Bmatrix} A_1 \\ A_2 \end{Bmatrix} = \begin{Bmatrix} 0 \\ 0 \end{Bmatrix} \quad (3-46)$$

For coefficients A_1 and A_2 to be nonzero, the determinant of the square matrix in this equation must be equated to zero, to obtain the frequency equation as

$$\sinh^2 aL - \sin^2 aL - \cos^2 aL - 2 \cosh aL \cos aL - \cosh^2 aL = 0 \quad (3-47)$$

which reduces to the form

$$\cos aL = -\frac{1}{\cosh aL} \quad (3-48)$$

The solution of this transcendental equation provides the values of aL which represent the eigenfrequencies of vibration of the BT. Figure (3-2) shows a plot of functions $\cos aL$ and $-\frac{1}{\cosh aL}$, and their crossing points give the values of aL which satisfy Equation (3-48).

Introducing the values of aL given by Equation (3-48) into Equation (3-36), the corresponding circular frequencies can be obtained as

$$\omega_i = (aL)_i^2 \sqrt{\frac{EI}{mL^4}} \quad i = 1, 2, 3, \dots \quad (3-49)$$

Either of Equation (3-46) can now be employed to express coefficient A_2 in terms of A_1 . The first gives

$$A_2 = -\frac{(\cos aL + \cosh aL)}{(\sin aL + \sinh aL)} A_1 \quad (3-50)$$

This result along with the previously obtained conditions $A_3 = -A_1$ and $A_4 = -A_2$, allows the mode shape expression of Equation (3-42) to be written in the form

$$\psi_i(x) = A_1 \left[\cos ax - \cosh ax - \frac{[(\cos(aL)_i + \cosh(aL)_i)]}{[\sin(aL)_i + \sinh(aL)_i]} (\sin ax - \sinh ax) \right] \quad (3-51)$$

Substituting the frequency equation roots for aL into this expression separately, one obtains the corresponding mode shape functions. Plots of these functions for the first three modes are shown in Figure (3-3) along with their corresponding circular frequencies.

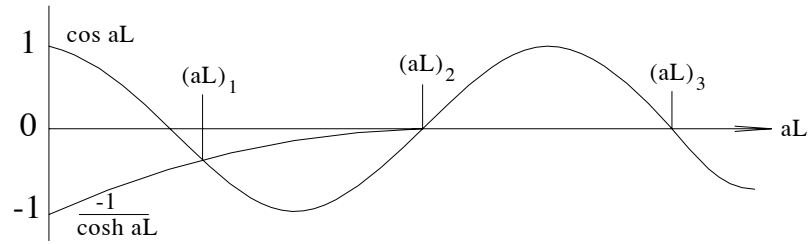


Figure 3-2 Roots of frequency equation

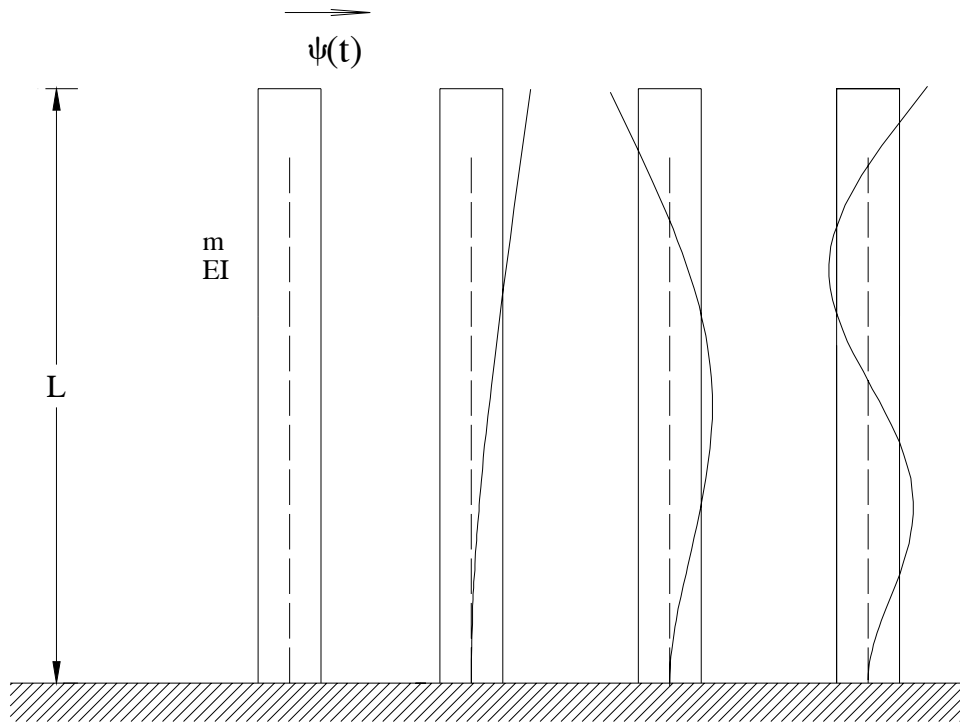


Figure 3-3 Mode shapes of the BT

$$\omega_1 = (1.875)^2 \sqrt{\frac{EI}{mL^4}} \quad \omega_2 = (4.694)^2 \sqrt{\frac{EI}{mL^4}} \quad \omega_3 = (7.855)^2 \sqrt{\frac{EI}{mL^4}} \quad (3-52)$$

3.3.3 Uncoupled equations of motion⁷

The mode shape (normal) coordinate transformation serves to uncouple the equations of motion of any linear dynamic system and therefore is applicable to the flexural equations of motion of a one dimensional member. Introducing the equation of flexural motion, leads to

$$M_n \ddot{Z}_n(t) + (a_0 M_n + a_1 \omega_n^2 M_n) \dot{Z}_n(t) + \omega_n^2 M_n Z_n(t) = P_n(t) \quad (3-53)$$

$$\ddot{Z}_n(t) + 2\zeta_n \omega_n \dot{Z}_n(t) + \omega_n^2 Z_n(t) = \frac{P_n(t)}{M_n} \quad (3-54)$$

$$\zeta_n = \frac{a_0}{2\omega_n} + \frac{a_1 \omega_n}{2} \quad (3-55)$$

$$M_n = \int_0^L \bar{m}(x) \psi_i^2(x) dx \quad (3-56)$$

$$P_n = \int_0^L \psi_i(x) P_n(x, t) dx \quad (3-57)$$

It is apparent that after the vibration mode shapes have been determined, the reduction to the normal coordinate form, involves exactly the same type of operations for all structures.

3.4 Vibration analysis of the BT

Following Equations (3-26) and (3-27) which were employed for the tower and the swinging pendulum, the first step in the dynamic response analysis will be the evaluation of mode shapes and frequencies of the BT which were discussed previously. As an example considering two mode shapes, the equations of motion can be written as follows

$$\begin{aligned} m_1 \ddot{Z}_1(t) + m_{1p}^* \psi_1(\ell_1) \ddot{Z}_1(t) + m_{1p}^* \psi_2(\ell_1) \ddot{Z}_2(t) + c_1 \dot{Z}_1(t) + k_1 Z_1(t) \\ + m_{1p}^* s(\ddot{\phi} \cos \phi - \dot{\phi}^2 \sin \phi) = -(m_1^* + m_{1p}^*) \ddot{Z}_g(t) \end{aligned} \quad (3-58)$$

⁷ Reference [6]

$$\begin{aligned}
m_2\ddot{Z}_2(t) + m_{2p}^*\psi_1(\ell_1)\ddot{Z}_1(t) + m_{2p}^*\psi_2(\ell_1)\ddot{Z}_2(t) + c_2\dot{Z}_2(t) + k_2Z_2(t) \\
+ m_{2p}^*s(\ddot{\phi}\cos\phi - \dot{\phi}^2\sin\phi) = -(m_2^* + m_{2p}^*)\ddot{Z}_g(t) \quad (3-59)
\end{aligned}$$

$$m_p s \cos\phi \psi_1(\ell_1)\ddot{Z}_1(t) + m_p s \cos\phi \psi_2(\ell_1)\ddot{Z}_2(t) + m_p s^2\ddot{\phi} + m_p s g \sin\phi = -m_p s \cos\phi \ddot{Z}_g(t) \quad (3-60)$$

Normalizing the mode shapes with reference to the pendulum's operating position ℓ_1 results in

$$\begin{aligned}
\psi_1(\ell_1) &= \psi_2(\ell_1) = 1 \\
m_{1p} &= m_{1p}^* = m_p \\
m_{2p} &= m_{2p}^* = m_p \quad (3-61)
\end{aligned}$$

Therefore the last three equations become

$$\begin{aligned}
(m_1 + m_p)\ddot{Z}_1(t) + m_p\ddot{Z}_2 + c_1\dot{Z}_1(t) + k_1Z_1(t) \\
+ m_p s(\ddot{\phi}\cos\phi - \dot{\phi}^2\sin\phi) = -(m_1^* + m_p)\ddot{Z}_g(t) \quad (3-62)
\end{aligned}$$

$$\begin{aligned}
(m_2 + m_p)\ddot{Z}_2(t) + m_p\ddot{Z}_1 + c_2\dot{Z}_2(t) + k_2Z_2(t) \\
+ m_p s(\ddot{\phi}\cos\phi - \dot{\phi}^2\sin\phi) = -(m_2^* + m_p)\ddot{Z}_g(t) \quad (3-63)
\end{aligned}$$

$$m_p s \cos\phi \ddot{Z}_1(t) + m_p s \cos\phi \ddot{Z}_2(t) + m_p s^2\ddot{\phi} + m_p s g \sin\phi = -m_p s \cos\phi \ddot{Z}_g(t) \quad (3-64)$$

By providing the time values of t , the solution of these three equations leads to the displacements of the tower for the first and second modes and the rotation angle of the pendulum in each time step.

3.5 Simulink controller of the BT

In this section Simulink controller of the hybrid nonlinear system is discussed. Consider Figure (3-1) where again the objectives in the control of this model are moving the tower and swinging angle of the pendulum.

The input of this system is a horizontal acceleration applied to the base of the tower. The pendulum rotates without friction. The Equations (3-62),(3-63) and (3-64) represent motions of this system in each time step, where g is the acceleration due to the gravity. Examining these equations, we notice that $\ddot{Z}_1(t)$, $\ddot{Z}_2(t)$ and $\ddot{\phi}(t)$ appear in each equation. The Simulink model using these equations contains an algebraic loop.

The model consists of a system with input $\ddot{Z}_g, Z_1, \dot{Z}_1, Z_2, \dot{Z}_2, \phi, \dot{\phi}$ and with output $\ddot{Z}_1, \ddot{Z}_2, \ddot{\phi}$ in each time step, as shown in Figure (3-4).

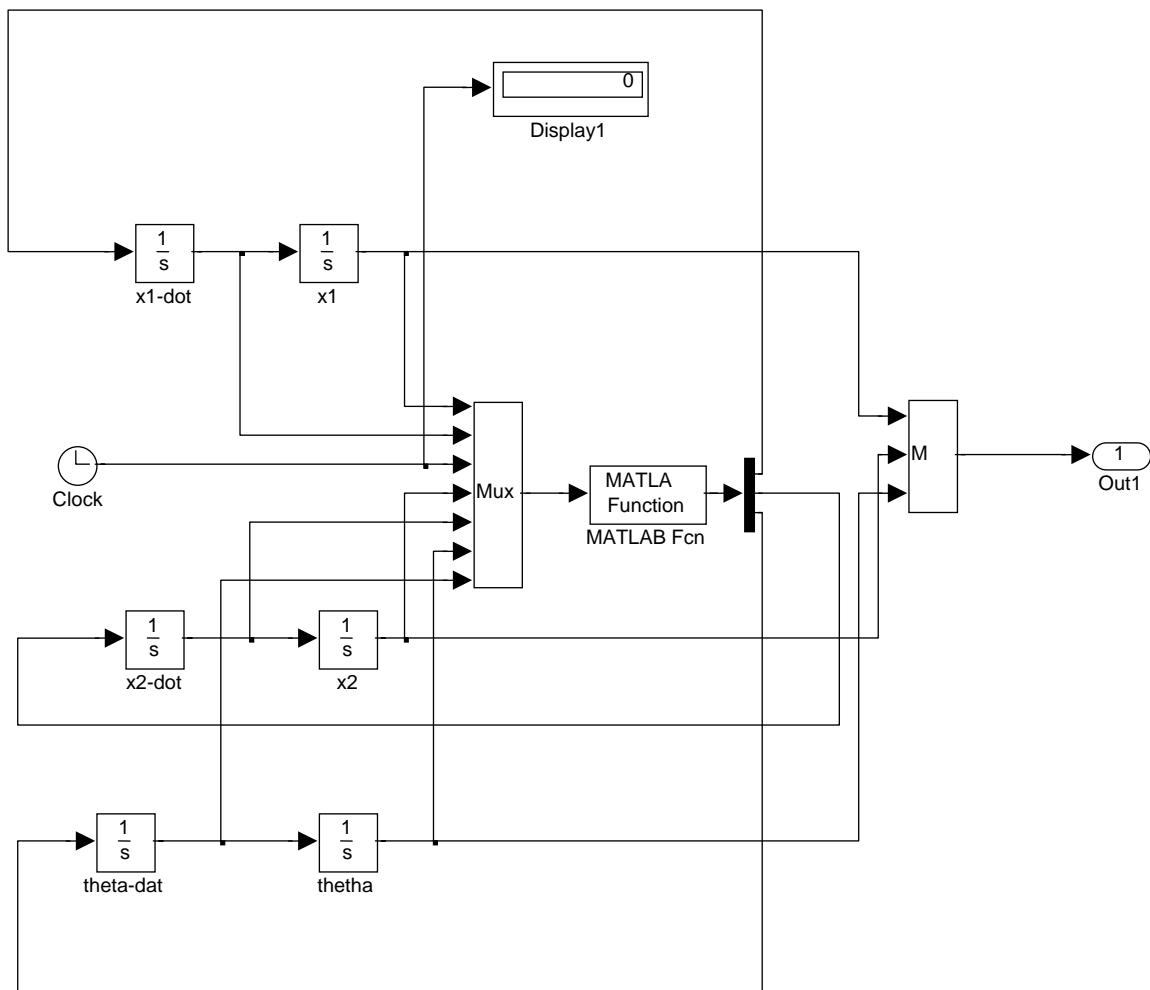


Figure 3-4 Simulink model of a hybrid system

The equations of motion are computed using the above mentioned model and the system parameters as well as mode shapes and frequencies are defined by Matlab7 software.

3.6 Numerical example for the BT

In order to follow the procedure of analysis of the hybrid system, a concrete tower of full circular cross-section is modeled and the mass of the pendulum is assumed to be concentrated at the end (mathematical pendulum), where the mass of the pendulum is 10% of the tower's mass shown in Figure (3-5). The numerical parameters of the system are assumed as follows:

$$L = 10m, E = 2.48e10 \frac{N}{m^2}, \bar{m} = 1884 \frac{kg}{m}, I = 0.0491m^4, \ell_1 = 10m, m_p = 1884kg$$

$$g = 9.81 \frac{m}{sec^2}, \zeta = 5\%, s = 1m \quad (3-65)$$

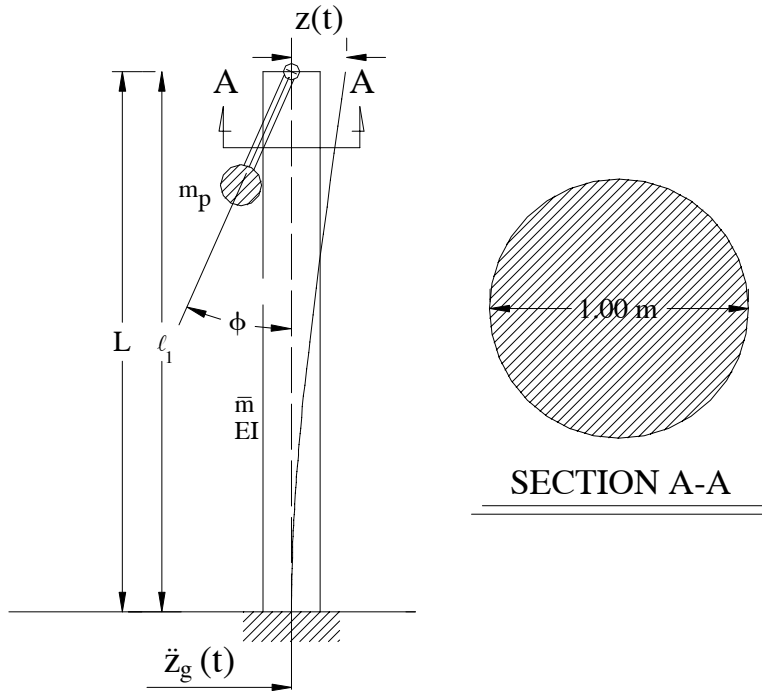


Figure 3-5 Bell-Tower specifications

Substituting the parameters of the tower in Equation (3-49) results in the linear eigenfrequencies of the main structure as

$$\begin{aligned}\omega_1 &= 28.26 \frac{rad}{sec} \\ \omega_2 &= 177.14 \frac{rad}{sec} \\ \omega_3 &= 496.00 \frac{rad}{sec}\end{aligned}\tag{3-66}$$

3.7 Analysis of the hybrid BT example

The coupled hybrid model of BT shown in Figure (3-5) is excited by the base acceleration, $\ddot{Z}_g(t)$. In the following section, the response of the BT is discussed considering different type of base excitations.

3.7.1 Unit acceleration base excitation

The hybrid system is excited by a base excitation of the Heaviside type⁸ $\ddot{Z}_g(t) = 1.H(t)$. Figure (3-6) shows the displacement of the top of the tower in the first and second modes as well as the rotation angle of the pendulum. In Figure (3-6), the Fast Fourier Transformation (FFT) in frequency domain is illustrated with regard to tower and pendulum. Zero crossing in time domain for the all records occurs simultaneously.

The results prove that the value of the first natural frequency of the system $\omega = 3.12 \text{ rad/sec}$ is smaller than the circular frequency of the simple pendulum

$$\omega_p = \sqrt{\frac{g}{s}} = 3.132 \text{ rad/sec}, \text{ and the first natural frequency of the tower } \omega_1 = 28.26$$

rad/sec . It can be seen that the oscillation of the pendulum and displacement of the tower are decreased and bounded in the time domain, although oscillation is not around the $Z = 0$ and $\phi = 0$ position.

⁸ Reference [1]

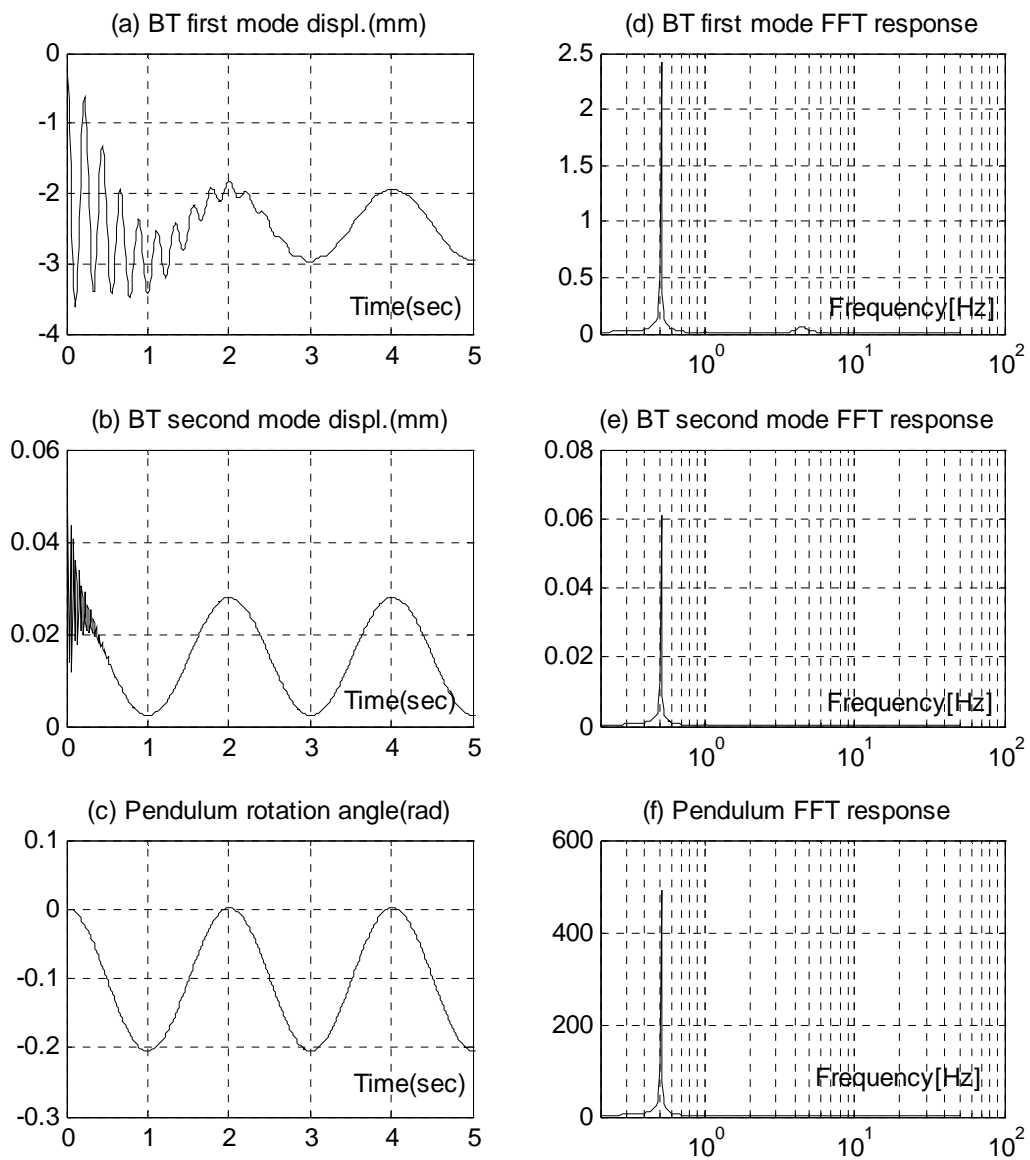


Figure 3-6 Constant initial excitation (Heviside step function) $\ddot{Z}_g = "1"$

3.7.2 Harmonic support excitation

The hybrid system is excited by a harmonic support excitation, $\ddot{Z}_g(t) = 1.0 \cos \nu t$. The excitation frequency ν is chosen as 1, 3, 5, 20, 28 and 177 *rad/sec*. The response of the system is connected to type of excitation and natural frequencies of the system. The base of the BT is excited by low and high frequencies and Figures (3-7) through (3-12) are obtained, indicating the response curve of displacement of the tower and oscillation angle of the pendulum, as well as the FFT in these miscellaneous circumstances. These figures show that frequency of the response is the combination of two parts. The first part shows the oscillation at the forcing or exciting frequency which is called steady state response, and second part shows the transient part of the system. By adjustment of excitation frequency around the natural frequencies of the BT as shown in Figures (3-8), (3-11) and (3-12) the amplitude of tower deformation and pendulum rotation grows enormously and it decreases by time. An additional resonance of the system also may be concluded whose frequency is changed by nonlinearity to $\omega_p \approx \frac{1}{3}\nu$ as the subharmonic resonance. Likewise an additional resonance of the system may be concluded whose frequency is changed by nonlinearity to $\omega_p \approx 3\nu$ as the superharmonic resonance.

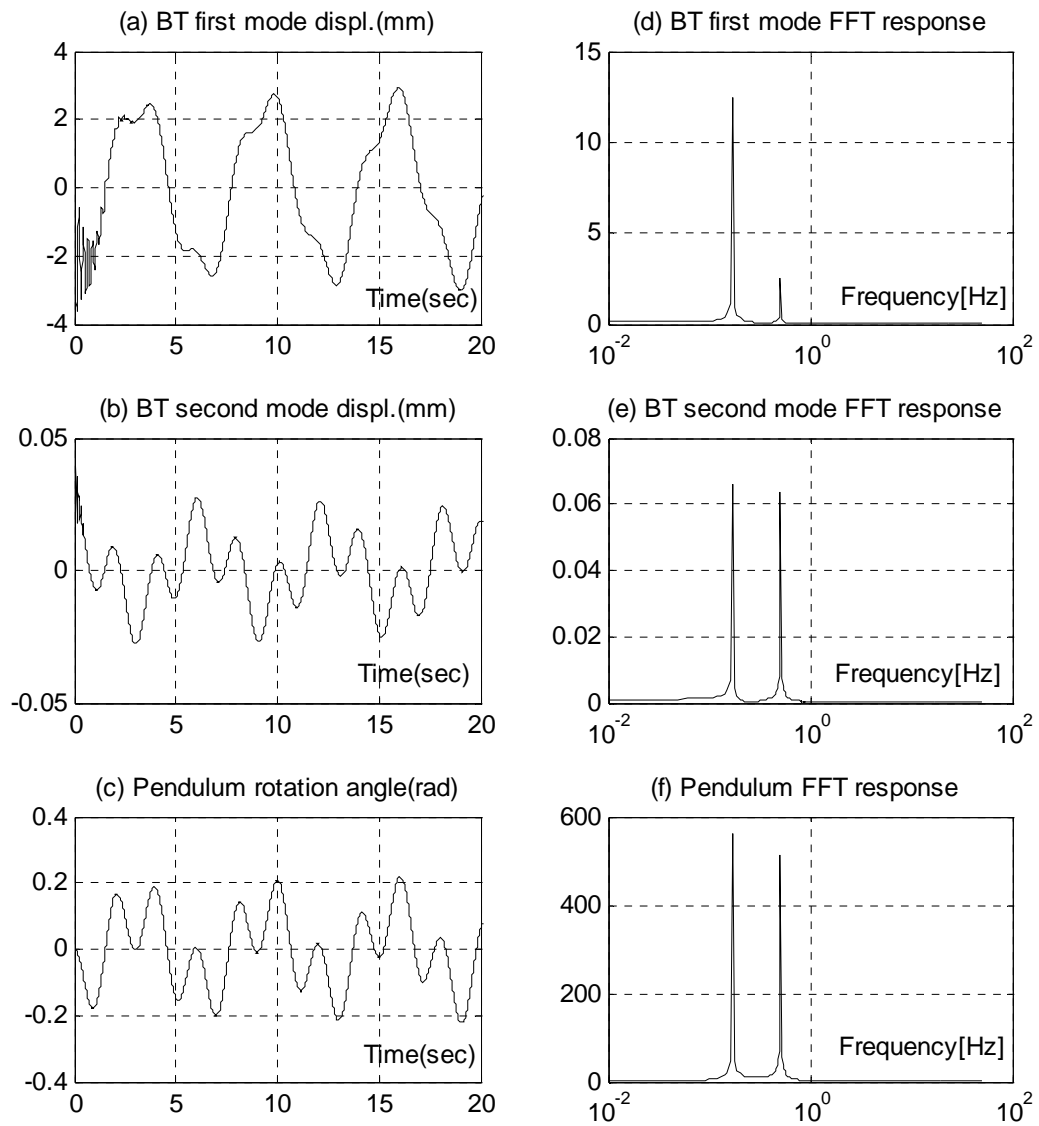


Figure 3-7 Harmonic base excitation $\ddot{Z}_g(t) = 1.0 \cos 1.0t$

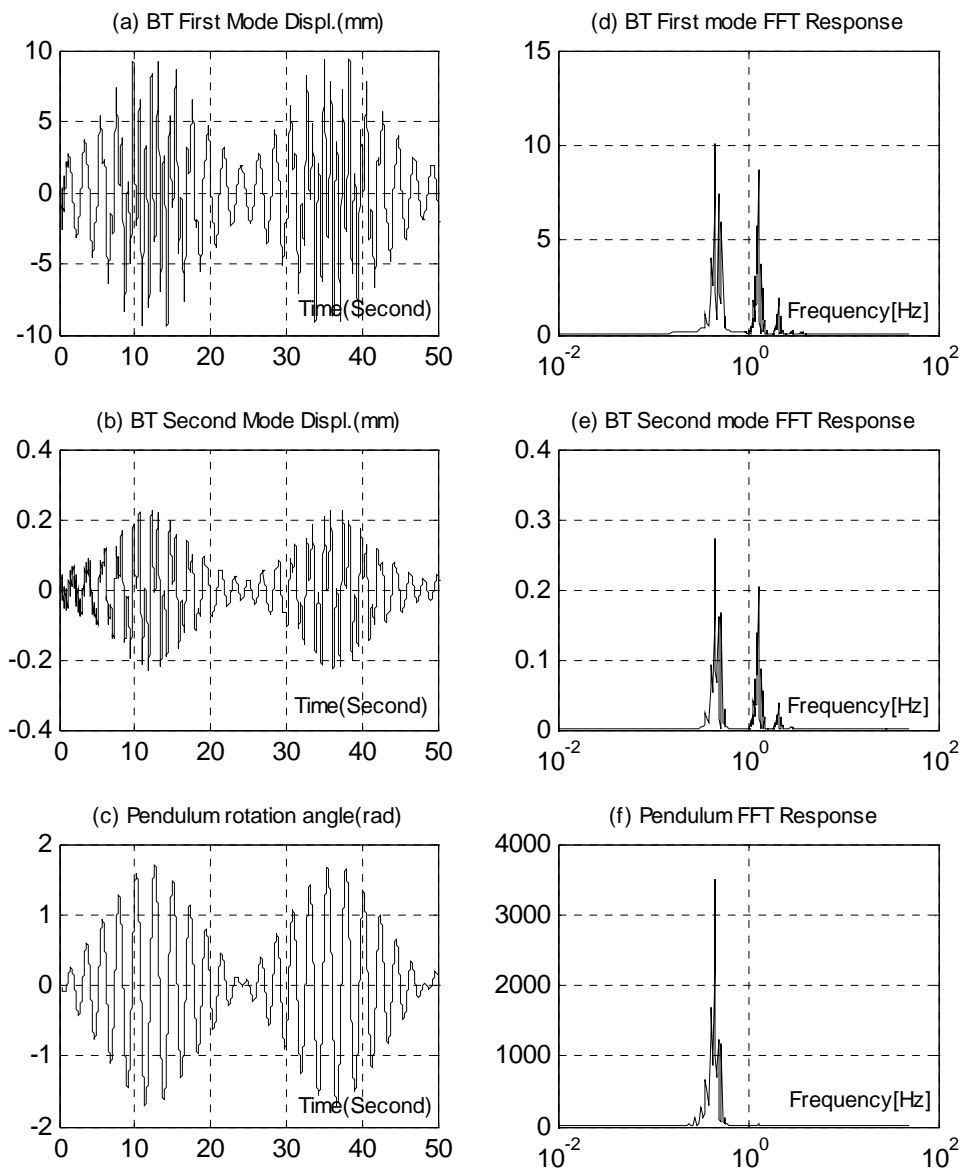


Figure 3-8 Harmonic base excitation $\ddot{Z}_g(t) = 1.0 \cos 3.0t$

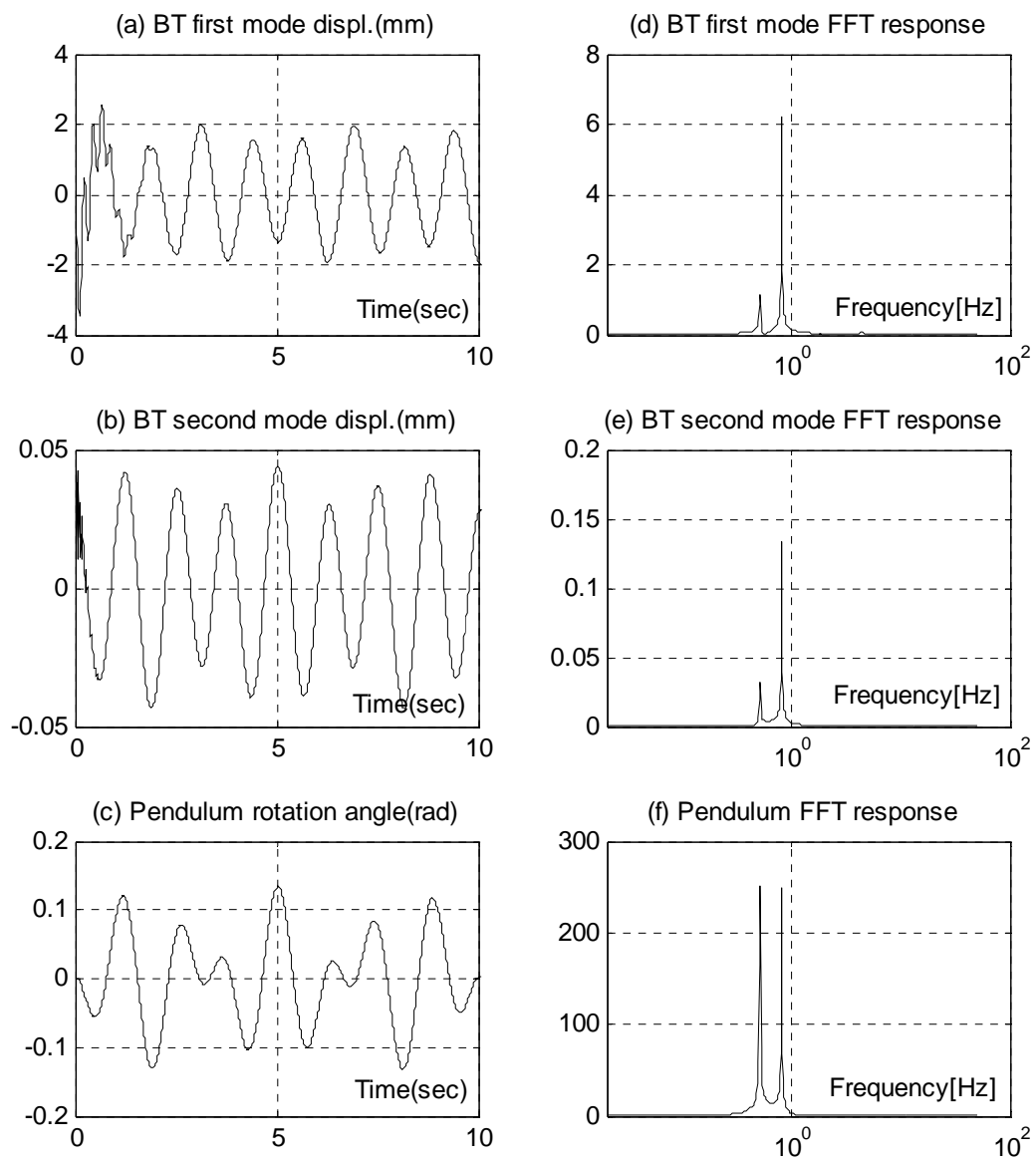


Figure 3-9 Harmonic base excitation $\ddot{Z}_g(t) = 1.0 \cos 5.0t$

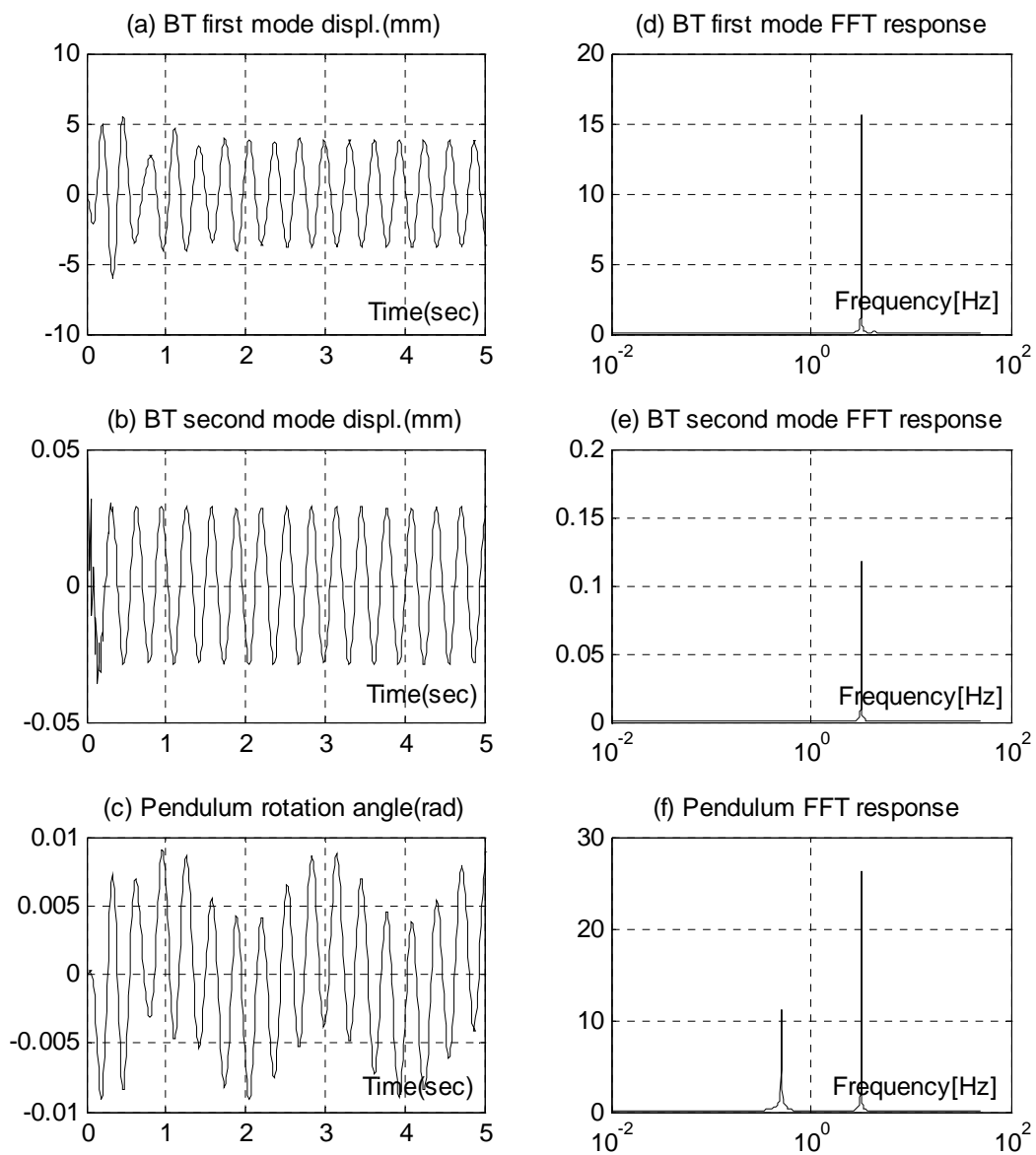


Figure 3-10 Harmonic base excitation $\ddot{Z}_g(t) = 1.0 \cos 20.0t$

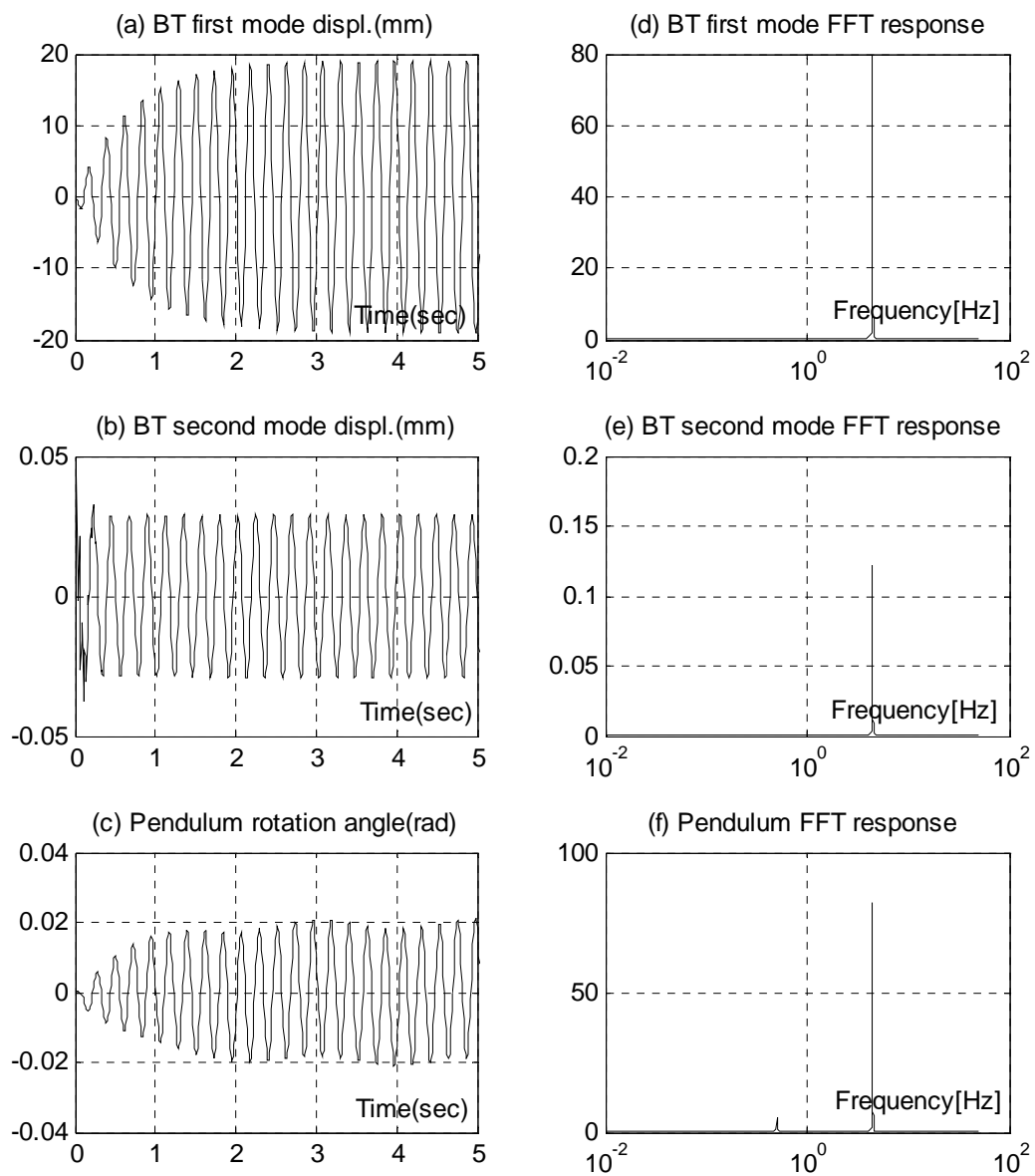


Figure 3-11 Harmonic base excitation $\ddot{Z}_g(t) = 1.0 \cos 28t$

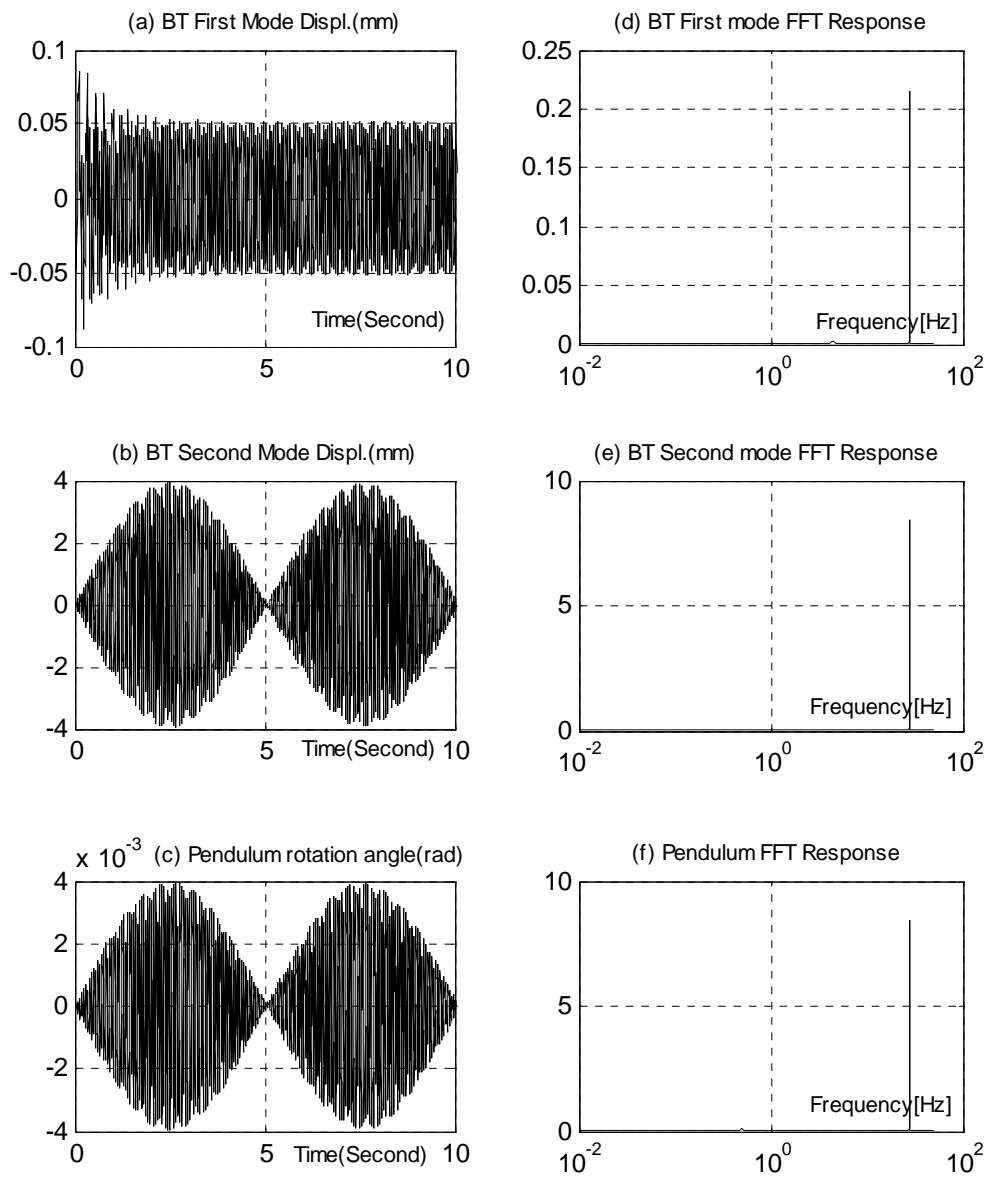


Figure 3-12 Harmonic base excitation $\ddot{Z}_g(t) = 1.0 \cos 177t$

3.7.3 Stationary random base excitation⁹

The excitation of the random process $\ddot{Z}_g(t)$ as discussed in Chapter 2, Part 2.7.5 is rendered as

$$\ddot{Z}_g(t) = \sum_{n=1}^N \sqrt{4S(\nu)\Delta\nu} \times \cos(n\Delta\nu t - \varphi) \quad (3-67)$$

where $S(\nu)$ expresses an ensemble spectral density function. $\nu_1, \nu_2, \dots, \nu_n$, and $S(\nu)$ are determined by numerical values, $\nu_i = i\Delta\nu$ and $\Delta\nu$ is equal to ν_1 . Moreover the phase angle within the interval between $0 \leq \varphi \leq 2\pi$ is selected in the form of random number. Thus the numerical values are evaluated as

$$S(\nu) = 1.5 \text{ m}^2 / \text{sec}^3$$

$$T = 100 \text{ sec}$$

$$\Delta\nu = \frac{2\pi}{T} = \frac{2\pi}{100} = 0.0628 \text{ rad/sec}$$

$$\nu_1 = \Delta\nu = 0.0628 \text{ rad/sec}$$

$$S(\nu) = 1.5 \text{ m}^2 / \text{sec}^3 \Rightarrow \ddot{Z}_g(t) = \sum_{n=1}^{50} 0.6138 \times \cos(0.0628nt - \varphi) \text{ m/sec}^2 \quad (3-68)$$

The Generated sample function is illustrated in Figure (3-13a) and the Fast Fourier transformation analysis is obtained in Figure (3-13b), indicating a constant energy level in time domain.

⁹ Reference [7]

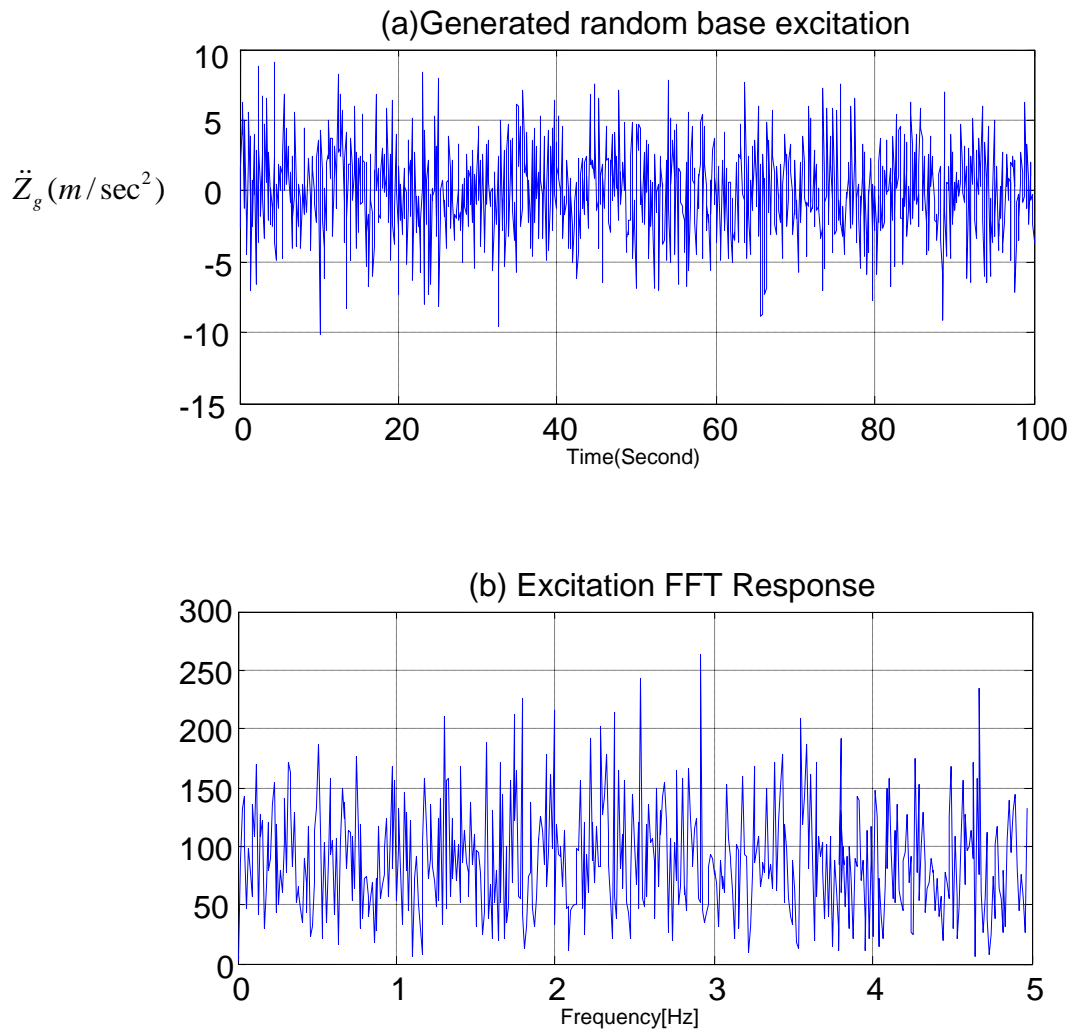


Figure 3-13 Random base excitation

The response curves of the tower and the pendulum in time domain are illustrated in Figure (3-14). The amplitude spectra of the system are illustrated in Figure (3-15). The response of the hybrid system depends on the type of excitation, natural frequency of system, the order of nonlinearity and the type of damping mechanism.

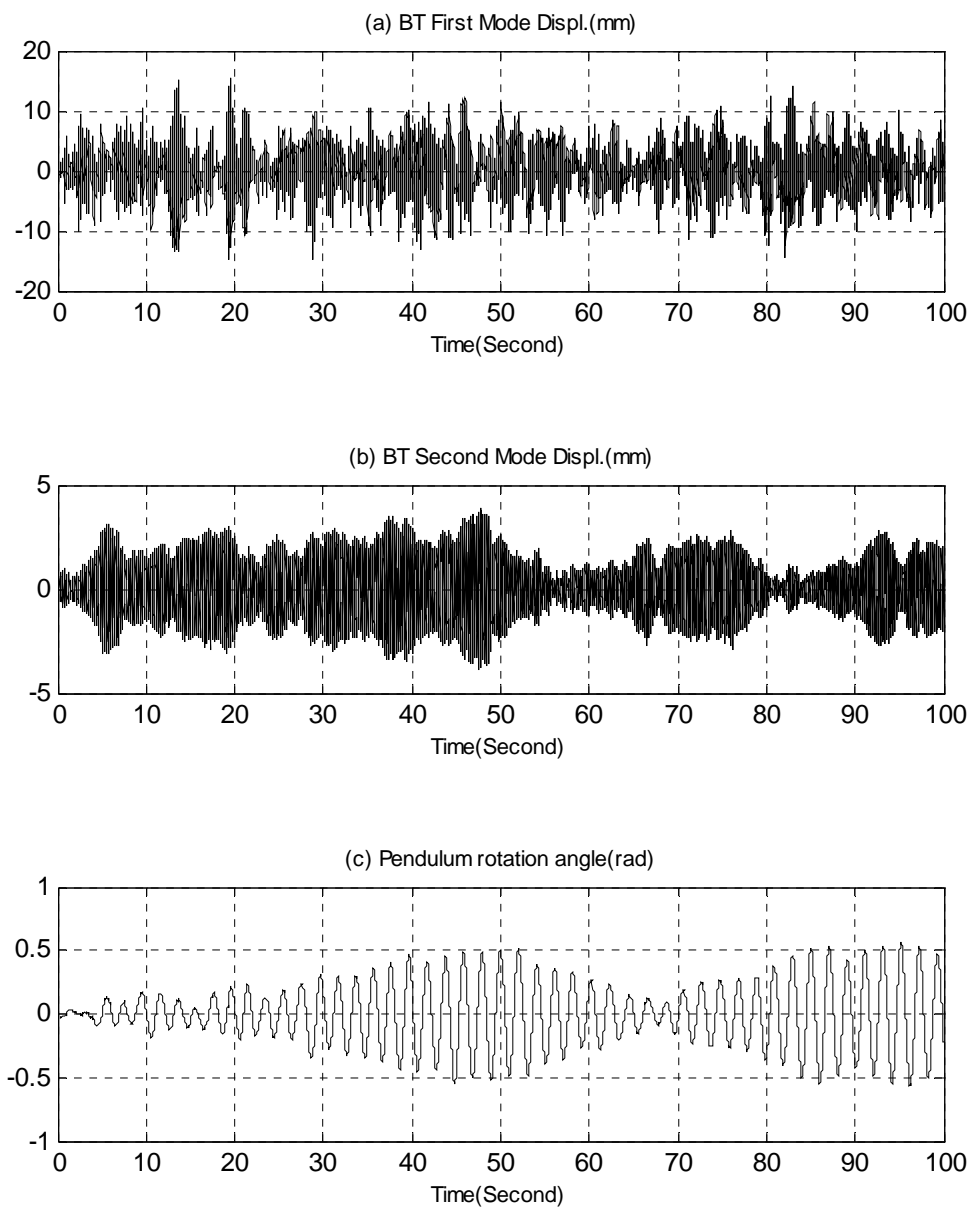
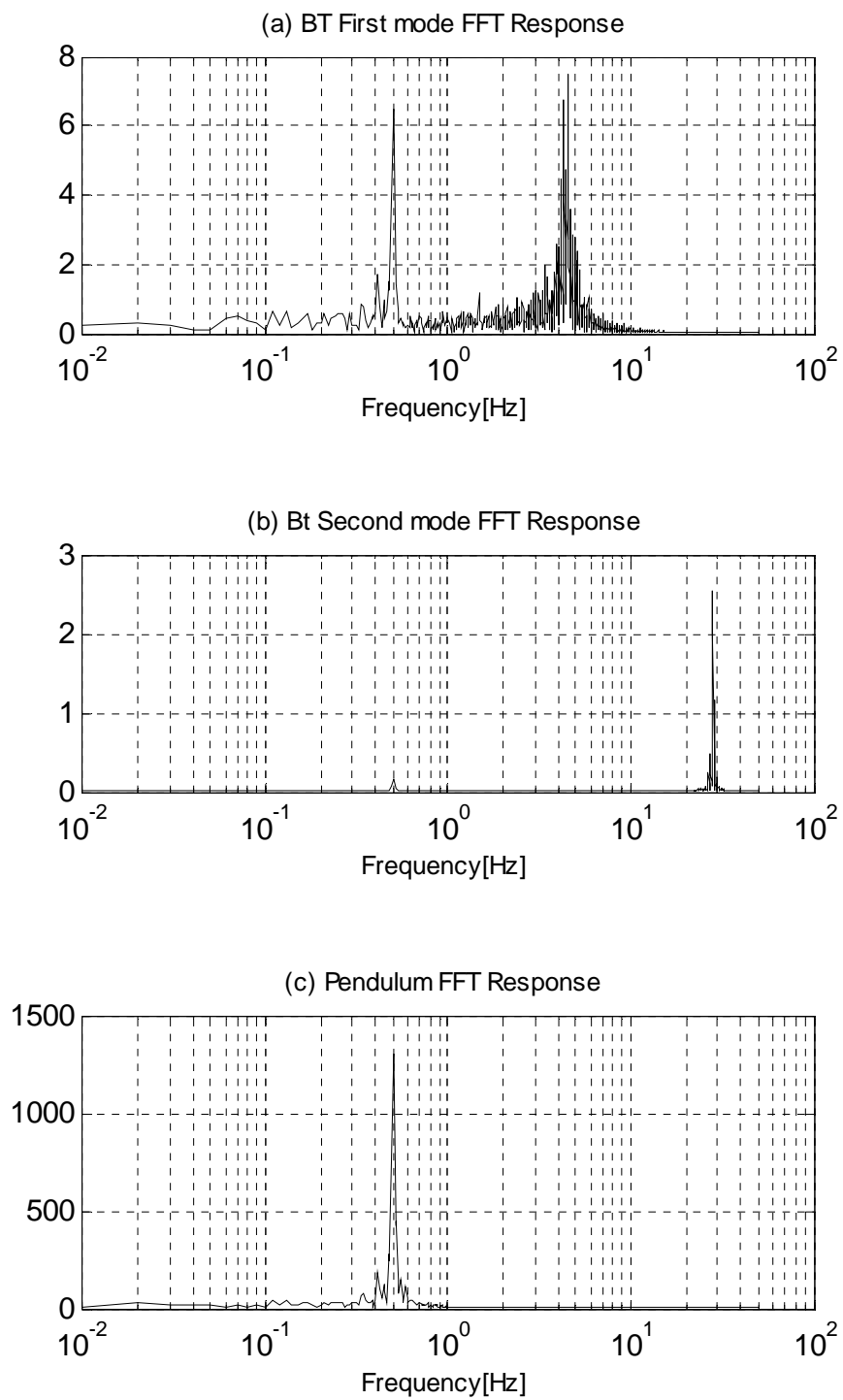


Figure 3-14 Random base excitation response in time domain

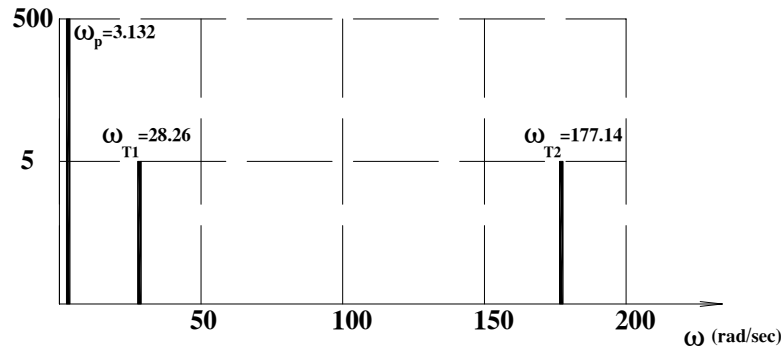
**Figure 3-15** Random base excitation FFT response

Comparing the circular frequencies of the uncoupled system

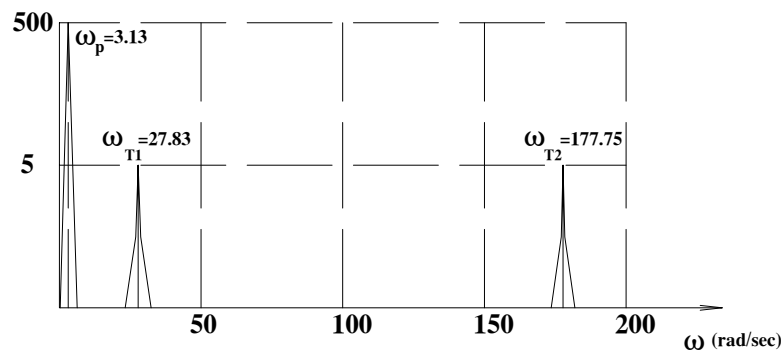
$$\begin{aligned}\omega_p &= 3.132 \frac{\text{rad}}{\text{sec}} \\ \omega_{T1} &= 28.26 \frac{\text{rad}}{\text{sec}} \\ \omega_{T2} &= 177.14 \frac{\text{rad}}{\text{sec}}\end{aligned}\tag{3-69}$$

with the frequencies in the hybrid coupled system, indicates that the second and third frequencies are obviously shifted. Deviation of the oscillation frequency of the pendulum, ω_p , is not remarkable.

Figures (3-16) shows the coupled system frequencies in contrast to the uncoupled system.



(a) UNCOUPLED SYSTEM



(b) COUPLED SYSTEM

Figure 3-16 Comparison between the coupled and uncoupled systems

3.8 References

1. Ziegler F., 'Mechanics of Solids and Fluids', Second edition, Technical University Vienna, Springer-Verlag New York-Vienna, 1998.
2. Weaver Jr.W., Timoshenko S.P., Young D.H., Department of Civil Engineering, Stanford University, 'Vibration Problems in Engineering', Fifth edition, John Wiley & Sons, 1989.
3. Shabana A. A., Department of Mechanical Engineering, University of Illinois at Chicago, 'Theory of Vibration', Springer-Verlag New York-Berlin Heidelberg, 1998.
4. Clough R.W., Penzien J., Department of Civil Engineering, University of California, 'Dynamic of Structures', McGraw-Hill, 1989.
5. Harris C.M., 'Shock and Vibration Handbook', Fourth edition, McGraw-Hill, 2003.
6. Chopra A.K., University of California at Berkeley, 'Dynamics of Structures', second edition, Prentice Hall, 2001.
7. Yang C.Y., University of Delaware Newark, Delaware, 'Random Vibration of Structure', John Wiley & Sons, 1985.

4

DYNAMIC BELL SWINGING ACTIONS IN THE BELL-TOWER

4.1 Introduction

Dynamic actions caused by bell ringing are typical characteristic aspects in BTs. Here the effect of the bell ringing on the BT is presented. Both the tower and bell system is estimated under the effect of forced bell vibrations. The bell acts like a pendulum and is supported at the top of the tower. Particular study of the nonlinear pendulum with special focus on subharmonics and superharmonics resonate frequencies is presented in this chapter. Vibrating forces are applied as an external moment, and nonstationary conditions in nonlinear pendulum is also discussed.

4.2 Dynamic reactions by bell ringing

One of the main external actions on the BT is the forces caused by ringing the bell. In the European systems the bells are swinging around the bell axis with rotation angles ranging up to 60 degrees. The (rigid) bell is modeled as a mathematical pendulum. If the amplitude of the pendulum is moderately large, the restoring moment is proportional to $\sin\phi$, which can be approximated by power series. Considering again the free vibration of simple mathematical pendulum, Equation (2-41) and substitution of the first two terms of the series results in

$$\ddot{\phi} + \frac{g}{\ell} \left(\phi - \frac{\phi^3}{6} \right) = 0 \quad (4-1)$$

4.2.1 Secondary resonance of the pendulum

An approximate method for simulating the motion of such a system consists of determining the particular solution that can be obtained by using the Lindstedt-Poincare technique¹

$\tau = \omega_N t$, ω_N is circular frequency of the nonlinear pendulum, $\omega = \sqrt{\frac{g}{\ell}}$ is the circular frequency of the linear pendulum. ω_N and ϕ can be expanded as

$$\phi = \varepsilon \phi_1(\tau) + \varepsilon^3 \phi_3(\tau) + \dots \quad (4-2)$$

$$\omega_N = \omega + \varepsilon^2 \omega_2 + \dots \quad (4-3)$$

where ε is a small dimensionless parameter characterizing the amplitude of motion. Substituting Equations (4-2) and (4-3) in Equation (4-1), and equating the coefficients for each power of ε to zero, leads to

$$\omega^2 (\phi_1'' + \phi_1) = 0 \quad (4-4)$$

$$\omega^2 (\phi_3'' + \phi_3) + 2\omega\omega_2\phi_1'' - \frac{1}{6}\omega^2\phi_1^3 = 0 \quad (4-5)$$

where ϕ'' is a second order derivative with respect to τ . Then the solution of Equation (4-4) is obtained as

$$\phi_1 = a \cos(\tau + \beta) \quad (4-6)$$

¹ Reference [7]

where a, β are constant values. Substituting in Equation (4-5) and eliminating condition of resonance becomes

$$\omega_2 = -\frac{1}{16}\omega a^2 \quad (4-7)$$

Thus the first approximation results in

$$\phi_1 = a \cos[\omega_N t + \beta] \quad (4-8)$$

$$\omega_N = \omega \left(1 - \frac{1}{16}\varepsilon^2 a^2\right)$$

If we limit our calculations to the second approximation, which is sufficient for practical problems, the corresponding solution becomes

$$\phi_3 = -\frac{1}{192}a^3 \cos(3\omega_N t + 3\beta) \quad (4-9)$$

and the total solution of ϕ by substituting in Equation (4-2) leads to

$$\phi = \varepsilon a \cos(\omega_N t + \beta) - \frac{\varepsilon^3 a^3}{192} \cos(3\omega_N t + 3\beta) \quad (4-10)$$

Considering the corresponding initial conditions (for $t=0$, $\phi = \varepsilon a$ and $\dot{\phi} = 0$) and substituting in Equation (4-2)

$$\begin{aligned} \varepsilon a &= \varepsilon \phi_1 + \varepsilon^3 \phi_3 + \dots \\ 0 &= \varepsilon \dot{\phi}_1 + \varepsilon^3 \dot{\phi}_3 + \dots \\ 0 &= \varepsilon \ddot{\phi}_1 + \varepsilon^3 \ddot{\phi}_3 + \dots \end{aligned} \quad (4-11)$$

These equations must hold for any amplitude of ε , thus

$$\phi_1(0) = a, \dot{\phi}_1(0) = 0 \quad (4-12)$$

$$\phi_3(0) = 0, \dot{\phi}_3(0) = 0$$

The general solution for ϕ_1 and ϕ_3 becomes

$$\phi_1 = a \cos \omega_N t \quad (4-13)$$

$$\phi_3 = c_1 \sin \omega_N t + c_2 \cos \omega_N t - \frac{1}{192} a^3 \cos 3\omega_N t \quad (4-14)$$

Consequently

$$\phi = \varepsilon a \cos \omega_N t + \frac{1}{192} \varepsilon^3 a^3 \cos \omega_N t - \frac{1}{192} \varepsilon^3 a^3 \cos 3\omega_N t \quad (4-15)$$

can be considered as a general solution of nonlinear pendulum free vibration by second approximation. Another characteristic of this equation is its secondary resonance which indicates that the free oscillations resonate terms are changed due to nonlinearity to one-third and three times of its natural frequency. For this reason the one-third subharmonic resonance and superharmonic resonance of order 3 may be considered in the response.

4.2.2 Forced introduced by bell ringing

The time-harmonic external moment is defined as

$$M(t) = M_0 \cos \nu t \quad (4-16)$$

where M_0 is the amplitude of the moment and ν is a constant forcing frequency. Figure (4-1) shows the action of oscillation in the simple pendulum induced by an external moment. The equation of motion for simple pendulum is given as²

$$m\ell^2 \ddot{\phi} + mg\ell \sin \phi = M_0 \cos \nu t \quad (4-17)$$

² Reference [2]

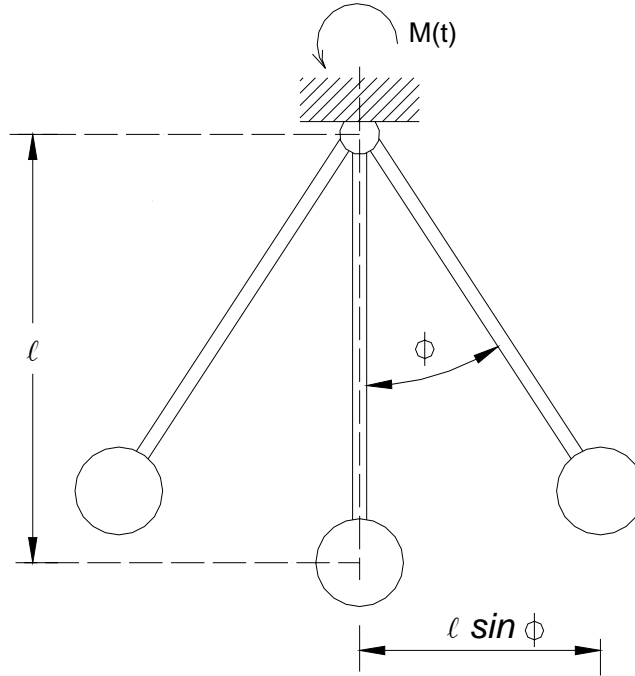


Figure 4-1 Simple pendulum, forced oscillation

4.3 Description of the BT

Figure (4-2) shows a BT system where the bell ringing action is considered to behave as a simple pendulum with concentrated mass at the end (mathematical pendulum). The numerical tower model uses the generalized continuous system having MDOF as described in Chapter 3.

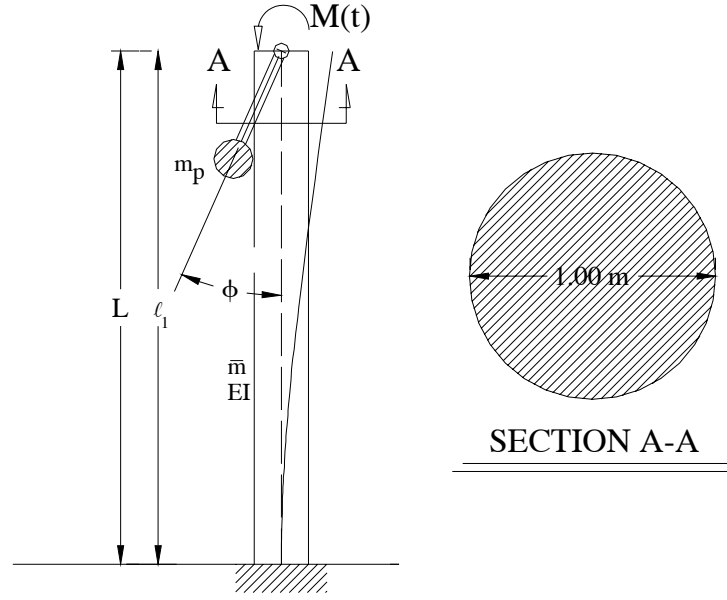


Figure 4-2 Tower plan and section

The main material used in the building is concrete and the cross-section of the tower is circular. Weight of the pendulum is 10% of the tower's total weight. The mechanical properties of the BT are considered as

$$L = 10\text{ m}, E = 2.48 \times 10^7 \frac{\text{N}}{\text{m}^2}, \bar{m} = 1884 \frac{\text{kg}}{\text{m}}, m_{\text{total}} = 18840\text{ kg}, m_p = 1884\text{ kg}$$

$$g = 9.81 \frac{\text{m}}{\text{sec}^2}, \zeta = 5\%, (A, I)_{\text{tower}} = (0.785\text{ m}^2, 0.0491\text{ m}^4), l_1 = 10\text{ m}, s = 1\text{ m} \quad (4-18)$$

4.4 Analysis of the BT

In this section the approach for simple pendulum is developed for the analysis of the forced vibration caused by bell ringing in the BT. The configuration of such a vibrating system is determined by using the forced vibration terms of the bell ringing in Equation (3-63) and substituting $\ddot{Z}_g = 0$ in Equations (3-62), (3-63) and (3-64). Thus the equations of motion are of the form

$$\begin{aligned}
(m_1 + m_p)\ddot{Z}_1(t) + m_p\ddot{Z}_2(t) + c_1\dot{Z}_1(t) + k_1Z_1(t) \\
+ m_p s(\ddot{\phi}\cos\phi - \dot{\phi}^2\sin\phi) = 0
\end{aligned} \tag{4-19}$$

$$\begin{aligned}
(m_2 + m_p)\ddot{Z}_2(t) + m_p\ddot{Z}_1(t) + c_2\dot{Z}_2(t) + k_2Z_2(t) \\
+ m_p s(\ddot{\phi}\cos\phi - \dot{\phi}^2\sin\phi) = 0
\end{aligned} \tag{4-20}$$

$$m_p s \cos \phi \ddot{Z}_1(t) + m_p s \cos \phi \ddot{Z}_2(t) + m_p s^2 \ddot{\phi} + m_p g s \sin \phi = M_0 \cos \nu t \tag{4-21}$$

4.4.1 Numerical modeling

The numerical modeling is based on details of the geometrical data of the tower and the pendulum. Simulink controller for such a vibrating system is used for computing in time domain. The excitation forces are originated from the swinging of the bell and the impact of forced vibration in the hinged support of the pendulum. The pendulum is assumed to rotate without friction. The solution of Equations (4-20), (4-21) and (4-22) gives the time domain response of the tower in first and second modes as well as rotation of the pendulum.

By inspecting these equations, we notice that $\ddot{Z}_1(t), \ddot{Z}_2(t)$ and $\ddot{\phi}(t)$ appear in each equation and thus indicates an inertia coupling. The model consists of a system with input $Z_1, \dot{Z}_1, Z_2, \dot{Z}_2, \phi, \dot{\phi}$ and $M(t)$ as well as output $\ddot{Z}_1, \ddot{Z}_2, \ddot{\phi}$ in each time step. Figure (4-3) shows the Simulink model of such a system. This model calculates the output response of the pendulum and the BT in each time step.

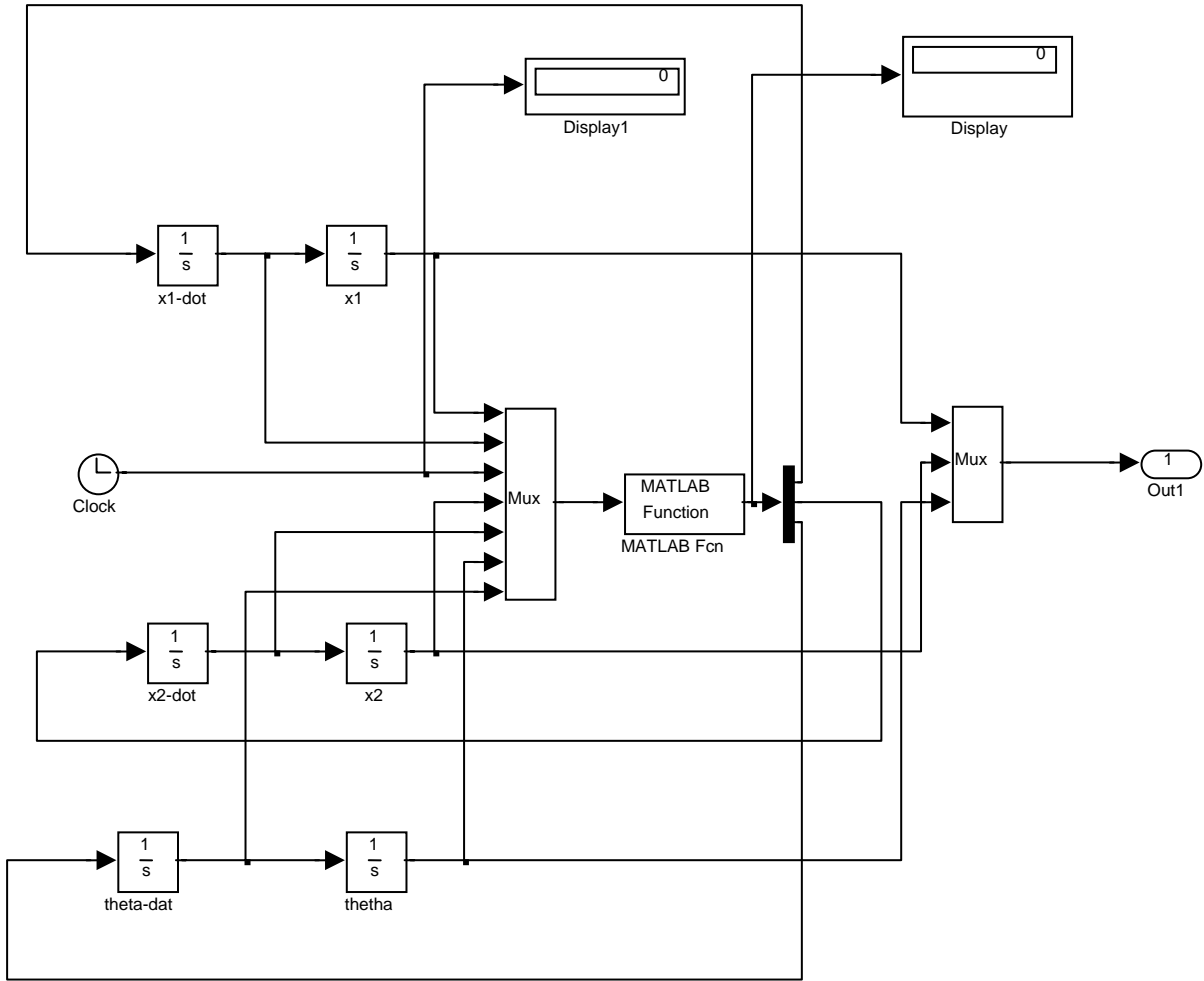


Figure 4-3 Simulink model (consists of the tower first & second mode and the pendulum)

According to the results of Section 3.6 in Chapter 3, the eigenfrequencies of the BT are

$$\omega_1 = 28.26 \frac{\text{rad}}{\text{sec}}, f_1 = 4.50 [\text{Hz}]$$

$$\omega_2 = 177.14 \frac{\text{rad}}{\text{sec}}, f_2 = 28.19 [\text{Hz}] \quad (4-22)$$

$$\omega_3 = 496.00 \frac{\text{rad}}{\text{sec}}, f_3 = 78.94 [\text{Hz}]$$

and

$$\omega_p = \sqrt{\frac{g}{\ell_p}} = 3.13 \frac{rad}{sec}, f_p = 0.50[Hz] \quad (4-23)$$

4.5 Analysis of the BT example

The coupled system of the BT and the bell is excited by an external dynamic moment $M(t)$. The response of the bell and the tower is discussed for variable types of moment.

4.5.1 Free oscillation

The BT system is excited by initial perturbation, $\phi_0 = 0.90 rad$, where ϕ_0 is the initial deviation angle of the pendulum which is allowed to oscillate without any external forces.

Figure (4-4) represents the displacement of the top of the BT for the first and second natural modes, and oscillation angle of the pendulum. In Figure (4-5) the amplitude spectras in frequency domain are shown for each mode of the tower and the pendulum. It is obvious that both the oscillations of the pendulum and the displacement of the tower are bounded by time decay. The $3\omega_p$ -subharmonic term is identified in the first and second modes of the tower. In contrast the effect of subharmonic resonance in the pendulum is low and negligible.

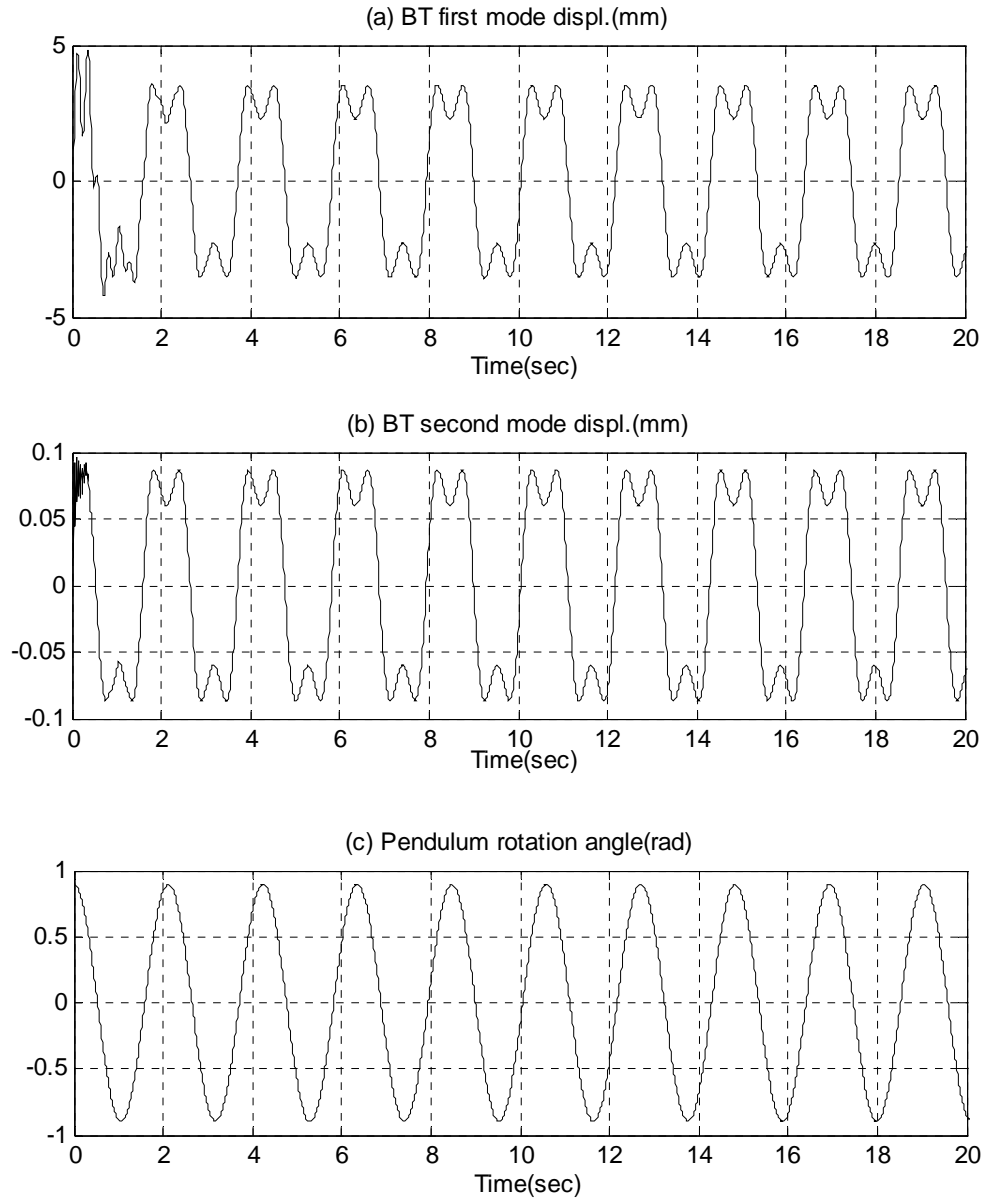


Figure 4-4 Time domain response due to initial perturbation $\phi_0 = 0.90 \text{ rad}$

- (a) Displacement at the top of the tower in the first natural mode
- (b) Displacement at the top of the tower in the second natural mode
- (c) Rotation angle of the pendulum

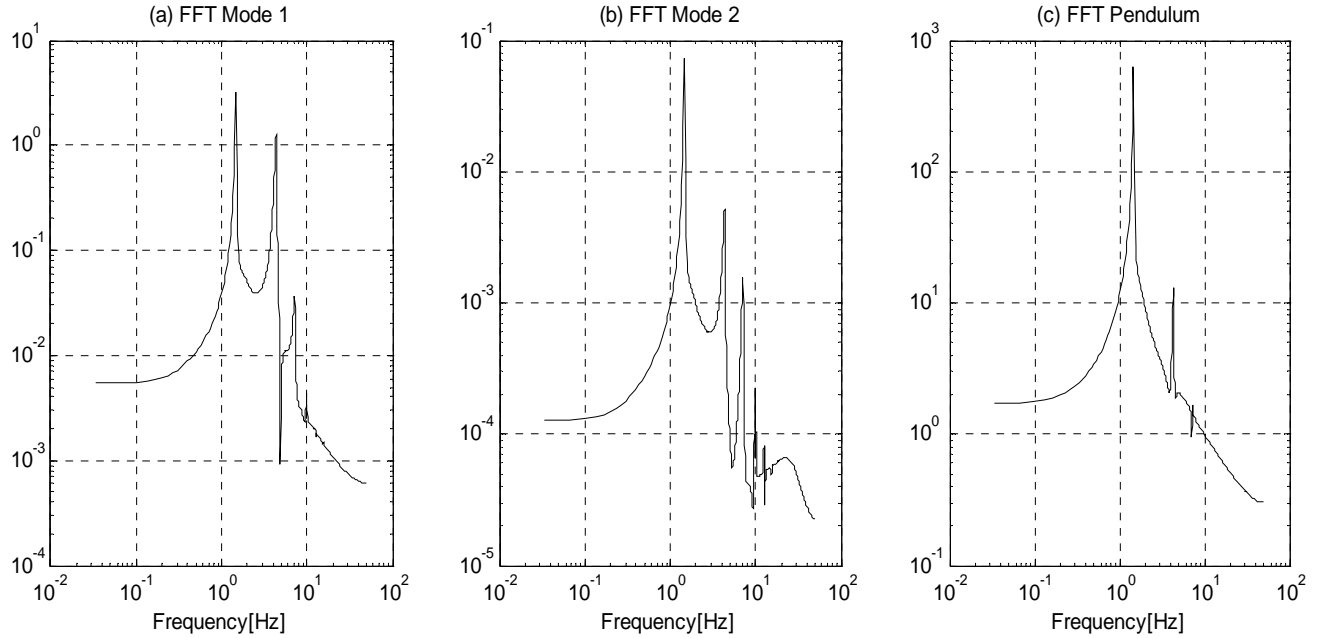


Figure 4-5 FFT spectrum response of BT effected by initial perturbation $\phi_0 = 0.90 \text{ rad}$

- (a) The tower first natural frequency
 (b) The tower second natural frequency
 (c) The pendulum

4.5.2 Harmonic external moment excitation

In this study the BT is excited by a harmonic external moment induced at the hinged support of the pendulum at the top of the tower. This excitation form is given as

$$M(t) = M_0 \cos vt, \quad M_0 = 6.47 \text{ kNm} \quad (4-24)$$

where M_0 represents the amplitude of the moment and in this case it is needed to rotate the pendulum by 20 degrees. Figures (4-6), (4-8), (4-10) and (4-12) show the response curve of the BT and oscillation angle of the pendulum in time domain. Figures (4-7), (4-9), (4-11) and (4-13) illustrate the FFT spectrum response of the BT and the pendulum.

The hybrid system is excited by a time-harmonic forced moment with forcing frequency of $\nu = \omega_p = 3.13 \text{ rad/sec}$ (linear resonance frequency of pendulum), $\nu = 5 \text{ rad/sec} > \omega_p$, $\nu = \omega_1 = 28.26 \text{ rad/sec}$ (first natural frequency of the tower) and $\nu = 1 \text{ rad/sec} < \omega_p$, respectively.

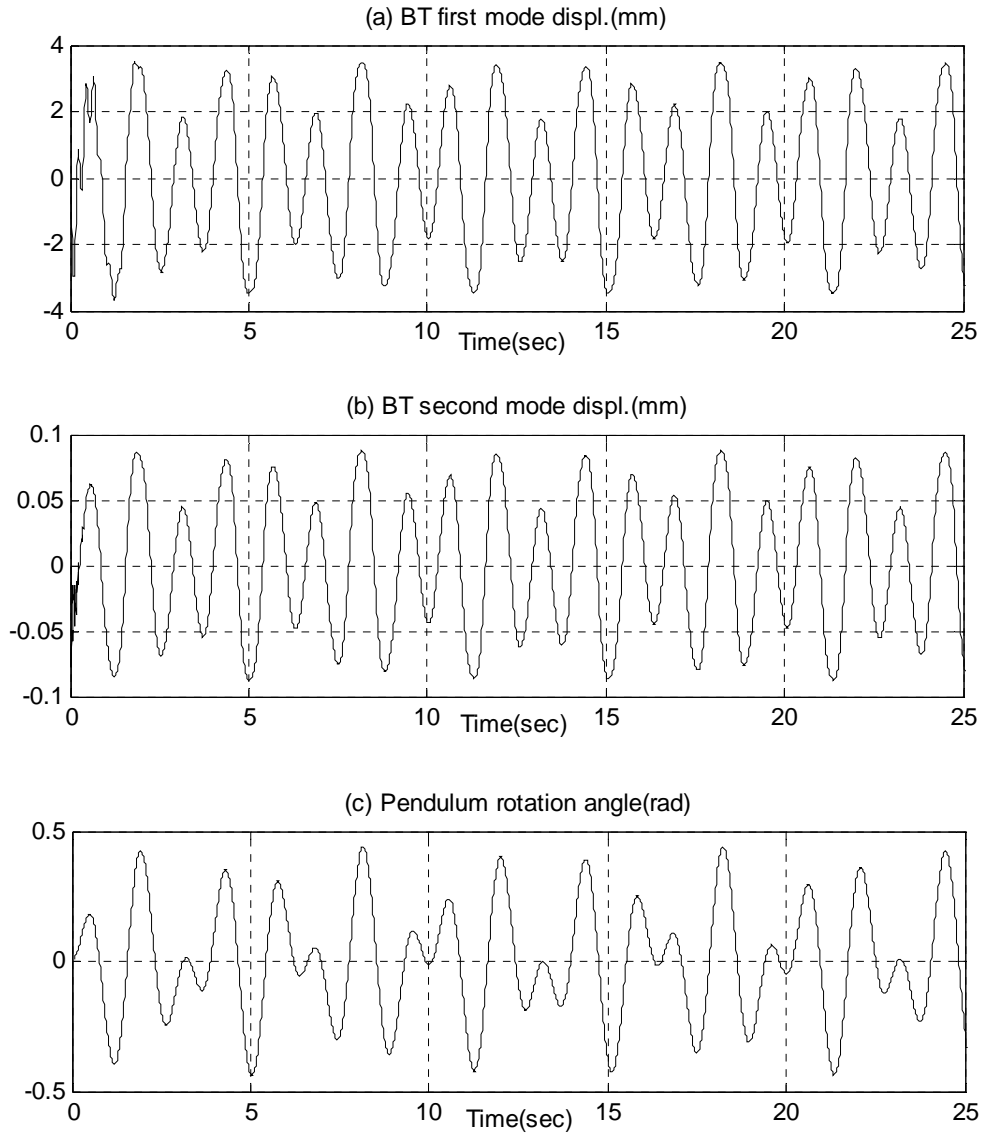


Figure 4-6 Time domain response due to harmonic moment excitation

$$M(t) = M_0 \cos \nu t, \quad M_0 = 6.47 \text{ kNm}, \quad \nu = 5 \text{ rad/sec}$$

- (a) Displacement at the top of the tower in the first natural mode
- (b) Displacement at the top of the tower in the second natural mode
- (c) Rotation angle of the pendulum

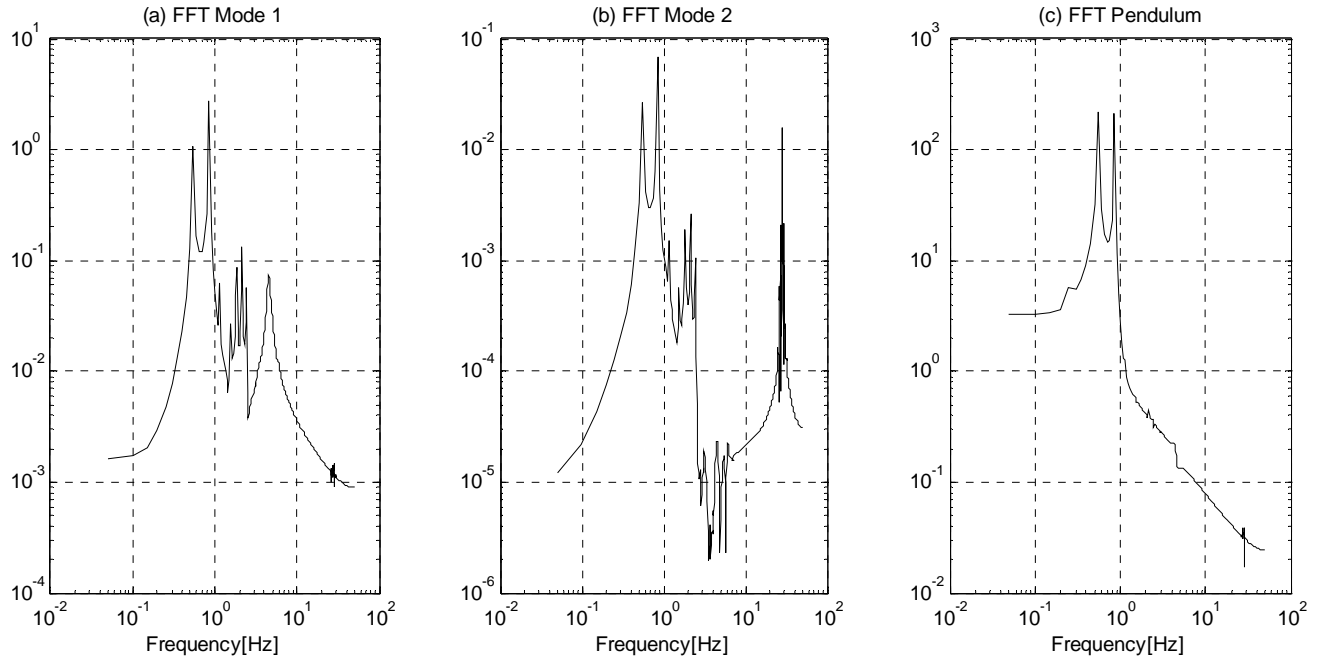


Figure 4-7 FFT spectrum response of the BT effected by harmonic moment

$$M(t) = M_0 \cos \nu t, \quad M_0 = 6.47 \text{ kNm}, \quad \nu = 5 \frac{\text{rad}}{\text{sec}}$$

- (a) The first natural frequency of the tower
- (b) The second natural frequency of the tower
- (c) The pendulum

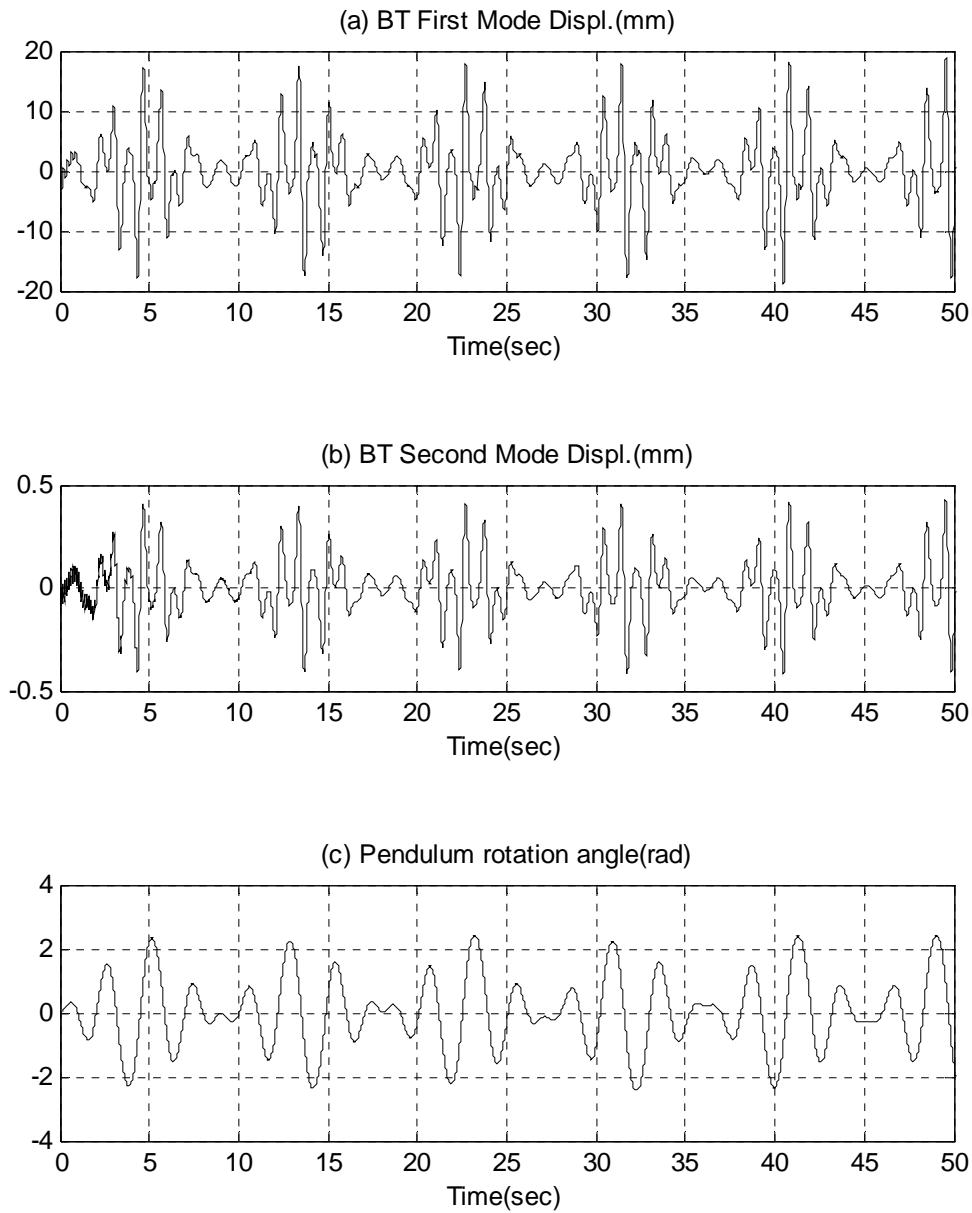


Figure 4-8 Time domain response due to harmonic moment

$$M(t) = M_0 \cos \nu t, \quad M_0 = 6.47 \text{ kNm}, \quad \nu = 3.13 \frac{\text{rad}}{\text{sec}}$$

- (a) Displacement at the top of the tower in the first natural mode
- (b) Displacement at the top of the tower in the second natural mode
- (c) Rotation angle of the pendulum

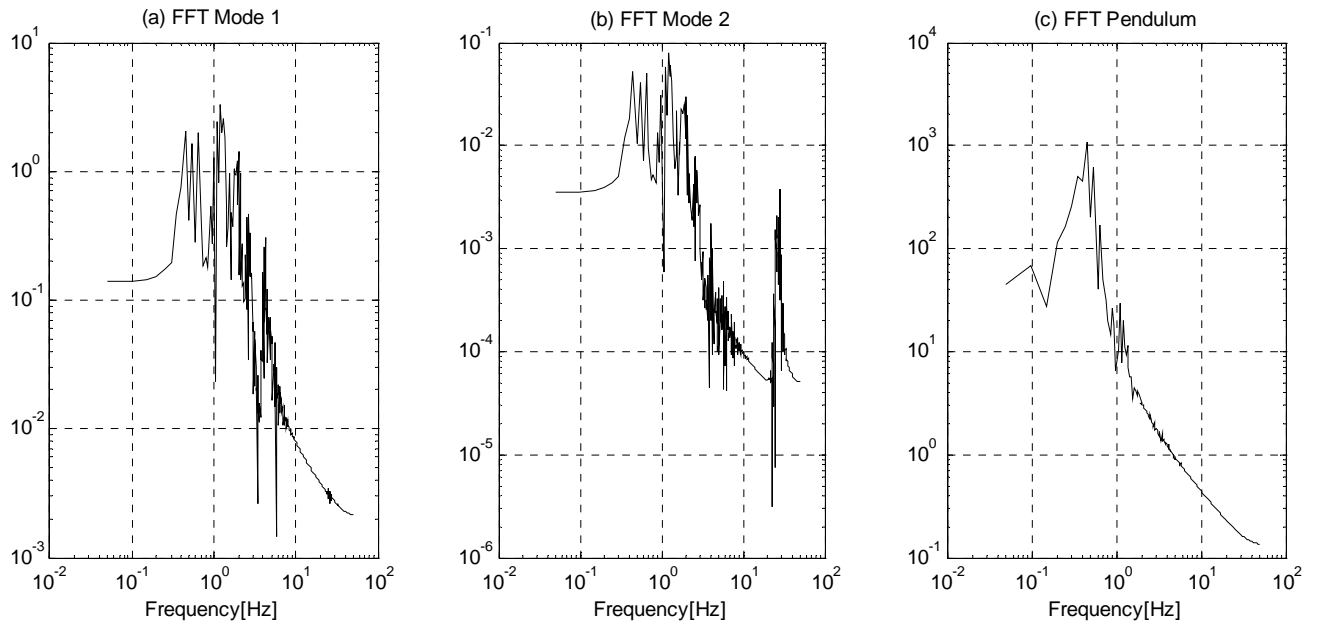


Figure 4-9 FFT spectrum response of the BT effected by harmonic moment

$$M(t) = M_0 \cos \nu t, \quad M_0 = 6.47 \text{ kNm}, \quad \nu = 3.13 \frac{\text{rad}}{\text{sec}}$$

- (a) The first natural frequency of the tower
- (b) The second natural frequency of the tower
- (c) The pendulum

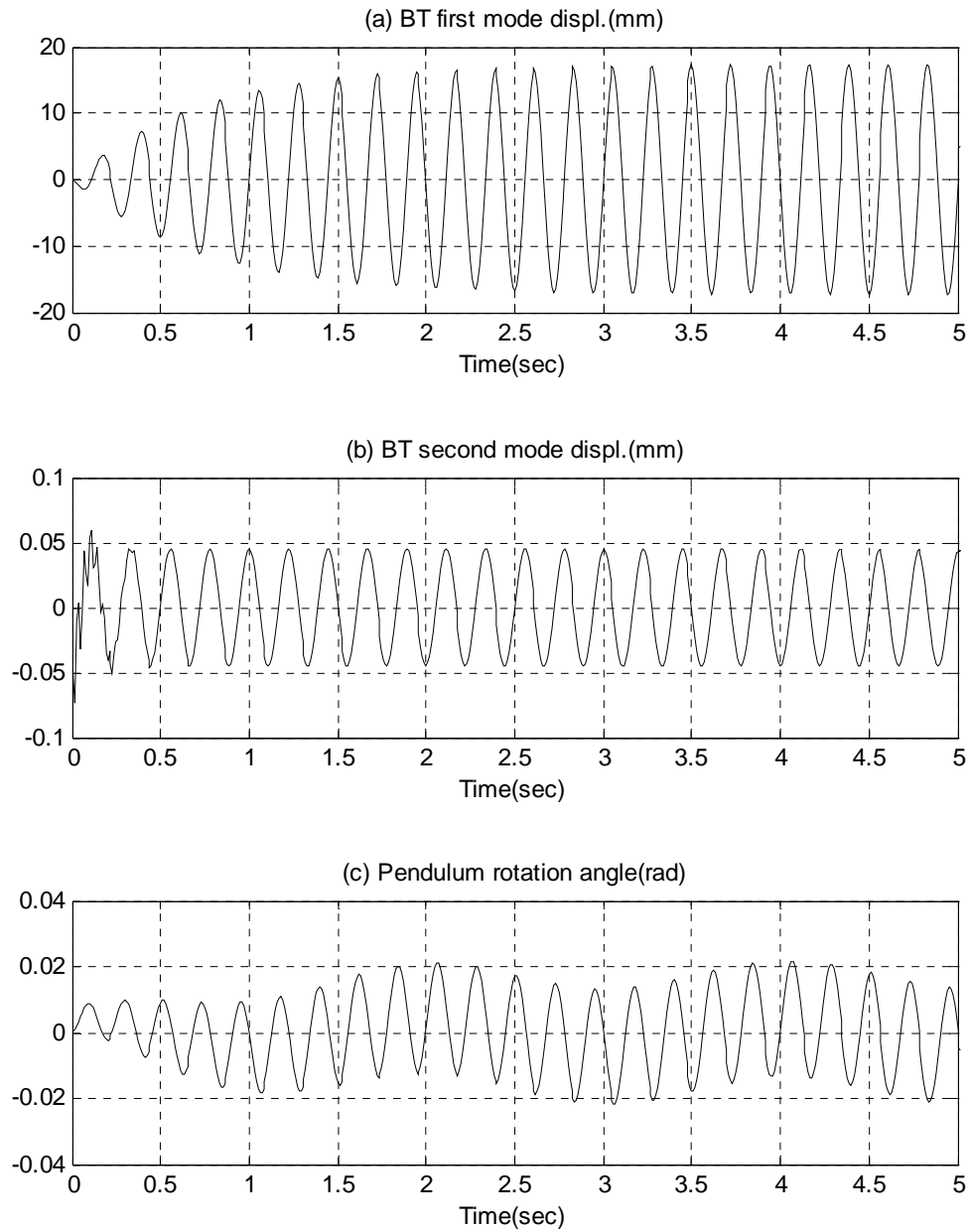


Figure 4-10 Time domain response due to harmonic moment

$$M(t) = M_0 \cos \nu t, \quad M_0 = 6.47 \text{ kNm}, \quad \nu = 28.26 \frac{\text{rad}}{\text{sec}}$$

- (a) Displacement at the top of the tower in the first natural mode
- (b) Displacement at the top of the tower in the second natural mode
- (c) Rotation angle of the pendulum

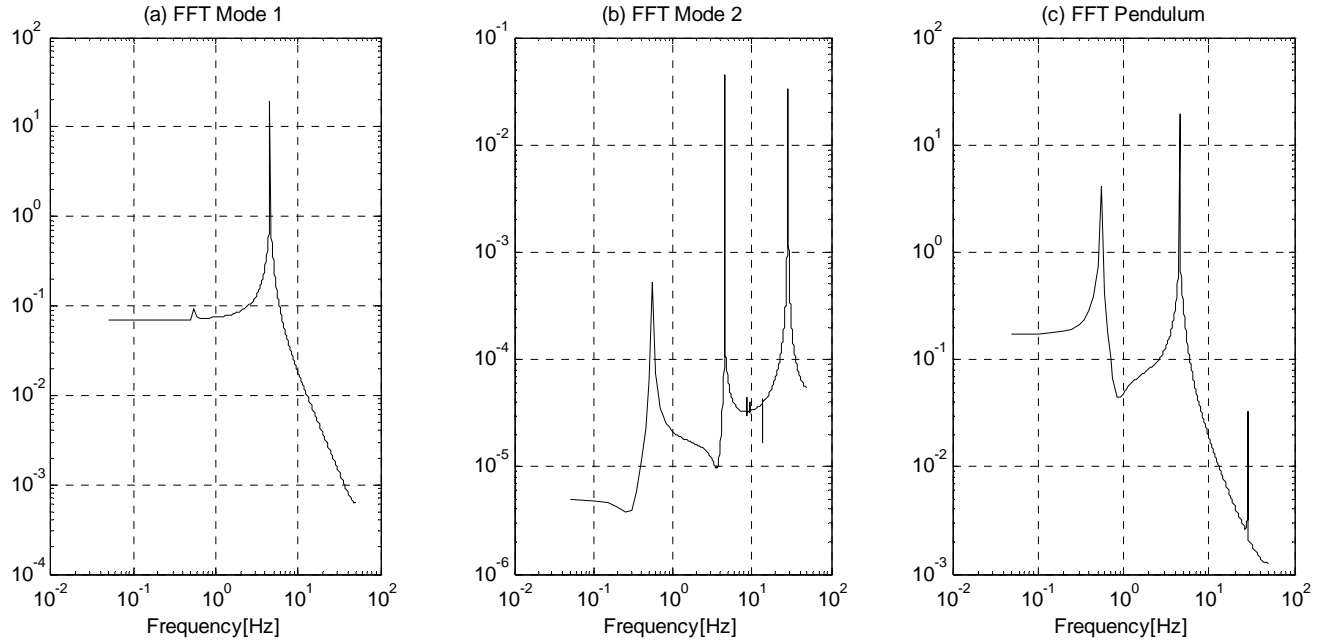


Figure 4-11 FFT spectrum response of the BT effected by harmonic moment

$$M(t) = M_0 \cos \nu t, \quad M_0 = 6.47 \text{ kNm}, \quad \nu = 28.26 \frac{\text{rad}}{\text{sec}}$$

- (a) The first natural frequency of the tower
- (b) The second natural frequency of the tower
- (c) The pendulum

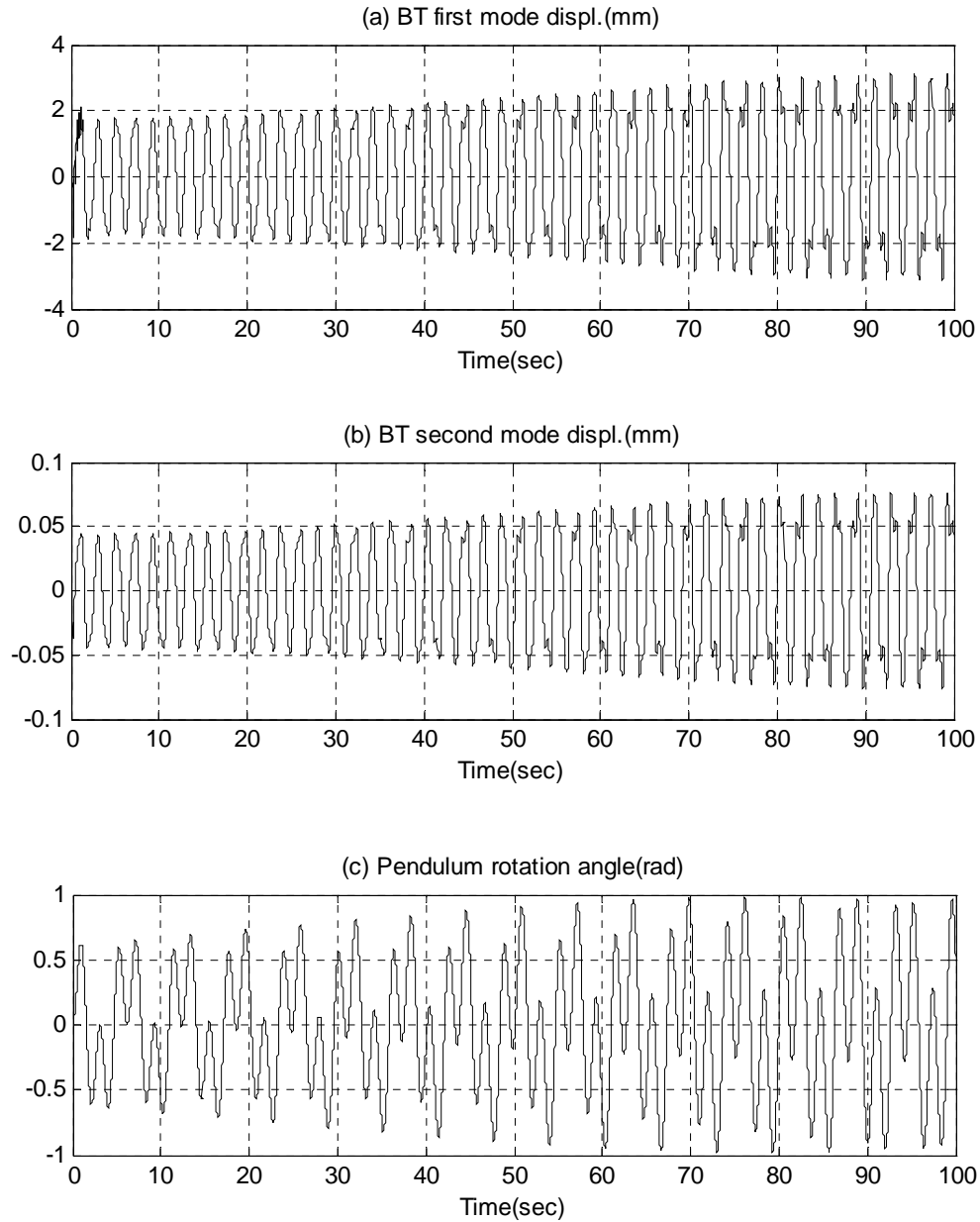


Figure 4-12 Time domain response due to harmonic moment

$$M(t) = M_0 \cos \nu t, \quad M_0 = 6.47 \text{ kNm}, \quad \nu = 1 \frac{\text{rad}}{\text{sec}}$$

- (a) Displacement at the top of the tower in the first natural mode
- (b) Displacement at the top of the tower in the second natural mode
- (c) Rotation angle of the pendulum

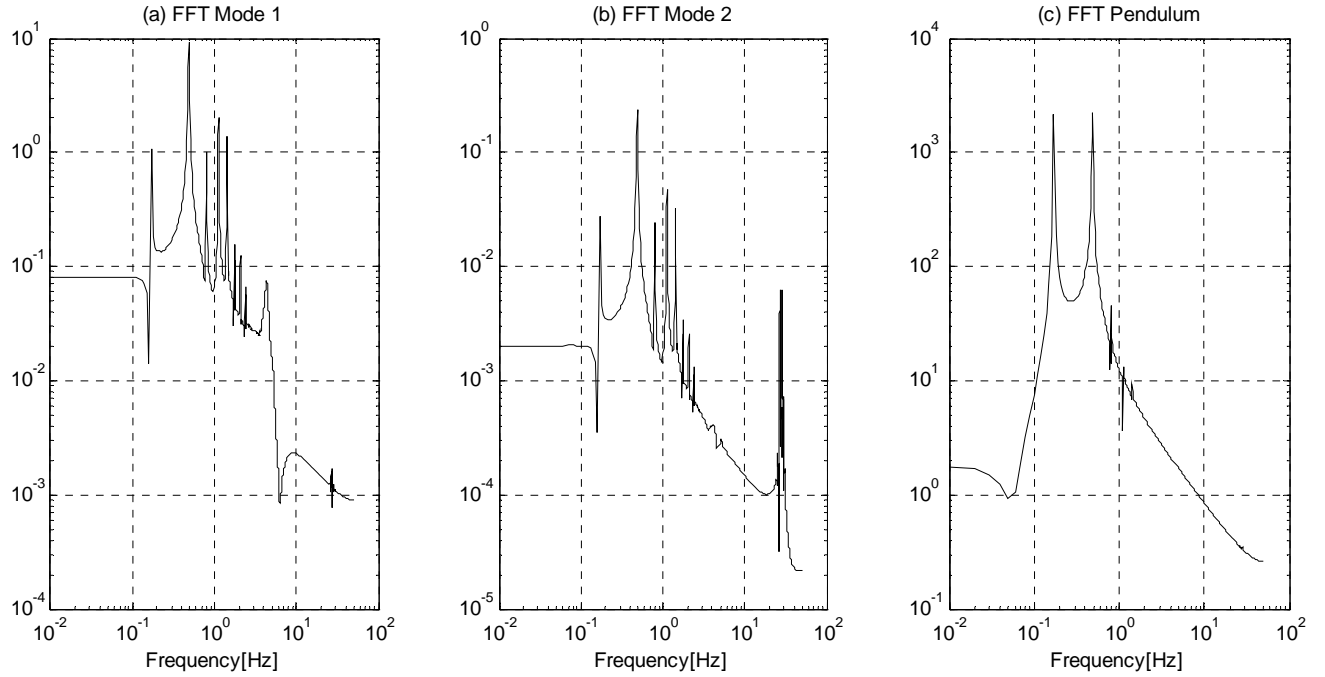


Figure 4-13 FFT spectrum response of the BT effected by harmonic moment

$$M(t) = M_0 \cos \nu t, \quad M_0 = 6.47 \text{ kNm}, \quad \nu = 1 \frac{\text{rad}}{\text{sec}}$$

- (a) The first natural frequency of the tower
- (b) The second natural frequency of the tower
- (c) The pendulum

Figure (4-12) shows the nonstationary effects for values $\phi > 0.4 \text{ rad}$ and $\nu < \omega_p$. It can be seen that the harmonic excitation with resonance frequency of the tower, illustrated in Figure (4-10), causes enormous increase of displacement response in the tower. Likewise excitation at resonance frequency of the pendulum causes an increase of the total system response and saturation in the time domain as shown in Figure (4-8). Maximum oscillation occurs when the frequency of excitation is adjusted to the natural frequency of each mode.

In the BT system with nonlinear influence of the pendulum ($\phi > 0.4\text{rad}$) in addition to the primary resonance, subharmonic resonance $\Omega_1 \approx 3\omega_p$ and the superharmonic resonance $\Omega_2 = \frac{1}{3}\omega_p$ appear in the tower displacement response, Figures (4-7) and (4-13). On the contrary these effects vanish in the pendulum rotation response.

4.6 Nonstationary vibration in the BT

In the preceding section of this chapter about nonstationary condition in the BT, only harmonic vibration of the coupled nonlinear pendulum is considered. According to Equation (4-21) and rearranging the terms

$$\ddot{\phi} + \omega_p^2 \sin \phi = a_0 \cos \nu t - \frac{1}{s} \cos \phi (\ddot{Z}_1(t) + \ddot{Z}_2(t)) \quad (4-25)$$

$$a_0 = \frac{M_0}{m_p s^2}, \quad \omega_p = \sqrt{\frac{g}{s}}$$

and substitution of the first two terms of the power series into the above equation

$$\begin{aligned} \sin \phi &= \phi - \frac{\phi^3}{6} \\ \cos \phi &= 1 - \frac{\phi^2}{2} \end{aligned} \quad (4-26)$$

results in

$$\ddot{\phi} + \omega_p^2 \left(\phi - \frac{\phi^3}{6} \right) = a_0 \cos \nu t - \frac{1}{s} \left(1 - \frac{\phi^2}{2} \right) (\ddot{Z}_1(t) + \ddot{Z}_2(t)) \quad (4-27)$$

This expression is related to the Duffing's equation³ of vibration.

As a first approximation we assume

$$\phi = a \cos \nu t \quad (4-28)$$

$$\ddot{Z}_1(t) + \ddot{Z}_2(t) = sb \cos(\nu t - \varepsilon)$$

where a and b are constant values. Substituting into the equation (4-27) gives

$$-\nu^2 a \cos \nu t + \omega_p^2 \left(a \cos \nu t - \frac{a^3 \cos^3 \nu t}{6} \right) = a_0 \cos \nu t - b \cos(\nu t - \varepsilon) \left(1 - \frac{a^2 \cos^2 \nu t}{2} \right) \quad (4-29)$$

$$b \cos(\nu t - \varepsilon) = b_1 \cos \nu t + b_2 \sin \nu t$$

Using the Ritz averaging method⁴ we obtain an approximate solution as

$$\begin{aligned} \int_0^\tau \left[-\nu^2 a \cos \nu t + \omega_p^2 \left(a \cos \nu t - \frac{a^3 \cos^3 \nu t}{6} \right) - a_0 \cos \nu t \right. \\ \left. + (b_1 \cos \nu t + b_2 \sin \nu t) \left(1 - \frac{a^2 \cos^2 \nu t}{2} \right) \right] \cos \nu t dt = 0 \end{aligned} \quad (4-30)$$

Integration and rearrangement of terms results in

$$-\frac{1}{8} a^3 - \frac{3}{8} \frac{b_1}{\omega_p^2} a^2 + \left(1 - \frac{\nu^2}{\omega_p^2} \right) a + \frac{b_1 - a_0}{\omega_p^2} = 0 \quad (4-31)$$

For any given values of the parameters ω_p, ν, b_1, a_0 Equation (4-31) represents an approximate relationship between the amplitude a and the forcing frequency ν for the steady state vibration. This system shows a softening in the stiffness.

³ Reference [8]

⁴ Reference [2]

Substitution of numerical values of the BT, $\omega_p = 3.13 \text{ rad/sec}$, $b_1 = 4 \text{ mm}$, $a_0 = 3.43 \text{ N/kgm}$, and solving a for given values of $\frac{\nu}{\omega_p}$ from Equation (4-31) results in the nonlinear frequency response curve as illustrated in Figure (4-14).

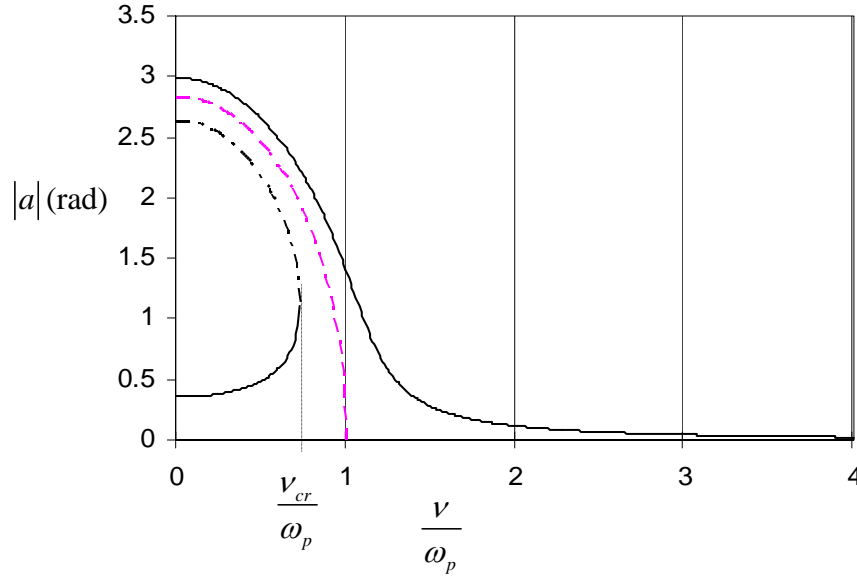


Figure 4-14 Pendulum amplitude versus harmonic excitation frequency ν in nonlinear condition

The amplitude-frequency relationship for free vibrations is obtained by setting a_0 and b_1 equal to zero in the Equation (4-31).

$$-\frac{1}{8}a^3 + \left(1 - \frac{\nu^2}{\omega_p^2}\right)a = 0 \quad (4-32)$$

ν represents the angular frequency of free nonlinear vibrations. The response spectrum shown in Figure (4-14) represents nonstationary phenomenon observed in nonlinear system of pendulum (bell) in contact with linear tower, where the hybrid system is subjected to harmonic forcing function.

Increasing the forcing frequency from $\nu = 0$ to $\nu > \nu_{cr}$ will cause a jump in the steady state amplitude response, where the phase angle shifts from 0° to 180° . On the other hand, decreasing the forcing frequency from $\nu > \nu_{cr}$ to zero will cause abrupt drop in the response curve, where the phase angle reverses from 180° to 0° . The dashed curve in Figure (4-13) shows free nonlinear vibration amplitude. Unstable region is represented by the dash-dot curve and the line $\nu = \nu_{cr}$ divides the left hand branch of the spectrum to unstable part.

In conclusion, once the numerical model is completed, the effect of the bell on the tower structure can be calculated for different bell tuning frequencies and different bell sizes.

In our case the effects of bell ringing on the tower is considerable. It is well known that, if the bell becomes small (low weight) in comparison to the weight of the tower, the effects of the bell ringing on the tower will be negligible in comparison with other excitations like earthquake and wind.

4.7 References

1. Ziegler F., 'Mechanics of Solids and Fluids', Second edition, Technical University Vienna, Springer-Verlag, New York-Vienna, 1998.
2. Weaver Jr.W., Timoshenko S.P., Young D.H., Department of Civil Engineering, Stanford University, 'Vibration Problems in Engineering', Fifth edition, John Wiley & Sons, 1989.
3. Shabana A.A., Department of Mechanical Engineering, University of Illinois at Chicago, 'Theory of Vibration', Springer-Verlag New York-Berlin Heidelberg, 1998.
4. Clough R.W., Penzien J., Department of Civil Engineering, University of California, 'Dynamic of Structures', McGraw-Hill, 1989.
5. Harris C.M., 'Shock and Vibration Handbook', Fourth edition, published by McGraw-Hill, 2003.
6. Chopra A.K., University of California at Berkeley, 'Dynamics of Structures', second edition, Prentice Hall, 2001.

7. Nayfeh A.H., Mook D.T., Department of Engineering Science and Mechanics Virginia, 'Nonlinear Oscillations', John Wiley & Sons, 1998.
8. Duffing G., 'Erzwungene Schwingungen bei veränderlicher Eigenfrequenz', F. Vieweg u. Sohn, 1918.

5

TOWER WITH PENDULUM TUNED MASS DAMPER SYSTEM

5.1 Introduction

Pendulum dynamic absorbers are extensively used to reduce tower's vibration level. A Pendulum Tuned Mass Damper (PTMD) is a device consisting of a suspended mass, and a damper that is attached to the tower in order to reduce the dynamic response of the structure. The frequency of the damper is tuned to a particular structural frequency so that when the system is excited by that frequency, the damper will resonate out of phase with the tower motion. Energy is dissipated by the damping inertia force acting on the structure.

This chapter starts with an introductory example of PTMD design and a description of the implementation of PTMDs in building structures like chimneys and BTs. Time history and frequency domain responses for a continuous system connected to optimally PTMD and subjected to harmonic and random support excitations in linear and nonlinear conditions are presented. An assessment is made for the optimal placement locations of PTMD in the tower. The tower response against earthquake with respect to seismic design criteria and record of real strong ground motion is also estimated.

5.2 An introductory sample of pendulum absorber

In this part, the concept of PTMD is illustrated using a two DOF system shown in Figure (5-1). It is assumed that a simple pendulum, suspended from the main mass, is connected to it by a rod and a viscous damper.

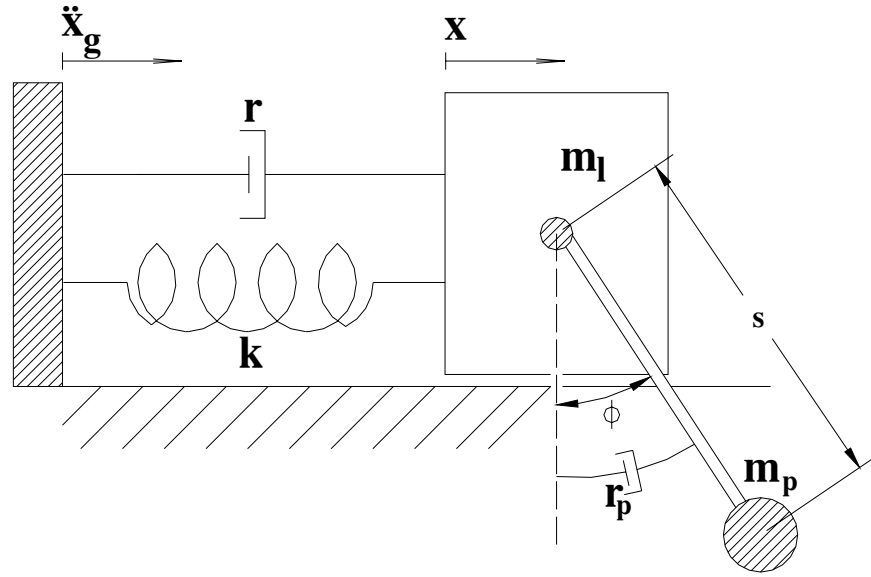


Figure 5-1 SDOF-PTMD system

Introducing the following notation

$$\omega^2 = \frac{k}{m_1} \quad (5-1)$$

$$r = 2\zeta\omega m_1 \quad (5-2)$$

$$\omega_p = \sqrt{\frac{g}{s}} \quad (5-3)$$

$$r_p = 2s^2\zeta_p m_p \omega_p \quad (5-4)$$

and defining μ as the mass ratio

$$\mu = \frac{m_p}{m_1} \quad (5-5)$$

the governing coupled equations of motion are given¹ for main mass as

$$(1 + \mu)\ddot{x} + \frac{r}{m_1}\dot{x} + \omega^2 x + \mu s(\sin \phi)\ddot{\phi} = -(1 + \mu)\ddot{x}_g \quad (5-6)$$

and for pendulum tuned mass as

$$\ddot{\phi} + \frac{r_p}{ms^2}\dot{\phi} + \omega_p^2 \sin \phi + \frac{\cos \phi}{s}\ddot{x} = -\cos \phi \ddot{x}_g \quad (5-7)$$

The purpose of adding the mass damper is to limit the motion of the main structure when subjected to a particular excitation.

A first approximation for the optimal linear frequency parameter of the damper is

$$\omega_p = \omega \quad (5-8)$$

which corresponds to tuning the damper to the period of the main structure.

5.3 Generalized MDOF system with PTMD

A method for reducing or eliminating the risk of oscillations induced by tower is to employ tuned mass dampers. There are mainly two types of tuned mass dampers, passive and active. An active mass damper requires an automatic engineering system to trigger the mass damper to counteract when oscillation occurs.

¹ Reference [7]

In this section passive tuned mass dampers are discussed². Several examples for a tuned mass damper are suggested in Figures (5-2), (5-3) and (5-4)

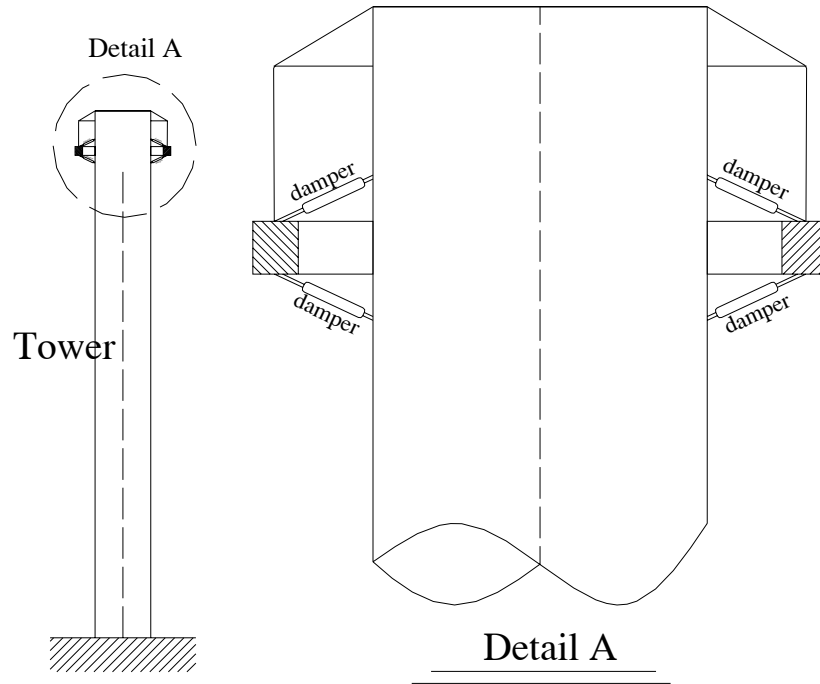


Figure 5-2 The tower is damped by using a pendulum ring connected to the tower by hydraulic dampers

² Reference [8]

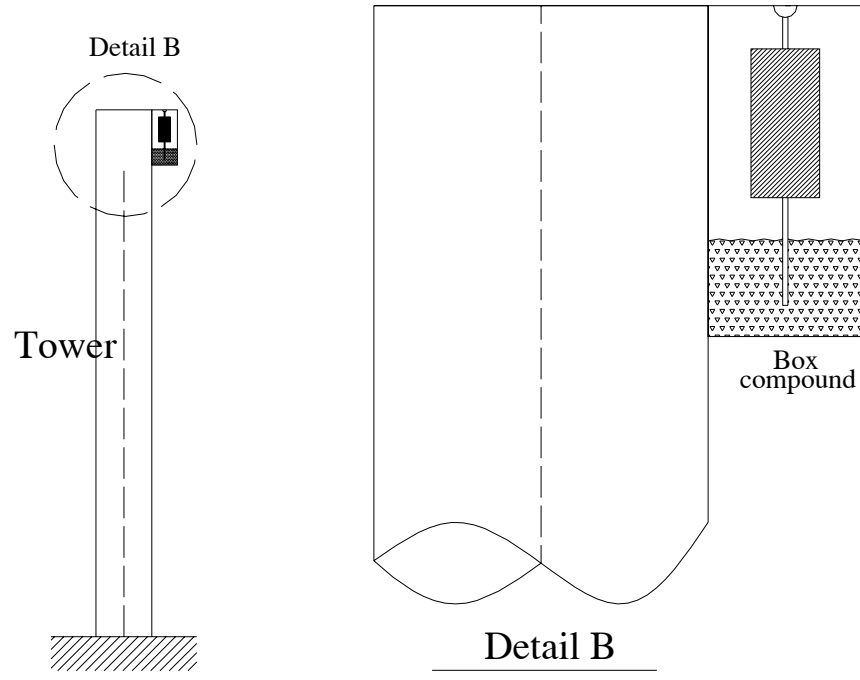


Figure 5-3 The tower is damped by using a pendulum mass with a bottom rod in a damping material

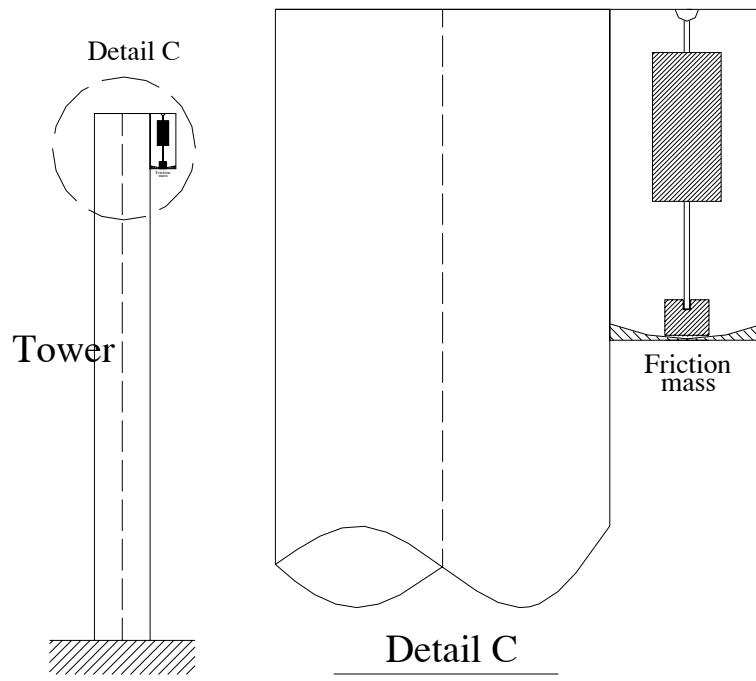


Figure 5-4 The tower is damped by using a pendulum mass with a bottom rod. The damping is achieved by the friction mass that slips on the bottom plate

Mechanical SDOF system with PTMD which was discussed in Section 5.2 is extended to continuous system consisting of distributed mass and elasticity. Figure (5-5) shows a tower system with pendulum which is allocated at the top of the tower. In order to follow numerical procedure we assume the tower to be made of concrete. Mass of the pendulum is 5% of total mass of the tower and it is assumed to be suspended at the top of the tower. The cross-section of the tower is circular as shown in Figure (5-5).

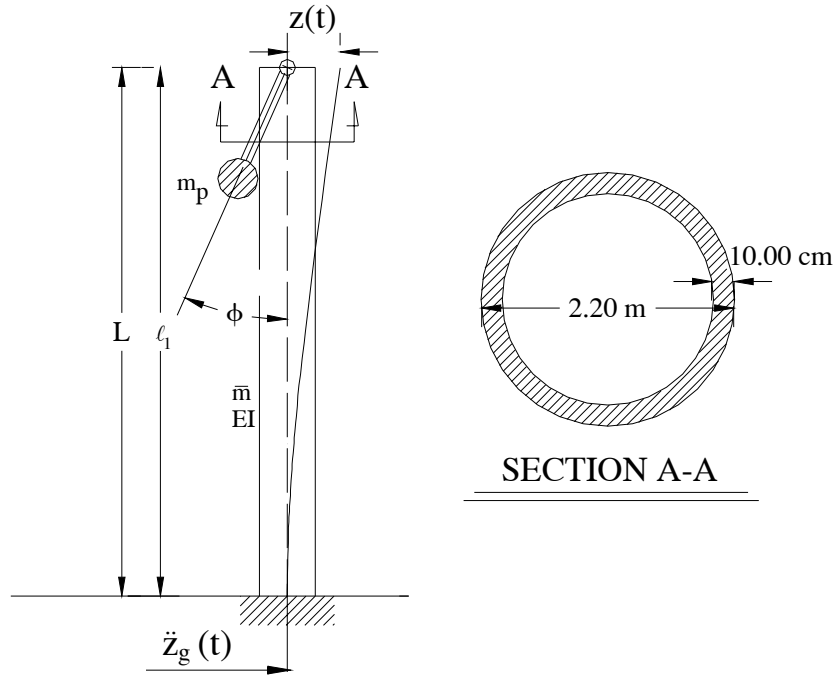


Figure 5-5 Tower plan and section

The mechanical parameters of the system are defined as

$$L = 50\text{ m}, E = 2.48 \times 10^9 \frac{\text{N}}{\text{m}^2}, \bar{m} = 1584 \frac{\text{kg}}{\text{m}}, m_{\text{total}} = 79200\text{ kg}, m_p = 3960\text{ kg}$$

$$g = 9.81 \frac{\text{m}}{\text{sec}^2}, \zeta_t = 5\%, (A, I)_{\text{tower}} = (0.66\text{ m}^2, 0.365\text{ m}^4), l_1 = 50\text{ m} \quad (5-9)$$

The parameters of the pendulum, s and ζ_p , are to be optimized. Substituting in Equations (3-49) gives the first and second circular frequency of the tower as

$$\begin{aligned}\omega_1 &= 3.36 \frac{\text{rad}}{\text{sec}} \\ \omega_2 &= 21.07 \frac{\text{rad}}{\text{sec}}\end{aligned}\tag{5-10}$$

Suppose the first modal response to be controlled, on the contrary when the external forcing frequency is close to ω_1 , the first mode response will dominate and it is reasonable to assume only first mode effects.

By considering the first mode shape of the tower and normalizing the mode shape with reference to pendulum operating position ℓ_1 , the equations of motion for the tower and pendulum can be expressed as

$$\begin{aligned}(m_1 + m_p)\ddot{Z}_1(t) + c_1\dot{Z}_1(t) + k_1Z_1(t) \\ + m_p s(\ddot{\phi} \cos \phi - \dot{\phi}^2 \sin \phi) = -(m_1^* + m_p)\ddot{Z}_g(t)\end{aligned}\tag{5-11}$$

$$m_p s \cos \phi \ddot{Z}_1(t) + m_p s^2 \ddot{\phi} + m_p s g \sin \phi = -m_p s \cos \phi \ddot{Z}_g(t)\tag{5-12}$$

noting that

$$\begin{aligned}m_1 &= m \int_0^l \psi_1^2(x) dx = 19799 \text{ kg} \\ k_1 &= EI \int_0^l [\psi_1''(x)]^2 dx = 223792 \frac{N}{m} \\ c_1 &= r_1 \int_0^l \psi_1^2(x) dx = 6652 \frac{Ns}{m} \\ m_{1p} &= m_p \psi_1^2(\ell_1) = 3960 \text{ kg} \\ m_1^* &= m \int_0^l \psi_1(x) dx = 31005 \text{ kg} \\ m_{1p}^* &= m_p \psi_1(\ell_1) = 3960 \text{ kg}\end{aligned}\tag{5-13}$$

Considering a hydraulic damper in pendulum connection as

$$c_p = 2s^2 \zeta_p m_p \omega_p \quad (5-14)$$

The Equation (5-12) leads to

$$\begin{aligned} m_p s \cos \phi \ddot{Z}_1(t) + m_p s^2 \ddot{\phi} + 2m_p s^2 \omega_p \zeta_p \dot{\phi} \\ + m_p s g \sin \phi = -m_p s \cos \phi \ddot{Z}_g(t) \end{aligned} \quad (5-15)$$

In case of small amplitude of the pendulum the coupled linearized system can be analyzed. By means of linearization $\phi = \sin \phi, \cos \phi = 1$ and neglecting the higher order terms of ϕ and its derivative, the equations reduce to the form

$$\begin{aligned} (m_1 + m_p) \ddot{Z}_1(t) + c_1 \dot{Z}_1(t) + k_1 Z_1(t) \\ + m_p s \ddot{\phi} = -(m_1^* + m_p) \ddot{Z}_g(t) \end{aligned} \quad (5-16)$$

$$m_p s \ddot{Z}_1(t) + m_p s^2 \ddot{\phi} + 2m_p s^2 \omega_p \zeta_p \dot{\phi} + m_p s g \phi = -m_p s \ddot{Z}_g(t) \quad (5-17)$$

considering periodic excitation

$$\ddot{Z}_g(t) = \ddot{Z}_g e^{i\omega t} \quad (5-18)$$

the response is given in the form

$$\begin{aligned} Z(t) &= Z e^{i\omega t} \\ \dot{Z}(t) &= i\omega Z e^{i\omega t} \\ \ddot{Z}(t) &= -\omega^2 Z e^{i\omega t} \end{aligned} \quad (5-19)$$

$$\begin{aligned} \phi &= \Phi e^{i\omega t} \\ \dot{\phi} &= i\omega \Phi e^{i\omega t} \\ \ddot{\phi} &= -\omega^2 \Phi e^{i\omega t} \end{aligned} \quad (5-20)$$

The Equations (5-16) and (5-17) may be written in the matrix form as

$$\begin{bmatrix} -\nu^2(m_1 + m_p) + c_1 i\nu + k_1 & -\nu^2 m_p s \\ -\nu^2 s & -s^2 \nu^2 + gs + 2s^2 \omega_p \zeta_p i\nu \end{bmatrix} \begin{bmatrix} Z \\ \Phi \end{bmatrix} = \begin{bmatrix} -(m_1^* + m) \\ -s \end{bmatrix} \ddot{Z}_g \quad (5-21)$$

The critical condition corresponds to the resonance condition.

Considering the parameters

$$\mu = \frac{m_p}{m_1} \quad (5-22)$$

$$\alpha = \frac{\nu}{\omega}, \beta = \frac{\omega_p}{\omega} \quad (5-23)$$

Treatment for optimal absorber parameters is contained in Den Hartog's text³.

Den Hartog has given the optimum frequency ratio as

$$\beta_{opt} = \frac{1}{1 + \mu} \quad (5-24)$$

and the optimal damping ratio as

$$\zeta_{opt} = \sqrt{\frac{3\mu}{8(1 + \mu)^3}} \quad (5-25)$$

However, due to the inherent damping in the main structure, the analytical expressions for the optimal tuning frequency and the optimal damping ratio can not be established in terms of the mass ratio.

In the following, solution corresponding to ground motion is examined and the optimal values of the damper properties for this condition are evaluated by Matlab7 program.

³ Reference [9]

Iteration for computing optimal parameters of pendulum leads to

$$\beta_{opt} = .76 \quad (5-26)$$

$$\zeta_p = 0.13 \quad (5-27)$$

Then the pendulum length and frequency are calculated as

$$(s, \omega_p) = (1.50 \text{ m}, 2.56 \frac{\text{rad}}{\text{sec}}) \quad (5-28)$$

Two variables of Equation (5-21), Z and Φ are calculated in frequency domain. Figure (5-6) shows the displacement of the tower at the top.

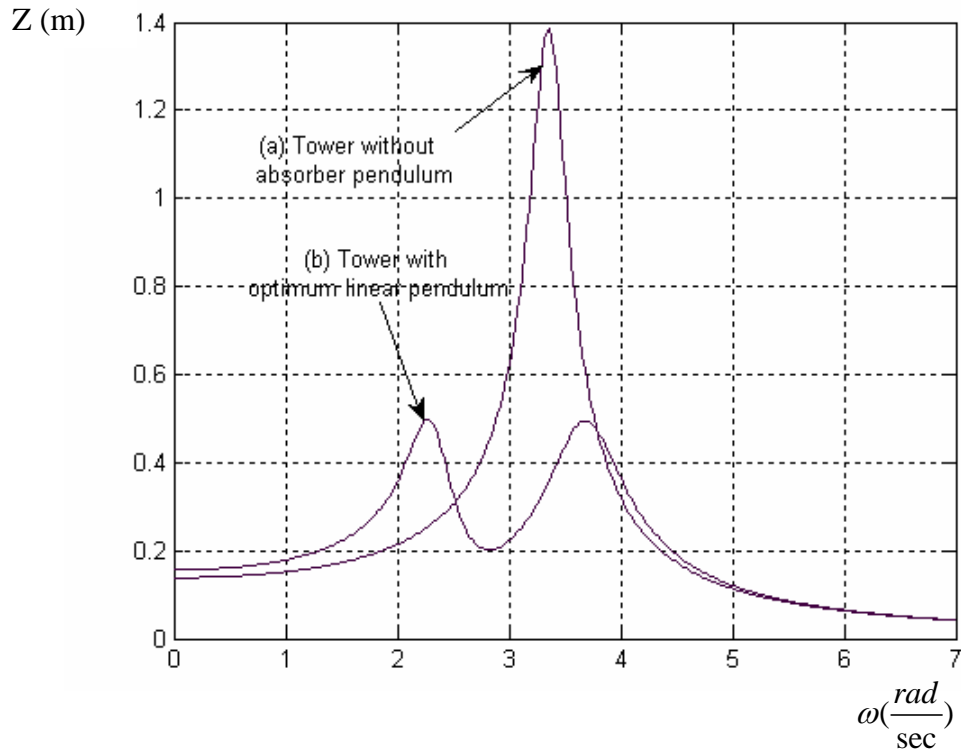


Figure 5-6 Tower displacement spectrum response in linear condition
 Z (displacement) versus ω (circular frequency)
 (a) Without pendulum
 (b) With pendulum by optimum parameters

5.4 The tower by nonlinear PTMD

The reason of considering absorber's nonlinear properties is the improvement of pendulum efficiency. The equations of the system vibrations relative to two mode shapes of the tower are written as

$$\begin{aligned} (m_1 + m_p)\ddot{Z}_1(t) + m_p\ddot{Z}_2(t) + c_1\dot{Z}_1(t) + k_1Z_1(t) \\ + m_ps(\ddot{\phi}\cos\phi - \dot{\phi}^2\sin\phi) = -(m_1^* + m_p)\ddot{Z}_g(t) \end{aligned} \quad (5-29)$$

$$\begin{aligned} (m_2 + m_p)\ddot{Z}_2(t) + m_p\ddot{Z}_1(t) + c_2\dot{Z}_2(t) + k_2Z_2(t) \\ + m_ps(\ddot{\phi}\cos\phi - \dot{\phi}^2\sin\phi) = -(m_2^* + m_p)\ddot{Z}_g(t) \end{aligned} \quad (5-30)$$

$$\begin{aligned} m_ps\cos\phi\ddot{Z}_1(t) + m_ps\cos\phi\ddot{Z}_2(t) + m_ps^2\ddot{\phi} \\ 2m_ps^2\omega_p\zeta_p\dot{\phi} + m_psg\sin\phi = -m_ps\cos\phi\ddot{Z}_g(t) \end{aligned} \quad (5-31)$$

The solution is found by numerical time-integration. The objectives are the evaluation of displacement of the tower and rotation angle of the pendulum in each time step. Computing these equations by algebraic loop of Simulink model which is shown in Figure (5-7) gives displacement and velocity of the tower as well as rotation angle and circular velocity in time step. The input of the system is a horizontal base acceleration which is generated by Matlab7 software and applied to the base of the tower.

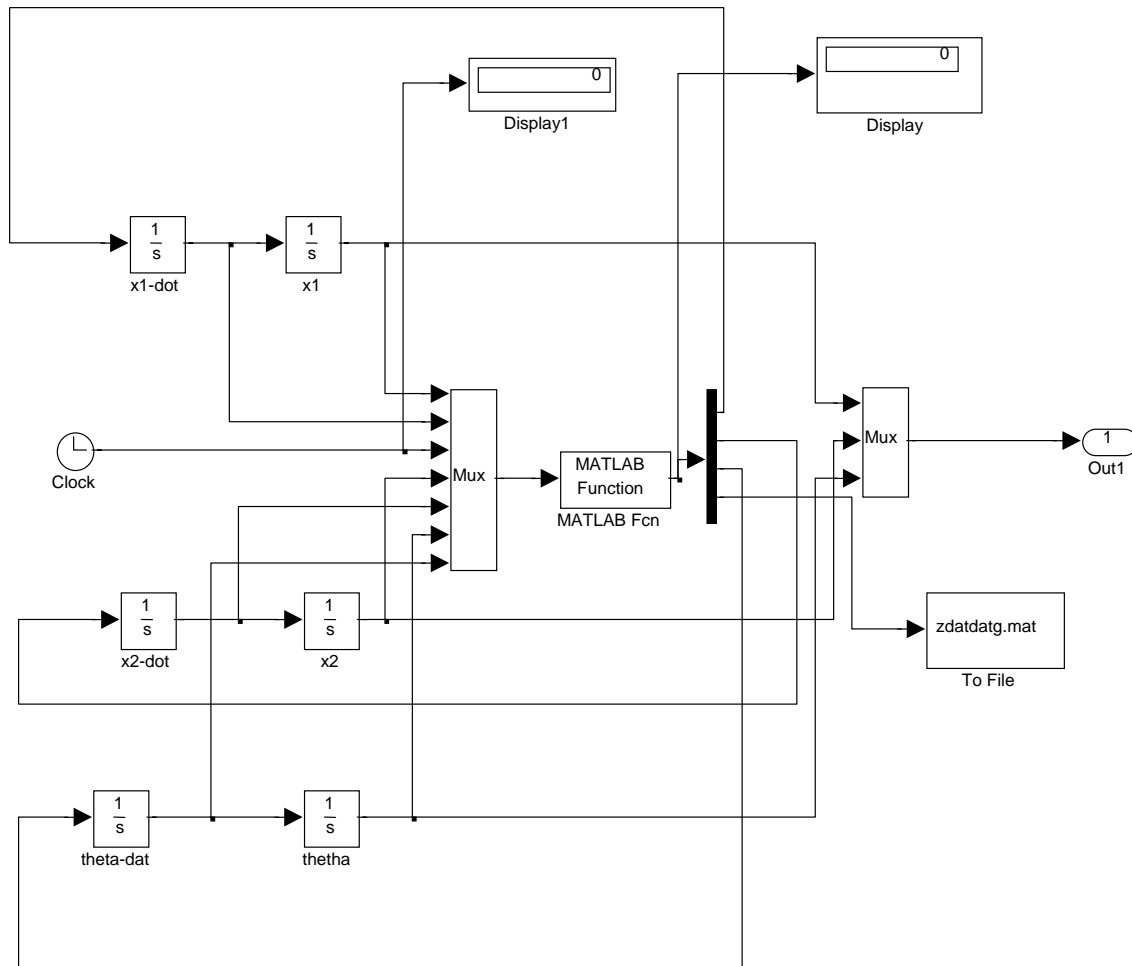


Figure 5-7 Simulink model (consisting the first & second modes of the tower and pendulum)

5.4.1 Time-Harmonic excitation

When a linear system is time-harmonically excited, the steady state response expresses the same frequencies as the input excitation. In the nonlinear case additional subharmonic and superharmonic parts can be detected. In Figure (5-8) and Figure (5-9) some results of Simulink calculations for external time-harmonic excitation (set to the first natural frequency of the tower) in linear and nonlinear conditions are shown.

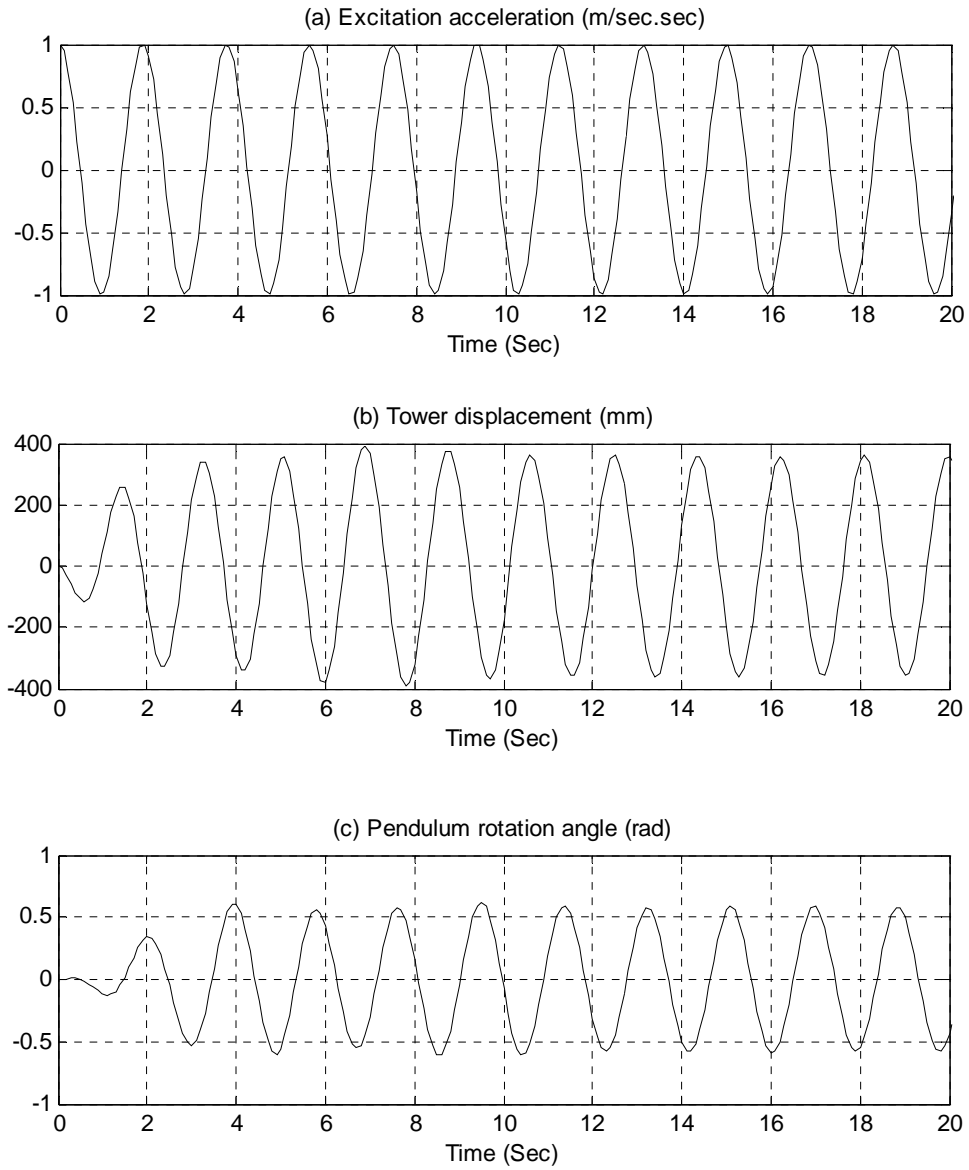


Figure 5-8 Time domain response by harmonic acceleration excitation

$$\ddot{Z}_g(t) = 1 \cos vt, \quad v = 3.36 \text{ rad in linear system}$$

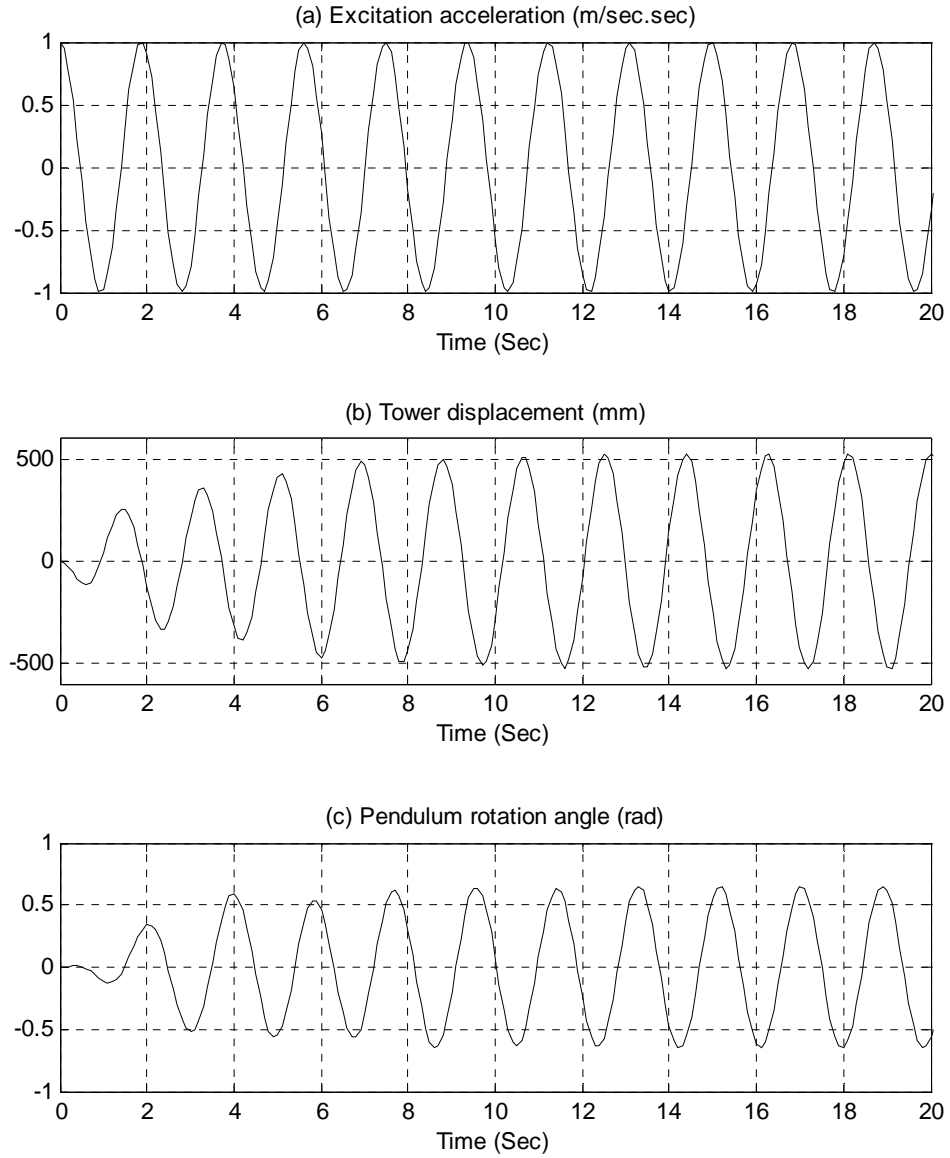


Figure 5-9 Time domain response by harmonic acceleration excitation

$$\ddot{Z}_g(t) = 1 \cos \nu t, \nu = 3.36 \text{ rad}$$

in nonlinear system

Figure (5-10) shows a 3-D plot of response function of the tower $\left| \frac{Z}{A} \right|$, where Z is displacement amplitude of the tower top point and A is the amplitude of the harmonic base excitation. The base excitation can be formulated as

$$\ddot{Z}_g(t) = A \cos vt \quad (5-32)$$

and steady-state harmonic response at the top of the tower is estimated as

$$Z(t) = Z \cos(vt - \alpha) \quad (5-33)$$

The geometrical specification of the tower is defined by Equation (5-9) and Equation (5-10). Likewise pendulum optimal parameters are evaluated in Equation (5-26) and Equation (5-27).

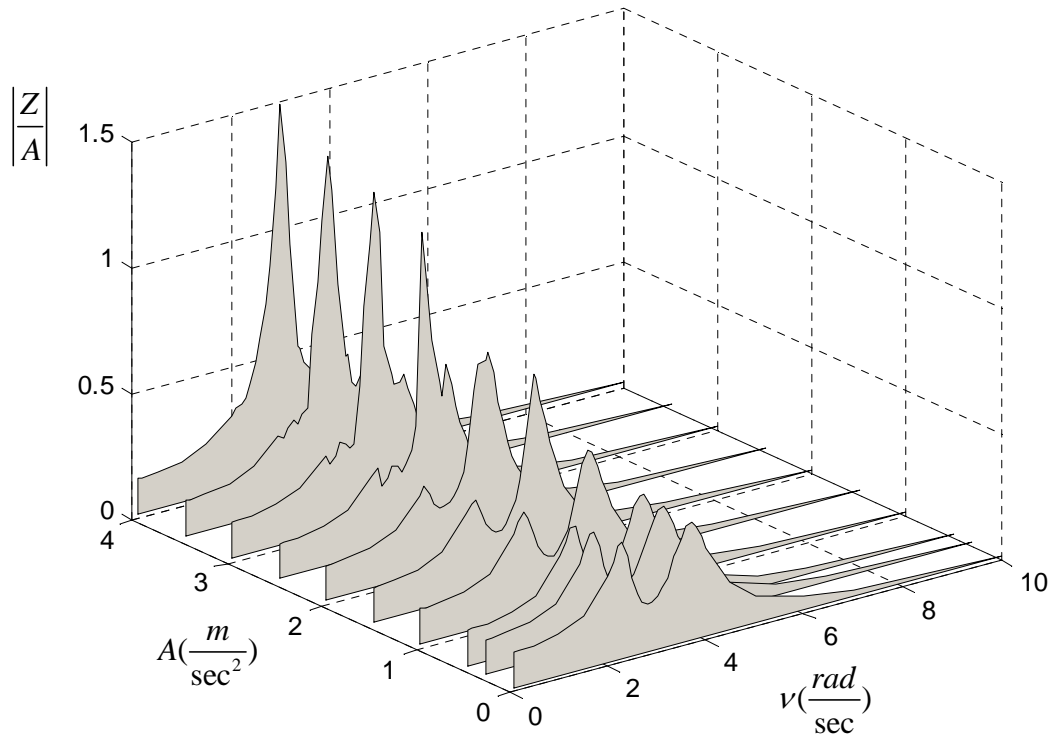


Figure 5-10 $\left| \frac{Z}{A} \right|$ (Z : displacement amplitude of the tower top point, A : amplitude of base excitation) versus ν (circular frequency) and A (amplitude of excitation)

Results for linear response of the tower are chosen on the condition of the pendulum absorber's optimum parameters set in front of the plot series.

Comparison due to increase of amplitude (A) shows unstable maximum frequency of the tower. It also shows that when the amplitude is less than $0.5m$ and $\phi_{\max} \leq 0.4rad$, the maximum optimal values of tuning mass is almost constant and it obeys the linear theory. Pendulum rotation angle (ϕ_{\max}) increases with increasing amplitude A . For $A \geq 1.65m$ and $\phi_{\max} > 0.9$, the pendulum starts to rotate.

The increase of the rotation angle of the pendulum increases the pendulum tuning values because of the system's nonlinearity.

Figure (5-10) shows the change of the pendulum optimum parameters according to the increase of the excitation amplitude. Note that for larger pendulum amplitudes, the absorption efficiency decreases and two peaks finally merge and form one peak only.

5.4.2 Fundamental statistical parameters⁴

For a random variable $X(t)$, fundamental statistical parameters consist of the mean $E\langle X \rangle$, the mean square $E\langle X^2 \rangle$, the variance σ^2 and the standard deviation σ as

$$E\langle X \rangle = \bar{x} = \frac{1}{N} \sum_{i=1}^n x_i = \frac{x_1 + x_2 + \dots + x_n}{N} \quad (5-34)$$

$$E\langle X^2 \rangle = \frac{1}{N} \sum_{i=1}^n x_i^2 = \frac{x_1^2 + x_2^2 + \dots + x_n^2}{N} \quad (5-35)$$

$$\text{var } X = \sigma^2 = \frac{1}{N} \sum_{i=1}^n (x_i - \bar{x})^2 = E\langle X^2 \rangle - [E\langle X \rangle]^2 \quad (5-36)$$

$$\sigma = \sqrt{\text{var } X} \quad (5-37)$$

⁴ Reference [6]

The standard deviation σ is a measure of the spread of the random variable about the mean, and variance σ^2 is interpreted by mean square minus the square of the mean and it is equals to mean square when $E\langle X \rangle = 0$.

5.4.3 Stationary random excitation⁵

Following the lines of Chapter 2, Part 2.7.5 artificial sample function for support excitation are generated by Simulink software, where stationary density function $S(\nu)$ and base random excitation $\ddot{Z}_g(t)$ can again be expressed according to

$$\ddot{Z}_g(t) = \sum_{n=1}^N \sqrt{4S(\nu)\Delta\nu} \times \cos(n\Delta\nu t - \varphi) \quad (5-38)$$

Numerical parameters are chosen as follows

$$S(\nu) = \text{const.} = 4 \frac{m^2}{\text{sec}^3}, \quad T = 100 \text{sec}, \quad \Delta\nu = \frac{2\pi}{100} = 0.0628$$

$$N = 100, \quad 0 \leq \varphi(\text{random}) \leq 2\pi \quad (5-39)$$

Due to the excitation in time domain, the response of the tower and the pendulum are computed (built by Simulink) and illustrated in Figure (5-11).

⁵ Reference [6]

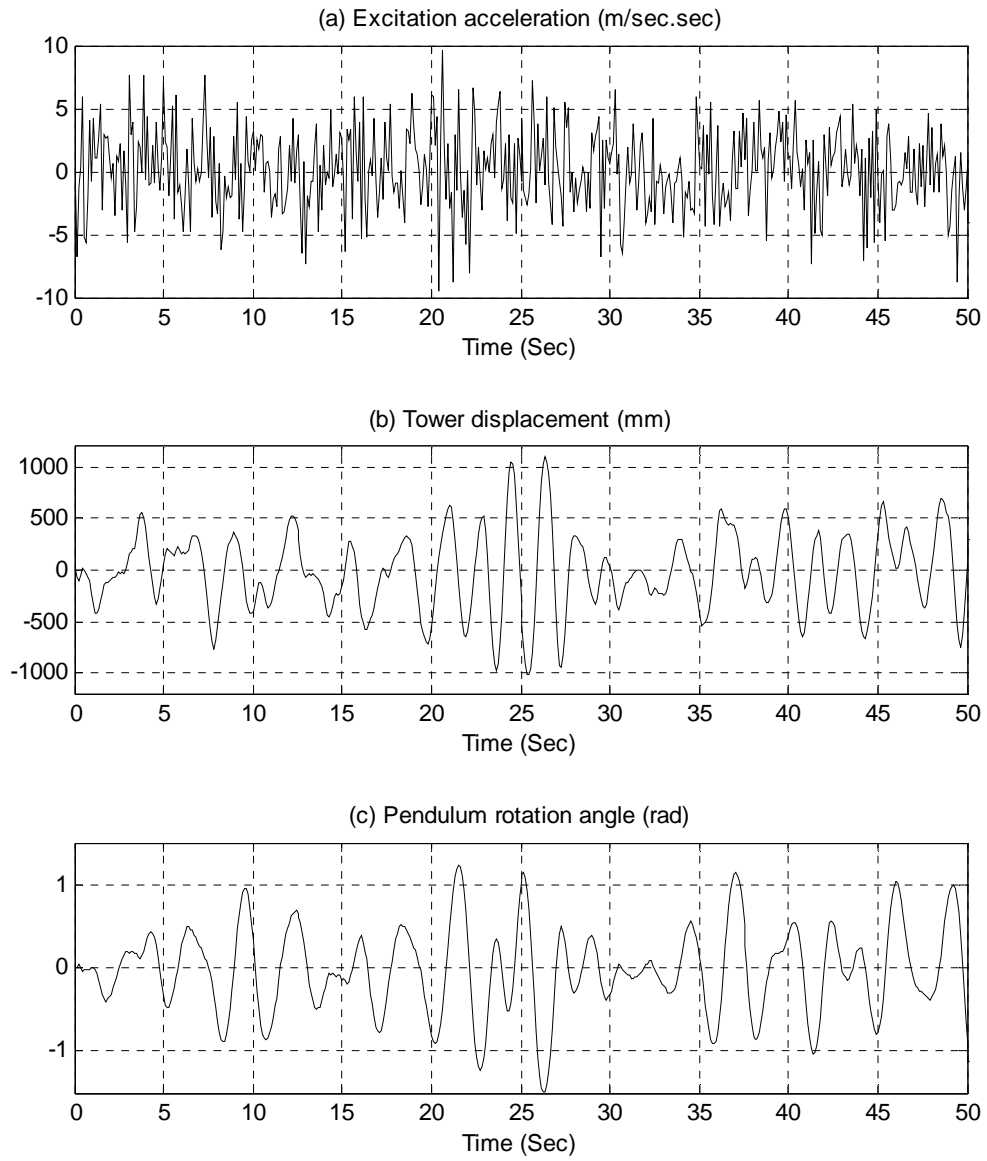


Figure 5-11 Time domain response by random acceleration excitation $S(\omega) = 4 \frac{m^2}{\text{sec}^3}$,

excitation amplitude $A = 1 \frac{m}{\text{sec}^2}$ in nonlinear system

By increasing the amplitude of excitation, the nonlinearity effect appears and changes the pendulum optimum parameters. Figure (5-12) and Figure (5-13) show the effects of increasing excitation amplitude on the system parameters.

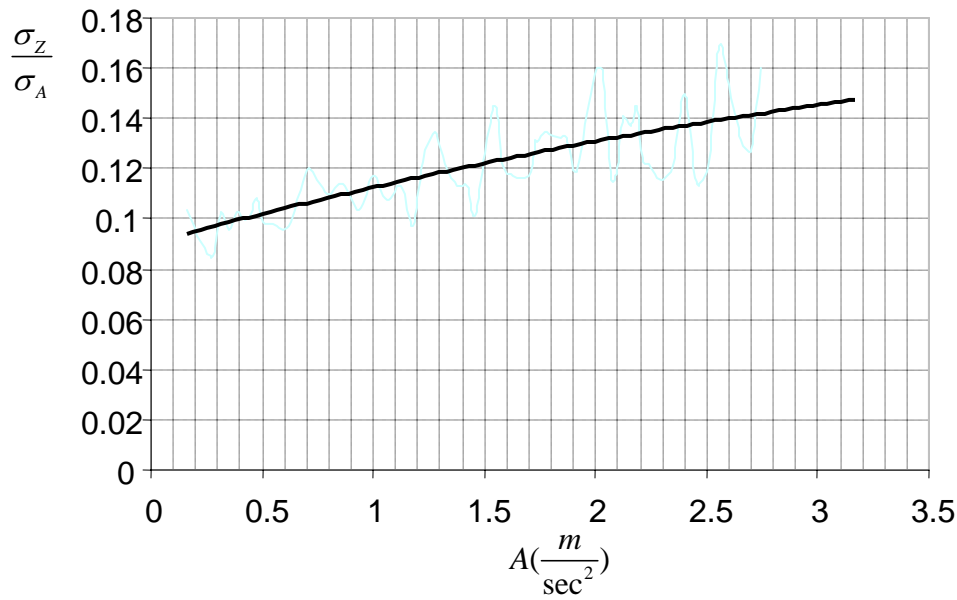


Figure 5-12 Dependence of the displacement amplitude of the tower (Z) upon excitation stationary amplitude (A) (σ_Z : standard deviation of displacement output, σ_A : standard deviation of excitation input)

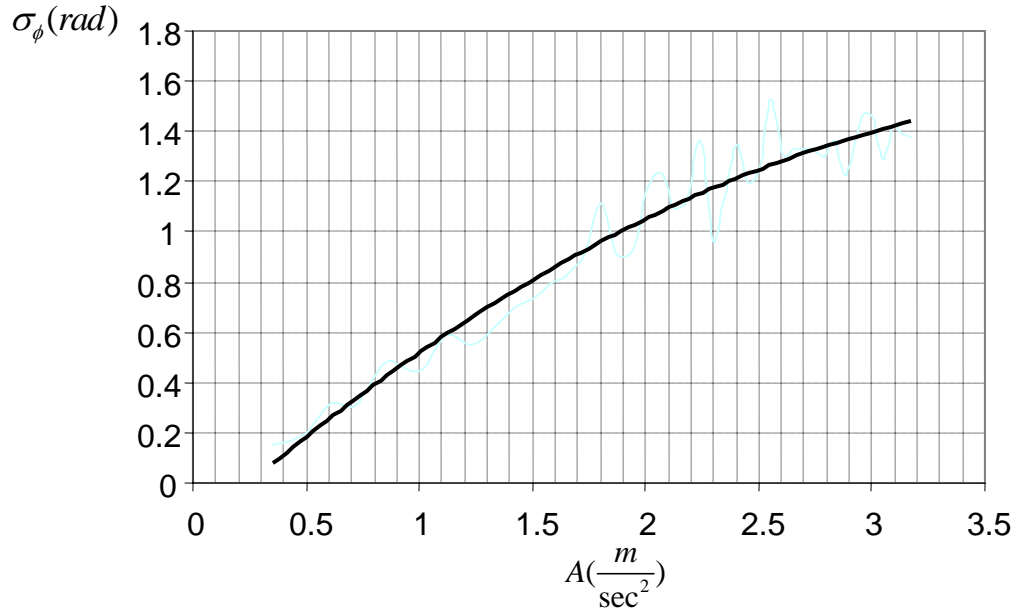


Figure 5-13 Maximum deviation angle of the pendulum (ϕ) versus excitation stationary amplitude (A) (σ_ϕ : standard deviation of rotation angle)

Figure (5-12) shows that for increasing excitation amplitude the corresponding response ($\frac{\sigma_z}{\sigma_A}$) will increase contrary to linear condition where the ratio remains constant.

Rotation angle of the pendulum versus the excitation amplitude is illustrated in Figure (5-13) and shows that the rotation angle increases as the excitation amplitude increases. When the amplitude exceeds $1.5m$, the pendulum begins to rotate after about 30 second of oscillation.

The value of μ should be increased in order to set a limit on the pendulum rotation angle when excitation amplitude increases. Figure (5-14) shows the maximum rotation angle of pendulum with μ for constant value of amplitude (A).

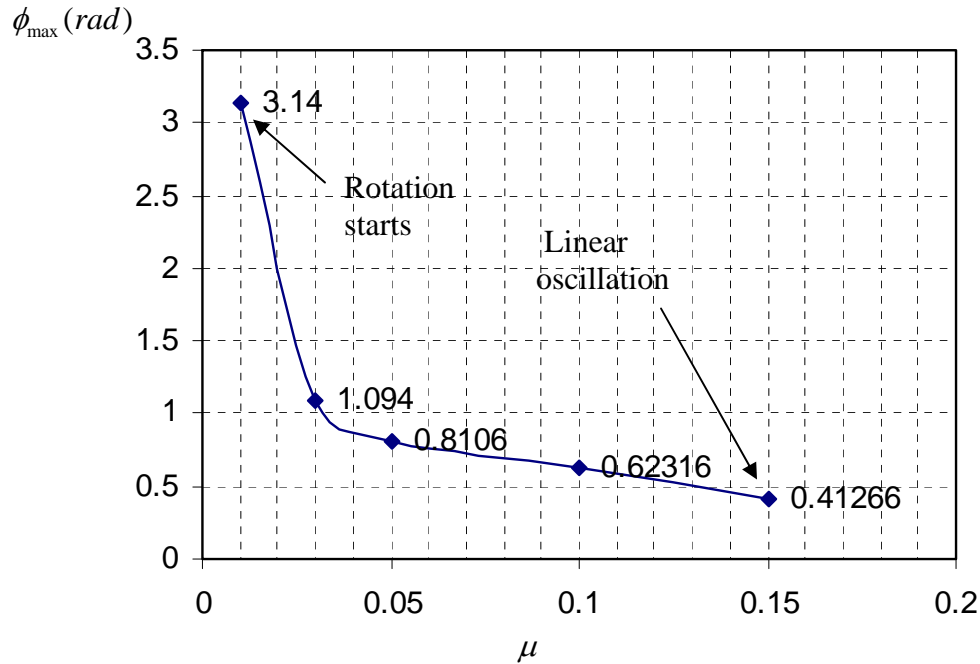


Figure 5-14 Maximum rotation angle of pendulum (ϕ_{\max}) versus pendulum mass ratio (μ) with excitation amplitude $A = 1.5 \text{ m/sec}^2$

As depicted in Figure (5-14), when pendulum weight increases to 15% of total weight of the tower, rotation angle of the pendulum decreases and the system yields to behave linearly. While the pendulum weight decreases to 1% of total weight of the tower, it begins to rotate.

5.4.4 Bam strong ground motion

Iran is one of the most vulnerable countries in the world to earthquake. Bam is located 193km southeast of Kerman city on a plane between Jebalbarez and Kabudi Mountains, approximately 1100 meters above sea level. In ancient times people lived in citadel, which is now known as Arg-e-Bam, one of the Persian historical sites and one of the most beautiful buildings of Ashkanian era. Structures with clay and straw as the main material components comprised the major type of construction in the city. The current city of Bam is located southeast of Arg-e-Bam. Bam city is located in a high seismic hazard zone of Iran and thus many earthquakes have been recorded around the Bam area. But

the city of Bam had no reports of great historical earthquakes before the 26 December 2003 earthquake.

The strong ground motions of Bam earthquake were recorded at 18 stations by Building and Housing Research center of Iran (BHRC). Larger residual displacements and damage in the E-W direction occurred and more than 26,000 people were killed and 30,000 injured. Although the impact of the earthquake was limited to a relatively small area of about 16 km in radius, in Bam city more than 85 percent of the buildings were completely destroyed. The impact on the surrounding rural areas was also severe. The 2,500 year-old historic city of Bam, an internationally renowned heritage site in the centre of Bam, was almost completely destroyed.

Figure (5-15) shows larger peak ground acceleration in E-W direction. Figure (5-16) shows acceleration response spectrum with a damping ratio coefficient of 0.05 to the critical⁶.

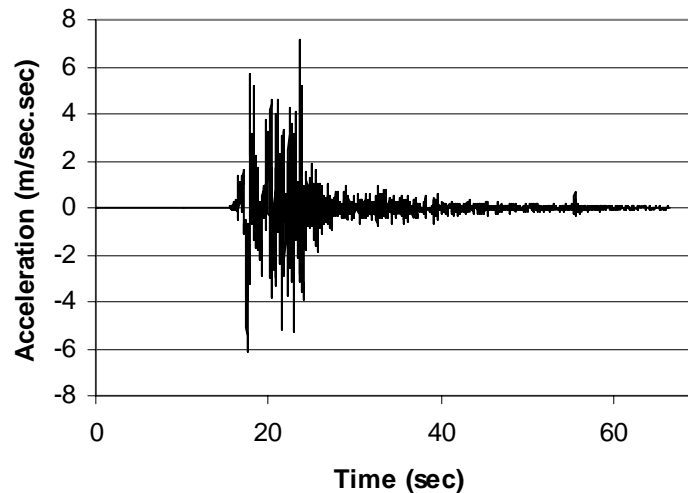


Figure 5-15 Strong ground motion in the E-W direction, Bam-Iran, recorded by Building and Housing Research Center (BHRC, 2003)

⁶ Reference [11]

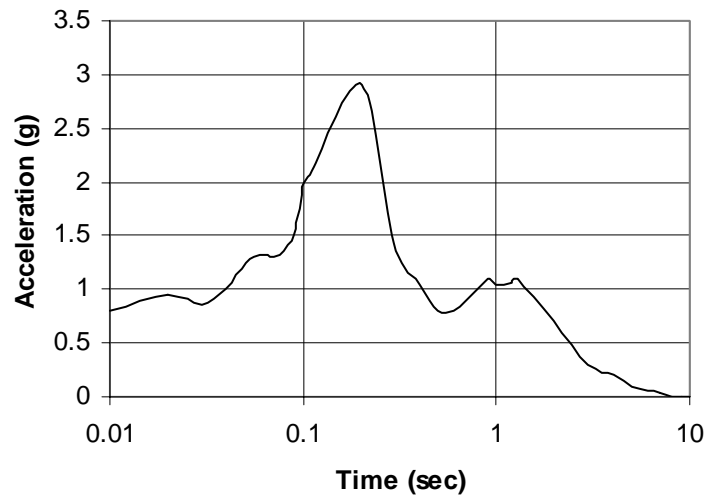


Figure 5-16 Acceleration response spectrum of Bam earthquake ($\zeta = 0.05$)

5.4.5 Earthquake excitation

The hybrid nonlinear tower with optimally adjusted pendulum shown in Figure (5-5) is excited by the strong ground motion of Bam, Iran 2003. It is defined as an input support excitation for the Simulink model illustrated in Figure (5-7). This calculation is one of the practical treatments of vibrations in the BT like structures. Figure (5-17) indicates the response curve of tip-displacement of the tower and rotation angle of the pendulum. Figure (5-18) shows the Fast Fourier Transformation curve of the output as well.

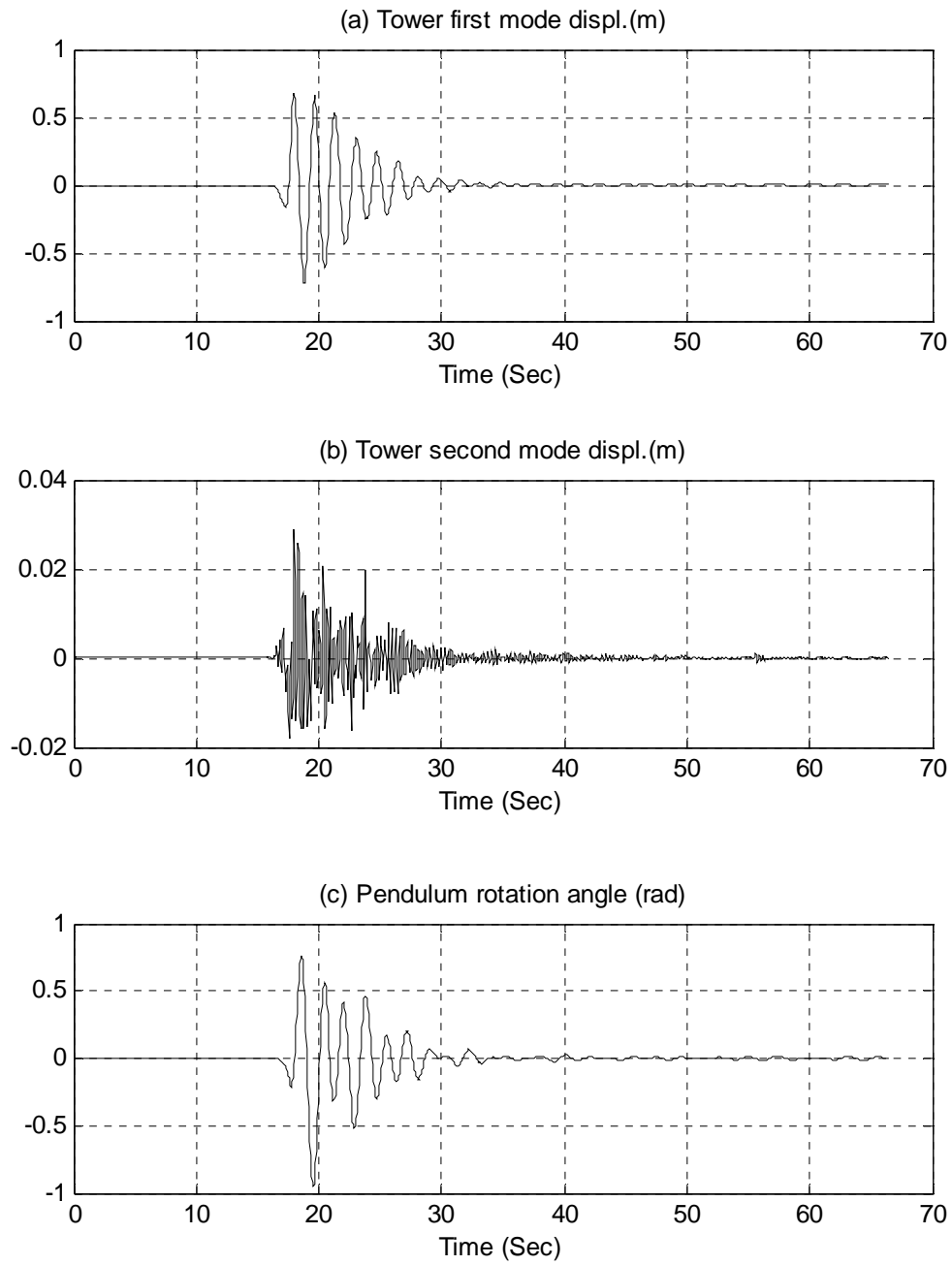


Figure 5-17 Time domain response of the top of the BT effected by Bam earthquake excitation

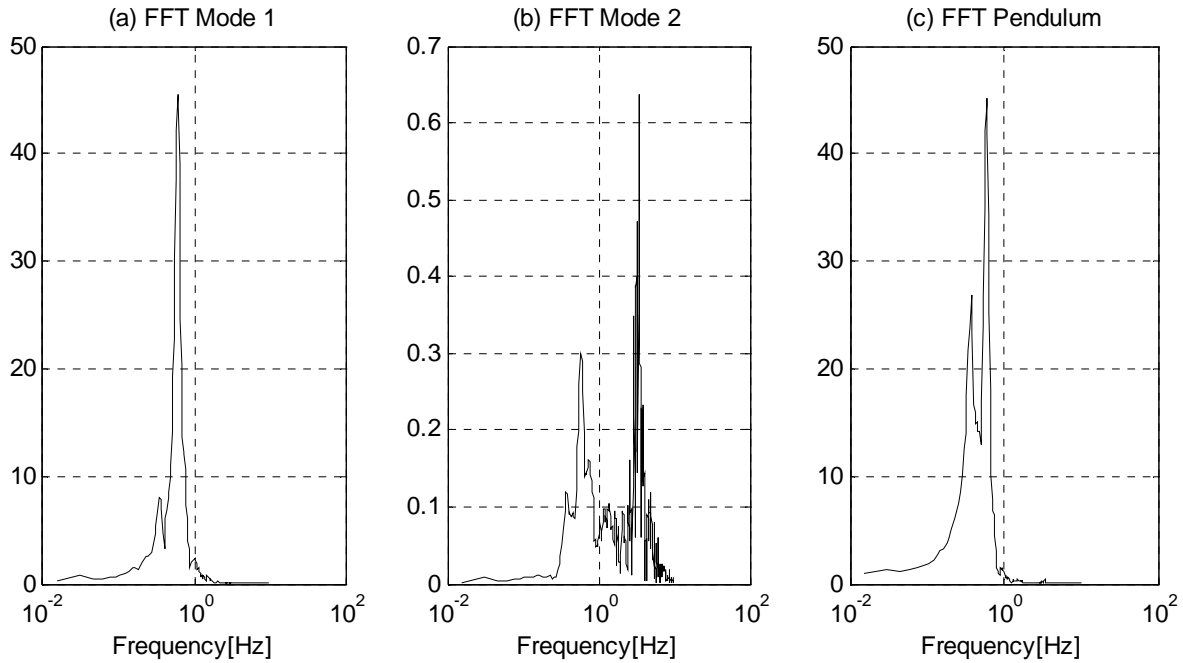


Figure 5-18 FFT spectrum response of the BT effected by Bam earthquake excitation

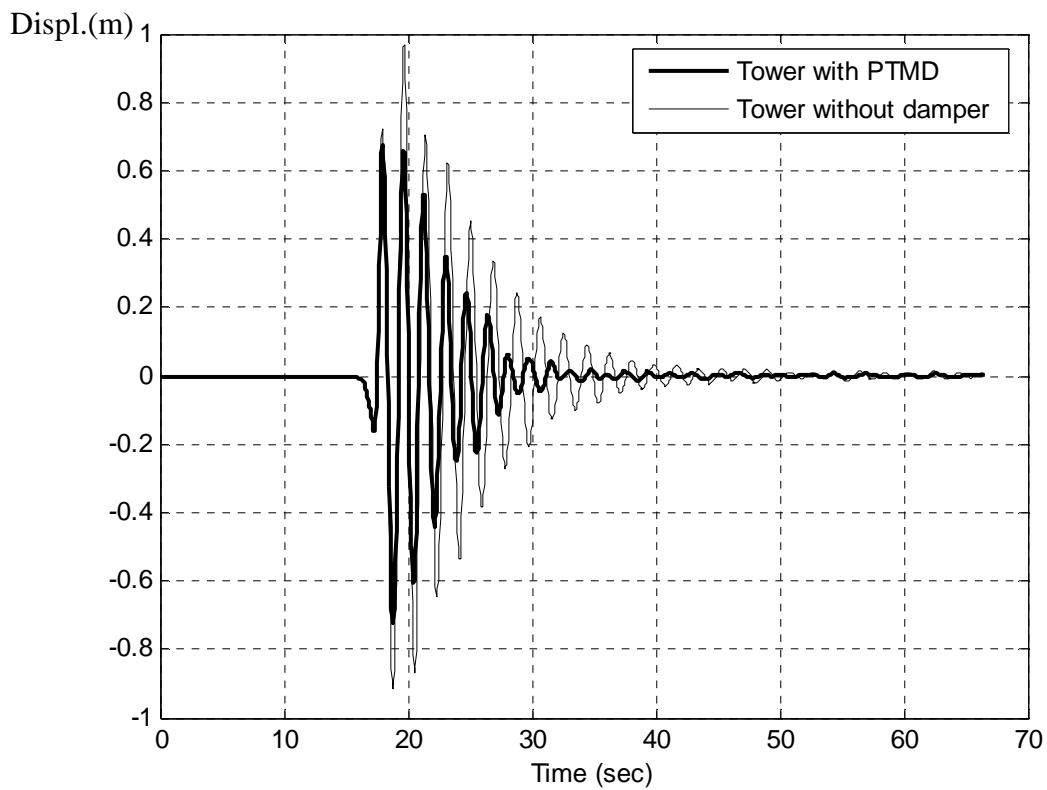


Figure 5-19 Time domain tip-displacement response of the tower with PTMD and without damper effected by Bam earthquake excitation

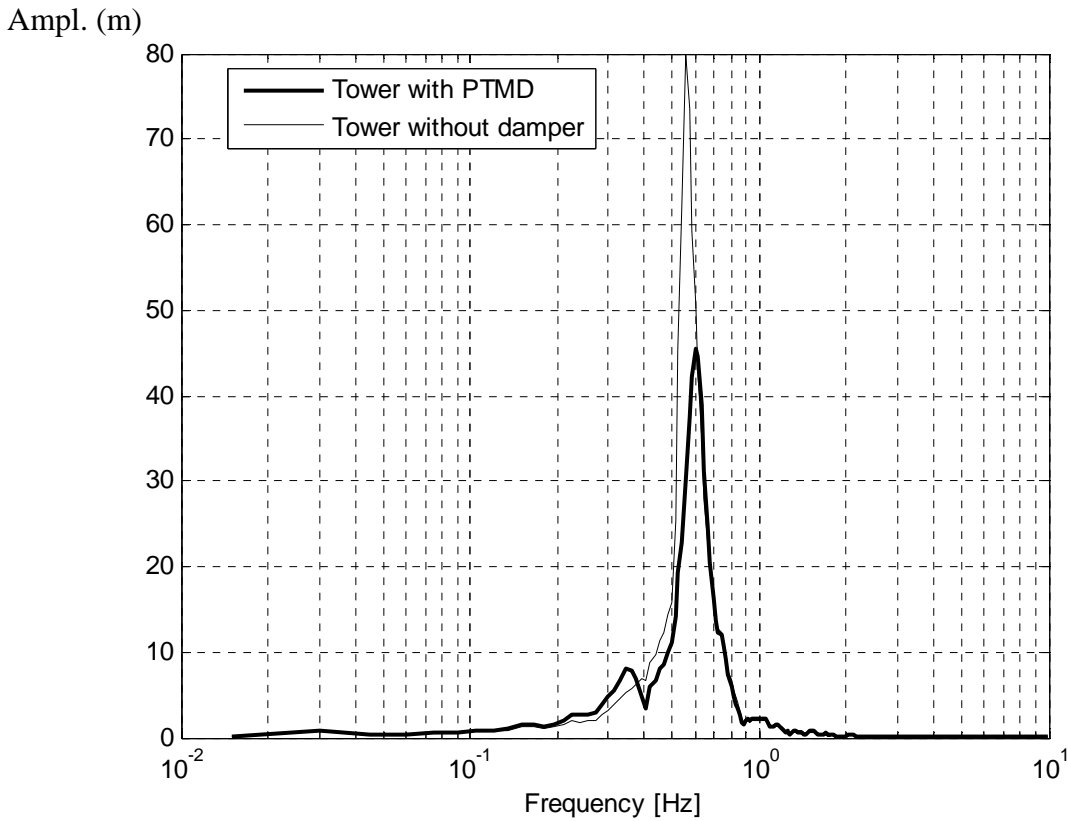


Figure 5-20 FFT response of the top of the tower with PTMD and without damper effected by Bam earthquake excitation

Figure (5-17) and Figure (5-18) show that the tower's first natural frequency is strongly excited and consequently PTMD adjusted to the first natural frequency of the tower has effectively decreased the deflections caused by earthquake excitation. The results indicate 35% reduction in deflection of the tower as illustrated in Figure (5-19) and Figure (5-20).

5.4.6 Optimal location of PTMD

Equations (5-29), (5-30) and (5-31) represent the 3DOF system, two degrees of freedom for the tower and one degree of freedom for the pendulum. Since PTMD is effective for a narrow frequency range, one has to decide on which

modal resonant response must be controlled with a PTMD⁷. The PTMD location should be selected to coincide with the maximum amplitude of mode shape to be controlled. In this case, the first mode is the target mode and the top of the tower has the maximum amplitude in the first mode shape. The second mode shape has a nodal point at $h = 0.78L$. Therefore locating a tuned mass at this point would have no effect on the second modal response, compare Figure (5-21). The optimal locations are $h = L$ and $h = 0.47L$. The first and second mode shapes of the tower are shown in Figure (5-21).

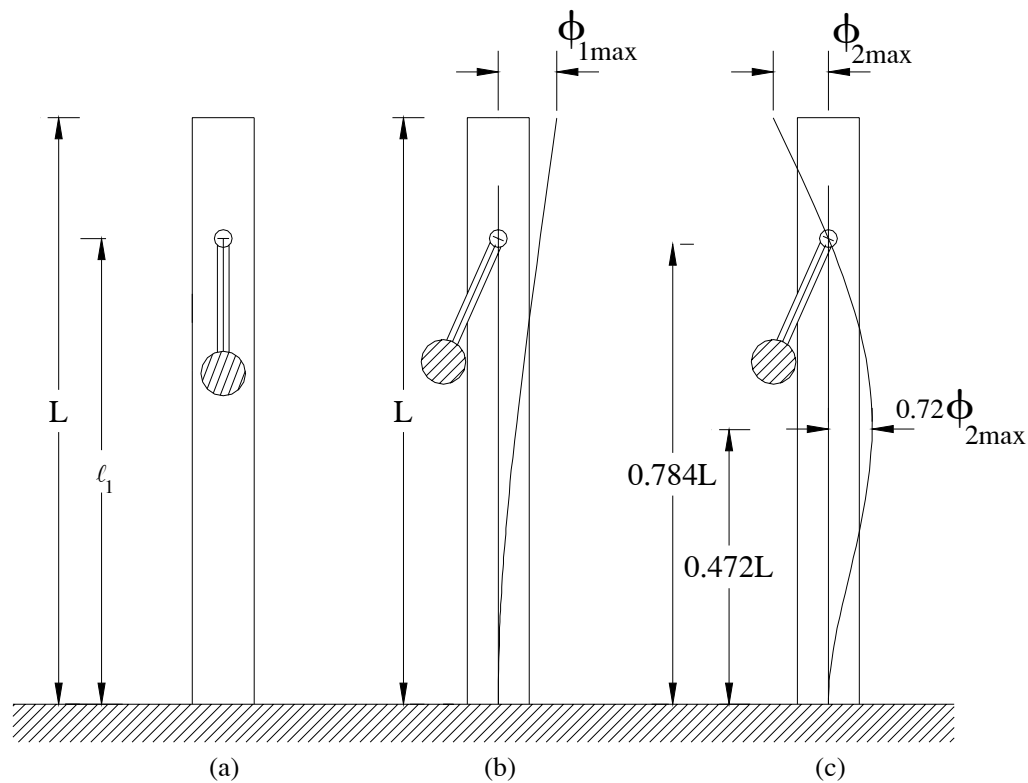


Figure 5-21 The tower
 (a) With pendulum
 (b) The first mode shape
 (c) The second mode shape

As a summary, during the analysis of the tower connected to optimally PTMD subjected to time-harmonic excitation and stationary random vibrations in

⁷ Reference [7]

linear and nonlinear condition, the results show that when the amplitude of excitation is not too high and causes small rotation angle ($\phi \leq 0.4 \text{ rad}$) in the pendulum, the maximum optimal values of tuning mass are almost constant and system behaves like a linear system. However if the amplitude of excitation is strong enough to oscillate pendulum more than 0.4 rad , the pendulum optimal tuning values will change because of system nonlinearity. In order to limit the pendulum deviation angle to less than 0.9 rad , the value of $\mu = \frac{m_p}{m_1}$ should be increased.

The displacement spectrum response of the tower in linear and nonlinear oscillation condition of pendulum in comparison to the response of the tower without pendulum is illustrated in Figure (5-22).

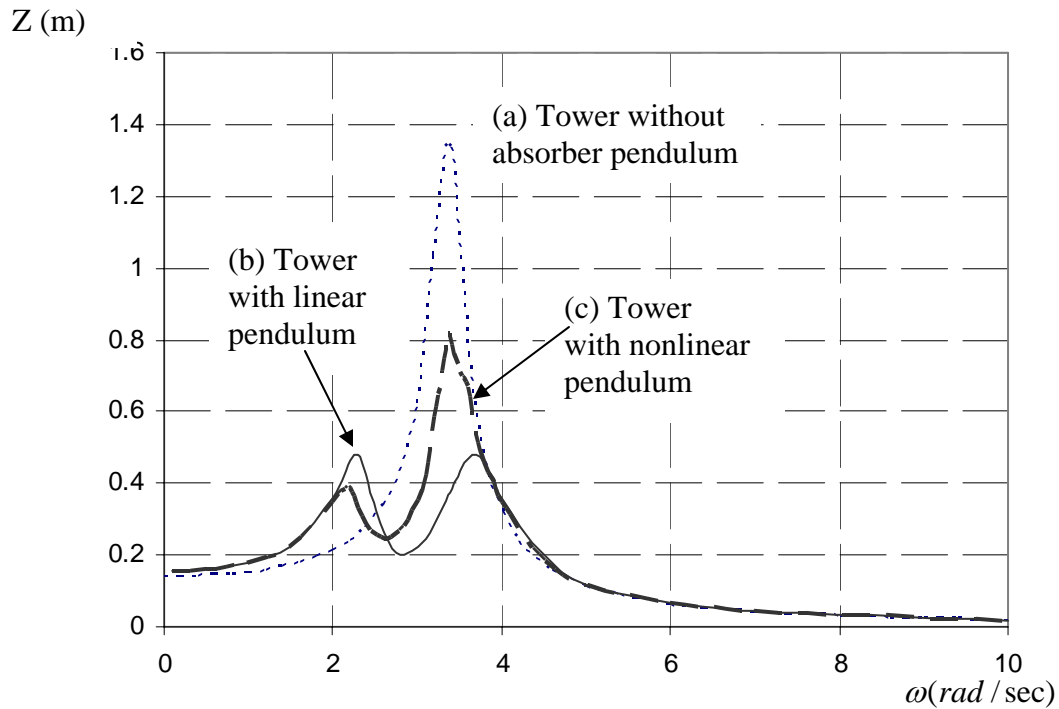


Figure 5-22 Tower displacement spectrum response
 $\phi_{\max} \approx 0.9 \text{ rad}$ (optimum tuning values set in linear system)
 (a) Without pendulum
 (b) With linear pendulum
 (c) With nonlinear pendulum

As illustrated in Figure (5-22), the maximum displacement of the tower decrease due to the nonlinear behavior of the pendulum, despite the fact that it changes the optimal tuning values.

This study reveals that a pendulum absorber can be computed according to the linear theory when $\phi \leq 0.4 \text{ rad}$, however when $0.4 \text{ rad} < \phi \leq 0.9 \text{ rad}$ it is necessary to allow nonlinearity effect, and in no circumstances $\phi > 0.9 \text{ rad}$ is recommended.

5.5 References

1. Ziegler F., 'Mechanics of Solids and Fluids', Second edition, Technical University Vienna, Springer-Verlag New York-Vienna, 1998.
2. Weaver Jr.W. , Timoshenko S.P., Young D.H., Department of Civil Engineering, Stanford University, 'Vibration Problems in Engineering', Fifth edition, John Wiley & Sons, 1989.
3. Shabana A.A., Department of Mechanical Engineering, University of Illinois at Chicago, 'Theory of Vibration', Springer-Verlag New York-Berlin Heidelberg, 1998.
4. Clough R.W., Penzien J., Department of Civil Engineering, University of California, 'Dynamic of Structures', McGraw-Hill, 1989.
5. Harris C.M., 'Shock and Vibration Handbook', Fourth edition, McGraw-Hill, 2003.
6. Yang C.Y., University of Delaware Newark, Delaware, 'Random Vibration of Structure', John Wiley & Sons, 1985.
7. Korenev B.G., Reznikov L.M., Moscow Civil Engineering Institute, 'Dynamic Vibration Absorbers, Theory and Technical Applications', John Wiley & Sons, 1993.
8. Petersen C., University of Munich, 'Dynamik der Baukonstruktionen', Vieweg 1996.
9. DenHartog J.P., 'Mechanical Vibrations', reprint of 4th edition, McGraw Hill, 1956.
10. Chopra A.K., University of California at Berkeley, 'Dynamics of Structures', second edition, Prentice Hall, 2001.
11. Mostafaei H., Kabeyasawa T.M., Earthquake Research Institute the University of Tokyo, 'Investigation and Analysis of Damage to Building during the 2003 Bam Earthquake', Vol.79 (2004), pp.107-132.

6

DYNAMIC SUBSTRUCTURE METHOD AND FORCE CALCULATIONS

6.1 Introduction

In the former chapters the numerical nonlinear behaviors of the BT have been discussed. In this chapter, dynamic analysis of the BT via substructure method is introduced, and then vibrations induced by bell (pendulum) movements are treated as externally applied excitations. When studying pendulum oscillatory movement, it is necessary to determine the time-variant forces applied to the tower. A numerical model is presented to compare the response of the BT in quasi-static analysis for this force.

The internal forces of the tower produced by dynamic excitations are evaluated by numerical nonlinear analysis.

6.2 Dynamic analysis via substructure method

The main concept of substructure analysis is to obtain the response of the entire system from the response of the individual substructures¹. The idea in such an approach is presented in the BT by means of modeling the pendulum and the tower as two substructures. Figure (6-1) shows the complete system of BT which is decomposed into two substructures. The tower substructure is contained in the first two mode shapes of vibration expressed as

¹ Reference [4]

$$(m_1 + m_p)\ddot{Z}_1(t) + m_p\ddot{Z}_2(t) + c_1\dot{Z}_1(t) + k_1Z_1(t) = -\ddot{Z}_g(m_1^* + m_p) + R(t) \quad (6-1)$$

$$(m_2 + m_p)\ddot{Z}_2(t) + m_p\ddot{Z}_1(t) + c_2\dot{Z}_2(t) + k_2Z_2(t) = -\ddot{Z}_g(m_2^* + m_p) + R(t) \quad (6-2)$$

where $R(t)$ stands for the dynamic interaction of the pendulum,

$$R(t) = -m_p s(\ddot{\phi} \cos \phi - \dot{\phi}^2 \sin \phi) \quad (6-3)$$

Definition of the generalized mass, stiffness and damping have been introduced in Equation (3-25).

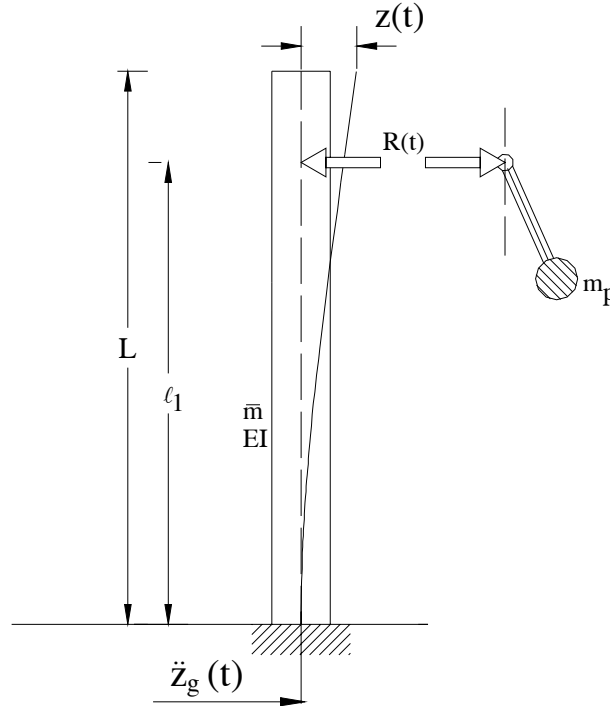


Figure 6-1 Substructure representation of the BT

On the other hand, the governing equation of motion of the pendulum can be expressed as

$$m_p s^2 \ddot{\phi} + m_p s g \sin \phi = -m_p s \cos \phi [\ddot{Z}_1(t) + \ddot{Z}_2(t) + \ddot{Z}_g] \quad (6-4)$$

By geometrical linearization of pendulum, $\sin \phi = \phi$, $\cos \phi = 1$ and neglecting higher order terms of ϕ and its derivatives, which holds for small oscillation about the position of equilibrium, Equations (6-3) and (6-4) yields

$$R(t) = -m_p s \ddot{\phi} \quad (6-5)$$

$$s \ddot{\phi} + g \phi = -\ddot{Z}_1(t) - \ddot{Z}_2(t) - \ddot{Z}_g \quad (6-6)$$

Considering a time-harmonic support excitation in the complex form of $\ddot{Z}_g = a e^{i\nu t}$, the steady-state response in terms of the complex frequency response function may be written as

$$Z_1(t) = Z_1 e^{i\nu t} \quad (a)$$

$$Z_2(t) = Z_2 e^{i\nu t} \quad (b)$$

$$\phi = \Phi e^{i\nu t} \quad (c) \quad (6-7)$$

Substituting Equation (6-7) into Equations (6-6) gives

$$\Phi = \frac{\nu^2 (Z_1 + Z_2) - a}{g - s\nu^2} \quad (6-8)$$

Moreover, considering $R(t)$ in terms of the complex frequency response function, from Equation (6-5)

$$R(\omega) = m_p s \nu^2 \Phi, \quad R(t) = R(\omega) e^{i\nu t} \quad (6-9)$$

Substitution of Equations (6-7), (6-8) and (6-9) in Equations (6-1) and (6-2), and solving two coupled equations in terms of the complex frequency response function leads to

$$Z_1 = \frac{\frac{a m_p g \nu^2}{g - s\nu^2} (m_1^* - m_2^*) - a S_2 (m_1^* + \frac{m_p g}{g - s\nu^2})}{\frac{-m_p g \nu^2}{g - s\nu^2} (S_1 - S_2) + S_1 S_2} \quad (6-10)$$

$$Z_2 = \frac{\frac{a m_p g v^2}{g - s v^2} (m_2^* - m_1^*) - a S_1 (m_2^* + \frac{m_p g}{g - s v^2})}{\frac{-m_p g v^2}{g - s v^2} (S_1 - S_2) + S_1 S_2} \quad (6-11)$$

where S_1 and S_2 are defined as

$$\begin{aligned} S_1 &= -v^2 m_1 + i c_1 v + k_1 \\ S_2 &= -v^2 m_2 + i c_2 v + k_2 \end{aligned} \quad (6-12)$$

Therefore the responses of the total system can be obtained from the complex frequency response function of the substructure.

6.3 Numerical example

The numerical parameters of the BT as defined in Chapter 4, Part 4.3, are a concrete tower of full circular cross-section, 1 meter in diameter and 10 meter in length. Two mode shapes are considered. Mass of the pendulum is 10% of the tower's total mass, which is hanged from top of the tower. The first and second eigenfrequencies of the tower are evaluated as

$$\begin{aligned} \omega_1 &= 28.26 \text{ rad/sec} & f_1 &= 4.5 \text{ [Hz]} \\ \omega_2 &= 177.14 \text{ rad/sec} & f_2 &= 28.19 \text{ [Hz]} \end{aligned} \quad (6-13)$$

Thus evaluation of generalized mass, stiffness and damping of the tower for first and second mode yields

$$\begin{aligned} m_1 &= m \int_0^l \psi_1^2(x) dx = 4709.70 \text{ kg} \\ k_1 &= EI \int_0^l [\psi_1''(x)]^2 dx = 3.77 \times 10^6 \frac{N}{m} \\ c_1 &= r_1 \int_0^l \psi_1^2(x) dx = 13310 \frac{Ns}{m} \\ m_1^* &= m \int_0^l \psi_1(x) dx = 7375.20 \text{ kg} \end{aligned} \quad (6-14)$$

$$\begin{aligned}
m_2 &= m \int_0^l \psi_2^2(x) dx = 4726.70 \text{ kg} \\
k_2 &= EI \int_0^l [\psi_2''(x)]^2 dx = 1.48 \times 10^8 \frac{N}{m} \\
c_2 &= r_2 \int_0^l \psi_2^2(x) dx = 83729 \frac{Ns}{m} \\
m_2^* &= m \int_0^l \psi_2(x) dx = -4107.80 \text{ kg}
\end{aligned} \tag{6-15}$$

Mass and length of the pendulum are chosen as follows

$$m_p = 1884 \text{ kg}, \quad s = 1 \text{ mtr} \tag{6-16}$$

By means of Matlab7 software, the Equations (6-10) and (6-11) are computed in frequency domain for the BT. Figure (6-2) and (6-3) illustrate displacement amplitude response by frequency. Two resonance frequency of the tower substructure are 4.52 [Hz] and 28.6 [Hz] for first and second dynamic modes, respectively.

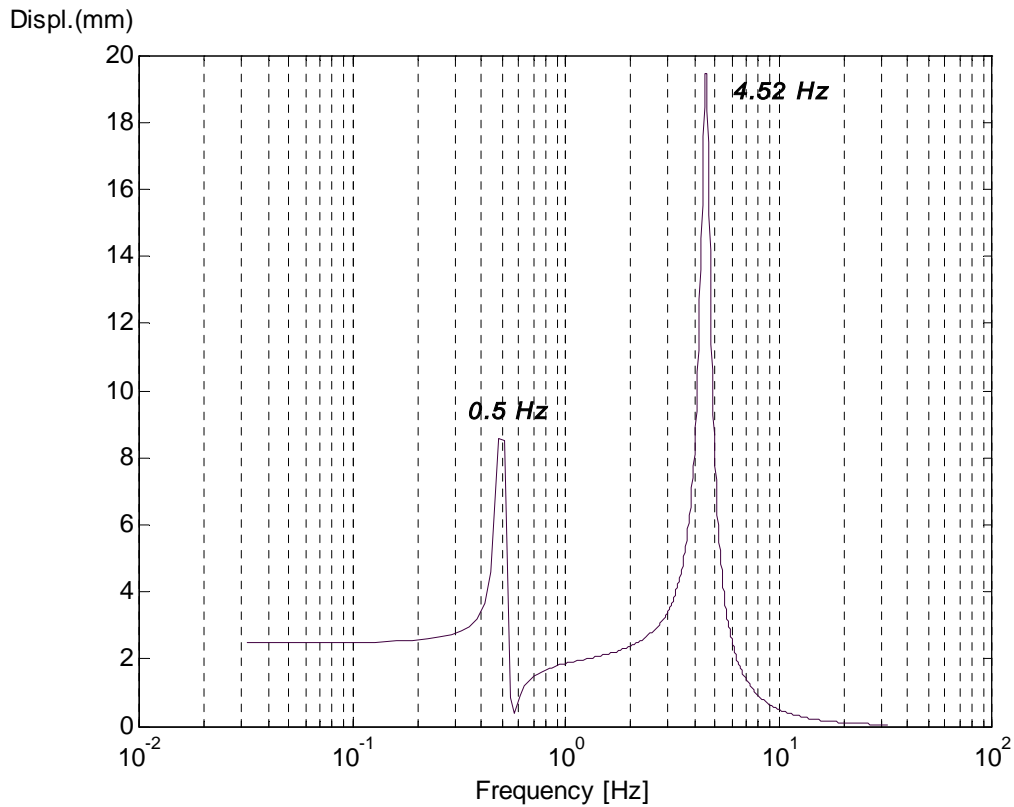


Figure 6-2 Tip-displacement response of the tower in frequency domain, the first mode contribution

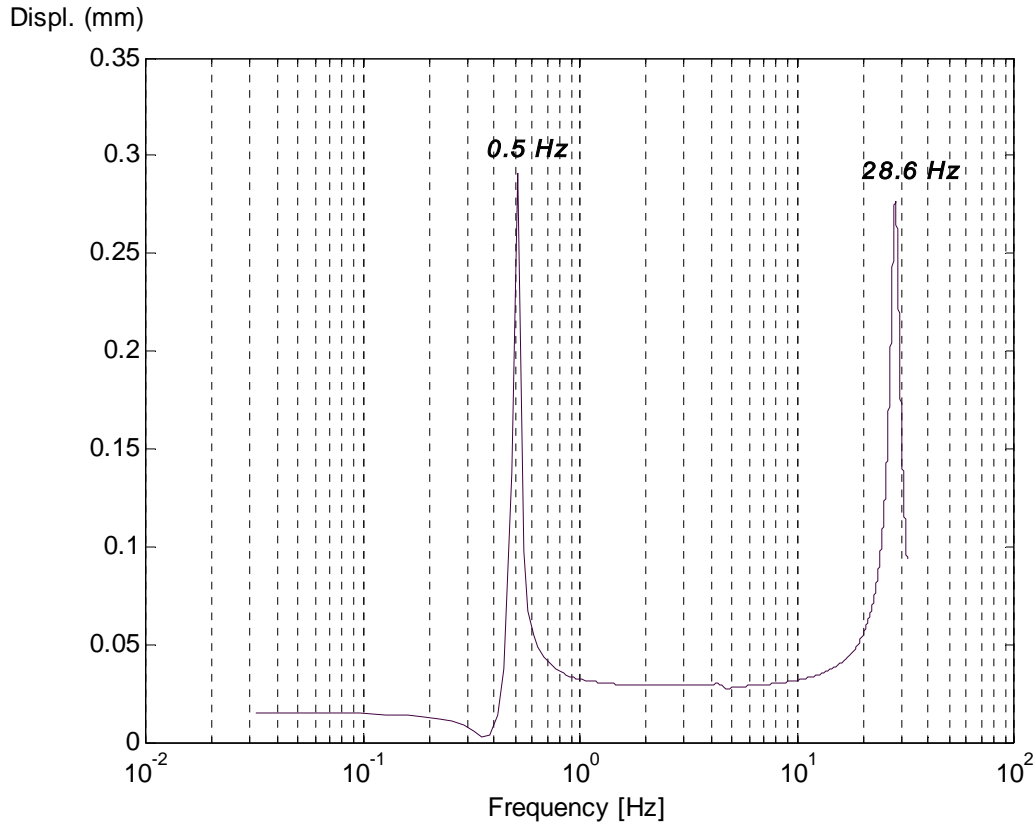


Figure 6-3 Tip-displacement response of the tower in frequency domain, the second mode contribution

Considering pendulum frequency response function as rendered in Equation (6-8), the tower interaction on the pendulum in comparison with excitation amplitude is small and negligible. Therefore Equation (6-8) yields

$$\Phi = \frac{-a}{g - s\nu^2} \quad (6-17)$$

Consequently Equations (6-10) and (6-11) reduce to

$$Z_1 = \frac{a m_p \nu^2 (m_1^* - m_2^*) - a S_2 (m_1^* + \frac{m_p g}{g - s\nu^2})}{-m_p \nu^2 (S_1 - S_2) + S_1 S_2} \quad (6-18)$$

$$Z_2 = \frac{a m_p \nu^2 (m_2^* - m_1^*) - a S_1 (m_2^* + \frac{m_p g}{g - s\nu^2})}{-m_p \nu^2 (S_1 - S_2) + S_1 S_2} \quad (6-19)$$

In the numerical BT substructure, for different values of ν , calculation of these two equations yields to displacement response of the tower tip-point for first and second mode, illustrated in Figures (6-4) and (6-5). Resonance frequency as depicted in these figures, are 3.80 [Hz] and 24.9 [Hz] for first and second mode subsequently.

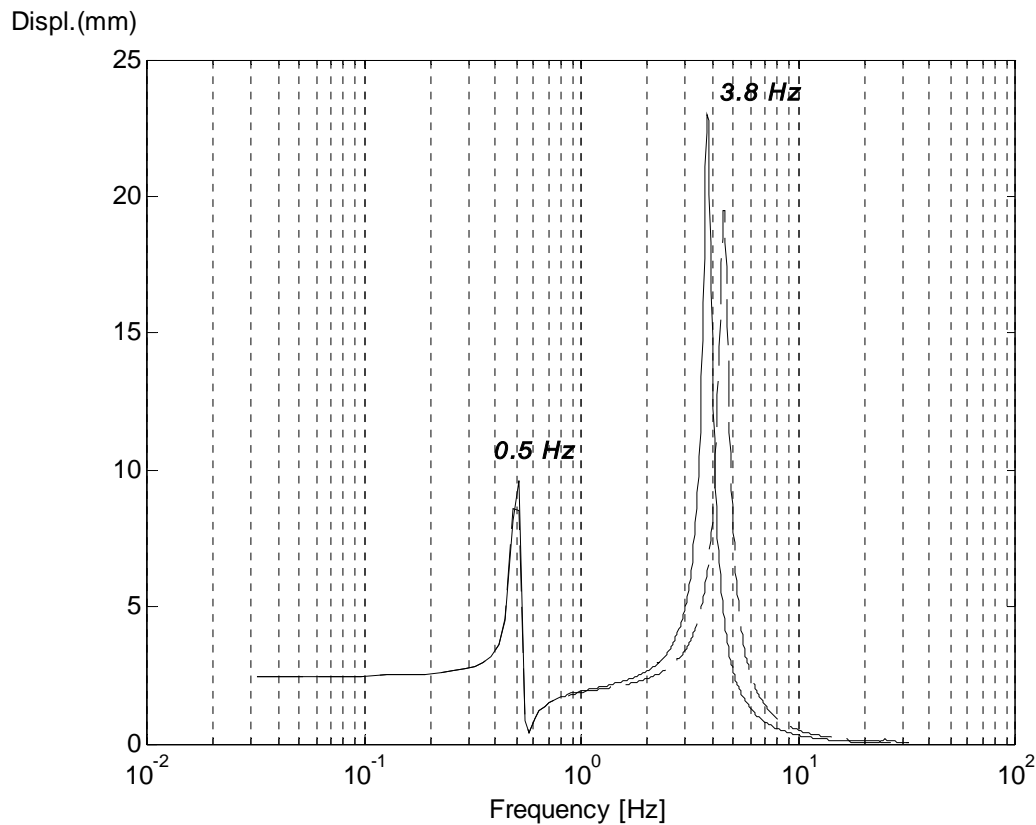


Figure 6-4 Tip-displacement response of the tower in frequency domain, the first mode contribution (interaction of tower on Bell ignored)

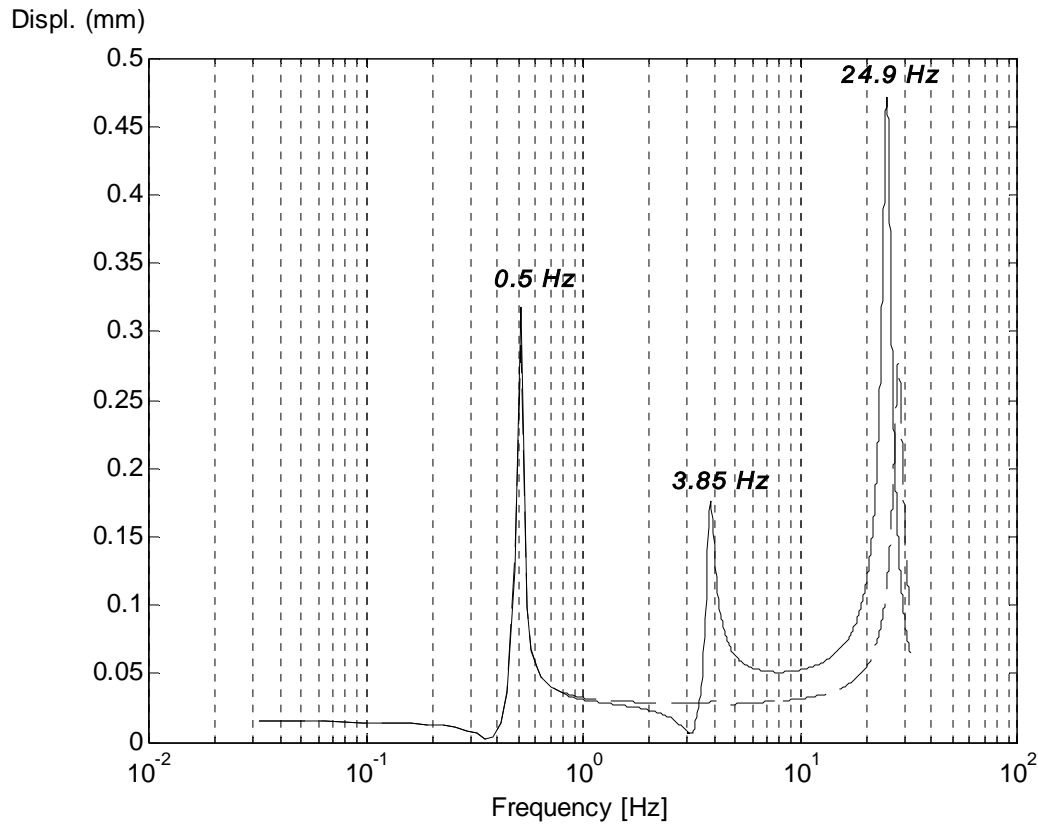


Figure 6-5 Tip-displacement response of the tower in frequency domain, the second mode contribution (interaction of tower on Bell ignored)

The results show 13% decrease of the tower substructure frequency for first mode contribution and 16% decrease of the tower substructure frequency for second mode contribution. Noting that in practical problems the fundamental tower frequency should be at least beyond 20% of the excitation frequency².

6.4 Pendulum dynamic actions

The forces associated with pendulum are periodic forces which can be considered as an external applied force in the tower.

Introducing the time displacement forces induced by the movement of the pendulum is of major relevance in the analysis of the tower. The free rotation of a simple pendulum with large oscillations around axis, as represented in Appendix B, is formulated as

$$m_p s^2 \ddot{\phi} + m_p g s \sin \phi = 0 \quad (6-20)$$

² Reference [6]

The mathematical solution of this equation leads to³

$$\phi(t) = 2 \arcsin[k \operatorname{sn}(\omega t)] \quad (6-21)$$

where sn is the elliptic Jacobean function, k is a constant depending on the initial conditions, and ω is the linear frequency of the mathematical pendulum $\omega = \sqrt{\frac{g}{s}}$.

As discussed in Chapter 4, Part 4.2, the general solution of the nonlinear free vibration may be formulated by a first approximation as

$$\phi(t) = \alpha \cos(\omega_N t + \beta) \quad (6-22)$$

The second approximation also reads

$$\phi(t) = \alpha \cos(\omega_N t + \beta) - \frac{\alpha^3}{192} \cos(3\omega_N t + 3\beta) \quad (6-23)$$

where ω_N is the frequency of nonlinear pendulum and α, β are constant values.

As a consequence of this oscillatory movement, the time-variant horizontal and vertical forces of the support are

$$H(t) = m_p s [\dot{\phi}^2 \sin \phi - \ddot{\phi} \cos \phi] \quad (6-24)$$

$$V(t) = m_p s [\dot{\phi}^2 \cos \phi + \ddot{\phi} \sin \phi] \quad (6-25)$$

The forces are periodic, where harmonic parts can be determined by means of the Fourier analysis⁴ as follows

$$H(t) = \sum_{j=1}^{\infty} H_j(t) = c m_p g \sum_{j=1}^{\infty} \gamma_j \sin \omega_j t \quad j = 1, 3, 5, \dots \quad (6-26)$$

$$V(t) = \sum_{j=1}^{\infty} V_j(t) = c m_p g \sum_{j=1}^{\infty} \beta_j \sin \omega_j t \quad j = 2, 4, 6, \dots \quad (6-27)$$

³ Reference [1]

⁴ Reference [5]

c is a shape factor expressed (see Chapter 2, Part 2.3) for the physical pendulum as

$$c = \frac{s^2}{i_s^2 + s^2} \quad (6-28)$$

and for mathematical pendulum

$$c = 1 \quad (6-29)$$

The corresponding Fourier coefficients γ_j, β_j are represented in Figures (6-6) and Figure (6-7). ω_N is the frequency of the nonlinear pendulum evaluated by the following equation in the standard form of the elliptic integral of the first kind,

$$\tau = \frac{4}{\omega} F\left(s, \frac{\pi}{2}\right) \quad \tau = \frac{1}{\omega_N} \quad \text{and} \quad s = \sin\left(\frac{a}{2}\right) \quad (6-30)$$

where a is the maximum rotation angle of the pendulum, see Appendix B.

Figure (6-8) shows the variation of frequency versus maximum amplitude of excitation a in the nonlinear pendulum.

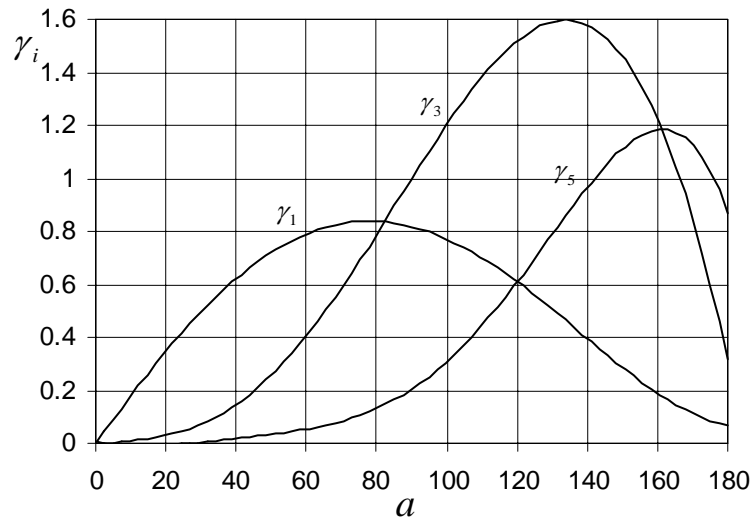


Figure 6-6 Horizontal force amplitudes of the harmonics of the pendulum oscillation
(a : pendulum rotation amplitude)

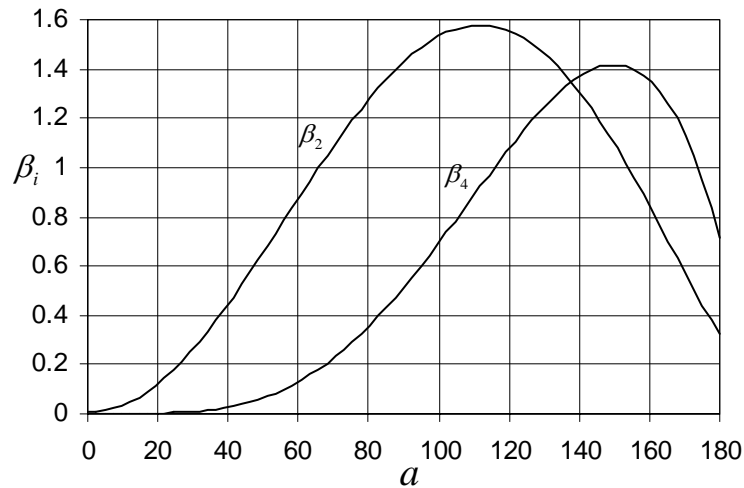


Figure 6-7 Vertical force amplitudes of the harmonics of the pendulum oscillation
(a : pendulum rotation amplitude)

For an angle greater than 80° , the amplitude of the third harmonic (subharmonic) for horizontal force is larger than the amplitude of fundamental frequency excitation, as shown in Figure (6-6). Then for free vibration of the tower, resonance with the components of the pendulum forces, particularly first and third harmonic should be avoided as described for some samples in Chapter 4.

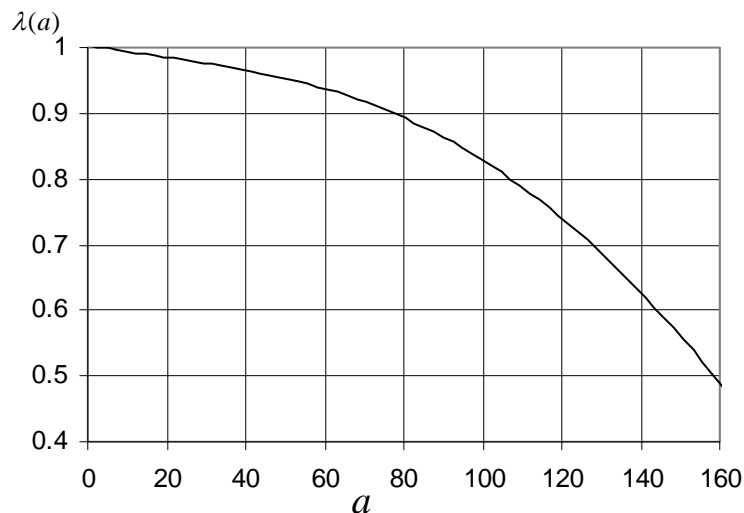


Figure 6-8 Ratio of nonlinear over linear frequency $\lambda(a) = \frac{\omega_N}{\omega}$ (a : pendulum maximum rotation)

Due to the geometry of the BT and the material utilized in the construction, most towers have significant higher resistance to axial loading than to torsion or bending. Therefore the horizontal component of induced forces is most critical and is applied to the BT model in the subsequent section.

6.5 Quasi-static analysis of the BT

A concrete BT of height $10m$ and of the circular diameter of $1m$ is considered for numerical investigation. Bell swinging is introduced at the top of the tower assuming the model of a simple mathematical pendulum, compare to Figure (4-2). The numerical geometry data of the BT are given in Equation (4-18). These data are introduced to Simulink software for time domain analysis. The forces induced by the bell can be evaluated by Equation (6-26) and Equation (6-27). Considering the geometry of the BT, horizontal forces of the bell are more critical than vertical forces, evaluated as

$$H(t) = 18482.04(\gamma_1 \sin \omega_N t + \gamma_3 \sin 3\omega_N t) \quad [N] \quad (6-31)$$

With the help of Figures (6-6), (6-7) and (6-8) and considering the maximum rotation angle of the pendulum ($a = 0.90 \text{ rad}$) one can write

$$\begin{aligned} \omega_N &= 0.95 \omega = 2.97 \text{ rad/sec} \\ \gamma_1 &= 0.73, \gamma_2 = 0.30 \end{aligned} \quad (6-32)$$

Substituting in Equation (6-31) results in

$$H(t) = 18482.04(0.73 \sin 2.97t + 0.30 \sin 8.91t) \quad [N] \quad (6-33)$$

Thus the equations of motion for the numerical BT-example consist of two mode shapes, compare Equations (6-14) and (6-15),

$$\begin{aligned} 6593.70\ddot{Z}_1 + 1884.00\ddot{Z}_2 + 13310.00\dot{Z}_1 + 3.77 \times 10^6 Z_1 = \\ 18482.04(0.73 \sin 2.97t + 0.30 \sin 8.91t) \end{aligned} \quad (6-34)$$

$$1884.00\ddot{Z}_1 + 6610.70\ddot{Z}_2 + 83729\dot{Z}_2 + 1.48 \times 10^8 Z_1 = 18482.04(0.73 \sin 2.97t + 0.30 \sin 8.91t) \quad (6-35)$$

Where the interaction between the tower and the pendulum is neglected, see Chapter 6, Part 6.2.

Those equations can be solved by numerical time step analysis. For this purpose Matlab7 and Simulink software are programmed and the response of the BT is computed. The force progress induced by bell swinging is shown in Figure (6-9). Tip-displacement response of the tower due to dynamic actions of bell in the first and second modes is illustrated in Figure (6-10) and Figure (6-11), respectively.

All figures show acceptable correlation with the results due to analysis of mechanical model of the BT (discussed in Chapter 4, Part 4.5), compare Figure (4-4).

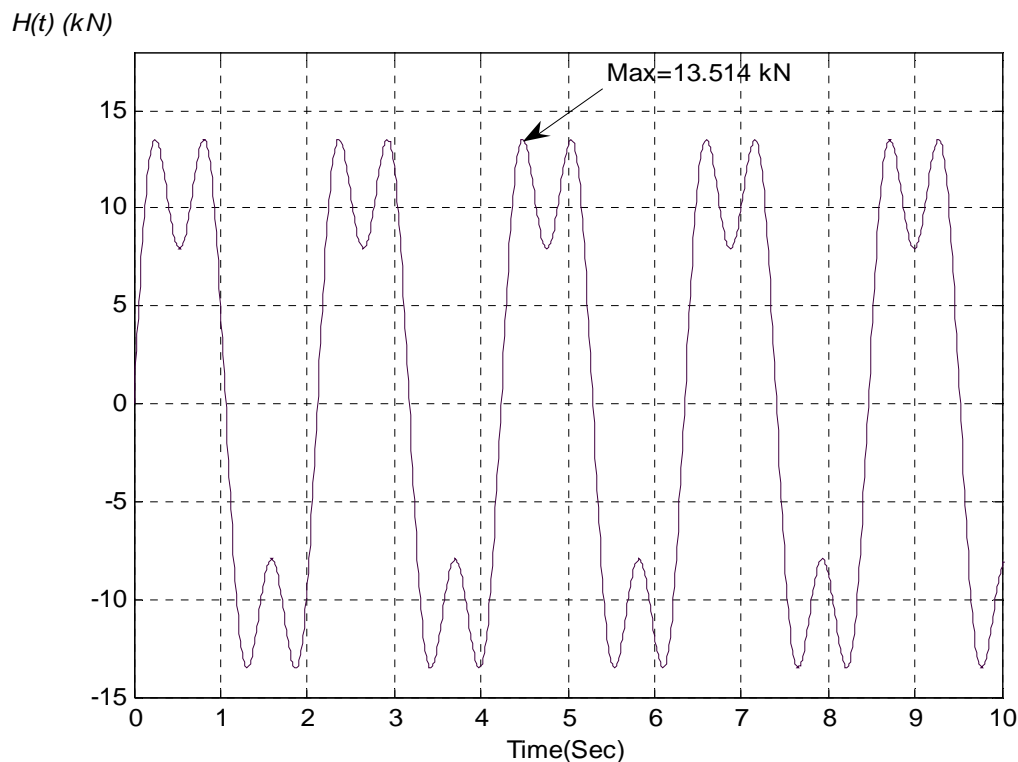


Figure 6-9 Periodic force induced by the swinging of bell

Figure (6-9) shows a maximum horizontal force of

$$[H(t)]_{\max} = 13514 \text{ N} \quad (6-36)$$

The expression of static stiffness of the BT with a single degree of freedom and without damping leads to

$$K_s = \frac{3EI}{L^3} = 3.65 \times 10^6 \frac{\text{N}}{\text{m}} \quad (6-37)$$

Due to dynamical effects, the stiffness of the tower depends on derivatives of modal displacement and is determined for the first mode of the numerical BT as

$$K = 3.77 \times 10^6 \frac{\text{N}}{\text{m}} \quad (6-38)$$

The quasi-static maximum deflection at the top of the tower can be evaluated as

$$\Delta_s = \frac{[H(t)]_{\max}}{K} = 3.58 \text{ mm} \quad (6-39)$$

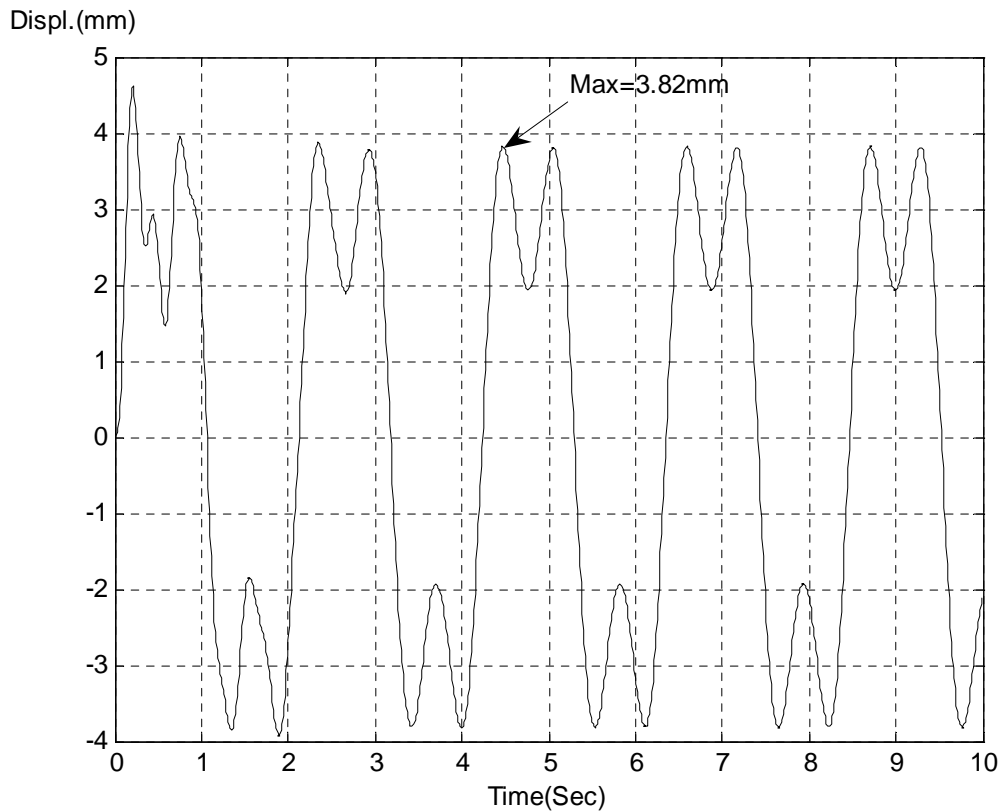


Figure 6-10 Tip-displacement response of the tower, the first mode contribution

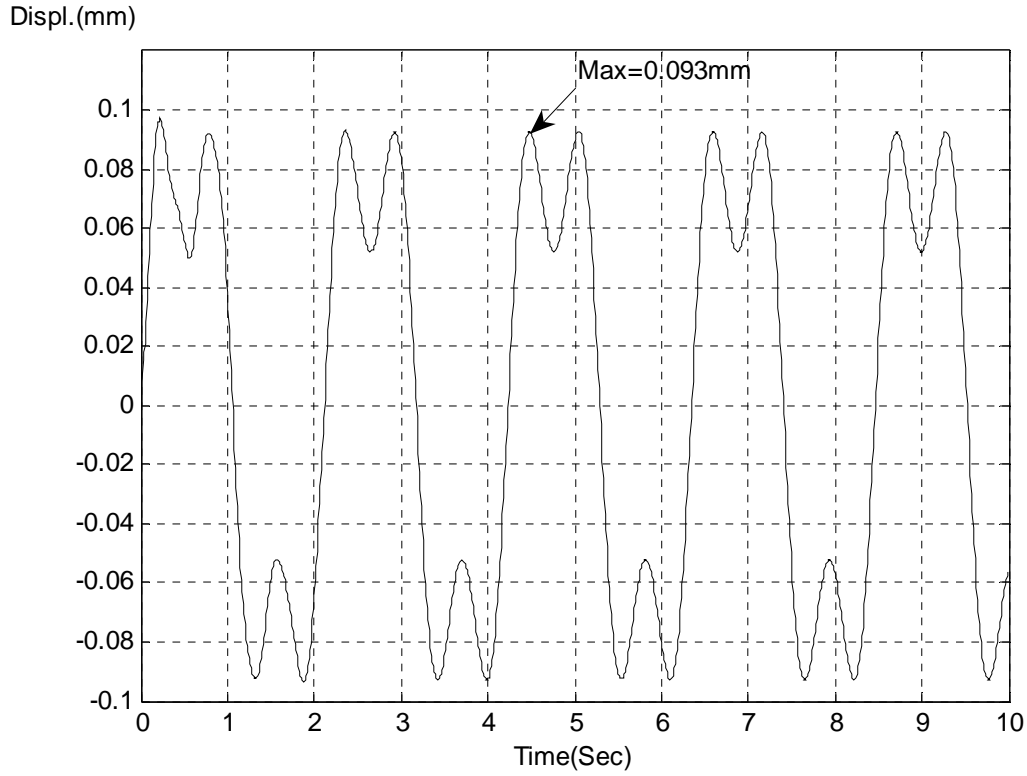


Figure 6-11 Tip-displacement response of the tower, the second mode contribution

The maximum amplitudes in the first and second modes marked in Figures (6-10) and (6-11) are

$$\Delta_{1\max} = 3.82\text{mm} \quad \text{and} \quad \Delta_{2\max} = 0.093\text{mm} \quad (6-40)$$

In order to evaluate the dynamic amplification factor introduced by bell swinging, the maximum displacements at the top of the tower for dynamic and static analyses are compared.

Results confirm that the maximum tip-displacement response of the tower, induced by bell swinging from dynamical analysis of the first vibration mode, is 1.07 times as that of the quasi-static analysis. It is defined as Dynamic Amplification Factor (DAF)

$$DAF = \frac{\Delta_{1\max}}{\Delta_s} = 1.07 \quad (6-41)$$

Thus any desired force and moment resultants in the tower section can be obtained by standard method of static analysis, multiply by DAF . For instance the base shear and moment can be written as

$$\begin{aligned} V_o &= 13514 \times DAF = 14460 \text{ N} \\ M_o &= 135140 \times DAF = 144600 \text{ Nm} \end{aligned} \quad (6-42)$$

6.6 BT forces induced by dynamic excitation

Considering only the first mode shape of the BT, the dynamic equilibrium of the system involves inertial, damping and elastic forces which are distributed along the axis⁵ and can be expressed as

$$f_I + f_D + f_s = 0 \quad (6-43)$$

f_I stands for inertial, f_D for damping and f_s for elastic force which are distributed along the tower axis, all force contributions are oriented in horizontal direction.

The Ritz approximation for a single degree of freedom system leads to

$$v(x,t) = \psi(x)Z(t) \quad (6-44)$$

The corresponding generalized forces are the same as for the problem discussed in Chapter 3, Part 3.2. Therefore, due to base excitation

$$f_I = m_i \ddot{Z}_i + m_i^* \ddot{Z}_g \quad f_D = c_i \dot{Z}_i \quad f_s = k_i Z_i \quad (6-45)$$

Thus Equation (6-43) results in

$$m_i \ddot{Z}_i + c_i \dot{Z}_i + k_i Z_i = -m_i^* \ddot{Z}_g \quad (6-46)$$

Furthermore, the external dynamic force can be formulated as

$$F = m_p g (\gamma_1 \sin \omega_N t + \gamma_3 \sin 3\omega_N t) \quad (6-47)$$

⁵ Reference [2]

Then the principal of virtual work, considering both internal and external forces according to Equations (6-46) and (6-47), leads to

$$m_i \ddot{Z}_i + c_i \dot{Z}_i + k_i Z_i = m_p g (\gamma_1 \sin \omega_N t + \gamma_3 \sin 3\omega_N t) \quad (6-48)$$

The solution of these equations can be obtained by numerical procedure and the displacement distribution follows from Equation (6-44).

The elastic forces depend on derivatives of the displacement shape and can be evaluated from the BT displacement acting on the stiffness properties. However, it is more effective to express these forces approximately in terms of the equivalent inertial forces developed in undamped free vibration⁶. Thus since the inertial force in free vibration is

$$f_I(x, t) = \bar{m} \ddot{v}(x, t) = -\omega^2 \bar{m} v(x, t) \quad (6-49)$$

where \bar{m} denotes mass per unit length.

For undamped oscillations Equation (6-43) reduces to

$$f_I + f_s = 0 \quad (6-50)$$

and further

$$f_s(x, t) = \omega^2 \bar{m} v(x, t) \quad (6-51)$$

Distributed elastic forces in the BT are depicted in Figure (6-12). The shear force at the base of the tower is expressed by

$$V_o = \int_0^L f_s(x, t) dx = \omega^2 \bar{m} Z(t) \int_0^L \psi(x) dx \quad (6-52)$$

and the base moment is given by

$$M_o = \int_0^L f_s(x, t) x dx = \omega^2 \bar{m} Z(t) \int_0^L \psi(x) x dx \quad (6-53)$$

⁶ Reference [2]

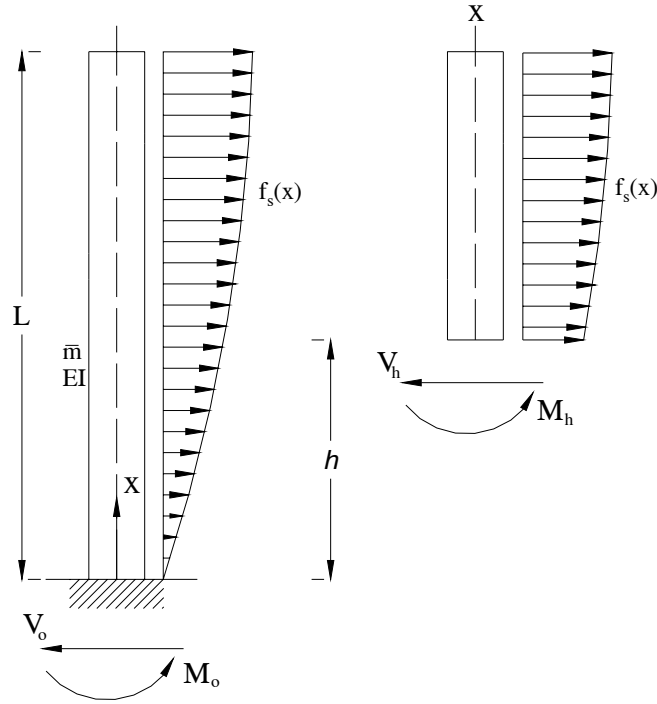


Figure 6-12 Elastic force of the BT

Expressions for moment and shear force at an arbitrary section with $x = h$, can be written as

$$V_h = \int_h^L f_s(x, t) dx = \omega^2 \bar{m} Z(t) \int_h^L \psi(x) dx \quad (6-54)$$

$$M_h = \int_h^L f_s(x, t) x dx = \omega^2 \bar{m} Z(t) \int_h^L \psi(x) x dx \quad (6-55)$$

Introducing the selected geometry for the BT given in Equation (4-18), time step analysis utilizing Matlab7 and Simulink software gives the time-variant response of the moment and shear forces, as illustrated in Figures (6-13) and (6-14).

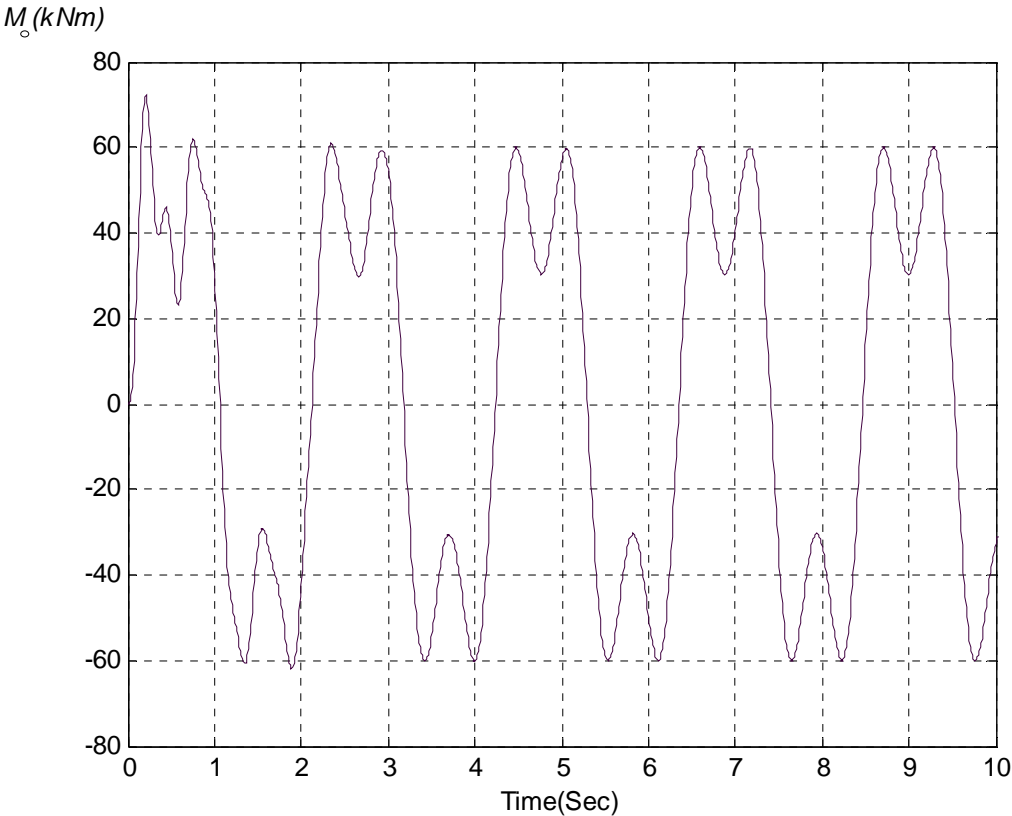


Figure 6-13 Base moment response of the BT, M_o (induced by pendulum)

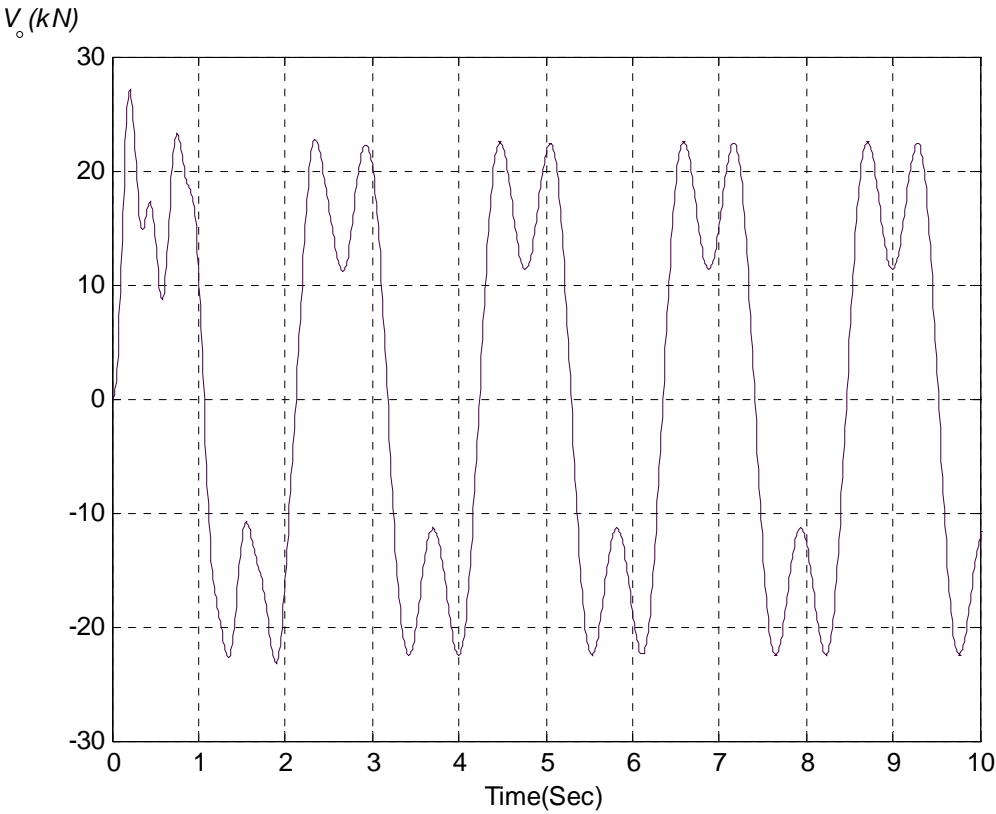


Figure 6-14 Base shear force response of the BT, V_o (induced by pendulum)

The maximum steady-state response values are

$$M_o(\max) = 60 \text{ kNm}$$

$$V_o(\max) = 22.5 \text{ kN} \quad (6-56)$$

As an additional practical study, the BT system formulated by Equation (3-62), (3-63) and (3-64) is excited by real earthquake excitation of Bam, Iran, (2003), (presented in Chapter 5, Part 5.4.5). Figures (6-15) through (6-17), as well as (6-20) through (6-22) illustrate the displacement responses of the BT in time and frequency domain, respectively.

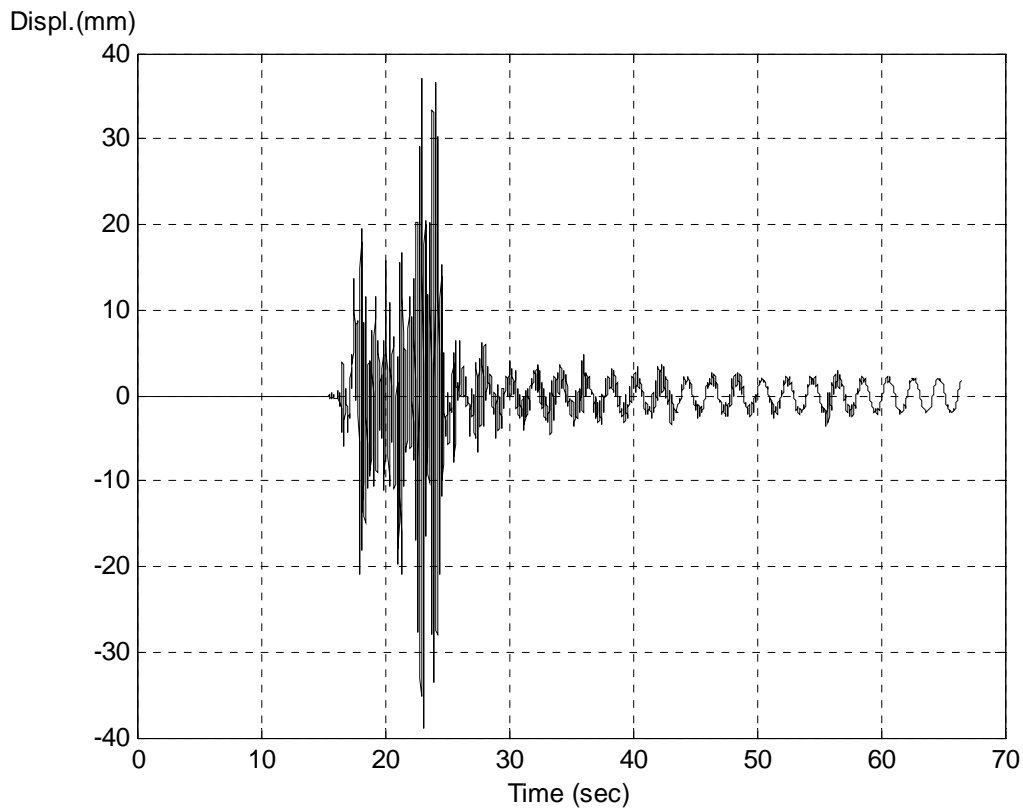


Figure 6-15 Tip-displacement of the first mode (BT induced by Bam strong ground motion)

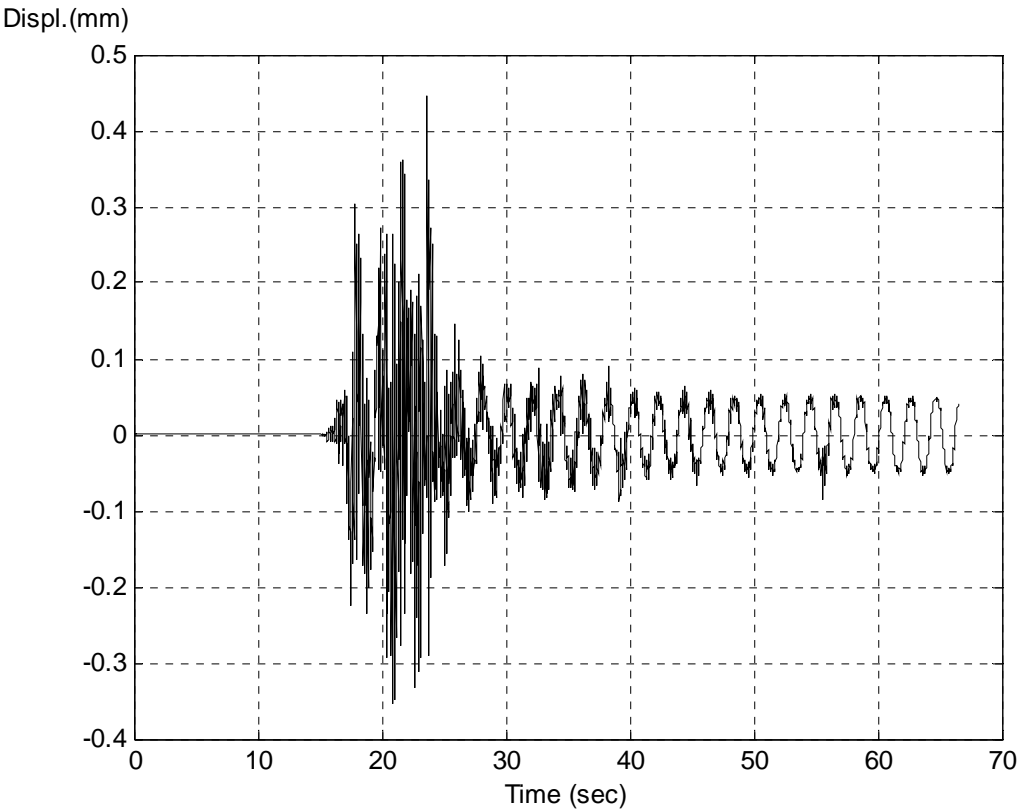


Figure 6-16 Tip-displacement of the second mode (BT induced by Bam ground motion)

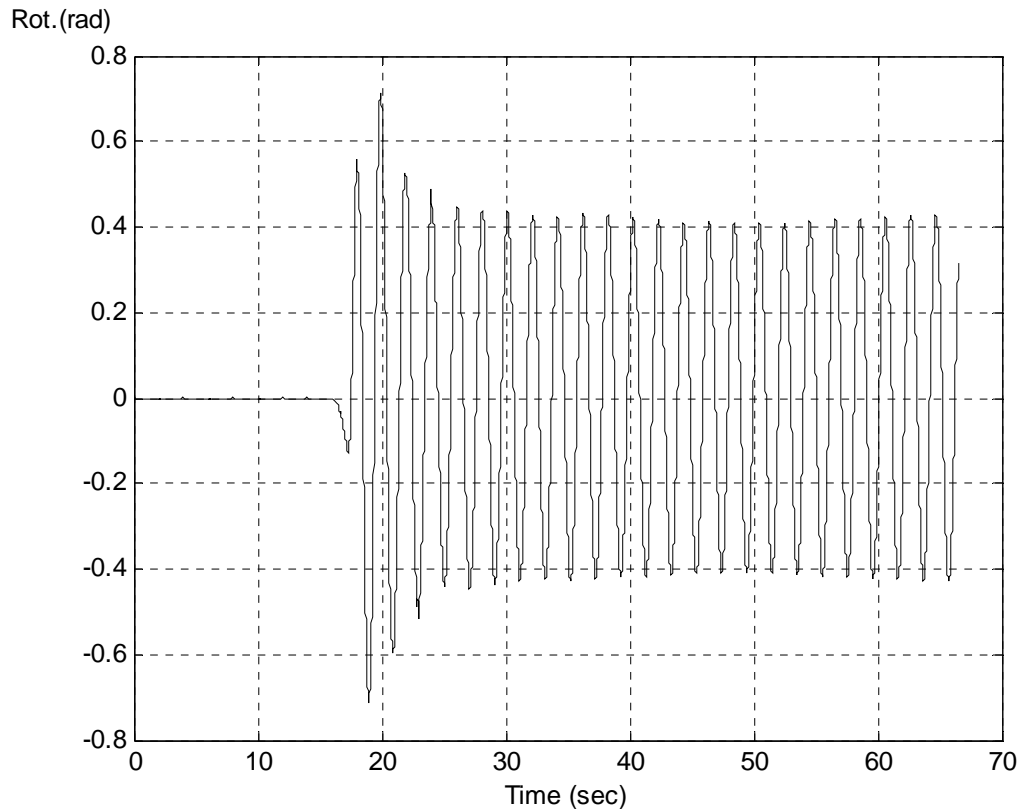


Figure 6-17 Pendulum rotation (BT induced by Bam strong ground motion)

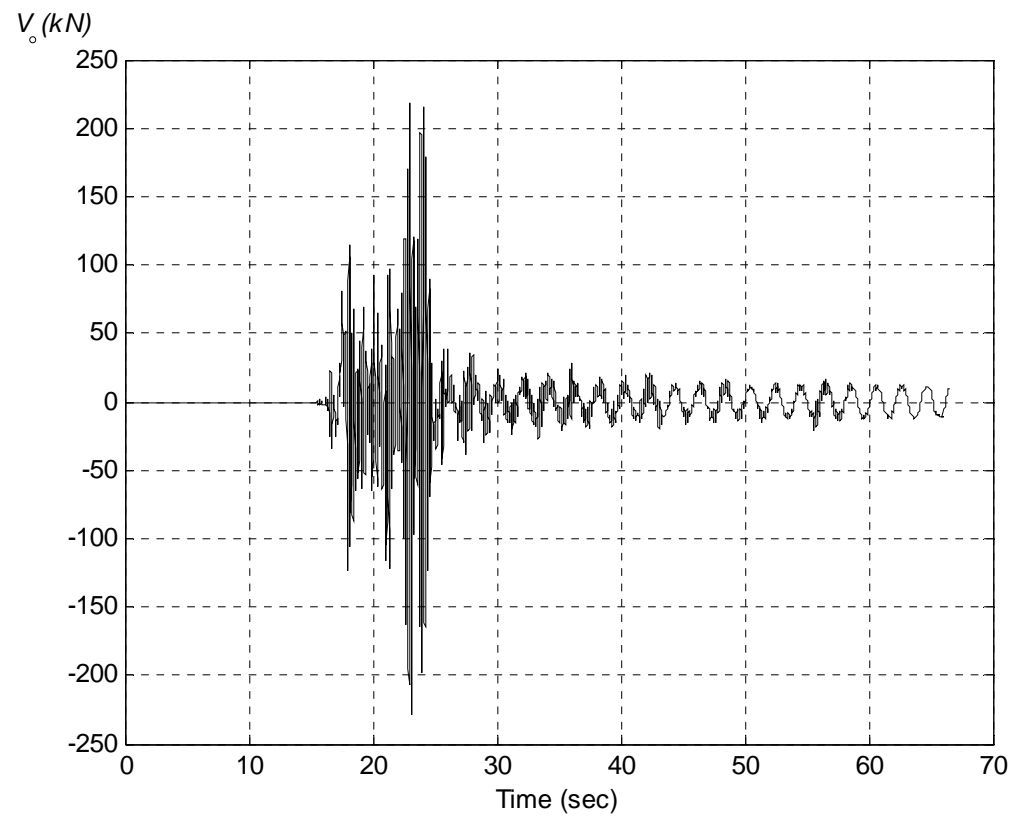


Figure 6-18 Base shear force response V_o (BT first mode)

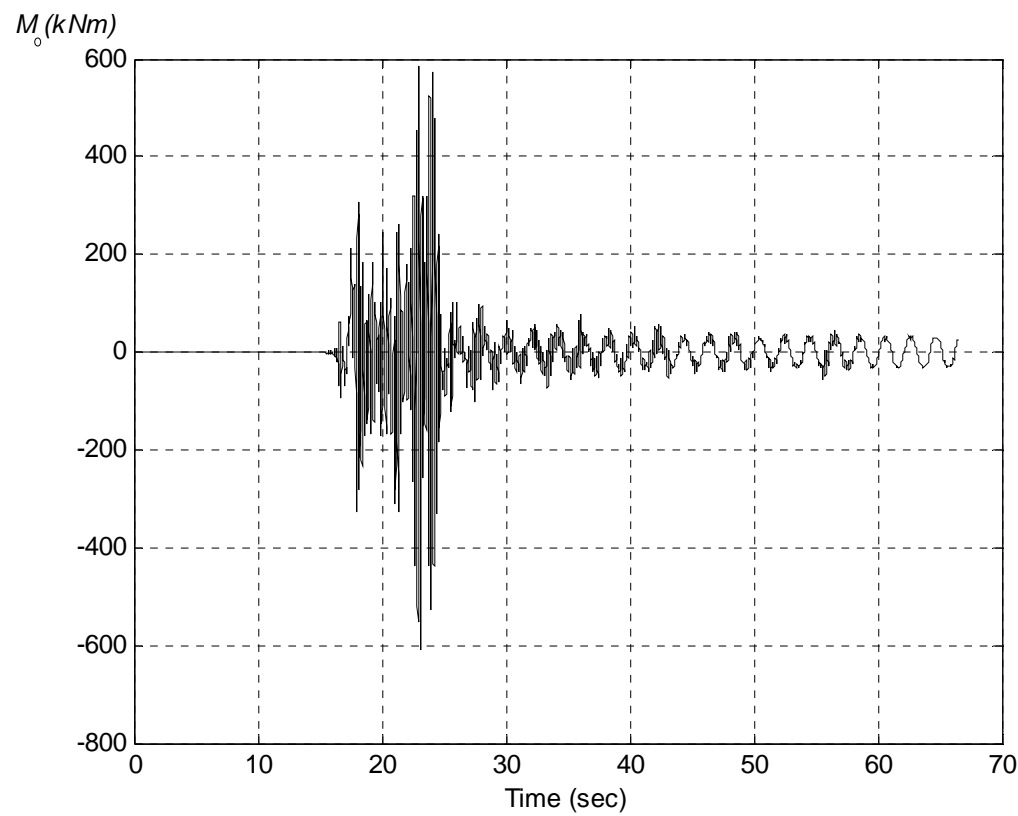


Figure 6-19 Base moment response M_o (BT first mode)

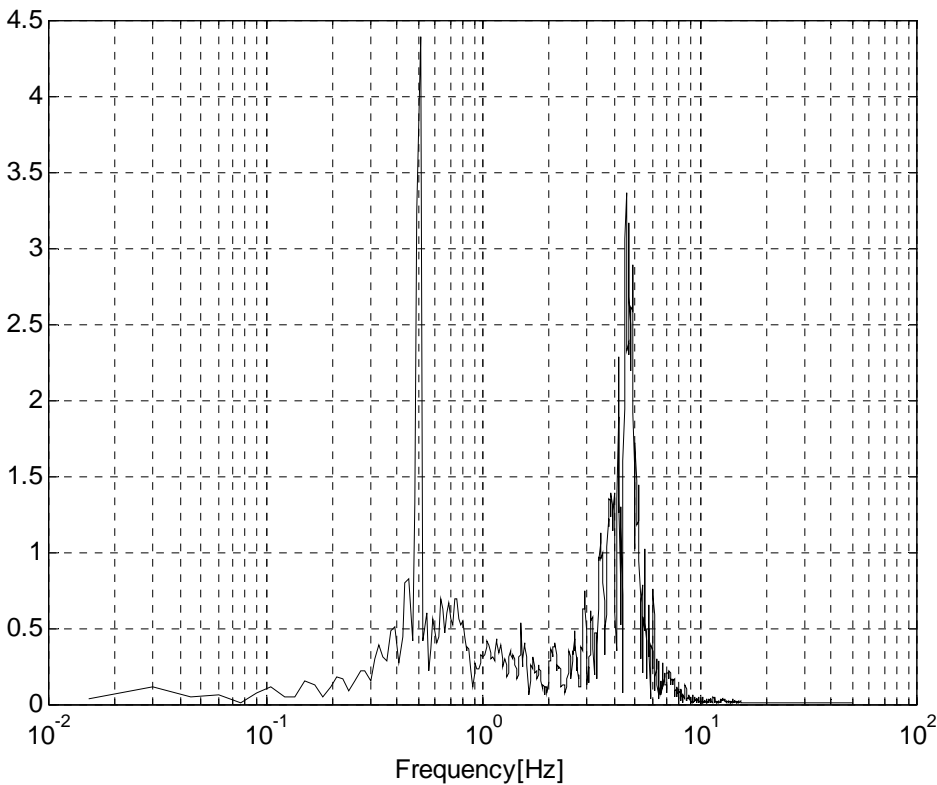


Figure 6-20 First mode tip-displacement FFT response
(BT induced by Bam strong ground motion)

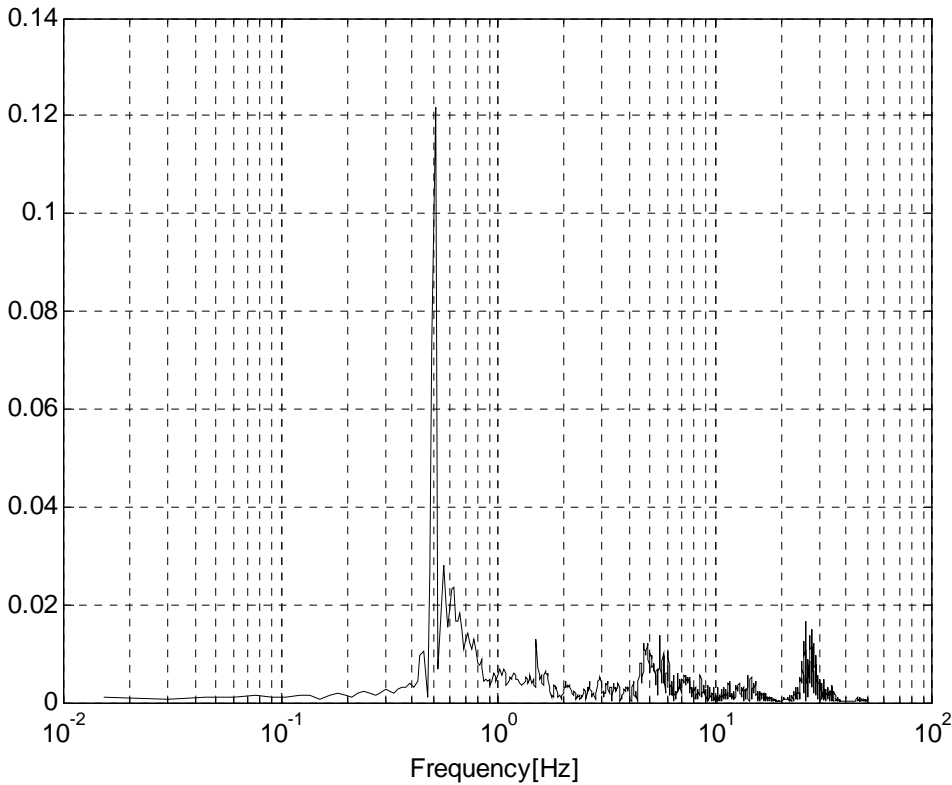


Figure 6-21 Second mode tip-displacement FFT response
(BT induced by Bam strong ground motion)

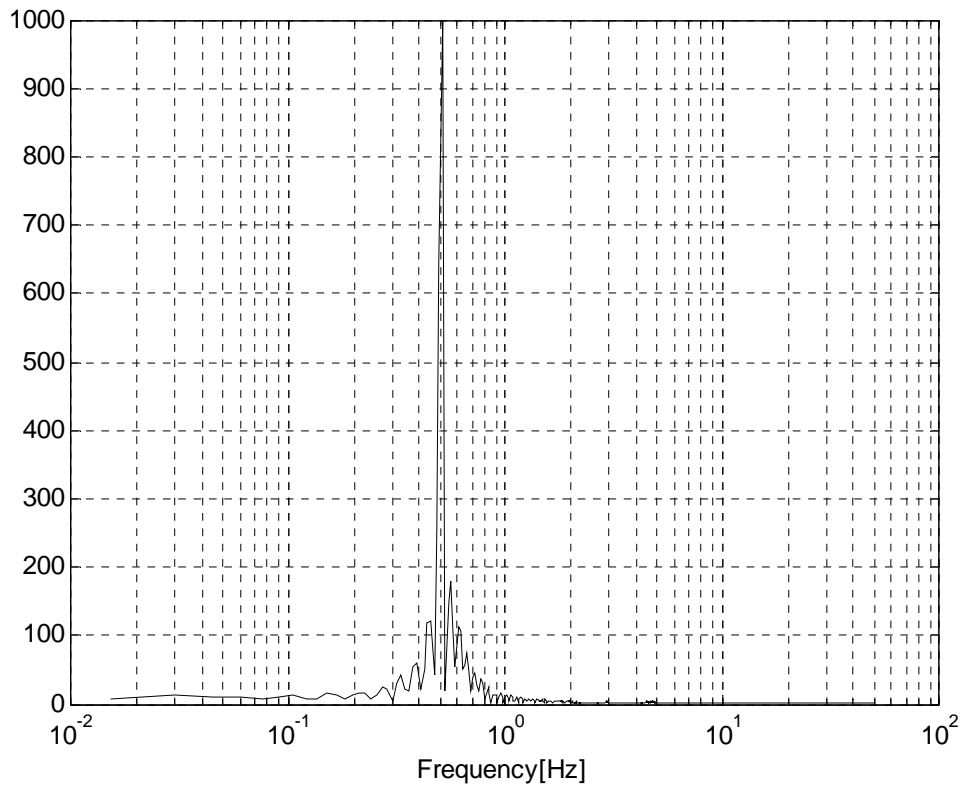


Figure 6-22 Pendulum mode FFT response (BT induced by Bam strong ground motion)

The maximum values of shear force and moment at the base of the tower for the first mode of vibration of the BT, shown in Figures (6-18) and (6-19), respectively are

$$M_o(\max) = 580 \text{ kNm}$$

$$V_o(\max) = 215 \text{ kN} \quad (6-57)$$

For the higher modes of vibration, forces can be obtained by a similar procedure. The maximum total response can be evaluated through superposition of modal values by the Square Roots of Sum of Squares (SRSS)⁷ method. However, when the frequencies of major contributing terms are very close to each other, the more general Complete Quadratic Combination (CQC)⁸ method is utilized. For the BT model with generalized coordinate system, the effects of higher modes are

⁷ Reference [3]

⁸ Reference [3]

negligible as compared to the first mode. Therefore, for this case only the first mode of vibration provides sufficient accuracy for the results.

6.7 References

1. Ziegler F., 'Mechanics of Solids and Fluids', Second edition, Technical University Vienna, Springer-Verlag New York-Vienna, 1998.
2. Clough R.W., Penzien J., Department of Civil Engineering, University of California, 'Dynamic of Structures', McGraw-Hill, 1989.
3. Chopra A.K., University of California at Berkeley, 'Dynamics of Structures', second edition, Prentice Hall, 2001.
4. Chakrabarti P., Chopra A.K., University of California at Berkeley, 'Earthquake Analysis of Gravity Dams Including Hydrodynamic Interaction', International Journal of Earthquake Engineering and Structural Analysis, Vol. 2, 1997 pp. 143-160.
5. Müller F-P., 'Berechnung und Konstruktion von Glockentürmen', Verlag Wilhelm Ernst & Sohn, 1968.
6. Bachman Hugo, 'Vibration Problems in Structures', Birkhäuser Verlag, 1995.

7

ACTIVE CONTROL IN THE BT

7.1 Introduction

In comparison with passive energy dissipation, research and development of active structural control technology has a more recent origin. In structural engineering, active structural control is an area of research in which the motion of structure is controlled or modified by means of the action of a control system through some external energy dissipation. Active control can be used for example, for motion control against wind and earthquake forces. In this chapter dynamic analysis of the BT by application of actual control system is investigated. A numerical nonlinear model is made and time step analysis is performed to compare the results.

7.2 Active Pendulum Tuned Mass Damper (APTMD)

The former studies were focused on the application of passive PTMD, for which no external forces needed to be added to the system, and the characteristic of stiffness and damping in the bell (pendulum) did not change with time. In contrast, the APTMD uses an external source of energy, in the form of an actuator, to reduce the level of vibration. A linear actuator placed between the structure and tuned mass and is known as a proof mass actuator¹. APTMDs have higher effectiveness than their passive counterparts and can be manually or automatically retuned (readjusted) via their electronic software. Moreover, a single active system can simultaneously be tuned to multiple frequencies. Those controllers are also smaller in size than their passive counterparts. Figure (7-1) shows a APTMD which has been installed on the top floor of a 70-story building with 296m height, and

¹ Reference [1]

also on the top of the tower of Akashi Kaikyo Bridge, having 300m height, by Matsumoto et al², 1990.

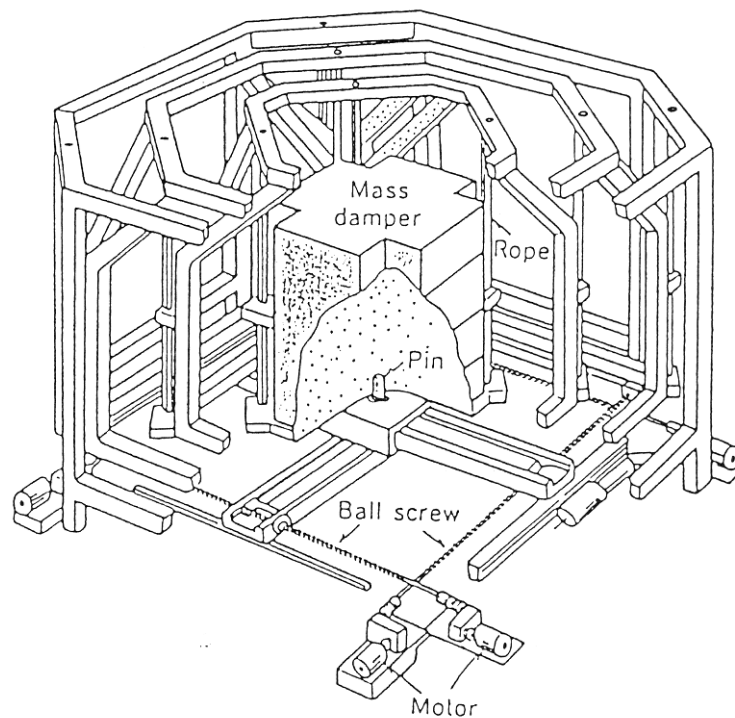


Figure 7-1 APTMD, Matsumoto et al 1990

7.3 BT with Active Pendulum Mass Damper (APMD)

For practical implementation, some analytical and numerical studies on the efficiency of APMD in the BT are made. Figure (7-2) shows the system of BT with control device. The tower is contained in the first two mode shapes of vibration. The bell (pendulum) and the actuator (shaker) are positioned directly at the top of the tower.

² Reference [3]

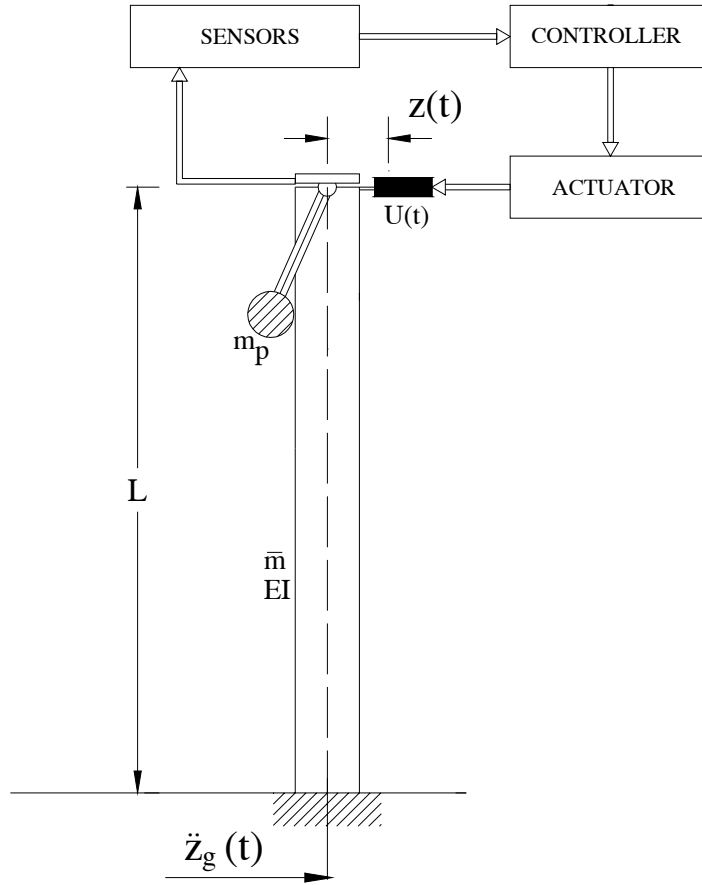


Figure 7-2 The active control loop for BT

The equations of motion are governed by the following

$$(m_1 + m_p)\ddot{Z}_1(t) + m_p\ddot{Z}_2(t) + c_1\dot{Z}_1(t) + k_1Z_1(t) + m_p s(\ddot{\phi} \cos \phi - \dot{\phi}^2 \sin \phi) = -(m_1^* + m_p)\ddot{Z}_g(t) + U(t) \quad (7-1)$$

$$(m_2 + m_p)\ddot{Z}_2(t) + m_p\ddot{Z}_1(t) + c_2\dot{Z}_2(t) + k_2Z_2(t) + m_p s(\ddot{\phi} \cos \phi - \dot{\phi}^2 \sin \phi) = -(m_2^* + m_p)\ddot{Z}_g(t) \quad (7-2)$$

$$m_p s \cos \phi \ddot{Z}_1(t) + m_p s \cos \phi \ddot{Z}_2(t) + m_p s^2 \ddot{\phi} + m_p s g \sin \phi = -m_p s \cos \phi \ddot{Z}_g(t) \quad (7-3)$$

Definition of the generalized mass, stiffness and damping have been introduced through Equation (3-25). Variable U stands for the reaction of the actuator and here it is dedicated to the first vibration mode shape. As discussed previously, the contribution of the first mode dominates the BT system, and it seems reasonable to

set the actuator to the first natural frequency of the tower. Thus, the systems reaction to any perturbation is expressed by a control force as³

$$U = U(Z_1, \dot{Z}_1, \phi, \dot{\phi}) \quad (7-4)$$

7.4 The optimal state feedback control ⁴

The control force U intends to keep system at zero state $\vec{X} = [Z_1 \ \dot{Z}_1 \ \phi \ \dot{\phi}]^T = 0$ and returns it back in case of any perturbations due to initial conditions or external forces. The actuator is designed as an optimal Linear Quadratic Regulator (LQR). Action force U based on a linearized model of unforced system. The linearized model of unforced system can be obtained from Equations (7-1), (7-2) and (7-3) if we ignore the external excitation \ddot{Z}_g , and linearize the corresponding equations for small values of ϕ and $\dot{\phi}$ in order to achieve a system of linear first order differential equations in the state space form

$$\dot{\vec{X}} = \underline{A}\vec{X} + \underline{B}U \quad (7-5)$$

Thus, system matrix \underline{A} and location matrix \underline{B} may be formulated as

$$\underline{A} = \begin{bmatrix} 0 & 1 & 0 & 0 \\ \frac{-k_1}{m_1} & \frac{-c_1}{m_1} & \frac{gm_p}{m_1} & 0 \\ 0 & 0 & 0 & 1 \\ \frac{k_1}{sm_1} & \frac{c_1}{sm_1} & \frac{-g(m_1 + m_p)}{sm_1} & 0 \end{bmatrix} \quad (7-6)$$

$$\underline{B} = \begin{bmatrix} 0 \\ \frac{1}{m_1} \\ 0 \\ \frac{-1}{sm_1} \end{bmatrix} \quad (7-7)$$

³ Reference [2]

⁴ Reference [3]

The control law for the optimal linear state feedback controller is

$$U = -\underline{D}\bar{\underline{X}} \quad (7-8)$$

Here, the optimal gain vector \underline{D} is chosen in order to minimize the performance index as a weighted sum of integrated control error and control effort

$$J = \int (\bar{\underline{X}}^T \underline{Q} \bar{\underline{X}} + RU^2) dt \rightarrow \min \quad (7-9)$$

\underline{Q} and R denote positive definitive weighting factors, that are chosen to reflect the value of control power.

The optimal solution for \underline{D} can be found in many publications on control theory, e.g. in reference [5].

$$\underline{D} = R^{-1} \underline{B}^T \underline{P} \quad (7-10)$$

Matrix \underline{P} is the solution to the algebraic Riccati's equation

$$\underline{A}^T \underline{P} + \underline{P} \underline{A} - R^{-1} \underline{P} \underline{B} \underline{B}^T \underline{P} + \underline{Q} = 0 \quad (7-11)$$

For given values of $\underline{A}, \underline{B}, \underline{Q}, R$, the Riccati's Matrix \underline{P} can be computed, for instance by using the built function in Matlab7. For given values of mass, damping and stiffness of the BT, the system matrix \underline{A} and the location matrix \underline{B} are computed using Equations (7-6) and (7-7). Then Ricatti Matrix solution is obtained by Equation (7-11) with chosen \underline{Q} and R to minimize the overall structural energy⁵.

Thus, considering both kinetic and static energy,

$$\underline{Q} = \begin{bmatrix} k_1 & 0 & 0 & 0 \\ 0 & m_1 & 0 & 0 \\ 0 & 0 & 0 & 0 \\ 0 & 0 & 0 & 0 \end{bmatrix} \quad (7-12)$$

$$R = \beta k_p \quad k_p = \frac{m_p g}{s} \quad (7-13)$$

⁵ Reference [4]

β is the weighing parameter, balancing the relative importance of response reduction (control effectiveness) and the control action requirements. Thus, small β minimizes the response and means that the response reduction is more important. Consequently, \underline{D} and the control force \underline{U} are calculated for any state of \vec{X} . The controller has the effect of adding positive linear stiffness and damping to the uncontrolled system. The control force \underline{U} can be used for time step analysis and is also applicable for the nonlinear BT.

7.5 Numerical analysis

Considering again the numerical example of BT as defined in Chapter 4, Part 4.3, the first and second natural frequencies of the tower are as follows

$$\begin{aligned}\omega_1 &= 28.26 \text{ rad/sec} & f_1 &= 4.5 \text{ [Hz]} \\ \omega_2 &= 177.14 \text{ rad/sec} & f_2 &= 28.19 \text{ [Hz]}\end{aligned}\tag{7-14}$$

The generalized mass, stiffness and damping of the tower for first and second mode were expressed in Equations (6-14) and (6-15). Thus the system matrix \underline{A} and the location matrix \underline{B} are calculated numerically by Equations (7-6) and (7-7) as

$$\underline{A} = \begin{bmatrix} 0 & 1 & 0 & 0 \\ -800.48 & -2.83 & 3.92 & 0 \\ 0 & 0 & 0 & 1 \\ 800.48 & 2.83 & -13.73 & 0 \end{bmatrix}\tag{7-15}$$

$$\underline{B} = \begin{bmatrix} 0 \\ 0.0002 \\ 0 \\ -0.0002 \end{bmatrix}\tag{7-16}$$

By considering matrix \underline{Q} and variable R as

$$\underline{Q} = \begin{bmatrix} 3.77 \times 10^6 & 0 & 0 & 0 \\ 0 & 4709.70 & 0 & 0 \\ 0 & 0 & 0 & 0 \\ 0 & 0 & 0 & 0 \end{bmatrix} \quad (7-17)$$

$$R = \beta \times 18482.04 \quad \beta = 1e-11 \quad (7-18)$$

the solution \underline{P} of the associated Riccati's matrix, optimal gain matrix \underline{D} and the linear quadratic state feedback control force U can be evaluated through Equations (7-8), (7-10) and (7-11) by using Matlab LQR function as

$$\underline{P} = \begin{bmatrix} 2.33e5 & 2.04e3 & 4.72e3 & 1.64e2 \\ 2.04e3 & 7.24e2 & 6.41 & 5.35e2 \\ 4.72e3 & 6.41 & 5.20e3 & 1.65 \\ 1.64e2 & 5.35e2 & 1.65 & 5.31e2 \end{bmatrix} \quad (7-19)$$

$$\underline{D} = [2.03e6 \quad 2.04e5 \quad 5.15e3 \quad 4.23e3] \quad (7-20)$$

$$U = 2.03 \times 10^6 Z_1 + 2.04 \times 10^5 \dot{Z}_1 + 5154\phi + 4229\dot{\phi} \quad (7-21)$$

Consequently, time step computation of Equations (7-1), (7-2) and (7-3) by means of Simulink software gives the time-variant response of the BT. Here, the BT is excited by real earthquake excitation of Bam, Iran, 2003 (presented in Chapter 5, Part 5.4.5) and the control force U is calculated for each time step, see Equation (7-1). Figures (7-3) illustrate the displacement responses of the controlled and uncontrolled BT in time domain. Figure (7-4) and (7-5) show the displacement FFT response of the controlled and uncontrolled BT, respectively. Base acceleration under the strong ground motion of Bam and control force U are depicted in Figure (7-6) and (7-7).

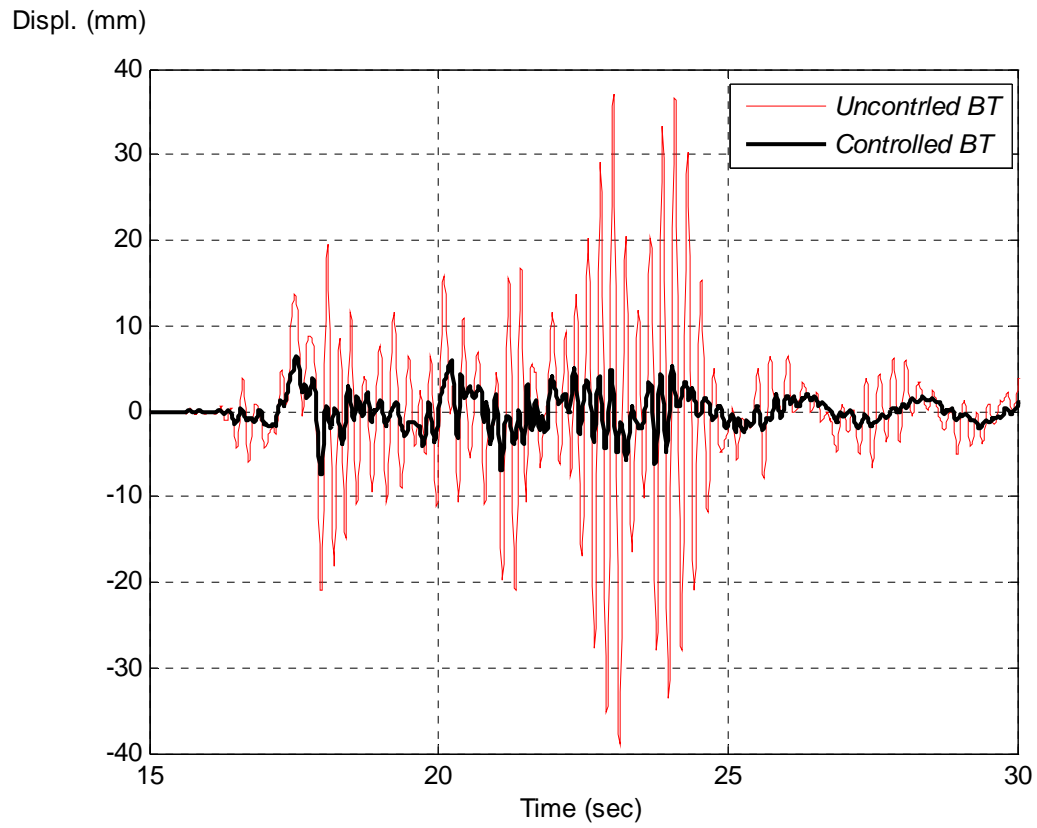


Figure 7-3 BT tip-point displacement with and without control force

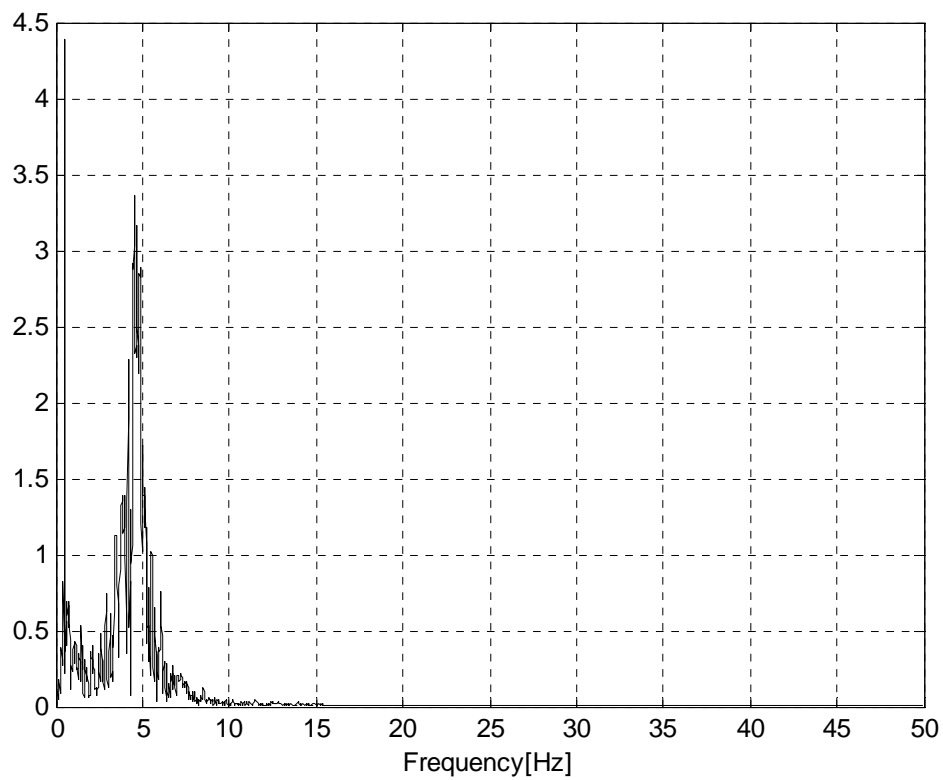


Figure 7-4 BT tip-point displacement FFT response without control force

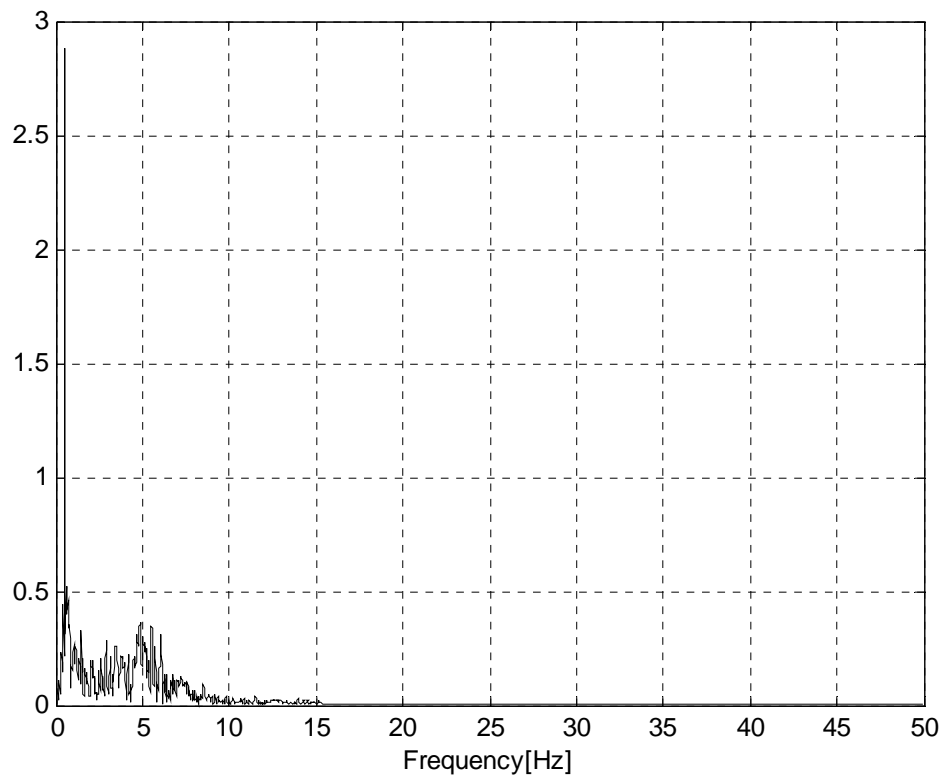


Figure 7-5 BT tip-point displacement FFT response, control force contribution

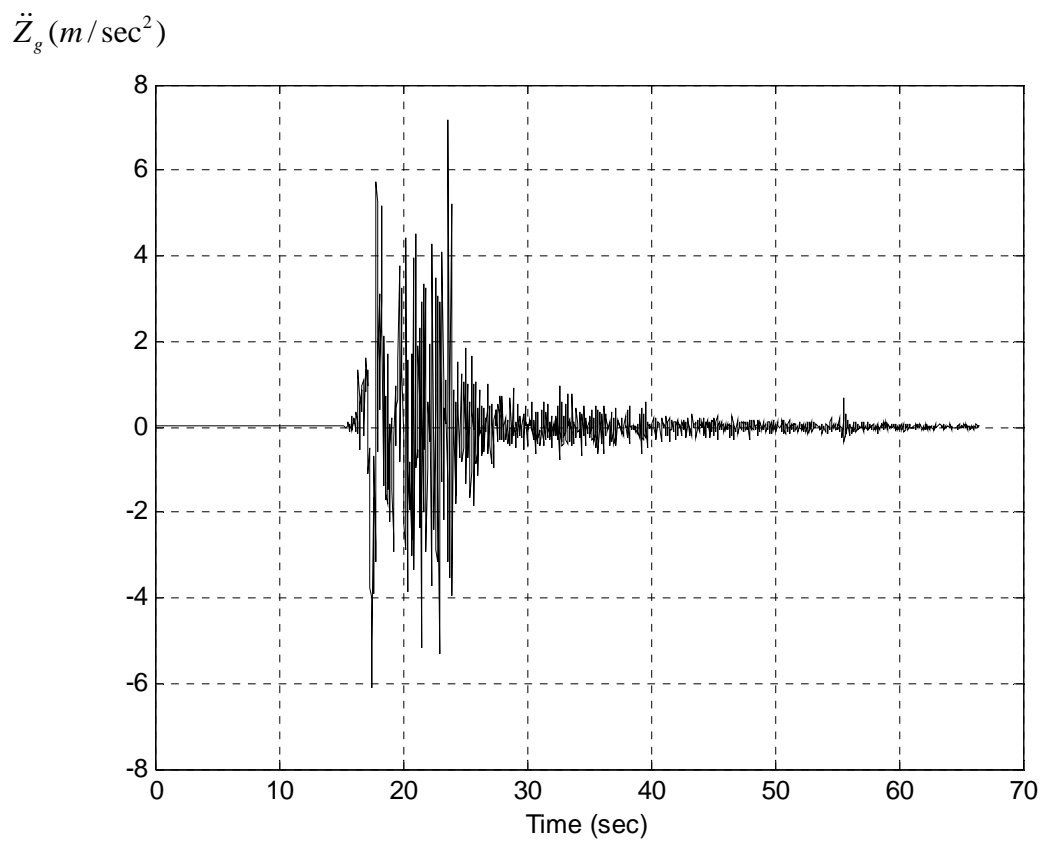


Figure 7-6 BT base acceleration, Bam strong ground motion

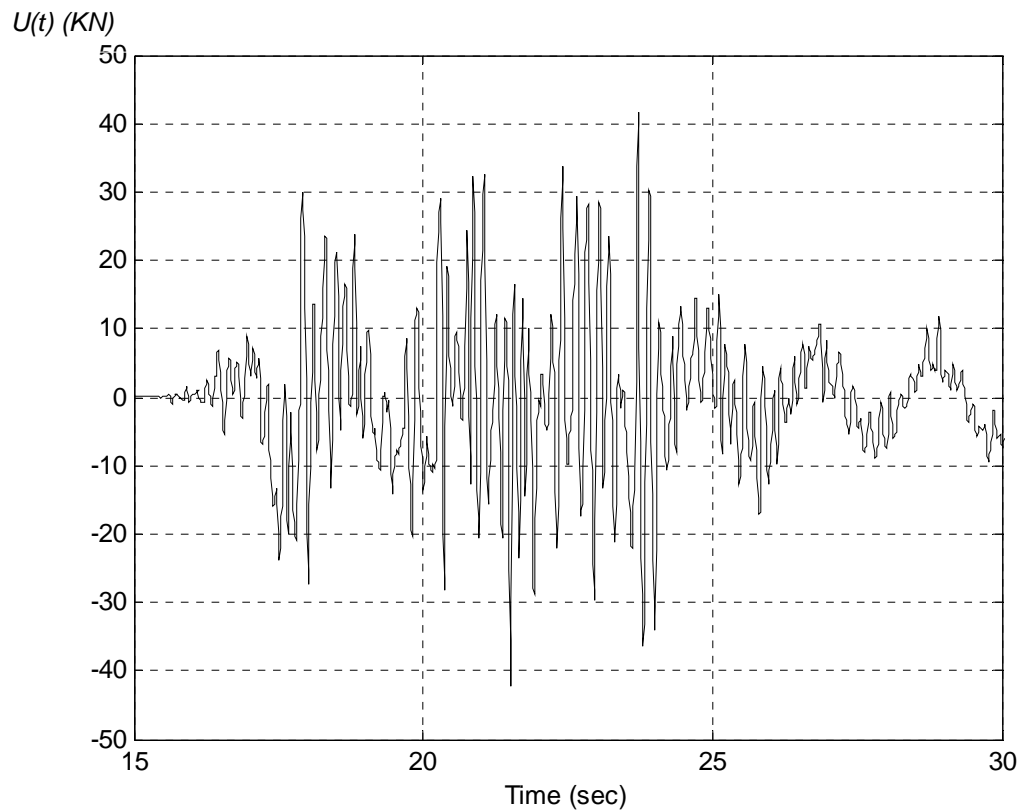


Figure 7-7 BT control force

The control coefficients are large compared to the parameters of the mechanical system and extensively decrease the displacement of the BT with respect to any perturbations.

7.6 References

1. Gawronski W.K., 'Advanced Structural Dynamics and Active Control of Structures', Springer-Verlag, New York, 2004.
2. Fidlin A., 'Nonlinear Oscillations in Mechanical Engineering', Springer-Verlag, Berlin Heidelberg, 2006.
3. Soong T.T., Constantinou M.C., 'Passive and Active Structural Vibration Control in Civil Engineering', Springer-Verlag, New York-Vienna, 1994.
4. Hochrainer M., 'Control Vibrations of Civil Engineering Structures with Special Emphasis on Tall Buildings', Dissertation, Technical University Vienna, Center of Mechanics and Structural Dynamics, 2001.
5. Preumont A., 'Vibration Control of Active Structures-An Introduction', Kluwer Academic Publishers, 2002.

8

CONCLUDING REMARKS

In this thesis the behavior of Bell-Tower like structures excited by various internal and external vibrations is studied. Governing equations for the dynamic response of the tower coupled with pendulum motion are derived based on Lagrange equations of motion. A 2DOF, sliding mass and simple pendulum, as a representative of pendulum (bell) combined with a tower are used. This system is developed for discretized MDOF model of tower coupled with mathematical pendulum. The BT is subjected to excitations due to base acceleration and pendulum swinging. The corresponding equations of motion are derived, considering nonlinear oscillations of the pendulum. Comparison is made between the characteristics in linear and nonlinear analyses, as well as coupled and uncoupled systems. In order to evaluate the nonlinear system, time-step analysis of numerical example by means of computer programming is performed. When the rotation angle of pendulum increases, the effects of nonlinearity appear. The nonlinear effects due to large motion of pendulum changes linear natural frequency of the pendulum and adds subharmonic resonate frequencies to the coupled system. It is observed that the tower is more sensitive than the pendulum to nonlinear effects. These effects reduce the displacement in the tower and rotation angle of the pendulum especially in the resonance circumstances.

The application of the pendulum as PTMD is studied to reduce the vibration of tower displacement. An introductory example of PTMD design and a description of the implementation of PTMDs in building structures like chimneys and BTs are presented. The optimal design parameters of the PTMD are found based on linearized system for small rotation of pendulum. Time history and frequency domain responses for a continuous system connected to optimally PTMD and subjected to harmonic and random support excitations in linear and nonlinear

conditions are compared. An assessment is made for optimal placement locations of PTMD in the tower. Results have confirmed that a pendulum absorber can be computed according to the linear theory when rotation angle of pendulum is small. When the rotation angle of pendulum rises, the effects of tuning parameters vanish. Response against earthquake force with respect to seismic design criteria and record of real strong ground motion of Bam (Iran, 2003) is also estimated.

The effect of the pendulum swinging on the tower is followed. Both the tower and pendulum are estimated under the effect of forced pendulum vibrations. Vibrating forces are applied as an external moment, and nonstationary conditions in nonlinear pendulum is discussed. While frequency of excitation is smaller than pendulum eigenfrequency, nonstationary happens in the responses of the tower and pendulum. Dynamic analysis of the tower by means of the substructure method is introduced. The vibrations induced by the pendulum movements treated as externally applied excitations and pendulum oscillatory movement formulated to determine the time-variant forces applied to the tower. Subsequently, the responses of the tower via quasi-static analysis compared and the internal forces of the tower produced by dynamic excitations are evaluated by numerical nonlinear analysis.

The forces associated with pendulum may be considered as an uncoupled external applied force in the tower. The oscillatory movement results in the time-variant horizontal and vertical forces of the support of the pendulum. Due to the geometry of the BT and the material utilized in the construction, the horizontal component of induced forces is most critical and is applied to the BT as a dynamic action of the pendulum, where the interaction between the tower and the pendulum is neglected.

Finally, the method of vibration control by application of nonlinear APMD in the towers is investigated. For this purpose, the mechanical model of the tower is represented by a continuous structure and is idealized as a MDOF system. The pendulum is modeled as an active mass damper to improve the response of the entire structure under dynamic loads. After applying appropriate analytical methods, parametric studies for forced vibration are performed by means of

computer simulations. The nonlinear dynamic analysis of the forced vibrations is chosen in time domain by using numerical investigation. By interpreting pendulum as an active absorber or APMD in the tower, it is intended to achieve a large decrease of displacement in the main tower structures. The optimal state feedback control method is introduced. The control force based on linear coupled system is evaluated and it is applied to the nonlinear system for time-step analysis. The results showed that control coefficients are large compared to the parameters of the mechanical system and extensively decrease the displacement of the tower with respect to any perturbations.

Appendix A

FUNDAMENTALS OF STRUCTURAL OSCILLATIONS

A.1 Formulation of the equations of motion

The primary objective of a deterministic structural dynamic analysis is the evaluation of the displacement-time history of a given structure subjected to a time-varying load. In most cases, an approximate analysis involving only a limited number of degrees of freedom will provide sufficient accuracy, and the problem thus can be reduced to the determination of the time history of these selected displacement components. The mathematical expressions defining the dynamic displacements or rotations are called the equations of motion of the structure, and the solution of these equations of motion provides the required displacement histories.

A.1.1 Direct Equilibration Using d'Alembert's Principle¹

The equations of motion of any dynamic system represent expressions of Newton's second law of motion, which states that rate of change of momentum of any mass m is equal to the force acting on it. This relationship can be expressed mathematically as the differential equation.

$$\vec{P}(t) = \frac{d}{dt} \left(m \frac{d\vec{x}}{dt} \right) \quad (\text{A-1})$$

where $\vec{P}(t)$ is the applied force vector and $\vec{x}(t)$ is the position vector of the mass m . For most problems in structural dynamics it may be assumed that the mass does not vary in time, and Equation (A-1) becomes

¹ Reference [1]

$$\vec{P}(t) = m \frac{d^2 \vec{x}}{dt^2} \equiv m \ddot{\vec{x}}(t) \quad (\text{A-2})$$

where a dot represents differentiation with respect to time. Equation (A-2), the familiar expression that force is equal to produce of mass and acceleration, may also be written

$$\vec{P}(t) - m \ddot{\vec{x}}(t) = 0 \quad (\text{A-3})$$

The second term $m \ddot{\vec{x}}(t)$ is called inertia force resisting the acceleration of the mass.

The concept that a mass develops an inertia force proportional to its acceleration is known as d'Alembert's principle. It is a very convenient device in problems of structural dynamics because it permits the equations of motion to be expressed as equations of dynamic equilibrium. The force $\vec{P}(t)$ may be considered to include many types of force acting on the mass such as elastic constraints, viscous forces, and independently defined external loads. Thus if an inertia force and resistances acceleration are introduced, the expression of the equation of motion is merely an expression of the equilibration of all of the forces acting on the mass. In many simple problems the most direct and convenient way of formulating the equations of motion is by means of such direct equilibration.

A.1.2 Principle of Virtual Displacements

If the structural system is complex and involves a number of interconnected mass points or bodies of finite size, the direct equilibration of all the forces acting in the system may be difficult. Frequently, the various forces involved may be expressed in terms of the displacement degrees of freedom, but their equilibrium relationships may be obscure. In this case, the principle of virtual displacements can be used to formulate the equations of motion as a substitute for the equilibrium relationships.

The principle of virtual displacements is expressed as follow. If a system which is in equilibrium under the action of a set of forces is subjected to a virtual displacement, any displacement compatible with the system constraints and the total

work done by the forces will be zero. With this principle, it is clear that the vanishing of the work during a virtual displacement is equivalent to a statement of equilibrium. Thus the response equations of a dynamic system can be established by identifying all the forces acting on the masses of the system, including inertia forces defined in accordance with d'Alembert's principle. Then the equations of motion are obtained by introducing virtual displacements corresponding to each degree of freedom and equating the mechanical work to zero. A major advantage of this approach is that the virtual work contributions are scalar quantities and can be added algebraically, whereas the forces acting on the structure are vectors and can only be superposed vectorially.

A.1.3 Hamilton's Principle²

Another procedure of avoiding the problems of establishing the vectorial equations of equilibrium is to make use of scalar energy quantities in a variation form. The most generally applicable variation concept is Hamilton's principle, which may be expressed as

$$\delta \int_{t_1}^{t_2} (T - V) dt + \int_{t_1}^{t_2} \delta W_{nc} dt = 0 \quad (\text{A-5})$$

where T is the total kinetic energy of system and V represents the potential energy, including both strain energy and potential of any conservative external forces.

W_{nc} denotes the work done by non-conservative forces acting on system, including damping and any arbitrary external loads.

Hamilton's principle states that variation of the kinetic and potential energy plus the variation of the work done by the non-conservative forces considered during any time interval t_1 to t_2 must equal zero. The application of this principle leads directly the initial boundary values problem for any given system. The process differs from the virtual-work analysis since the inertia and elastic forces are not explicitly involved, since variations of the kinetic and potential energy terms are

² Reference [1]

utilized. This formulation has the advantage of dealing only with purely scalar energy quantities, whereas the forces and displacements used to represent corresponding effects in the virtual-work analysis are all vectorial in character even though the work terms themselves are scalar.

A.1.4 Lagrange's equations of motion

The equations of motion for a Multi-Degree-of-Freedom (MDOF) system can be derived directly from the variational statement of dynamics, Hamilton's principle, Equation (A-5). By simply expressing the total kinetic energy T , the total potential energy V , and the total virtual work δW_{nc} in terms of a set of generalized coordinates, q_1, q_2, \dots, q_N . For most mechanical or structural systems, the kinetic energy can be expressed in terms of the generalized coordinates and their first time derivatives, and the potential energy can be expressed in terms of the generalized coordinates only. In addition, the virtual work which is performed by the non-conservative forces as they act through the virtual displacements caused by an arbitrary set of variations in the generalized coordinates can be expressed as a linear function of those variations. In mathematical terms the above three statements are expressed in the form

$$T = T(q_1, \dots, q_N, \dot{q}_1, \dots, \dot{q}_N) \quad (\text{A-6})$$

$$V = V(q_1, q_2, \dots, q_N) \quad (\text{A-7})$$

$$\delta W_{nc} = Q_1 \delta_1 + Q_2 \delta_2 + \dots + Q_N \delta_N \quad (\text{A-8})$$

where the coefficients Q_1, Q_2, \dots, Q_N are the generalized forcing function corresponding to the coordinates q_1, q_2, \dots, q_N , respectively.

Introducing Equation (A-6) into Equation (A-5), and completing the variation of the first term gives

$$\begin{aligned}
& \int_{t_1}^{t_2} \left(\frac{\partial T}{\partial q_1} \delta q_1 + \frac{\partial T}{\partial q_2} \delta q_2 + \cdots + \frac{\partial T}{\partial q_N} \delta q_N + \frac{\partial T}{\partial \dot{q}_1} \delta \dot{q}_1 + \frac{\partial T}{\partial \dot{q}_2} \delta \dot{q}_2 + \cdots \right. \\
& \quad + \frac{\partial T}{\partial \dot{q}_N} \delta \dot{q}_N - \frac{\partial V}{\partial q_1} \delta q_1 - \frac{\partial V}{\partial q_2} \delta q_2 - \cdots - \frac{\partial V}{\partial q_N} \delta q_N \\
& \quad \left. + Q_1 \delta q_1 + Q_2 \delta q_2 + \cdots + Q_N \delta q_N \right) dt = 0
\end{aligned} \tag{A-9}$$

Integrating the velocity dependent terms in Equation (A-9) leads to

$$\int_{t_1}^{t_2} \frac{\partial T}{\partial \dot{q}_i} \delta \dot{q}_i dt = \left[\frac{\partial T}{\partial \dot{q}_i} \delta q_i \right]_{t_1}^{t_2} - \int_{t_1}^{t_2} \frac{\partial}{\partial t} \left(\frac{\partial T}{\partial \dot{q}_i} \right) \delta q_i dt \tag{A-10}$$

The first term on the right-hand side of Equation (A-10) is equal to zero for each coordinate since $\delta q_i(t_1) = \delta q_i(t_2) = 0$ is the basic condition imposed upon the variations. Substituting Equation (A-10) into Equation (A-9), after rearranging terms

$$\int_{t_1}^{t_2} \left\{ \sum_{i=1}^N \left[-\frac{d}{dt} \left(\frac{\partial T}{\partial \dot{q}_i} \right) + \frac{\partial T}{\partial q_i} - \frac{\partial V}{\partial q_i} + Q_i \right] \delta q_i \right\} dt = 0 \tag{A-11}$$

Since all variations $\delta q_i (i = 1, 2, \dots, N)$ are arbitrary, Equation (A-11) can be satisfied in general only when the term in brackets vanishes, then

$$\frac{d}{dt} \left(\frac{\partial T}{\partial \dot{q}_i} \right) - \frac{\partial T}{\partial q_i} + \frac{\partial V}{\partial q_i} = Q_i \tag{A-12}$$

Equation (A-12) is the Lagrange's equations of motion, which have found widespread application in various fields of science and engineering.

With the Hamilton's variational principle, the energy and work terms can be expressed in terms of the generalized coordinates, and of their time derivatives and variations, as indicated in Equations (A-6), (A-7) and (A-8). Thus Lagrange's equations are applicable to all nonlinear and linear systems which satisfy these restrictions.

A.2 Linear Single Degree of Freedom (SDOF) systems

A.2.1 Free Vibration³

Figure (A-1) shows a SDOF system with a linear elastic spring (stiffness k) and viscous damper (parameter r). The differential equation of free motion of mass (parameter m) for the damped system is

$$m\ddot{x} + r\dot{x} + kx = 0 \quad (\text{A-13})$$

The form of the solution of this equation depends upon whether the damping coefficient is equal to, greater than, or less than the critical damping coefficient r_c

$$r_c = 2\sqrt{km} = 2m\omega, \quad \omega = \sqrt{\frac{k}{m}} \quad (\text{A-14})$$

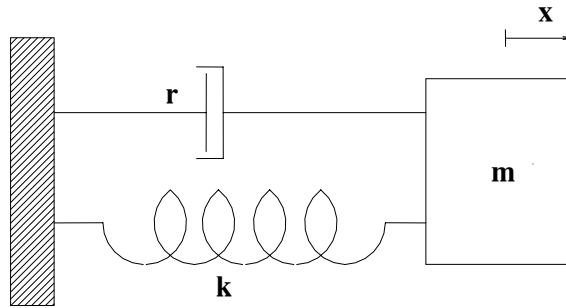


Figure A-1 SDOF system with linear elastic spring and viscous damper

The ratio $\zeta = \frac{r}{r_c}$ is defined as the fraction of critical damping. If the damping of the system is less than critical $\zeta < 1$, then the solution of Equation (A-13) is

$$\begin{aligned} x &= e^{-\zeta\omega t} (A \sin \omega_d t + B \cos \omega_d t) \\ &= C e^{-\zeta\omega t} \sin(\omega_d t + \phi) \end{aligned} \quad (\text{A-15})$$

The constants C and ϕ follow from the initial conditions, and the damped natural frequency is related to the undamped natural frequency

³ Reference [2]

$$\omega = \sqrt{\frac{k}{m}} \quad \text{rad/sec}$$

$$\omega_d = \omega \sqrt{1 - \zeta^2} \quad \text{rad/sec} \quad (\text{A-16})$$

Equation (A-16), relating the damped and undamped natural frequencies, is plotted in Figure (A-2).

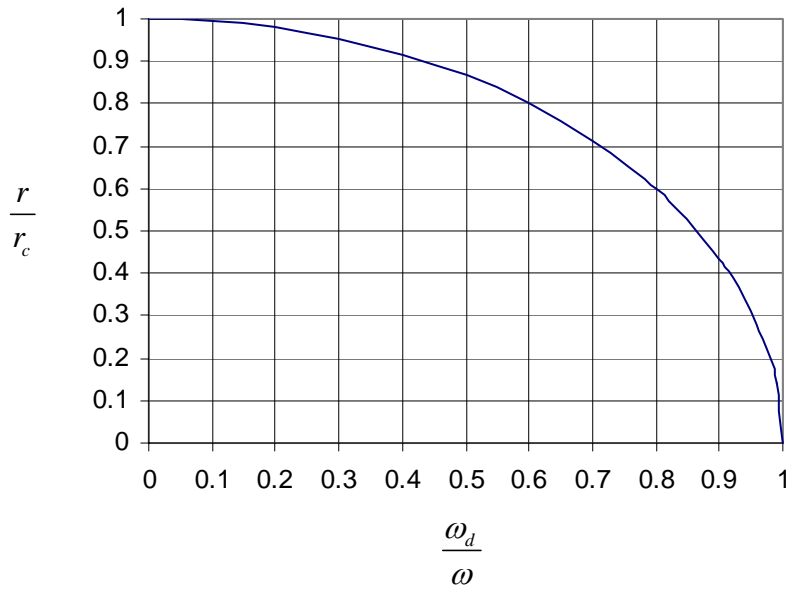


Figure A-2 Damped natural frequency as a function of undamped natural frequency ω_d / ω versus fraction of critical damping $\zeta = r / r_c$

When $r = r_c$ (critical damping) there is no oscillation and the solution of Equation (A-13) becomes

$$x = (A + Bt)e^{-\zeta\omega t} \quad (\text{A-17})$$

When $\zeta > 1$, the solution of Equation (A-13) is

$$x = e^{-\zeta\omega t} \left(Ae^{\omega\sqrt{\zeta^2-1}t} + Be^{-\omega\sqrt{\zeta^2-1}t} \right) \quad (\text{A-18})$$

This is a nonoscillatory motion. Thus, if the system is displaced from its equilibrium position, it tends to return gradually.

A.2.2 Forced vibration

Dynamic stresses and deflections may be induced in a structure by motions of its support points. Important examples of such excitation are the motions of a building foundation caused by an earthquake. A simplified model of the earthquake-excitation problem is shown in Figure (A-3), in which the horizontal ground motion caused by the earthquake is indicated by the displacement x_g of the structure's base relative to the fixed reference axis.

The horizontal girder in this frame is assumed to be rigid and to include all the moving mass of the structure. The vertical columns are assumed to be weightless and inextensible in the vertical (axial) direction, and the resistance to girder displacement provided by each column is represented by its spring constant $\frac{k}{2}$. The mass has a single degree of freedom, $x(t)$, which is associated with column flexure, the damper c provides a velocity-proportional resistance of this deformation.

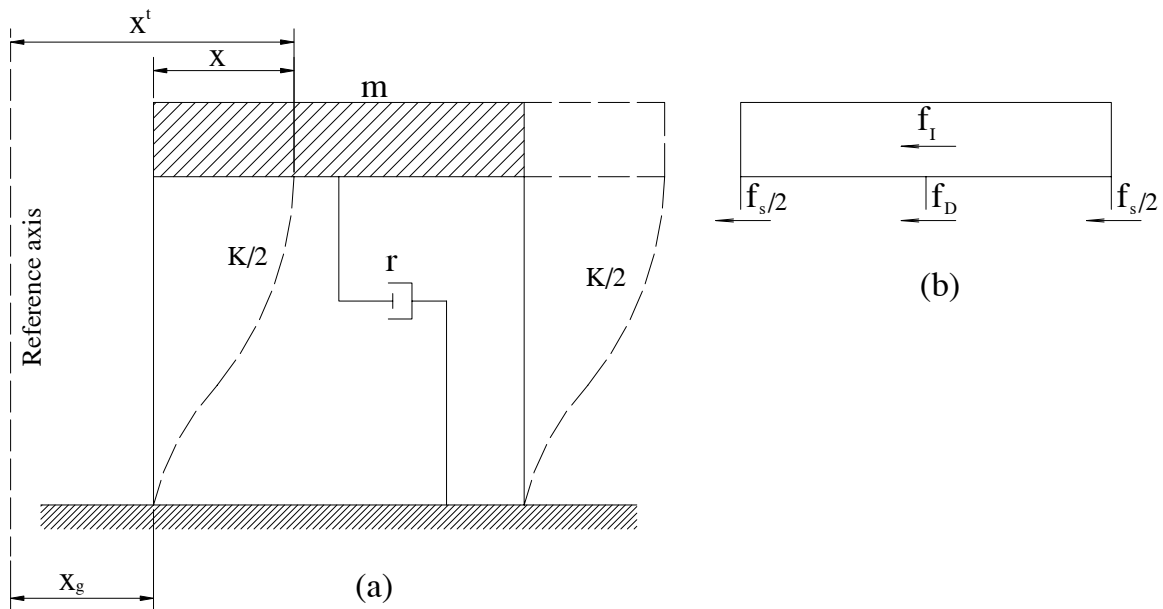


Figure A-3 Influence of support excitation on SDOF equilibrium: (a) motion of system; (b) equilibrium forces

As shown in Figure (A-3a), the equilibrium of forces for this system may be written

$$f_I + f_D + f_S = 0 \quad (\text{A-19})$$

However, the inertia force in this case is given by

$$f_I = m\ddot{x}_t \quad (\text{A-20})$$

where x_t represents the total displacement of the mass from the reference axis.

Substituting for the inertia, damping and elastic forces in Equation (A-19) yields

$$m\ddot{x}' + r\dot{x} + kx = 0 \quad (\text{A-21})$$

Before solving this equation all forces must be expressed in terms of single variable, which can be accomplished by noting that the total motion of the mass can be expressed as the sum of the ground motion and the column distortion then

$$x' = x + x_g \quad (\text{A-22})$$

Expressing the inertia force in terms of the two acceleration components obtained by differentiation of Equation (A-22) and substituting into Equation (A-21) yields

$$m\ddot{x} + m\ddot{x}_g + r\dot{x} + kx = 0 \quad (\text{A-23})$$

or since the ground acceleration represents the specified dynamic input to the structure, the equation of motion may be written

$$m\ddot{x} + r\dot{x} + kx = -m\ddot{x}_g(t) \equiv p_{eff}(t) \quad (\text{A-24})$$

$p_{eff}(t)$ denotes the effective external loading due to support excitation.

A.3 Reference

1. Clough R.W., Penzien J., Department of Civil Engineering, University of California, 'Dynamic of Structures', published by McGraw Hill, 1989.
2. Chopra A.K., University of California at Berkeley, 'Dynamics of Structures', second edition, published by Prentice Hall, 2001.
3. Ziegler F., 'Mechanics of Solids and Fluids', Second edition, Technical University Vienna, Springer-Verlag New York-Vienna, 1998.

Appendix B

VIBRATION OF A SIMPLE PENDULUM

B.1 Nonlinear vibration of the simple pendulum¹

A simple mathematical pendulum of length ℓ having a lumped mass m , as shown in Figure (B-1) is considered. The linearized differential equation governing free vibration is

$$m\ell^2\ddot{\phi} + mg\ell\phi = 0 \quad (\text{B-1})$$

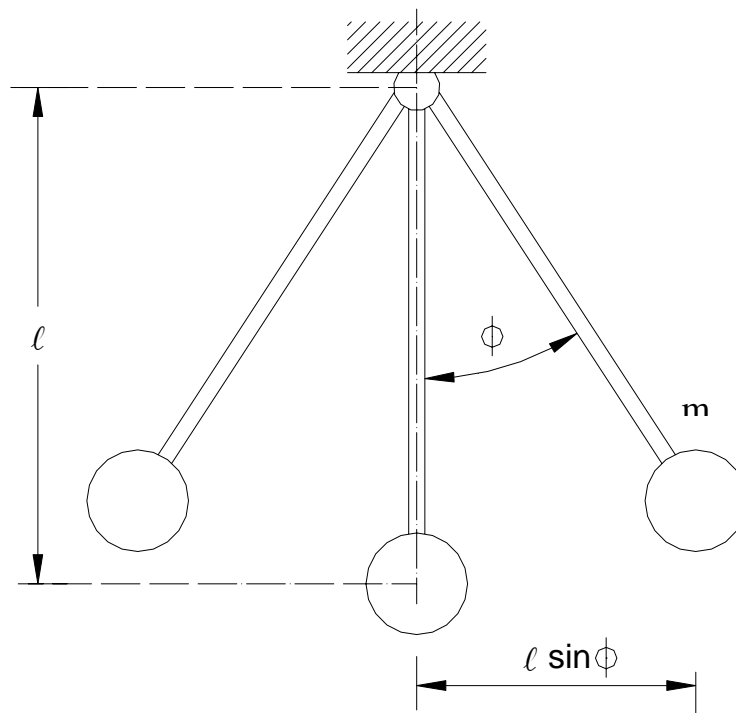


Figure B-1 Simple pendulum

¹ Reference [1]

That holds only for small oscillation about the position of equilibrium where the assumption $\sin \phi \approx \phi$ holds. The exact nonlinear equation of motion reads

$$m\ell^2\ddot{\phi} + mg\ell \sin \phi = 0 \quad (\text{B-2})$$

or

$$\ddot{\phi} + \omega^2 \sin \phi = 0, \quad \omega = \sqrt{\frac{g}{\ell}} \quad (\text{B-3})$$

Equation (B-2) may be written as

$$m\ddot{\phi} + F(\phi) = 0 \quad (\text{B-4})$$

or

$$\ddot{\phi} + \omega^2 f(\phi) = 0 \quad (\text{B-5})$$

in which the term $\omega^2 f(\phi) = \frac{F(\phi)}{m}$ represents the nonlinear resorting force per unit mass as a function of rotation(ϕ). The acceleration derivative of the velocity may be further expressed

$$\ddot{\phi} = \frac{d\dot{\phi}}{dt} = \frac{d\dot{\phi}}{d\phi} \frac{d\phi}{dt} = \frac{d\dot{\phi}}{d\phi} \dot{\phi} = \frac{1}{2} \frac{d(\dot{\phi})^2}{d\phi} \quad (\text{B-6})$$

Substituting the last expression into Equation (B-5) leads to

$$\frac{1}{2} \frac{d(\dot{\phi})^2}{d\phi} + \omega^2 f(\phi) = 0 \quad (\text{B-7})$$

where the resorting force $\omega^2 f(\phi) = \omega^2 \sin \phi$ per unit mass is given by the function shown in Figure (B-2) and the velocity corresponding to ϕ_m in an extreme position is zero. Thus the Equation (B-7) may be integrated as

$$\frac{1}{2} \dot{\phi}^2 = -\omega^2 \int_{\phi_m}^{\phi} f(\phi') d\phi' = \omega^2 \int_{\phi}^{\phi_m} f(\phi') d\phi' \quad (\text{B-8})$$

For any position of the undamped vibrating system its kinetic energy per unit mass is equal to the potential energy represented by the hatched area under the curve in

Figure (B-2). The maximum kinetic energy is attained in the equilibrium position, $\phi = 0$, the total energy remains constant and the maximum kinetic energy must be equal to the maximum potential energy.

$$T_{\max} = \frac{1}{2} \dot{\phi}_m^2 = \omega^2 \int_0^{\phi_m} f(\phi') d\phi' = V_{\max} \quad (\text{B-9})$$

Equation (B-8) yields an expression for the velocity $\dot{\phi}$ of the vibrating mass in any position as

$$\dot{\phi} = \frac{d\phi}{dt} = \pm \omega \sqrt{2 \int_{\phi}^{\phi_m} f(\phi') d\phi'} \quad (\text{B-10})$$

The time for any portion of cycle may be obtained by second integration. Hence, the time for a full cycle becomes

$$\tau = \frac{4}{\omega} \int_0^{\phi_m} \frac{d\phi}{\sqrt{2 \int_{\phi}^{\phi_m} f(\phi') d\phi'}} \quad (\text{B-11})$$

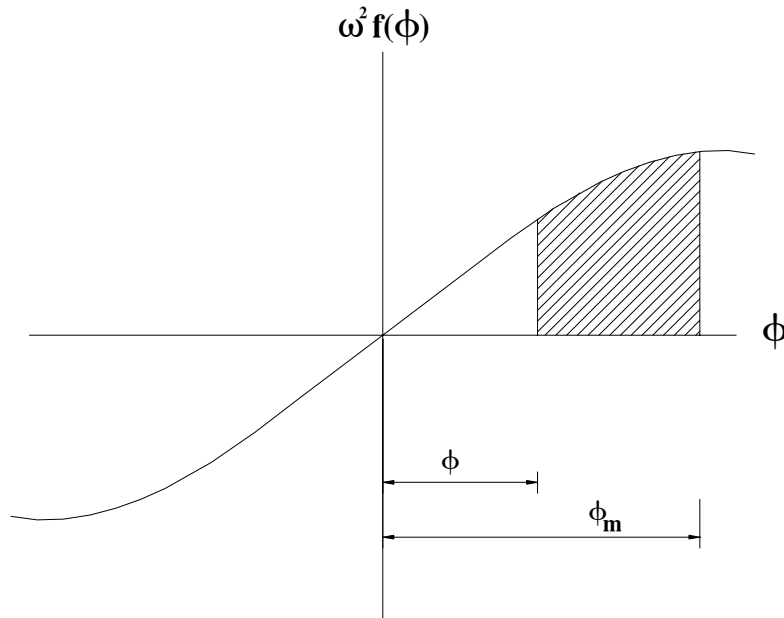


Figure B-2 Force in simple pendulum

Therefore, if an analytical expression for the restoring force is given, the natural period of the system may be evaluating the integrals in Equation (B-11).

Furthermore, the relationship between the velocities $\dot{\phi}_m$ in an extreme position may be obtained from Equation (B-9). This expression is useful for finding the maximum velocity of a nonlinear system that is initially displaced and allowed to vibrate freely. It also may be used to calculate the maximum displacement due to an initial velocity. The mass might be affected by an impulse of initial velocity that is of short duration in comparison with the period of the system.

For the pendulum free vibration according to Equation (B-3), Equation (B-10) becomes

$$\dot{\phi}_m = \pm \omega \sqrt{2(1 - \cos \phi_m)} \quad (\text{B-12})$$

and

$$\tau = \frac{4}{\omega} \int_0^{\phi_m} \frac{d\phi}{\sqrt{2(\cos \phi - \cos \phi_m)}} = \frac{2}{\omega} \int_0^{\phi_m} \frac{d\phi}{\sqrt{\sin^2(\frac{\phi_m}{2}) - \sin^2(\frac{\phi}{2})}} \quad (\text{B-13})$$

introducing the notation $s = \sin(\frac{\phi_m}{2})$ and a new variable θ ,

$$\sin(\frac{\phi}{2}) = s \sin \theta = \sin(\frac{\phi_m}{2}) \sin \theta \quad (\text{B-14})$$

It is obtained

$$d\phi = \frac{2s \cos \theta d\theta}{\sqrt{1 - s^2 \sin^2 \theta}} \quad (\text{B-15})$$

substituting expressions (B-14) and (B-15) into Equation (B-13) and observing from Equation (B-14) that θ varies from 0 to $\frac{\pi}{2}$ while ϕ varies from 0 to ϕ_m ,

$$\tau = \frac{4}{\omega} \int_0^{\pi/2} \frac{d\theta}{\sqrt{1 - s^2 \sin^2 \theta}} = \frac{4}{\omega} F(s, \frac{\pi}{2}) \quad (\text{B-16})$$

which is in the standard form of the elliptic integral of the first kind. Thus the numerical value of the integral in Equation (B-16) corresponding to any value of s can be evaluated.

When the maximum rotational displacement ϕ_m of the pendulum is small, the value of s is also small and the quantity $s^2 \sin^2 \theta$ in Equation (B-16) can be neglected. Then the integral becomes equal to $\frac{\pi}{2}$ and we obtain the natural period $\tau = \frac{2\pi}{\omega}$ for the pendulum with small rotations.

B.2 References

1. Weaver Jr. W., Timoshenko S. P., Young D. H., Department of Civil Engineering, Stanford University, 'Vibration Problems in Engineering', Fifth edition, published by John Wiley & Sons, 1989.

Appendix C

NUMERICAL ANALYSIS OF NONLINEAR RESPONSE

C.1 Incremental formulation of nonlinear system¹

For a SDOF system at any instant of time t the equilibrium of forces acting on the mass m requires

$$f_I(t) + f_D(t) + f_S(t) = p(t) \quad (C-1)$$

After a short time Δt the equation reads

$$f_I(t + \Delta t) + f_D(t + \Delta t) + f_S(t + \Delta t) = p(t + \Delta t) \quad (C-2)$$

Subtracting Equation (C-1) from Equation (C-2) then yields the incremental form of the equation of motion for the time interval t

$$\Delta f_I(t) + \Delta f_D(t) + \Delta f_S(t) = \Delta p(t) \quad (C-3)$$

The incremental forces in this equation may be expressed as follows

$$\Delta f_I(t) = f_I(t + \Delta t) - f_I(t) = m\Delta\ddot{x}(t) \quad (C-4)$$

$$\Delta f_D(t) = f_D(t + \Delta t) - f_D(t) = c(t)\Delta\dot{x}(t)$$

$$\Delta f_S(t) = f_S(t + \Delta t) - f_S(t) = k(t)\Delta x(t)$$

$$\Delta p(t) = p(t + \Delta t) - p(t)$$

It is assumed that the mass remains constant. The terms $c(t)$ and $k(t)$ represent the damping and stiffness properties corresponding to the velocity and displacement. In practice, the secant slopes could be evaluated only by iteration because the velocity and displacement at the end of the time increment depend on these

¹ Reference [1]

properties. For this reason tangent slopes defined at the beginning of the time intervals.

$$c(t) = \left(\frac{df_D}{d\dot{x}} \right)_t \quad k(t) = \left(\frac{df_S}{dx} \right)_t \quad (\text{C-5})$$

Substituting the force expressions of Equation (C-4) into Equation (C-3) leads to the final form of the incremental equilibrium equations for time t

$$m\Delta\ddot{x}(t) + c(t)\Delta\dot{x}(t) + k(t)\Delta x(t) = \Delta p(t) \quad (\text{C-6})$$

C.2 Step-by-Step integration

Many procedures are available for the numerical integration of Equation (C-6), e.g. Euler-Gauß Method, Newmark Beta Method and Runge-Kuta Method. The basic approximate assumption of the computational process is that the acceleration varies linearly during each time increment while the properties of the system remain constant during this interval. The equation of motion during the time interval for linear variation of the acceleration and the corresponding quadratic and cubic variations of the velocity and displacement respectively are assumed. Evaluating these latter expressions at the end of the interval ($\tau \equiv \Delta t$) leads to the following equations of the increments of velocity and displacement

$$\Delta\dot{x}(t) = \ddot{x}(t)\Delta(t) + \Delta\ddot{x}(t)\frac{\Delta t}{2} \quad (\text{C-7})$$

$$\Delta x(t) = \dot{x}(t)\Delta(t) + \ddot{x}(t)\frac{\Delta t^2}{2} + \Delta\ddot{x}(t)\frac{\Delta t^2}{6} \quad (\text{C-8})$$

Now it will be convenient to use the incremental displacement as the basic variable of the analysis. Hence Equation (C-7) is solved for the incremental acceleration, and this expression is substituted into Equation (C-8) to obtain

$$\Delta\ddot{x}(t) = \frac{6}{\Delta t^2} \Delta x(t) - \frac{6}{\Delta t} \dot{x}(t) - 3\ddot{x}(t) \quad (\text{C-9})$$

$$\Delta \dot{x}(t) = \frac{3}{\Delta t} \Delta x(t) - 3\dot{x}(t) - \frac{\Delta t}{2} \ddot{x}(t) \quad (\text{C-10})$$

Substituting Equation (C-9) and (C-10) into Equation (C-6) leads to the following form of the equation of motion

$$m \left[\frac{6}{\Delta t^2} \Delta x(t) - \frac{6}{\Delta t} \dot{x}(t) - 3\ddot{x}(t) \right] + c(t) \left[\frac{3}{\Delta t} \Delta x(t) - 3\dot{x}(t) - \frac{\Delta t}{2} \ddot{x}(t) \right] + k(t) \Delta x(t) = \Delta p(t) \quad (\text{C-11})$$

Finally transferring all terms associated with the known initial conditions to the right-hand side gives

$$\tilde{k}(t) \Delta x(t) = \Delta \tilde{p}(t) \quad (\text{C-12})$$

in which

$$\tilde{k}(t) = k(t) + \frac{6}{\Delta t^2} m + \frac{3}{\Delta t} c(t) \quad (\text{C-13})$$

$$\Delta \tilde{p}(t) = \Delta p(t) + m \left[\frac{6}{\Delta t} \dot{x}(t) + 3\ddot{x}(t) \right] + c(t) \left[3\dot{x}(t) + \frac{\Delta t}{2} \ddot{x}(t) \right] \quad (\text{C-14})$$

After solving Equation (C-12) for the displacement increment, this value is substituted into Equation (C-10) to obtain the incremental velocity. The initial conditions for the next time step result from the addition of these incremental values to the velocity and displacement at the beginning of the time step.

C.3 References

1. Clough R.W., Penzien J., Department of Civil Engineering, University of California, 'Dynamic of Structures', published by McGraw-Hill, 1989.
2. Chopra A.K., University of California at Berkeley, 'Dynamics of Structures', second edition, Prentice Hall, 2001.

REFERENCES

- Bachman Hugo, 'Vibration Problems in Structures', Birkhäuser Verlag, 1995.
- Building and Housing Research Center, <http://www.bhrc.ir/>
- Chakrabarti P., Chopra A.K., University of California at Berkeley, 'Earthquake Analysis of Gravity Dams Including Hydrodynamic Interaction', International Journal of Earthquake Engineering and Structural Analysis, Vol. 2, 1997, pp. 143-160.
- Chopra A.K., University of California at Berkeley, 'Dynamics of Structures', second edition, Prentice Hall, 2001.
- Civil Engineering Database, <http://pubs.asce.org>.
- Clough R.W., Penzien J., Department of Civil Engineering, University of California, 'Dynamic of Structures', McGraw-Hill, 1989.
- Dabney, J.B., 'Mastering Simulink', Pearson Prentice Hall, 2004.
- DenHartog J.P., 'Mechanical Vibrations', reprint of 4th edition, McGraw-Hill, 1956.
- Duffing G., 'Erzwungene Schwingungen bei veränderlicher Eigenfrequenz', F. Vieweg u. Sohn, 1918.
- EERC, structures with TMDs, <http://nisee.berkeley.edu/>
- Flügge W., 'Handbook of Engineering Mechanics', McGraw-Hill, 1962.
- Fidlin A., 'Nonlinear Oscillations in Mechanical Engineering', Springer-Verlag Berlin Heidelberg, 2006.

- Gawronski W.K., 'Advanced Structural Dynamics and Active Control of Structures', Springer-Verlag New York, 2004.
- Hanselman D.C., 'Mastering Matlab 6', Pearson Prentice Hall, 2001.
- Harris C.M., 'Shock and Vibration Handbook', Fourth edition, McGraw-Hill, 2003.
- Haskett T., Breukelman B., Robinson J., Kottelenberg J., 'Tuned mass dampers under excessive structural excitation', Monitoring Inc, Guelph, Ontario, Canada.
- Hochrainer M., 'Control Vibrations of Civil Engineering Structures with Special Emphasis on Tall Buildings', Dissertation, Technical University Vienna, Center of Mechanics and Structural Dynamics, 2001.
- Korenev B.G., Reznikov L.M., Moscow Civil Engineering Institute, 'Dynamic Vibration Absorbers, Theory and Technical Applications', John Wiley & Sons, 1993.
- Mostafaei H., Kabeyasawa T.M., Earthquake Research Institute the University of Tokyo, 'Investigation and Analysis of Damage to Building during the 2003 Bam Earthquake', Vol.79 (2004), pp. 107-132.
- Müller F-P., 'Berechnung und Konstruktion von Glockentürmen', Verlag Wilhelm Ernst & Sohn, 1968.
- Nayfeh A.H., Mook D.T., Department of Engineering Science and Mechanics Virginia, 'Nonlinear Oscillations', John Wiley & Sons, 1998.
- Petersen C., University of Munich, 'Dynamik der Baukonstruktionen', Vieweg 1996.

- Preumont A., 'Vibration Control of Active Structures-An Introduction', Kluwer Academic Publishers, 2002.
- Shabana A.A., Department of Mechanical Engineering, University of Illinois at Chicago, 'Theory of vibration', Springer-Verlag New York-Berlin Heidelberg, 1998.
- Soong T.T., 'Passive and Active Structural Vibration Control in Civil Engineering', Springer-Verlag, New York-Vienna, 1994.
- Weaver Jr.W., Timoshenko S.P., Young D.H., Department of Civil Engineering, Stanford University, 'Vibration problems in engineering', Fifth edition, John Wiley & Sons, 1989.
- Wikipedia, The Free Encyclopedia, <http://en.wikipedia.org>.
- Wylie C.R., 'Advanced Engineering Mathematics', McGraw-Hill, 1985.
- Yang C.Y., University of Delaware Newark, Delaware, 'Random vibration of structure', John Wiley & Sons, 1985.
- Ziegler F., 'Mechanics of Solids and Fluids', Second edition, Technical University Vienna, Springer-Verlag, New York-Vienna, 1998.

PERSONAL INFORMATION

S. Mehdi Yousefi

Date of Birth: 19 Sep 1975

Marital status: married, no children

Email: s.mehdiyousefi@gmail.com

Mobile: +43-6507053164

EDUCATION

- Ph.D. Candidate, Civil Engineering, Structural Dynamics, Technical University of Vienna, Vienna, Austria, Mar 2005 to Jan 2008.
Thesis: Dynamic Behavior of Bell (Pendulum) Tower Like Structures in Earthquake Environment, in English language.
- M.Sc. Civil Engineering, Earthquake Engineering, Building and Housing Research Center (BHRC), Tehran, Iran, Oct 1997 to Mar 2000.
Thesis: Dynamic Analysis of Dome Space Structures.
- B.Sc. Civil Engineering, Civil, Technical Faculty, University of Tabriz, Tabriz, Iran, Oct 1993 to Aug 1997.
- High School Diploma, Math and Physics, Taleghani High school, Tabriz, Iran, Oct 1989 to Jun 1993.

WORK EXPERIENCE

- Mar 2005 to Jan 2008
Technical University of Vienna (TUW), Center of Mechanics and Structural Dynamics, Vienna, Austria
Research work related to nonlinear analysis of (bell) towers and chimneys under dynamic loads utilizing external Pendulum Tuned Mass Damper to mitigate vibration.
- Jul 2001 to Feb 2005
MAPNA Company (EPC Contractor, Power Plant Project), Tehran, Iran

Project civil engineer, design and construction of industrial projects, Isfahan power plant project, Mobin power plant project, Abadan power plant project.

- Oct 1999 to Jun 2001

Mab Sazeh Company (Design and Construction) , Tehran, Iran

Associate engineer, construction of Sarab gas pressure reduction station project, house building projects designed with engineering design software (up to 20 storey buildings), research on modeling and analysis of space structures.

- Nov 1998 to Sep 1999

Monenco Iran Inc (Iran Office for AGRA Monenco Inc, Canada), Tehran, Iran
Civil engineer & drafter, Civil Engineering Department, 6CCPP power plant projects.

- Nov 1997 to Dec 1998

Ivan-E-Behesht Consulting Engineers Company, Tehran, Iran

Structural engineer, design and directing house building projects, tall building projects, research on reinforcement of structures against earthquake with knee braced connections.

- Jun 1994 to Sep 1997

Azar Khat Construction Company, Tabriz, Iran

Civil technologist & technical office staff, construction of house building projects.